



CONTROL PERFORMANCE EVALUATION AND DIAGNOSIS

BY

NIVES STANFELJ,

B.Sc.

McMASTER UNIVERSITY LIBRARY
TS 156.8 .S73 1990
Control performance evaluation C.2



3 9005 0473 3452 3

CONTROL PERFORMANCE EVALUATION AND DIAGNOSIS

**CONTROL PERFORMANCE EVALUATION
AND DIAGNOSIS**

by NIVES STANFELJ, B.Sc.

A Thesis

Submitted to the School of Graduate Studies
in Partial Fulfilment of the Requirements
for the Degree
Master of Engineering

McMaster University

(c) Copyright by Nives Stanfelj, October 1990

MASTER OF ENGINEERING (1990)
(Chemical Engineering)

McMASTER UNIVERSITY
Hamilton, Ontario

TITLE: Control Performance Evaluation and Diagnosis

AUTHOR: Nives Stanfelj, B.Sc. (University of Waterloo)

SUPERVISOR: Professor T.E. Marlin
Professor J.F. MacGregor

NUMBER OF PAGES: xii, 240

ABSTRACT

A working definition of "good" control performance was considered and the criteria for its measurement were then determined. This study is focused on a time series approach to control performance evaluation and diagnosis, in which statistical tools such as the autocorrelation and crosscorrelation functions and the power spectrum, as well as the input and output variances are used. This technique allows the use of normal operating data for control system performance evaluation, thus requiring minimal effort.

Several simulation and industrial cases were investigated for this research, including SISO feedback and feedforward-feedback strategies as well as MIMO applications. The basis of this approach is the comparison of the existing controller statistical properties to that of a theoretical optimum. In this manner, it is possible to ascertain whether the potential for controller improvement exists and is warranted. The diagnostic procedure then allows for the determination of the likely cause of inadequate control performance, with the ability to distinguish between poor tuning and model mismatch and between poor feedforward or

feedback control or the specific controlled or manipulated variable in a MIMO system.

ACKNOWLEDGEMENTS

I would like to express my appreciation to Shell Canada Ltd. for their support of this research and in particular the Scotford Refinery personnel for all of their assistance. Special thanks go to Steve Kelly and Dave Onderwater for their continued technical help and guidance. I would also like to take this opportunity to thank my thesis supervisors, Tom Marlin and John MacGregor, without whose technical and moral support this final product would not have been possible.

TABLE OF CONTENTS

	PAGE
Abstract	
1.0 Introduction	1
2.0 Control Performance Monitoring and Diagnosis	5
2.1 Conventional Analysis	7
2.1.1 Statistical Analysis	8
2.2 Control Performance Evaluation and Diagnosis	13
2.2.1 Establishing Best Achievable Control	17
2.2.2 Control Performance Diagnosis	22
2.3 Summary	49
3.0 SISO Control Systems	52
3.1 Feedback Control	52
3.1.1 Model Based Feedback Control	65
3.1.2 Industrial Case Study	77
3.2 SISO Feedforward-Feedback Control System	94
3.2.1 Simulation Results	95
3.2.2 Empirical Study of a Distillation Tower at Shell Scotford Refinery	120

TABLE OF CONTENTS

	PAGE
4.0 MIMO Control Systems	150
4.1 Simulation Results	151
4.2 Multivariable Control Case Study using QDMC	168
5.0 Conclusions and Recommendations	187
6.0 References	190
7.0 Glossary of Terms	194
A.0 Statistical Analysis Review	197
B.0 SISO Feedback Control Simulation Results	209
C.0 SISO Model Based Feedback Control System Simulation Results	211
D.0 Paper Mill Data Industrial Case Study	213
E.0 Shell Heat Exchanger Industrial Case Study	214
F.0 SISO Feedforward-Feedback Control Simulation Results	216
G.0 Shell Stabilizer Industrial Case Study	222
H.0 MIMO Control System Simulation Results	227
I.0 Shell HCU QDMC Industrial Case Study	239

LIST OF FIGURES

	PAGE	
2.1	Performance and Variance	12
2.2	Control Performance, Evaluation and Diagnosis	14
2.3	Feedback-Only Control Block Diagram	18
2.4a	Feedback Control Block Diagram	25
2.4b	Model Based Feedback Control Block Diagram	26
2.5	Feedforward-Only Control Block Diagram	30
2.6	Feedforward-Feedback Control Block Diagram	32
2.7	Feedforward-Feedback Analysis Sequence	33
2.8	Feedforward-Feedback Correlation Matrix	40
2.9	MIMO Performance Diagnosis Correlation Matrix	47
3.1	SISO Feedback-Only Control Block Diagram	53
3.2	SISO Feedback-Only, Uncontrolled Case	55
3.3	SISO Feedback-Only, MVC Case	57
3.4	SISO Feedback-Only, CMVC Case	60
3.5	SISO Feedback-Only, Model Mismatch (Increased K)	63
3.6	SISO Feedback-Only, Model Mismatch (Decreased K)	64
3.7	Smith Predictor Control Block Diagram	66
3.8	Smith Predictor (MVC), Base Case	67
3.9	Smith Predictor (PI), Detuned Case	70

LIST OF FIGURES

	PAGE
3.10 Smith Predictor (MVC), Model Mismatch	73
3.11 Smith Predictor (MVC), Model Mismatch (Setpoint Changes)	75
3.12 Domtar Paper Mill Data Case Study	78
3.13 Kruger Paper Mill Data Case Study	81
3.14 Process Schematic for Rich Amine Heat Exchanger	84
3.15 Rich Amine Heat Exchanger Control Block Diagram	85
3.16 Rich Amine Heat Exchanger, Normal Operation	86
3.17 Rich Amine Heat Exchanger, MVC Case	89
3.18 Rich Amine Heat Exchanger, Overtuned Case	92
3.19 Feedforward-Feedback Control Block Diagram	96
3.20 Feedforward-Feedback, Base Case	98
3.21 Feedforward-Feedback, Detuned Feedback	101
3.22 Feedforward Control Decommissioned, Perfect Models	104
3.23 Feedforward-Feedback, Model Mismatch with Cancelling Errors	106

LIST OF FIGURES

	PAGE
3.24 Feedforward Control Decommissioned, Cancelling Model Errors	109
3.25 Feedforward-Feedback, Process Model Mismatch	111
3.26 Feedforward-Feedback, Disturbance and Process Model Mismatch	114
3.27 Feedforward-Feedback, Detuned Feedback Correlation Matrix	119
3.28 Feedforward-Feedback, Process Model Mismatch Correlation Matrix	119
3.29 Process Schematic for the HCU Stabilizer	122
3.30 HCU Stabilizer Control Block Diagram	135
3.31 HCU Stabilizer, Initial Control Case	129
3.32 HCU Stabilizer, Decreased Feedforward Gain	132
3.33 HCU Stabilizer, Increased Feedback Gain	135
3.34 HCU Stabilizer, Increased Feedforward Gain	138
3.35 HCU Stabilizer, No Feed Perturbations	142
3.36 HCU Stabilizer, No Feedforward Control	144
3.37 HCU Stabilizer, Excessive Feedforward Gain	147
4.1 Control Block Diagram for the 2X2 MIMO System	152
4.2 MIMO Base Case	154

LIST OF FIGURES

		PAGE
4.3	MIMO, Penalty Weights on u_1 and u_2	155
4.4	MIMO, Penalty Weight on u_1	156
4.5	MIMO, Model Mismatch in $G_m(1,2)$ and/or $G_m(1,2)$	157
4.6	MIMO, Model Mismatch in y_1 and y_2	160
4.7	MIMO, Correlated Noise with Model Mismatch in $G_m(2,2)$	162
4.8	MIMO, Independent Noise with Model Mismatch in $G_m(2,2)$	162
4.9	MIMO, Imbalanced Dead Times	164
4.10	MIMO, Balanced Dead Times	166
4.11	MIMO, Sparse System Correlation Matrix	168
4.12	Process Schematic for First Stage Hydrotreater	171
4.13	Controlled Variable Dynamic Matrix	172
4.14	HCU QDMC, Autocorrelation	177
4.15	HCU QDMC, Crosscorrelation ($d_t \times C.V._{t+k}$)	179
4.16	HCU QDMC, Crosscorrelation ($u_t \times ER_{t+k}$)	181
4.17	HCU QDMC, Crosscorrelation ($u_t \times ER_{t+k}$)	182
4.18	HCU QDMC, Crosscorrelation ($u_t \times u_{t+k}$)	183

LIST OF TABLES

		PAGE
2.1	Conventional Monitoring Parameters	7
3.1	Summary of Rich Amine Heat Exchanger Study	88
3.2	HCU Stabilizer Conditions During Model Identification	124
3.3	Summary of Stabilizer Study	126
4.1	Minimum Variance Predictions	178

1.0 INTRODUCTION

Presently, industry has many control schemes implemented, whose benefits are judged against the pre-control plant performance. Some of the conventional criteria used to measure performance are the controlled variable mean (as compared to a target value) and standard deviation and the control loop service factor. Hence, normal operating data is being used extensively in industry to monitor applications, whereby the process performance is deemed acceptable or not with respect to traditional process requirements such as product specifications. If the key criteria are being satisfied then further effort is not required. Since monitoring is generally based on a comparison to prior performance there is no information on the improvement that still may be available. Furthermore, this monitoring phase does not provide a means to determine why unsatisfactory or non-optimal performance is being experienced. The evaluation and diagnostic procedure being proposed in this research is designed to address these two shortcomings of current practice.

As the number and complexity of implemented control loops increase, focus will be placed on existing control scheme maintenance and improvement. This control performance evaluation and diagnosis tool becomes valuable in that a theoretical optimum is established and used for comparison against which the actual controller is measured. If a significant deviation exists between the actual and the best achievable performance and more aggressive control action is desirable, control modifications can be recommended.

This study has investigated Single-Input-Single-Output (SISO) systems for both feedback-only and combined feedforward-feedback control schemes. The study of these simple systems is important as many cases having negligible interaction can be evaluated and diagnosed in this manner. Furthermore, study of SISO systems provides a solid basis for the approach being used. It is important to note that these cases are not limited to isolated control loops having no other interaction. In these cases it is assumed that the process involved is the physical process plus the other control schemes implemented. As long as the latter remains consistent throughout the analysis the results obtained are reliable. The techniques and criteria developed for these simple structures have also been extended to Multi-Input-Multi-Output (MIMO) systems, both multiple single loop and multivariable control schemes. The aforementioned cases have

been examined both in simulation studies and in industrial applications.

The aim of this research is to utilize readily available normal operating data to accomplish control performance evaluation and diagnosis. A simple analysis method is proposed relying primarily on graphical analyses. As a result of these inherent factors, limited effort is required to fulfil the objectives of this diagnostic technique.

As a result of this study a methodology has been developed by which industrial control applications can be evaluated. Upon observation of simple statistical parameters control performance can be deemed satisfactory or inappropriate. A theoretical optimum is generated against which the control scheme's success can be judged. If there is a sufficient discrepancy between the optimal and actual performances the diagnostic procedure can locate areas of inadequacy. In this manner the many existing control applications can be examined and modifications can be identified which will attempt to fulfil the control objectives.

The remaining chapters of this thesis will provide some of the statistical arguments supporting this approach,

discussion of the simulation case studies used to develop and test the methodology and the industrial examples illustrating the potential and limitations of this analysis technique. As mentioned previously SISO feedback-only and feedforward-feedback control systems will be addressed first and the methodology will then be extended to MIMO schemes.

2.0 CONTROL PERFORMANCE MONITORING AND DIAGNOSIS

Before control "performance" can be evaluated, the measures of performance must be defined. These qualitative and quantitative measures of control performance should be based on safety, product quality, equipment protection, plant data, site economics and facilities. The next obvious question becomes how to use these measures to distinguish between good and poor performance. All of these concerns must be answered with engineering judgement and a sound understanding of the process and its objectives.

The desirable features of any controller are "good" performance in both regulatory (compensate for disturbances entering the process) and servo (controlled variable must follow frequent setpoint changes) operating modes, and robustness to modelling errors. Servo control performance may be assessed by the inspection of the process response to infrequent setpoint step changes. Key performance indicators are rise time, magnitude of overshoot and decay ratio, all of which can be observed by visual examination of the process transient response to the requested setpoint change. Measures such as the integral error or absolute integral error can also be used to evaluate the control performance. Desired response

characteristics are dependent on the process specifications. [Marlin et al., 1987; Stout & Cline, 1976] This technique is also applicable to the case of step disturbances affecting the process, but is not valid in the case of stochastic disturbances.

Regulatory control performance in the presence of stochastic disturbances is more difficult to assess as there is no definite pattern to represent good control performance in the dynamic response. This specific challenge is the focus of this research. The evaluation techniques include variance, the autocorrelation and crosscorrelation functions and the power spectrum. These will be discussed in greater detail in the following sections.

The remainder of this chapter introduces the conventional analyses, which provide necessary parameters for monitoring the performance of process control systems, and the diagnostic tools proposed in this research to evaluate and diagnose the control performance. To satisfy the latter, the statistical tools already mentioned including variance, autocorrelation, crosscorrelation and power spectrum will be introduced. These measures have been chosen as they are effective with the use of normal operating data and they are straightforward to use and to understand. These statistical techniques and the diagnostic procedure will be discussed in

detail in the following sections. The methodology described in this chapter is then demonstrated through simulation and industrial examples in Chapters 3 and 4.

2.1 CONVENTIONAL ANALYSIS

Historically, control effectiveness has been quantified using simple statistical calculations using readily available process information. Table 2.1 lists common parameters used in conventional analyses. The basis of this conventional analysis is the comparison of these measures between the controlled and uncontrolled cases.

Table 2.1 Conventional Monitoring Parameters

- * control loop service factor
- * controlled variable mean and standard deviation
- * product specification and giveaway
- * manipulated variable variance
- * number of constraint/specification violations
- * maximum value of violations and integral error of violations
- * number of incidents (off-specification products, alarms, runaways, shutdowns)

Although these quantities provide useful information, their value is limited to a monitoring capacity. These measures enable one to establish the improvement achieved over the uncontrolled case and how well the control system is achieving key plant objectives, but they do not provide information on the potential for further improvement nor a means to diagnose any shortcomings in the control performance. These parameters should be used, however, in a preliminary 'monitoring' phase in which control schemes can be screened in order to identify unsatisfactory performance. Only those cases deemed unacceptable in this monitoring phase should be further addressed in the diagnostic phase. This diagnostic procedure will be introduced and demonstrated in the latter section of this chapter.

2.1.1 STATISTICAL ANALYSIS

Statistical analysis can be performed on batch systems or on continuous processes. In the case of the latter, sampled data points are taken at a constant frequency and are assumed to be representative of the long term nature of the process. These assumptions hold if the variation in sampling frequency is not large and if the process is stationary or possesses stationary random properties. [Pryor, 1982] For this reason it is imperative that the data analyzed is

stationary or that stationarity conditions be imposed. This is discussed in Appendix A, Time Series Review, which contains information on model identification, the autocorrelation and crosscorrelation functions and power spectrum, confidence intervals and the differencing of nonstationary series. Furthermore, the data which is collected should reflect typical plant conditions in order to ensure that the statistical parameters generated are representative of the normal operation. In addition to this, enough data must be collected or sufficient forcing should be present in the system to ensure accurate statistical estimates.

Once the data has been collected, conventional statistical analyses will provide useful information about the process. Some of the most useful properties and the calculations which provide the sample estimates are defined below. The nomenclature used throughout this report is defined in a glossary of terms included in section 7.0.

$$\text{Mean} = E(y) = \bar{y} = \sum_{i=1}^N \frac{y_i}{N} = \frac{1}{N} \sum_{i=1}^N y_i \quad (2.1)$$

$$\text{Error} = Er_i = y_i - \bar{y} \quad (2.2)$$

$$\text{Average Absolute Error} = \overline{ER} = \frac{1}{N} \sum_{i=1}^N |ER_i| \quad (2.3)$$

$$\text{Variance} = V = E(y-\mu)^2 = \frac{1}{N} \sum_{i=1}^N ER_i^2 = \frac{1}{N} \sum_{i=1}^N (y_i - \bar{y})^2 \quad (2.4)$$

$$\text{Standard Deviation} = S = \sqrt{V} = \left(\frac{1}{N} \sum_{i=1}^N (y_i - \bar{y})^2 \right)^{\frac{1}{2}} \quad (2.5)$$

The measure of the standard deviation, or variance, is of great importance. Improved control performance reduces the variance of key process variables, and hence this statistical value can be used as an initial screening of control performance.

The standard deviation of a variable can be attributed to real variations and instrument or measurement errors. Improved process control reduces the standard deviation by reducing the former. This real variability can in turn be traced back to changes in the independent variables. [Stout & Cline, 1976, Marlin et al., 1987] In many cases performance can be related to one key variable, which may be a temperature, concentration or product quality, and a measure of performance such as profit or cost can be expressed as a

function in this variable.

A frequently encountered situation is one in which the performance function, P , is linear,

$$P_{avg} = A \pm BM \quad (2.6)$$

where A, B are constants, M is the variable average, which is symmetrically distributed, and the variable is constrained at some minimum or maximum limit. Reducing the variability of the output in this case, will allow the operating point to be moved closer to the acting constraint. The change in profit or cost is then given by,

$$\Delta P_{avg} = B \Delta M \quad (2.7)$$

If we refer to Figure 2.1 tighter control, resulting in a lower variance, allowed the process to move to a more favourable operating point, M_2 .

While these statistics are useful, they do not allow for further diagnosis of the control system as important, frequency-dependent information is combined and therefore masked in these moments, such that the dynamic behaviour cannot be evaluated. The control performance evaluation techniques being studied in this research are based on a time series approach. This method is being pursued as it is

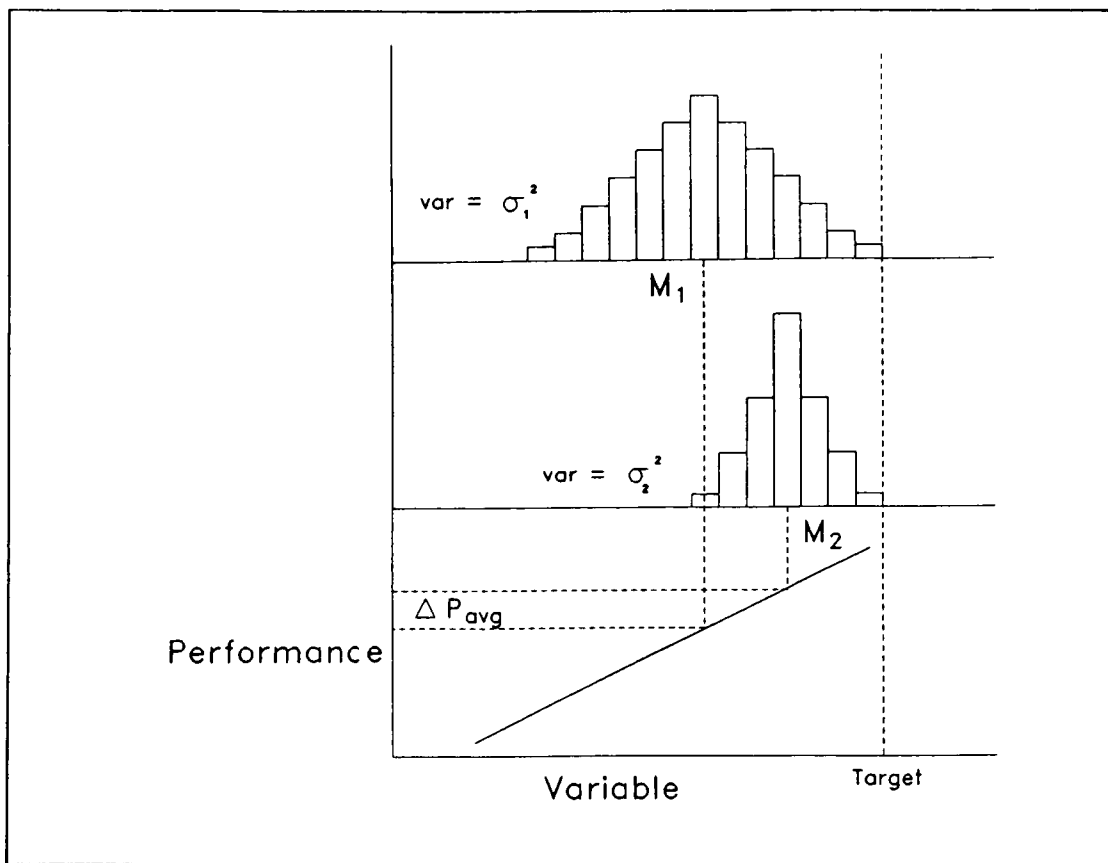


Figure 2.1 Performance and Variance

presently the only way in which to address stochastic processes and to preserve the important dynamic information. Statistical analyses such as the autocorrelation and crosscorrelation functions and the power spectrum are used to compare the existing controller to a theoretical optimum and to identify problem areas. Depending on the system being evaluated, problem areas may be within the process model (in model-based controllers) or the controller tuning or execution frequency. In many of these cases it is possible to further isolate the controller inadequacy, such as to the feedforward

or feedback component or the specific component in a multivariable scheme.

A basic understanding of time series techniques is assumed in this report. A quick review of the key statistical parameters is provided in Appendix A.

2.2 CONTROL PERFORMANCE EVALUATION AND DIAGNOSIS

In this section the three tier approach to a monitoring, evaluation and diagnosis system will be presented. The first level is comprised of conventional analyses which provide the monitoring phase of this technique while the remaining two complete the diagnostic phase. The hierarchy of monitoring, control evaluation and control diagnosis is presented in Figure 2.2.

At the pyramid apex we have 'normal operating data' which is abundant and easily accessible given the present status of industrial computer data storage and manipulation capabilities. It is important to stress the use of normal operating data as this limits the amount of effort required to fulfil the analysis. Control performance monitoring is the first level in this procedure and would be executed for all control loops. As numerous control schemes exist in any

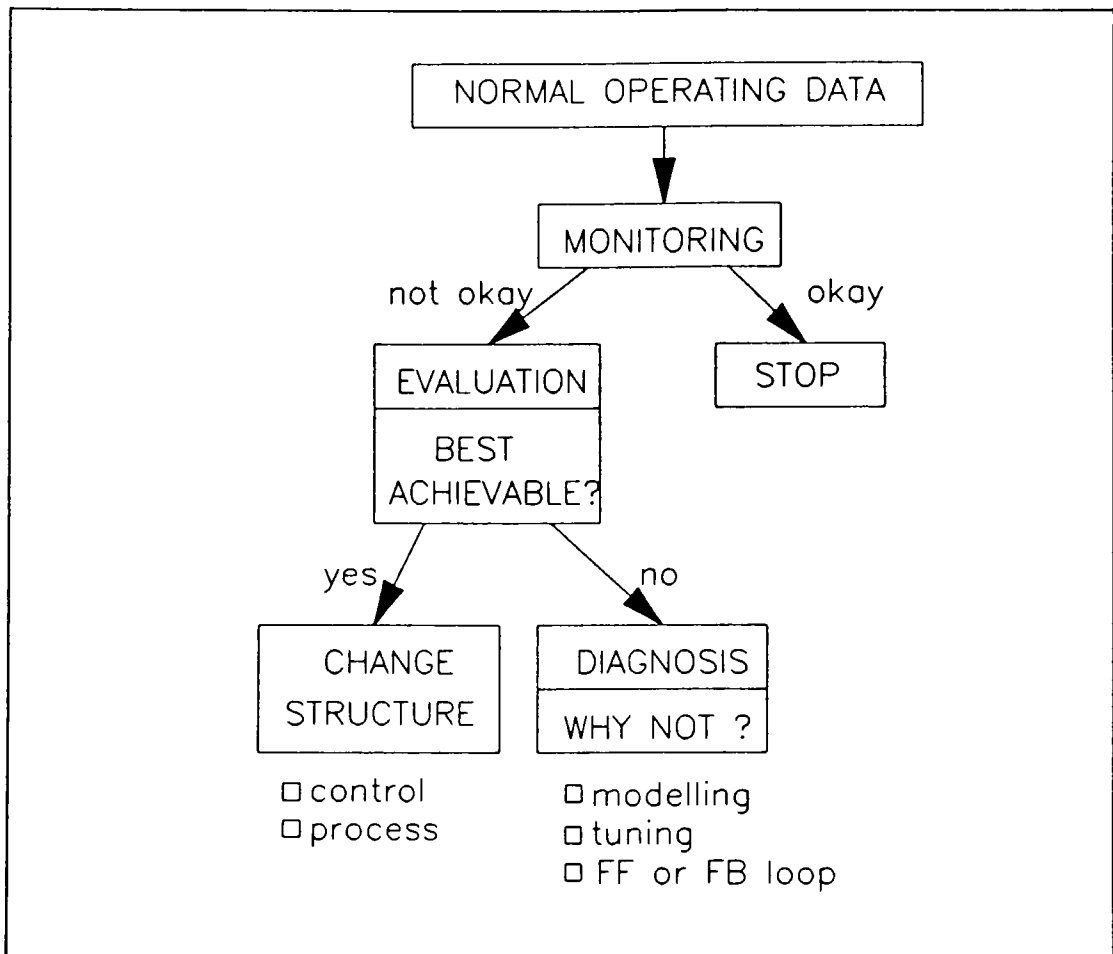


Figure 2.2 Control Performance Monitoring, Evaluation and Diagnosis

plant, this level acts as a screen to discriminate between acceptable and unacceptable performance. The monitoring criteria would include those variables listed in Table 2.1. If the control scheme is meeting its objectives then further analysis is not necessary. Only those applications deemed unsatisfactory in this initial monitoring phase would be diagnosed in the second level.

It is the development of these diagnostic levels which comprises this research. The initial step in the diagnostic procedure is to establish whether the best achievable performance is being realized. If this is not the case then an estimate of the best achievable control performance is generated and compared against the actual control system performance. This idea is not new as it has been presented in Box & Jenkins [1976] and used in MacGregor, Taylor & Wright [1988] and Harris [1989].

For the purposes of this research, variance is used as a measure of control performance with the theoretical minimum acting as the basis for comparison. This bound on achievable performance, therefore, is the Minimum Variance Controller (MVC) or in the case of multivariable systems, the Linear Quadratic Gaussian Controller (LQG). These controllers provide the theoretically lowest variance for the variables controlled and are thus valuable in establishing performance limits. It is important, however, that in achieving this level of performance that the variance of the manipulated variable(s) is also reasonable. A controller which requires the harsh manipulation of the input variable(s) is not desirable and is therefore not generally useful in industrial applications. Thus, in the practical application of this analysis it may be necessary to generate other bases for comparison, such as the best achievable performance with a PI

controller. This will also be specific to the problem being examined and will require knowledge of the process and its goals.

If the best achievable bound does not present a significant improvement over the actual performance but the performance is still not satisfactory then either the structure of the controller or process must be changed. The former may be achieved, for example, by changing the loop pairing or introducing feedforward control. The latter may involve reducing the dead time of the process or attenuating the disturbances. This solution path is not the concern of this research since modifications made must be the result of process and cost analyses of each specific control system.

If the estimated best achievable performance is significantly better than that which is being experienced, then the source of this inadequate or sub-optimal performance must be diagnosed in order for it to be corrected. It is this step which constitutes the main contribution of this research. The causes of this poor control performance may be in the controller tuning or in incorrect process model representation. In more complex schemes the poor performance may be attributed to the feedforward or feedback controller or to a specific output or input variable in a MIMO scheme.

In order to accomplish this challenging task a new approach, one differing from conventional monitoring, is required. Because we are limited to large quantities of normal operating data describing stochastic processes a statistical approach is most appropriate. Moreover, many of these stochastic processes are identified using the time series technique, hence the concepts of this approach are familiar to process engineers. Specifically, the use of the autocorrelation and crosscorrelation functions will be demonstrated in fulfilling the objectives of this research.

2.2.1 ESTABLISHING BEST ACHIEVABLE CONTROL

"For processes described by linear transfer functions with additive disturbances, the best achievable control in the mean square sense is realized when an MVC is implemented." [Box & Jenkins, 1976] The minimum variance controller (MVC) provides the smallest variance of any controller at the given sampling intervals. It is rarely applied industrially, however, as it often requires harsh input manipulations and often lacks robustness. The MVC and its statistical properties, are useful in providing a basis against which to compare the performance of industrially implemented controllers. The minimum variance controller provides a bound on achievable feedback performance, beyond which improvements

are not possible given the physical process configuration.

It can be shown that an estimate of the best achievable control can be obtained by fitting a univariate time series model to process data collected under routine feedback control. At this point it should be mentioned that this research deals exclusively with discrete, sampled data systems. It is not necessary to introduce perturbations in the manipulated variable and 'identifiability' constraints need not be imposed. [Harris, 1989] Given the general block diagram for a univariate system, shown in Figure 2.3, the closed loop process model is given by,

$$Y_t = \left(\frac{N}{1 + G_c G_p} \right) a_t \quad (2.8)$$

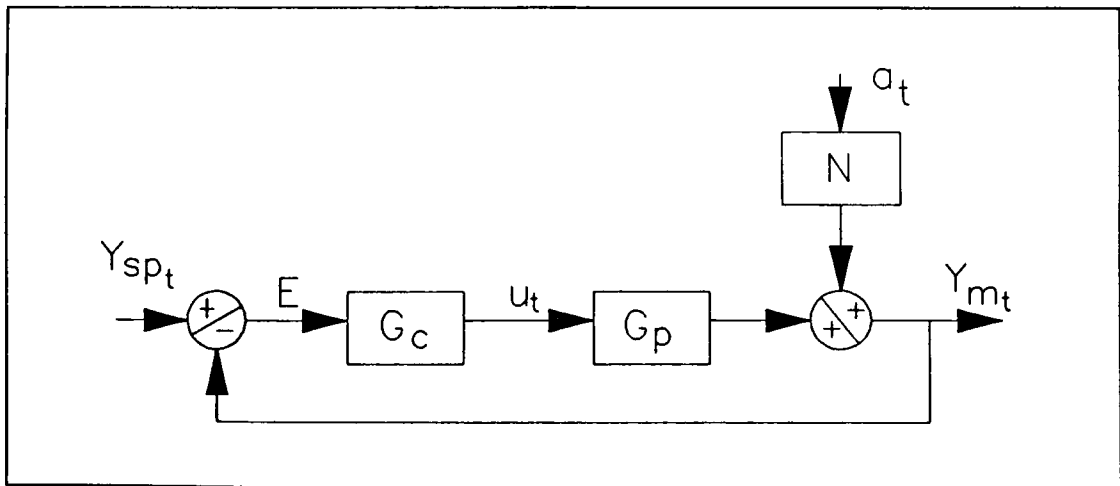


Figure 2.3 Feedback-Only Control Block Diagram

which can be represented by,

$$Y_t = \frac{\theta(z^{-1})}{\phi(z^{-1})} * a_t = \psi(z^{-1}) * a_t \quad (2.9)$$

This representation can be expanded through long division to give a moving average time series model,

$$Y_t = [1 + \psi_1(z^{-1}) + \psi_2(z^{-2}) + \dots + \psi_f(z^{-f}) + \psi_{f+1}(z^{-(f+1)}) + \dots] a_t \quad (2.10)$$

where f is the true process dead time. The first $(f+1)$ terms cannot be affected by feedback control as the effect of the input manipulations, u_t , can only be observed after the process delay. Therefore, these terms remain unchanged regardless of manipulated variable perturbations. The presence of feedback control only affects the remaining terms in equation 2.10. In the case of minimum variance control these terms are reduced to zero as all incoming disturbances are completely attenuated. This reduces the process model, for perfect control, to a moving average model of order f ,

$$\begin{aligned} (Y_t)_{MVC} &= a_t + \psi_1 a_{t-1} + \psi_2 a_{t-2} + \dots + \psi_f a_{t-f} \\ &= [1 + \psi_1(z^{-1}) + \psi_2(z^{-2}) + \dots + \psi_f(z^{-f})] a_t \end{aligned} \quad (2.11)$$

Testing for Best Achievable Control

A moving average (MA) process of order f has the property that the autocorrelation function is zero beyond lag f . Therefore, given the time series response of the process being examined the simple generation of the autocorrelation plot can show whether MVC is being achieved by observing the lag at which the autocorrelation is effectively eliminated. If the autocorrelations are reduced to zero at or soon after the process dead time, then the best achievable control is being realized and further improvements can only be attained through structural modifications. If the autocorrelation function is significant after the process dead time then control modifications can improve the process performance. In order to decide whether modifications are warranted the available improvement can be quantified. As noted previously, if the variance is used as an indication of process performance then an estimate of the minimum variance can provide the necessary justification.

Estimating Best Achievable Performance

Given the moving average model in equation 2.10 the variance is calculated by,

$$\text{VAR}\{Y_t\} = (1 + \psi_1^2 + \psi_2^2 + \dots + \psi_f^2 + \psi_{f+1}^2 + \dots) \sigma_a^2 \quad (2.12)$$

where ψ_i are the coefficients of the model, estimated from the raw data and σ_a^2 is the variance of the residuals obtained after fitting the ARMA model. In the case of minimum variance control only the first $f+1$ terms are required, as shown in Equation 2.11, reducing the calculation of the variance to,

$$\text{VAR}\{Y_t\}_{MVC} = (1 + \psi_1^2 + \psi_2^2 + \dots + \psi_f^2) \sigma_a^2 \quad (2.13)$$

This is the minimum variance which is attainable for the given process configuration under the existing disturbance conditions. Further reductions in the process output variance cannot be achieved at the given sampling interval. Additional reductions in the variance can only be attained through structural modifications such as the reduction of disturbances (σ_a^2), the reduction of dead time (f), the incorporation of feedforward control or the use of another manipulated variable for control purposes.

The use of the minimum variance as a performance bound provides a significant simplification to the evaluation and diagnosis methodology. The only information required is the process dead time, (f), and the ψ weights up to lag f , which can be calculated from any open or closed loop data. The future performance of any other controller, which deviated

from minimum variance, would need to be calculated from a simulation of the control system subject to the specific stochastic disturbance. In the latter case both the process, G_p , and the disturbance, G_d , transfer functions would have to be known. Although model identification is not difficult, plant perturbations would be necessary.

In the case where the estimated best achievable control is a significant improvement over the current control performance, alternate controller tuning or algorithms can be considered in order to reduce the controlled variable variability, if this improved performance is desired.

2.2.2 CONTROL PERFORMANCE DIAGNOSIS

Once the controlled variable, $(Y_m)_t$, autocorrelation has shown inadequacy in the control performance and the estimate of the best achievable performance, calculated as described in the previous section, shows a significant improvement over the actual performance then further control diagnosis is warranted. The basis for this diagnosis is the analysis of the correlation between the various process variables and other calculated quantities. Depending on which variables are correlated it will be possible to deduce the likely cause of control deficiency. The following sections

will demonstrate the diagnosis methodology used for several control strategies.

Feedback-only Control

If the autocorrelation of $(Y_m)_t$ shows non-optimal control and the estimated best achievable performance is a significant improvement over the existing performance then the control system must be examined. The crosscorrelation between the input, u_t , and the output, $(Y_m)_{t+k}$, duplicates the information provided in the output autocorrelation. In the case of perfect control significant correlation will only exist from the input to the output, γ_{uy} , up until the dead time of the process, in the positive lag direction. As discussed in section 2.2.1 feedback-only control can have no effect on the process output until after the process delay.

The reason why only the positive lag direction is considered falls directly from the relationship between the two crosscovariances of a bivariate system. As presented in Appendix A,

$$\gamma_{uy}(k) = \gamma_{yu}(-k) \quad (2.14)$$

Therefore, the crosscovariance from u_t to y_{t+k} , γ_{uy} , in the positive lag direction is equal to the crosscovariance from y_t to u_{t+k} , γ_{yu} , in the negative lag direction. The converse is also true,

$$\gamma_{uy}(-k) = \gamma_{yu}(+k) \quad (2.15)$$

As the systems being dealt with are under the influence of feedback control the output has a direct effect on the input moves which are implemented by way of the controller. As a result of this, correlation will always exist from the input to the output in the negative direction and is therefore of no concern.

It should be noted that the presence of a large negative autocorrelation at lag zero usually indicates that the data has been generated under closed loop conditions as in most dynamic, discrete time systems there can be no instantaneous transfer of the input to the output. [Box & MacGregor, 1974]

The control block diagram for the feedback-only controller is given in Figure 2.4a. The process model G_m is not used explicitly in the control algorithm but is used for model prediction purposes only. The output predicted by the identified process model can be calculated and used to verify

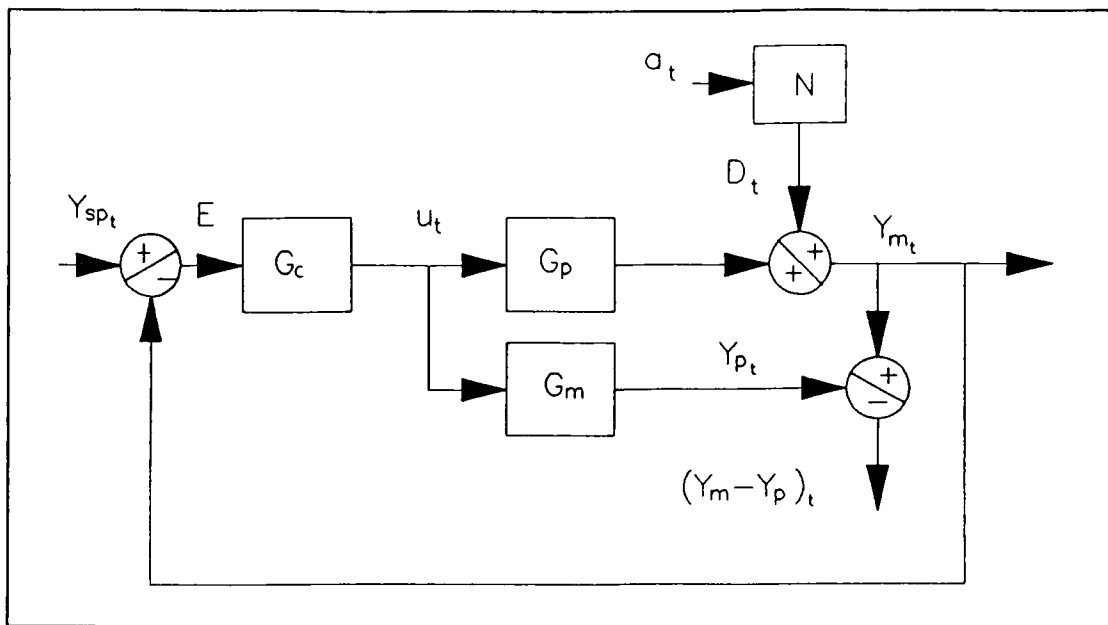


Figure 2.4a Feedback Control Diagram

the accuracy of model. The controller can also be implemented in IMC form as shown in Figure 2.4b, in which case the prediction error calculation is used in the control system. The prediction error is then given by,

$$(Y_m - Y_p)_t = (Y_m)_t - G_m * U_t \quad (2.16)$$

Degradation in performance can be the result of model/process error or poor controller tuning. The goal of the diagnosis, therefore, is to determine the source(s) of this poor performance, if possible.

Using the model-based feedback control system shown in Figure 2.4b and assuming a constant setpoint, block diagram

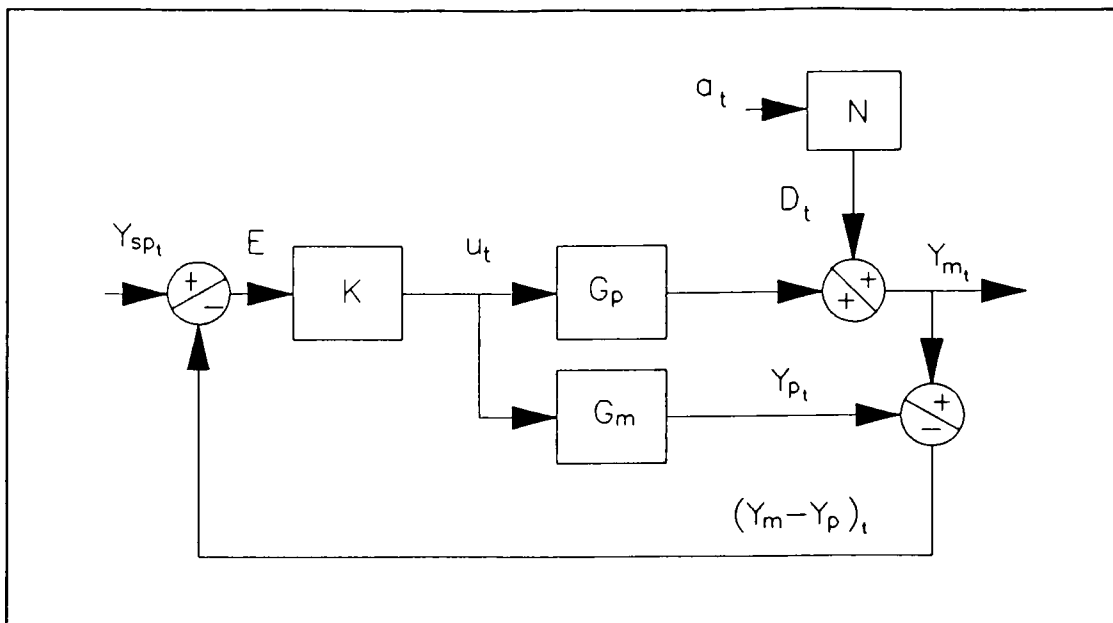


Figure 2.4b Model-Based Feedback Control Diagram

manipulation yields the following expression for the model prediction,

$$(Y_m - Y_p)_t = H * N a_t \quad (2.17)$$

where,

$$H = \frac{1}{1 + K(G_p - G_m)} \quad (2.18)$$

As evident from Equations 2.17 and 2.18, the prediction error reduces to the disturbance when the model exactly matches the plant, $H=1$. The manipulated variable can be represented by,

$$u_t = -K * H * N a_t \quad (2.19)$$

As both the prediction error and the input are influenced by the model accuracy, in H , a possible method for diagnosing control performance would be to compare the behaviour of the two. The crosscorrelation can be used for this comparison, and is described in detail in Appendix A. The crosscovariance from the input to the prediction error is given by,

$$\gamma_{u, (Y_m - Y_p)} = E [(-K * H * N a_t) (H * N a_{t+k})] \quad (2.20)$$

The simplest scenario results if the model is perfect, $H=1$, and the disturbance is white noise, $N=1$. In this case all crosscorrelations reduce to zero as $E(a_t a_{t+k})=0$ for $k>0$, and the controller, K , uses only the current and past values of the feedback signal. Therefore, given a system in which the disturbance is white noise, non-zero crosscorrelations are indicative of model error. A more realistic situation, however, is one of autocorrelated disturbances, $N \neq 0$. In this case $E[(N a_t) (N a_{t+k})] \neq 0$ for $k>0$, therefore, even with a perfect model some significant crosscorrelations would result from Equation 2.20. Although model error will contribute to the crosscorrelation from the input to the prediction error, it is not the only factor. Hence, non-zero crosscorrelations cannot be used as an unequivocal test for model error. Given normal operating data, therefore, it is not possible to diagnose whether poor control performance is the result of modelling errors or poor tuning.

This distinction can be accomplished, however, with the addition of setpoint changes to the process. In the presence of setpoint changes, the prediction error becomes,

$$(Y_m - Y_p)_t = H * D_t + K * [G_p - G_m] * H * Y_{sp_t} \quad (2.21)$$

The crosscovariance from the setpoint to the prediction error is given by,

$$\gamma_{Y_{sp}, (Y_m - Y_p)} = E[(Y_{sp_t}) (H * D_{t+k})] + E[(Y_{sp_t}) (K * (G_p - G_m) * H * Y_{sp_{t+k}})] \quad (2.22)$$

As the imposed setpoint changes should be independent of future disturbances, the first term in Equation 2.22 is eliminated. Hence, the crosscorrelation between the setpoint and the prediction error is only dependent on the model error, as expressed in the second term. Therefore, if the model is perfect no correlation would exist between the setpoint and the prediction error. Conversely, if the model error is significant, significant correlation will exist in Equation 2.22. This analysis can therefore be used to identify the presence of model error. It is important to note that the amount of forcing provided by the magnitude, frequency and number of setpoint changes must be significant enough to result in significant values of the calculated crosscorrelations.

If the model is deemed adequate by the above analysis, the only other possible cause of poor performance is the controller. Deviations from minimum variance control performance can be the result of poor tuning or non-optimal algorithm structure. Of course, aggressive control manipulations resulting from a minimum variance controller may not be appropriate to achieve the desired control objectives. Therefore, once the cause of non-optimal performance is established judgement must be used in improving the performance. A compromise between the variances of the controlled and manipulated variables must be reached.

It has been shown, therefore, that given unsatisfactory performance as indicated by a non-optimal output autocorrelation, the crosscorrelation between the setpoint, $(Y_{sp})_t$, and the model prediction error, $(Y_m - Y_p)_{t+k}$, can be used to distinguish between tuning inadequacy or a poor process model representation.

Feedforward Control

Figure 2.5 shows the control block diagram for feedforward-only control. The closed loop equation is,

$$Y_m = d * G_d + d * G_{c_{FF}} * G_p \quad (2.23)$$

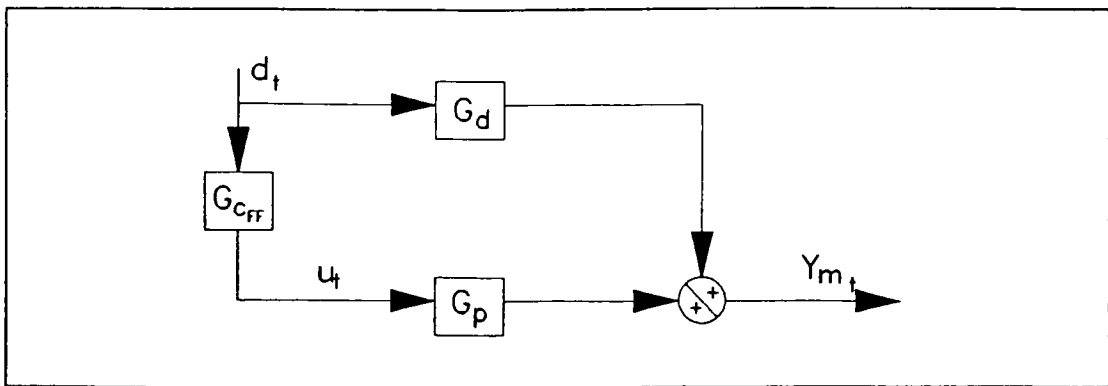


Figure 2.5 Feedforward-Only Control Block Diagram

For perfect feedforward control, resulting in complete disturbance rejection, the feedforward control algorithm is given in Equation 2.24.

$$G_{c_{FF}} = - \frac{G_d}{G_p} \quad (2.24)$$

The resulting closed loop equation becomes,

$$\begin{aligned} Y_m &= d * G_d + d * \left(- \frac{G_d}{G_p}\right) * G_p \\ &= 0 \end{aligned} \quad (2.25)$$

If the process and disturbance models identified are correct and the feedforward controller has been designed as given in equation 2.24, the output, $(Y_m)_t$, will not deviate from its target value. Therefore, the crosscorrelation from the disturbance, d_t , to the output, $(Y_m)_{t+k}$, will not show any significant correlation. Conversely, if either or both of G_d

and G_p are in error perfect disturbance rejection will not be attained and Equation 2.25 will no longer be valid. In this case the output, $(Y_m)_{t+k}$, will be a function of the disturbance, d_t , hence the crosscorrelation from d_t to $(Y_m)_{t+k}$ will show significance.

It has been shown, therefore, that the crosscorrelation from the disturbance to the output can be used to establish whether perfect feedforward compensation has been achieved. If this perfect control has not been attained then either or both of the process and disturbance models is in error.

Feedforward - Feedback Control

The combination of feedforward and feedback control is shown in Figure 2.6. Most of the concepts used for the diagnosis of this control strategy have been covered in the previous discussions. Of course, the first level of performance monitoring remains unchanged. The second level of performance evaluation, however, must be modified to evaluate the performance of both the feedforward and feedback controllers. In the diagnostic level which follows, the cause of poor performance, model mismatch or poor tuning, can then sometimes be determined.

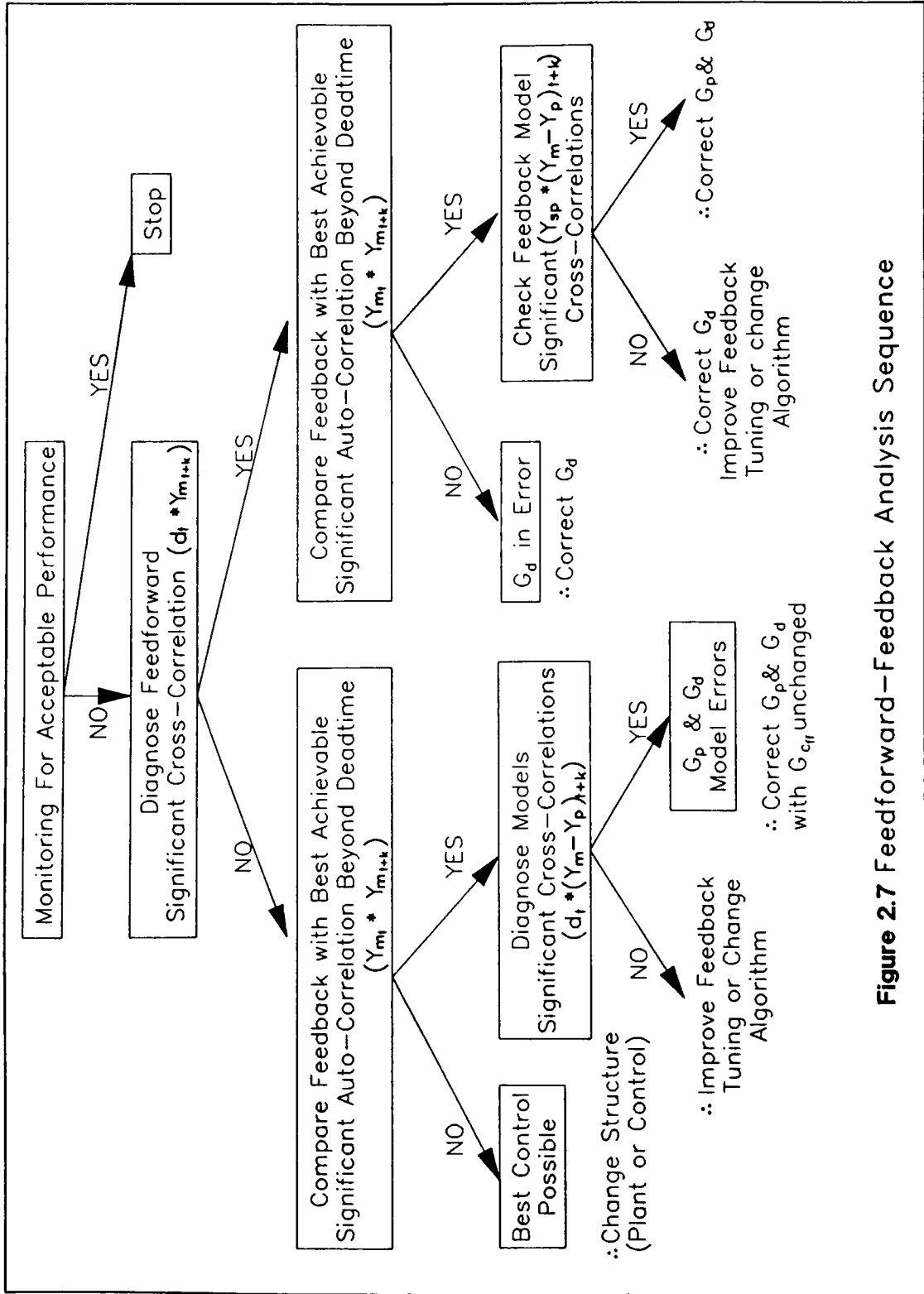


Figure 2.7 Feedforward-Feedback Analysis Sequence

The inherent models used in designing the feedforward and feedback controllers are used to generate an output prediction, $(Y_p)_t$, given the process input and disturbance sequences. The value $(Y_m - Y_p)_t$ represents the model prediction error and is composed of any error in both the process and disturbance models and the unmeasurable noise or disturbances entering the process. This quantity will again be used to check for modelling errors. In the case of the feedforward-feedback control scheme there are two models to consider, one each for the disturbance and the process.

The initial step is to evaluate the performance of the feedforward controller. Block diagram manipulation of Figure 2.6 yields the following expression for the controlled variable,

$$Y_{m_t} = (G_d + G_{c_{FF}} * G_p) * d_t + D_t + G_p * U_{FB_t} \quad (2.26)$$

If the feedforward controller is designed for perfect disturbance rejection,

$$G_{c_{FF}} = -\frac{G_{m_d}}{G_{m_p}} \quad (2.27)$$

and is realizable, with the disturbance dead time being greater than or equal to the feedback dead time, then the first term in Equation 2.26 becomes zero. The measured disturbance, d_t , is also not correlated with future unmeasured disturbances, D_{t+k} , or feedback control manipulations, $(u_{FB})_{t+k}$. Therefore, perfect control results in absence of correlation between the measured disturbance and the future values of the controlled variable. This gives the first diagnostic step in Figure 2.7, which determines the performance of the feedforward controller.

Proceeding down the left branch of Figure 2.7, in which case the feedforward controller is providing perfect compensation for the measured disturbance, the feedback controller can then be evaluated in a similar manner to the feedback-only control case. The autocorrelation of the controlled variable is examined next. If the autocorrelations are eliminated after the dead time, the combination of the feedback control and the perfect feedforward control are providing the best achievable control performance given the current process and control structure. If the feedback control deviates from the best achievable performance, as indicated by the autocorrelation of the controlled variable, the diagnosis is extended. Given the block diagram in Figure 2.6 the prediction error is expressed in Equation 2.28. The crosscorrelation from the measured disturbance, d_t , to the

$$\begin{aligned}
(Y_m - Y_p)_t = & \frac{1 + G_{c_{FB}} * G_{m_p}}{1 + G_{c_{FB}} * G_p} * D_t + \frac{G_{c_{FB}} * (G_p - G_{m_p})}{1 + G_{c_{FB}} * G_p} * Y_{sp_t} \\
& + \frac{(G_d - G_{m_d})}{1 + G_{c_{FB}} * G_p} * d_t + \frac{(G_p - G_{m_p}) * G_{c_{FF}}}{1 + G_{c_{FB}} * G_p} * d_t \\
& - \frac{G_{c_{FB}} * (G_d * G_{m_p} - G_p * G_{m_d})}{1 + G_{c_{FB}} * G_p} * d_t
\end{aligned} \tag{2.28}$$

prediction error, $(Y_m - Y_p)_{t+k}$, can now be investigated. Because the feedforward control has already been deemed adequate the last term in Equation 2.28 reduces to zero, as $G_d * G_{m_p} - G_p * G_{m_d} = 0$. Although the third and fourth terms are non-zero, they essentially cancel one another even in the presence of model mismatch due to the design of the feedforward controller, $G_{c_{FF}}$. Moreover, the unmeasured disturbance and the setpoint changes are independent of the measured disturbance and are therefore not correlated. Hence, the proposed crosscorrelation between the measured disturbance and the prediction error is not a useful diagnostic.

Under feedback-only conditions, however, the crosscorrelation between d_t and $(Y_m - Y_p)_{t+k}$ does provide useful diagnostic information. There is still no correlation from d_t to D_{t+k} and $(Y_{sp})_{t+k}$, eliminating the first two terms in Equation 2.28, and terms 4 and 5 disappear entirely. The third term, however, can be correlated with the measured disturbance and

is a function of the accuracy of the disturbance model. If the measured disturbance model is perfect then there will be no correlation in the previously mentioned crosscorrelation. Conversely, in the presence of significant measured disturbance model error, the crosscorrelation will be non-zero. The data necessary for this diagnostic is easily obtained by decommissioning the feedforward component of the control system for a short period of time. Recall, however, that the feedforward controller has already been established to be perfect and therefore an error in the disturbance model implies a compensating error in the process model. If it is determined that model error does not exist but the feedback control deviates from minimum variance, the poor performance must be the result of inadequate tuning or the choice of control algorithm.

If the evaluation of the feedforward controller showed non-optimal performance then the right hand branch of Figure 2.7 is followed. Once again, the autocorrelation of the controlled variable is examined for the presence of significant correlation beyond the dead time of the feedback process. If there is absence of correlation then the feedback control is tentatively accepted as being minimum variance. Although the feedback control performance appears perfect under these conditions, it should be rechecked once the feedforward control is corrected. This should be done because

the feedback system experiences different disturbances dependent on the quality of the feedforward control.

Lastly, if the feedforward controller is not perfect and the feedback control is not performing to minimum variance the individual models cannot be evaluated from normal operating data. The process model, G_{mp} , however can be evaluated as described in the section on feedback-only control, using periodic setpoint changes.

Because the statistical parameters used in this analysis are only estimates for the data sample in question, statistical significance becomes important. Enough data and/or enough forcing must be present to ensure accurate statistical estimates. The input and output variables should exhibit enough variability such that relationships can be observed in the correlation analyses. Any error seen in the output sequence is assumed to be correct while the absence of visible error is subject to two interpretations. A stable output can be the result of either excellent control or the absence of disturbances. In the latter situation the output would not be adversely affected by disturbances entering the system, hence no input manipulations would be required and the output would not show variability. In those cases in which enough data is not available or the variability is insufficient the statistical significance of the results can

be examined via quantities such as 'confidence intervals'.

Confidence intervals, which are discussed in Appendix A, verify that correlation estimates beyond a certain lag are effectively zero and therefore are not statistically significant. Moreover, the question often arises of the size of error needed before it can be detected using this diagnostic tool. It must therefore be stressed that it is not the absolute size of the parameter variation which is the critical issue but whether this variation contributes significantly to the final control performance. Confidence intervals are thus used to distinguish between statistical significance and random error. Therefore, in the analyses presented in this document only the correlations appearing outside these confidence bounds are considered.

In order to facilitate the analysis, a visual representation of all the information is beneficial. A 'correlation matrix' is shown in Figure 2.8. The controlled variable, measured disturbance and setpoint, at time "t", are the rows of the matrix. The columns of the matrix show the controlled variable and model prediction error at time "t+k", where $k > 0$. The specific matrix elements of interest are indicated with a numbered box. It is intended that significant correlation between any two variables on the matrix axes will be signified with an 'X' in the corresponding

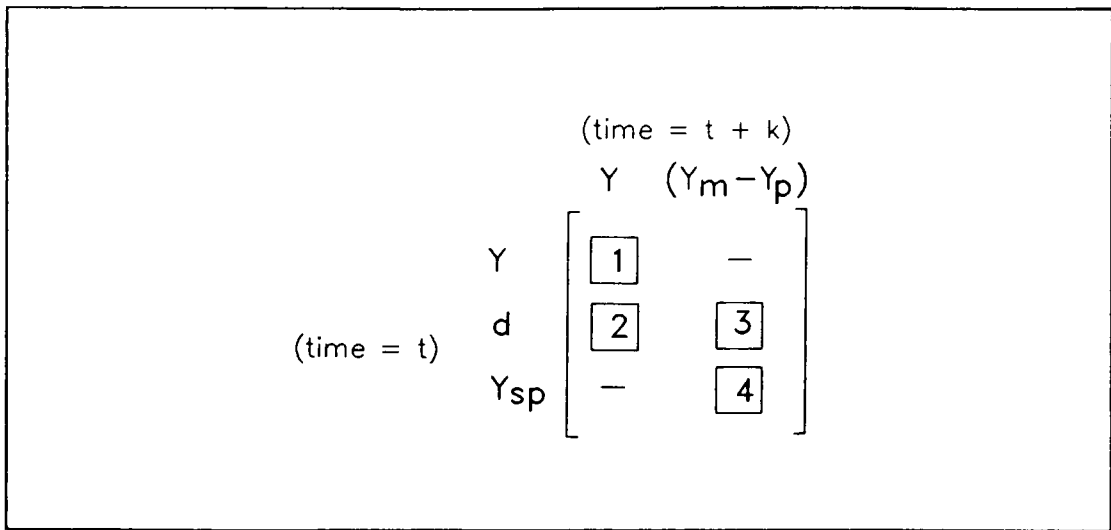


Figure 2.8 Feedforward-Feedback Control Correlation Matrix

box. Absence of significant correlation will be denoted by a blank box.

Depending on which matrix elements show significant correlation, as determined through the diagnoses explained previously, control system inadequacy can be distinguished. Element 1 represents the output autocorrelation. An "X" would be placed in this position if significant correlation existed between Y_t and Y_{t+k} beyond the process dead time. This then indicates that the feedback control deviates from minimum variance. The crosscorrelation from the measured disturbance, d_t , to the controlled variable, $(Y_m)_{t+k}$, is shown in element 2. An "X" in this position indicates poor feedforward control performance. Element 3 represents the crosscorrelation between d_t and $(Y_m - Y_p)_{t+k}$. An "X" would be placed in this box

if under feedback-only control this correlation was significant, suggesting an error in the disturbance model. Finally, element 4 shows the crosscorrelation between $(Y_{sp})_t$ and $(Y_m - Y_p)_{t+k}$. An "X" in this box results from non-zero correlation between the setpoint and future values of the prediction error and is indicative of an inadequate feedback model. The diagnostic matrix, therefore, provides a concise display of the control performance diagnosis information.

This matrix representation is helpful but may not be crucial in the analysis of this low dimension problem. It clearly simplifies the diagnosis in the multidimensional problems to be encountered in the MIMO examples. Matrix representation will be further developed in the MIMO section of this report, but the concepts follow directly from the previous examples.

Creation of the diagnostic matrix does not require the subjective visual evaluation of the auto and crosscorrelation plots. Overall statistics can be used to determine significance. [Box & Jenkins, 1976] An example of this is,

$$Q = n \sum_{k=j}^L r_{xy}^2(k) \quad (2.29)$$

where n is the number of data points. If the true values of the correlation function are zero, between values j and L , then Q is distributed as a Chi-squared distribution with $(L-j-1)$ degrees of freedom. This value of Q can then be compared with the upper $100(1-\alpha)\%$ critical value of the Chi-squared distribution, having the appropriate degrees of freedom. If Q exceeds this critical value then an "X" is placed in the diagnostic matrix. If the level of significance is chosen to be small, $\alpha=0.01$, then only relatively large deviations from the best achievable performance would be indicated in the matrix.

Multivariable Control

The calculation of the best achievable performance for SISO control problems was discussed in section 2.2.1. The extension of Harris' approach to calculating the bound on achievable performance, as given by the variance under minimum variance control conditions, is not directly applicable to the general MIMO control problem. A multivariable ARMA model is fit to the outputs of the process under the current control conditions, shown in Equation 2.30.

$$\Phi(z^{-1}) \underline{Y}_t = \underline{\Theta}(z^{-1}) \underline{a}_t \quad (2.30)$$

This can be expanded to,

$$\underline{Y}_t = \underline{a}_t + \underline{\psi}_1 \underline{a}_{t-1} + \underline{\psi}_2 \underline{a}_{t-2} + \dots + \underline{\psi}_f \underline{a}_{t-f} \quad (2.31)$$

The variance can then be calculated from,

$$\begin{aligned} \text{VAR}\{\underline{Y}\}_{MVC} = & \Sigma_a + \underline{\psi}_1 \Sigma_a \underline{\psi}_1^T + \underline{\psi}_2 \Sigma_a \underline{\psi}_2^T + \dots \\ & + \underline{\psi}_f \Sigma_a \underline{\psi}_f^T \end{aligned} \quad (2.32)$$

It is important to note that some of the values of the ψ 's are dependent upon the particular control scheme active at the time of data collection.

The simplest system to study has uncorrelated disturbances and minimum dead times which appear on the diagonal. This latter condition can also be satisfied if the rows or columns of the matrix can be rearranged such that the minimum dead times appear on the diagonal. Complexities such as correlated disturbances, which are more common in industrial settings, and dead time imbalances establish the capabilities and limitations of this diagnostic procedure. Finally, sparsity introduced in the system matrix demonstrates the analysis simplifications which can be attained.

As the diagnosis technique is based on correlation analysis, having independent or uncorrelated disturbances is

an important simplification. As the disturbances affecting the controlled variables become correlated the moves implemented by the controller and any modelling errors incurred will themselves become highly correlated, adversely affecting the analysis. As will be shown in the illustrative examples in Chapter 4, correlated disturbances introduce added complexity to the diagnosis and as such the conclusions drawn from the analysis are not as specific.

In the case in which the minimum dead times appear on the diagonal it is obvious that the minimum dead time for each output variable, which corresponds to perfect control conditions, is this diagonal value. Once the dead times are imbalanced the minimum realizable dead time for each controlled variable becomes unclear and accurate performance evaluation is adversely affected. Any well tuned controller can reduce the correlations to zero between the lower and upper limits as given by the theoretical settling times of the process. The lower limit for each output is obtained if all the emphasis is placed on that output alone. The upper limit is given by the minimum settling time for a dynamically decoupled system. [Holt & Morari, 1985] The actual achievable performance under minimum variance control must lie between these upper and lower limits.

The MIMO cases studied can be divided into two

distinct groups according to the transfer function dead times. Each one experiences a different level of success using this evaluation and diagnostic procedure. The first group can be classified as having minimum dead times on the diagonal and is the simplest to address. Conversely, the second group does not have minimum dead times appearing on the diagonal. In the case of the former, if the diagonal elements of the transfer function not only have the minimum dead time but all other row elements have greater dead times, then an extension of the SISO minimum achievable variance calculations is possible.

Let us consider a 2x2 example with independent disturbances for which the minimum dead time for Y_1 is f_1 , which corresponds to u_1 , while a greater f_2 corresponds to u_2 . The following relationship can be written,

$$\begin{aligned}
 Y_{1t} = & a_t + \psi_{1_1} a_{1_{t-1}} + \dots + \psi_{1_{f_1}} a_{1_{t-f_1}} + \psi_{1_{f_1+1}} a_{1_{t-(f_1+1)}} + \dots \\
 & + \psi_{1_{f_1+f_2}} a_{1_{t-(f_1+f_2)}} + \dots
 \end{aligned}
 \tag{2.33}$$

It is important to note that the same holds for Y_2 but will not be presented here. Similar to the SISO case nothing can affect the first f_1 terms in Equation 2.33. Under minimum variance control conditions, however, all remaining terms will be eliminated by input u_1 . Since input u_2 will have had no effect until f_2 , the first f_1 ψ terms are unaffected by both u_1 and u_2 . Therefore, the problem reduces to that of the SISO

example, whose disturbance includes the other controller, and the minimum variance for Y_1 can be calculated from,

$$\text{VAR}\{Y_1\}_{MVC} = (1 + \psi_1^2 + \psi_2^2 + \dots + \psi_{f_1}^2) \sigma_a^2 \quad (2.34)$$

If the minimum dead times do not appear on the diagonal, however, a best achievable performance reference cannot be generated using the techniques established in this research.

As introduced already, the representation of this correlation information is a very important aspect of the analysis. In MIMO systems which deal with many inputs, outputs and disturbances it may be difficult to interpret the cumbersome correlation results and thus to locate the area of difficulty. In order to facilitate this process of deduction a simple, visual means of representing the information is provided. The correlation matrix representation introduced in the feedforward-feedback analysis proves extremely useful in the more complicated MIMO examples. The correlation matrix used for the performance diagnosis is shown in Figure 2.9. Once again, the rows and columns represent the variables at times "t" and "t+k", respectively, and elements of interest are indicated with a box. For display purposes in this document an "X" placed in one of the correlation matrix elements will denote significant correlation between the

		(time = t + k)			
		Y_1	Y_2	∇ER_1	∇ER_2
(time = t)	Y_1	1	—	—	—
	Y_2	—	2	—	—
	u_1	3	4	—	—
	u_2	5	6	—	—
	Y_{sp_1}	—	—	7	8
	Y_{sp_2}	—	—	9	10

Figure 2.9 MIMO Performance Diagnosis Correlation Matrix

variables appearing on the matrix axes, while blank elements indicate absence of correlation.

Elements 1 and 2 show the autocorrelations for the two controlled variables, 3 through 6 represent the crosscorrelations between the inputs and the controlled variables and lastly, elements 7 to 10 show the crosscorrelations from the controlled variable setpoint changes to the model prediction errors. In the case of perfect LQG control for the balanced dead time case, with equal output weighting and no input penalties, the correlation matrix would only show significant correlation in the controlled variable autocorrelations up until their respective dead times. Following the diagnostic procedure already

outlined in the SISO examples, significant output autocorrelation and significant crosscorrelation between the inputs and the outputs beyond the minimum process dead time indicate non-optimal control performance. Finally, the crosscorrelations between the setpoint changes and the model prediction errors provide information on the accuracy of the process models.

The MIMO cases presented in Chapter 4 will demonstrate some of the limitations of this performance evaluation and diagnosis methodology, encountered specifically in the presence of correlated disturbances and imbalanced dead times. In the simplest case of independent disturbances and minimum dead times appearing on the diagonal, the methodology is a direct extension of the SISO case and is virtually as specific in its diagnostics. The control performance can be tested against optimal behaviour, the best achievable control can be evaluated and problems within the control scheme can be attributed to one or more of the inputs or outputs. The diagnosis becomes more complex and less resolute, however, in the presence of correlated disturbances and imbalanced dead times. All of these concepts will be treated in greater detail in Chapter 4.

2.3 SUMMARY

The development of this analysis tool demonstrating its success and limitations will be shown in the many examples to follow commencing with the simple pure feedback SISO scheme, an extension to a feedforward-feedback strategy and ending with a MIMO control scheme. These examples will demonstrate the use of this diagnostic tool, following the analyses discussed in this chapter, as they pertain to the system being examined and indicate the conclusions which can be drawn. Both simulation results and industrial case studies will be presented for various control schemes which will address the many aspects of the diagnostic procedure.

In the examples to follow it will be assumed that the initial monitoring phase has been completed and the performance is deemed unsatisfactory. If we refer to the hierarchy displayed in Figure 2.2 further evaluation and diagnosis is required at this stage. The initial step is to generate the controlled variable autocorrelation which tests for the existence of optimal control. If near optimal control is present the evaluation diagnostic procedure is halted. At this point the structure of the process or the control algorithm must be examined. If the best achievable control is not being realized then an estimate of the best achievable performance is generated, and the actual performance is

compared against it. If a sufficient difference exists between the two and the improvement in performance is desired then further diagnosis is required to establish the source of control inadequacy. Diagnosis of inadequate performance will then proceed as discussed in the previous sections, specific to the type of control scheme being examined. Conclusions can then be drawn according to the results of this correlation analysis.

During the course of this research various limitations of the procedure have been established. Some of these have been introduced in the previous section, according to the control scheme being examined, and will be discussed in greater detail as they are encountered in specific examples. In some cases additional analyses, such as spectral analysis, could provide needed information but in the attempt of simplicity these steps have not been included in the method. In its present form this diagnostic tool provides the user with useful information for establishing the presence of a problem and in deducing the likely source. As the technology is developed and automated, further analyses could be added. Presently, the key concern in developing this methodology is in keeping it quicker and simpler to use than recommencing the control design procedure. In some cases, however, process reidentification and controller redesign are inevitable if improvements are desired.

Presently, this is an interactive procedure requiring the direct involvement of qualified personnel. Ultimately, the process could be automated as the technology is developed. This automatization could take the form of an on-line expert system to initially screen the control schemes in the monitoring phase and then to analyze only those showing unsatisfactory performance in the diagnosis phase. An appropriate rule base could be structured to convey the results or recommendations of the analysis. The personnel in question can then review these results and decide whether adequate incentive for improvement exists.

Various software was used in the course of this research. The MIDSA™ [Taylor, 1990] software package was used to simulate the feedback-only process under open and closed loop operation, and was used to analyze the process performance of all the simulation and industrial cases examined. The Smith Predictor and Feedforward-Feedback simulation cases were simulated in a spreadsheet environment. [Stanfelj, 1990] The power spectrum plots shown for the paper mill data were generated using the TIMESLAB™ time series and identification software package. [Newton, 1988] The LQG controllers designed for the simulated MIMO 2x2 case study were generated using the LQDESIGN software package. [Kozub, Swanson & Wong] The closed loop system was then simulated in a general fortran program. [Stanfelj, 1990]

3.0 SISO CONTROL SYSTEMS

The first phase of research focussed on Single-Input-Single-Output (SISO) processes. These schemes are important as they are most prevalent in industrial practice and therefore should be well understood. Moreover, they are the simplest schemes to study and once the methodology is proven successful in these applications the results will provide a knowledge base for the more complex schemes examined in later sections. This section covers the initial feedback-only and combined feedforward-feedback simulation studies. In the case of the former a model based feedback controller was also examined. The analysis methodology and simulation results were then tested and confirmed in a series of industrial examples from both the pulp and paper and petrochemical industries.

3.1 FEEDBACK CONTROL

A simulation study was initially performed on a SISO process with a feedback-only control system. The process is represented by the following transfer function,

$$Y(z) = \frac{0.2 z^{-3}}{1 - 0.8 z^{-1}} * u(z) + \frac{1}{(1 - 0.8 z^{-1}) \nabla} * a_t \quad (3.1)$$

with the variance of a_t , σ_a^2 , equal to 0.001. It is important to note the nonstationarity introduced to the process as a result of the nonstationary disturbance model. The underlying continuous process is represented by the following,

$$Y(s) = \frac{e^{-2s}}{s + 1} * u(s) \quad (3.2)$$

with a sampling period of one unit. A block diagram of the system is shown in Figure 3.1.

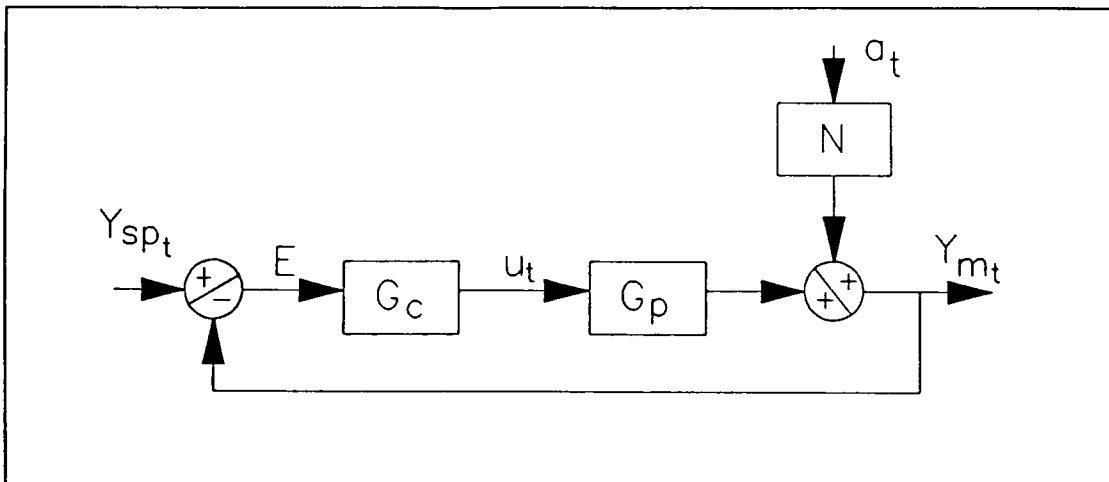


Figure 3.1 SISO Feedback-Only Block Diagram

The open loop response for this process is shown in Figure 3.2a. It is important to note that the only input is the white noise specified in the process model. The estimated autocorrelations are displayed in Figure 3.2b. Because of the

nonstationarity of the disturbance model the autocorrelations do not decrease rapidly but are maintained for a long period of time. The power spectrum for this open loop process is shown in Figure 3.2c. The power spectrum for this case is very large at low frequencies and reduces rapidly at increasing frequency. This is again characteristic of a slowly drifting, nonstationary disturbance model which was used in this example.

Therefore, the initial step of testing for optimal control has shown that there are many large correlations beyond the dead time of the process. An ARMA model, (refer to Appendix A), was then fit to the time series data to yield the following relationship,

$$Y_t \approx \frac{1}{(1 - 0.769 z^{-1})(1 - z^{-1})} * a_t \quad (3.3)$$

with a variance of 0.00101 for a_t . Long division of the above transfer function yields,

$$Y_t \approx (1 + 1.769 z^{-1} + 2.306 z^{-2} + \dots) a_t \quad (3.4)$$

Because the process is nonstationary the coefficients in Equation 3.4 are increasing, indicating an infinite variance for the nonstationary process. Given the sample set for this example, having a dead time of two units and the given noise

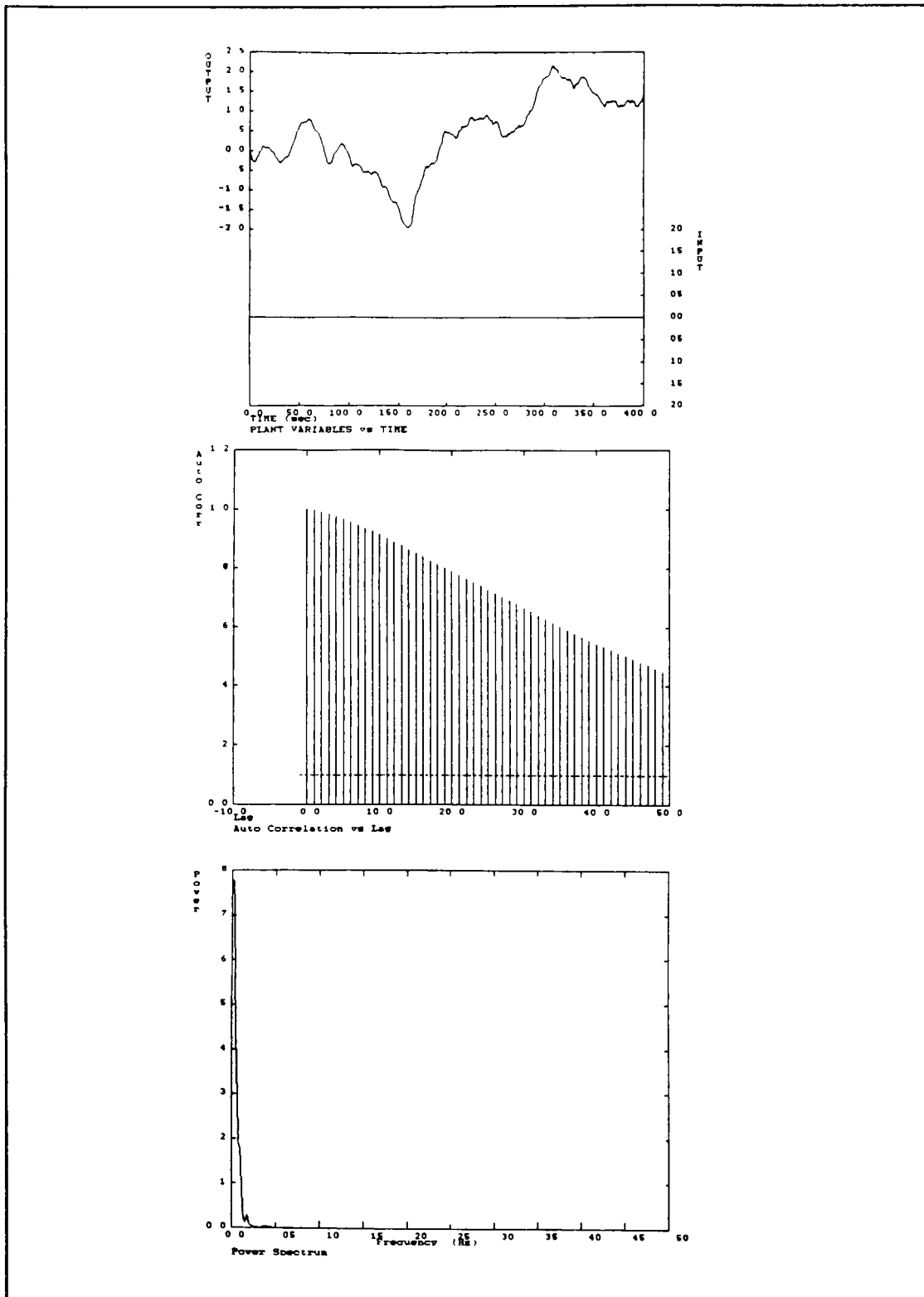


Figure 3.2(a,b,c) SISO Feedback-only, Uncontrolled Case

variance the estimated best achievable performance is derived from,

$$\begin{aligned} \text{VAR}\{Y_t\}_{MVC} &= (1^2 + 1.769^2 + 2.360^2) * 0.00101 \\ &= 0.0098 \end{aligned} \quad (3.5)$$

This minimum variance prediction of 0.0098 units shows that great improvement can be achieved over the uncontrolled case which produced a variance of 0.871 units. These results indicate that control should be implemented in this system.

A minimum variance controller, MVC, was designed for the given process model, and the system was simulated. All calculations and equations are included in Appendix B. Figure 3.3 shows the process response, autocorrelation and power spectrum for the process under MVC. The output response is now stationary as a result of the integral action of the controller.

If we refer to the autocorrelation plot we observe the rapid decrease of the autocorrelations which confirms the stationarity of the controlled process. The autocorrelations beyond lag two, which is the true process dead time, are effectively zero since they are within the confidence intervals. Hence, the presence of an MVC is confirmed as all autocorrelations beyond the dead time have been eliminated.

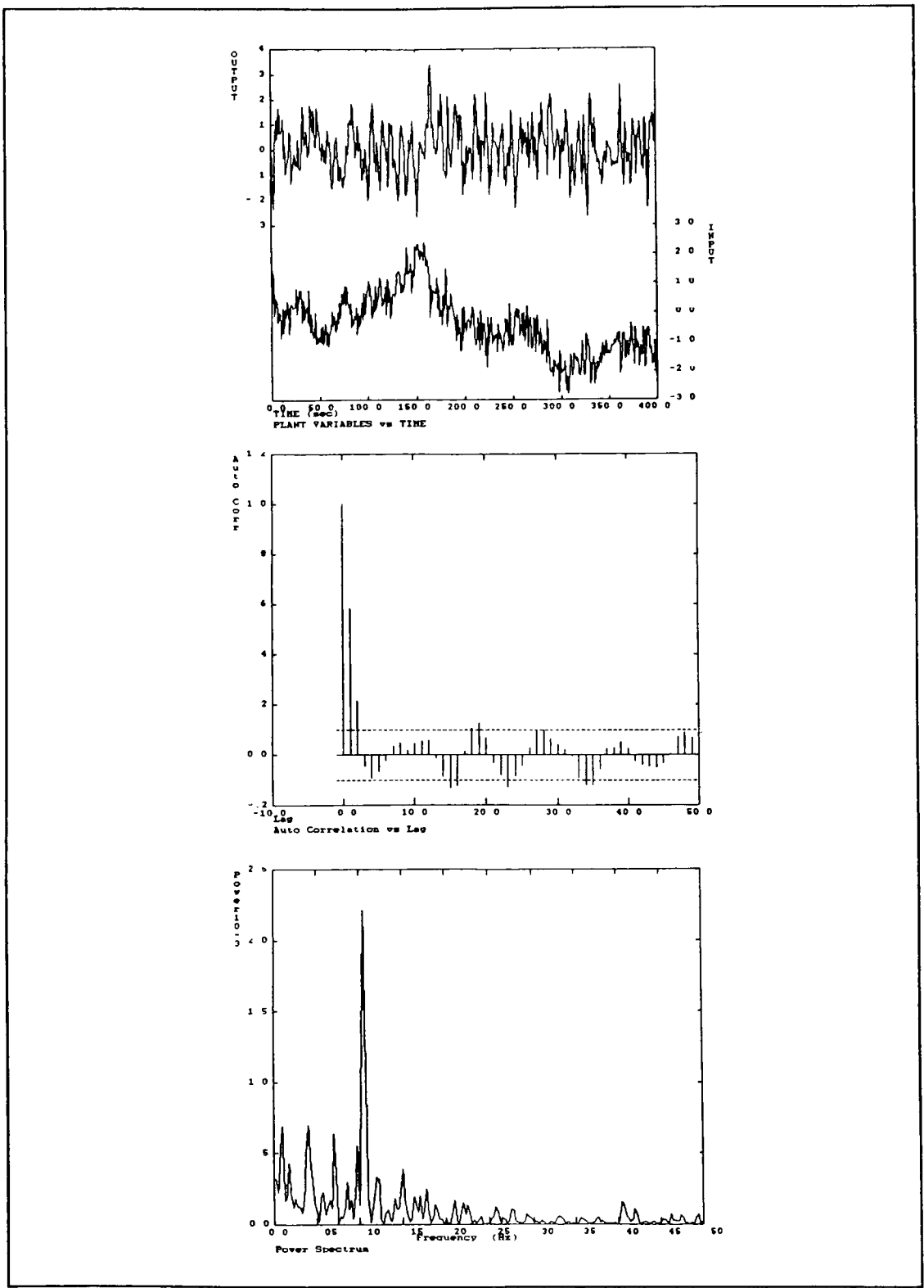


Figure 3.3(a,b,c) SISO Feedback-only, MVC Case

As would be expected the actual MVC variance of 0.0099 compares well with the predicted minimum of 0.0098, confirming the presence of optimal control. Any differences experienced between the theoretical and actual results can be partially attributed to the finite simulation period. This control scheme has reduced the output variance from 0.871 to 0.0099 but has resulted in a highly oscillatory input response, which may not be desirable.

The power spectrum for this process is displayed in Figure 3.3c. A substantial reduction in the power spectrum at low frequency levels has also been achieved as compared with the open loop simulation. A more equal distribution of power over the entire frequency range has been attained, which is characteristic of a process under minimum variance control.

In this particular example the presence of minimum variance control has reduced the process to a moving average of order 2, $MA(2)$, as a result of the two periods of delay in the process model. As discussed in section 2.2.1 a minimum variance controller may require harsh manipulations of the input variable and often lacks robustness to modelling errors. To reduce the effect of these undesirable characteristics several other controllers were designed and the closed loop process was simulated. These include a constrained minimum variance controller (CMVC, $\lambda=1.0$), with a penalty imposed on

the input manipulations, a PI controller designed to minimize the integral of absolute error (IAE) and a Dahlin algorithm with several values of the closed-loop time constant (λ). All controller calculations are included in Appendix B. The results obtained with these three controllers are similar, thus, only the CMVC case will be discussed in detail.

Figure 3.4 exhibits the simulation results using the constrained MVC. The closed-loop output response remains stationary using this controller while the input manipulations are now considerably smoother. The autocorrelation plot once again decreases rapidly with those lags beyond five effectively being reduced to zero. Because the controller being used is a constrained MVC and therefore not "perfect", there are still some significant autocorrelations beyond the process dead time of two time intervals. Therefore, the autocorrelation plot demonstrates that minimum variance control has not been realized and thus improvement can be achieved if it is desired. The power spectrum reflects these results in that the power at low frequencies has been greatly reduced from the open loop case but is slightly higher than in the MVC simulation. The estimate of the best achievable control performance, MVC, indicates that a 68% reduction in the output variance can be achieved with tighter control. A decision must therefore be made whether this decrease in output variance is desired and warrants the large increase in

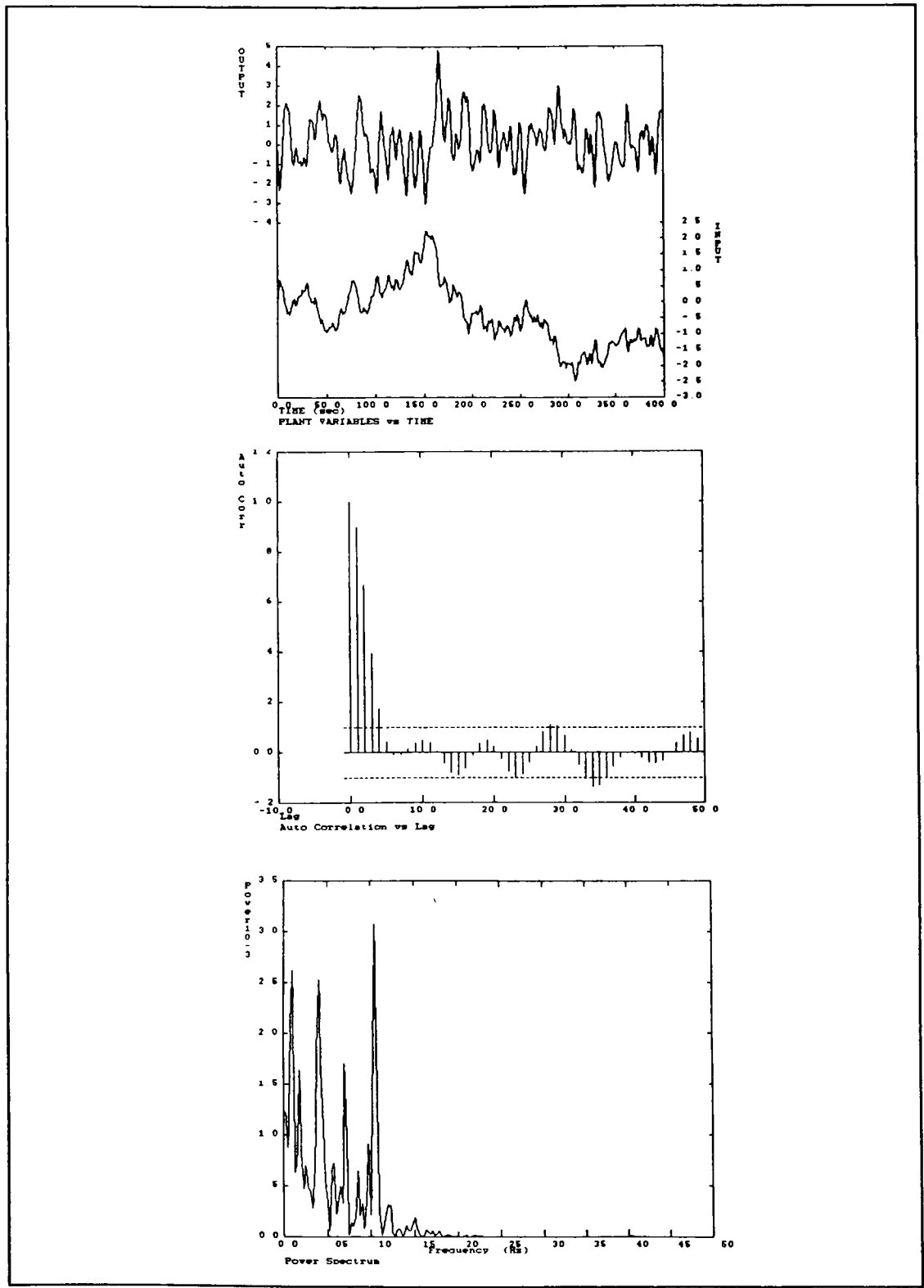


Figure 3.4(a,b,c) SISO Feedback-only, CMVC Case

input requirements.

Although it is evident that the system is not under theoretically optimal control the performance of the implemented controller may be satisfactory. Comparison of the output variance between the MVC and CMVC cases shows only a moderate difference in the variance which is accompanied by harsh input manipulations. Whether this improvement is desired must be decided by qualified personnel using process knowledge.

Model Mismatch

The analysis methodology was then tested in model mismatch cases. It is of interest to investigate whether this evaluation and diagnostic technique is successful in identifying modelling errors. In all model mismatch simulations of the process under minimum variance control the process became unstable. This verifies earlier claims that the minimum variance controller often lacks robustness to modelling errors, and hence finds limited use in industrial applications.

The model mismatch simulations performed on the process with more robust controllers, including the CMVC, PI

and Dahlin remained stable. Once again only the results for the CMVC case will be discussed. Refer to Appendix B for all calculations. With the controller tuned to the base case model a 50% increase in process gain was made on the plant, G_p . The results are displayed in Figure 3.5. Due to this particular mismatch the output response became more oscillatory and the input actions more aggressive compared with the true model responses shown in Figure 3.4. The output autocorrelations and power spectrum are plotted in Figures 3.5b and 3.5c respectively. The autocorrelation function displays significant oscillatory behaviour with an approximate period of ten sampling intervals, which can be attributed to the mismatch. Model mismatch is also apparent from observation of the power spectrum which shows a large peak at 0.1 Hz, corresponding to these oscillations. It is apparent that the output autocorrelations and power spectrum plots indicate definitively a deviation from minimum variance control.

Figure 3.6 shows the simulation results for the process under constrained minimum variance control with model mismatch occurring as a 50% decrease in the process gain. This particular mismatch results in a detuned controller. Similar to the open loop case, the autocorrelation does not damp out quickly and the power spectrum shows high power content at low frequency. Therefore, it is evident from the

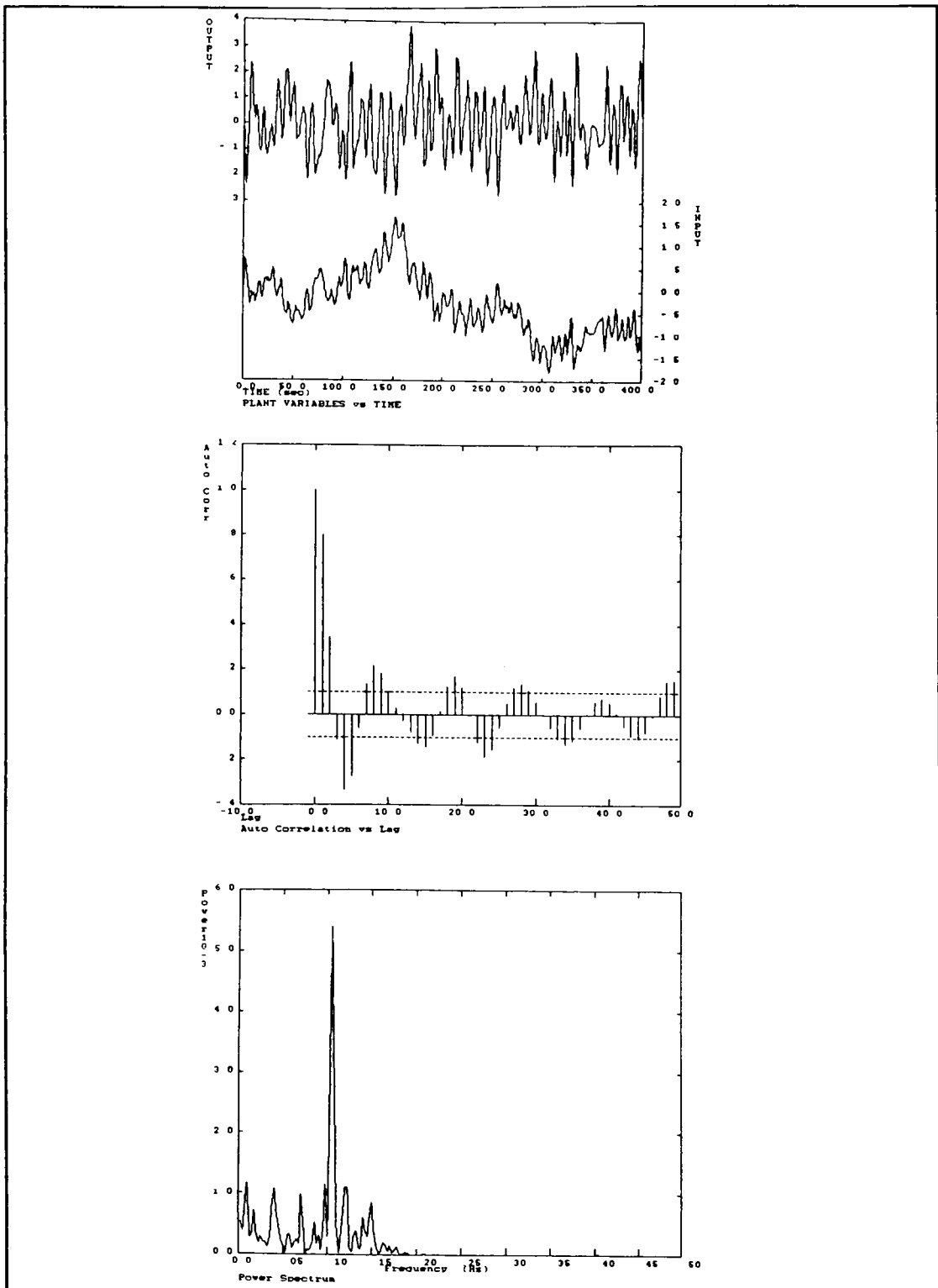


Figure 3.5(a,b,c) SISO Feedback-only, Model Mismatch Example, Increased K

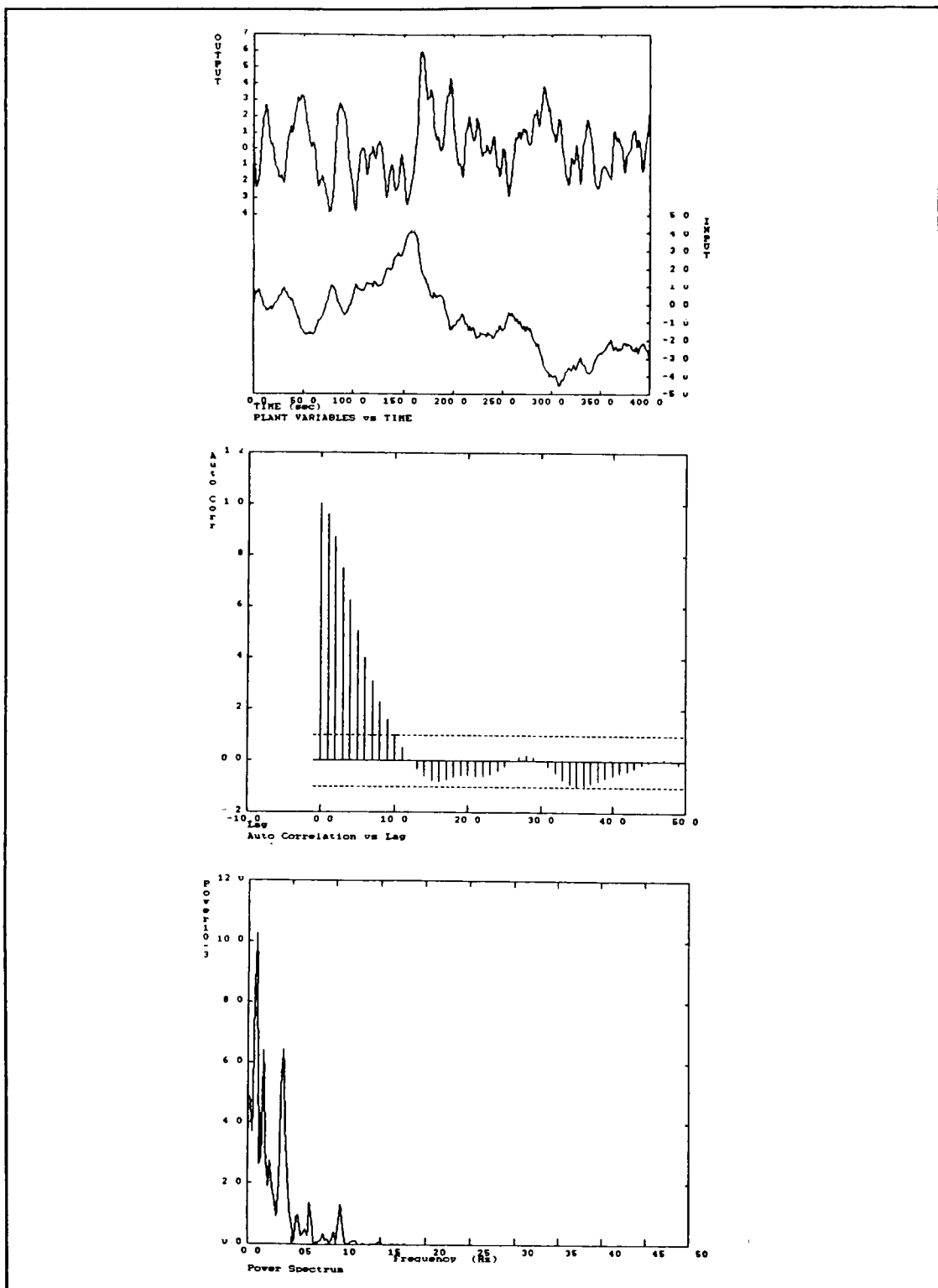


Figure 3.6(a,b,c) SISO Feedback-only, Model Mismatch Example, Decreased K

autocorrelation and power spectrum of the controlled variable that the controller is not aggressive enough resulting in a sluggish process response.

Thus far it has been established that poor control performance resulting from an overtuned or a detuned controller can be diagnosed. The former can be identified by oscillations in the autocorrelation plot and a corresponding peak in the power spectrum while the latter system shows a slowly damping autocorrelation and a power spectrum with high power at low frequency. Additional analyses will be required to differentiate between tuning and modelling errors.

3.1.1 MODEL-BASED FEEDBACK CONTROL

To further investigate the effects of model mismatch on controller diagnosis a simulation study of a model-based feedback control scheme was performed. A block diagram of the system is given in Figure 3.7 showing the Smith Predictor control structure. [Smith, 1957]

As discussed in Chapter 2 the quantity $(Y_m - Y_p)_t$, which is the difference between the actual and the predicted output, will be used to distinguish between tuning and modelling errors. The following examples will demonstrate the use of

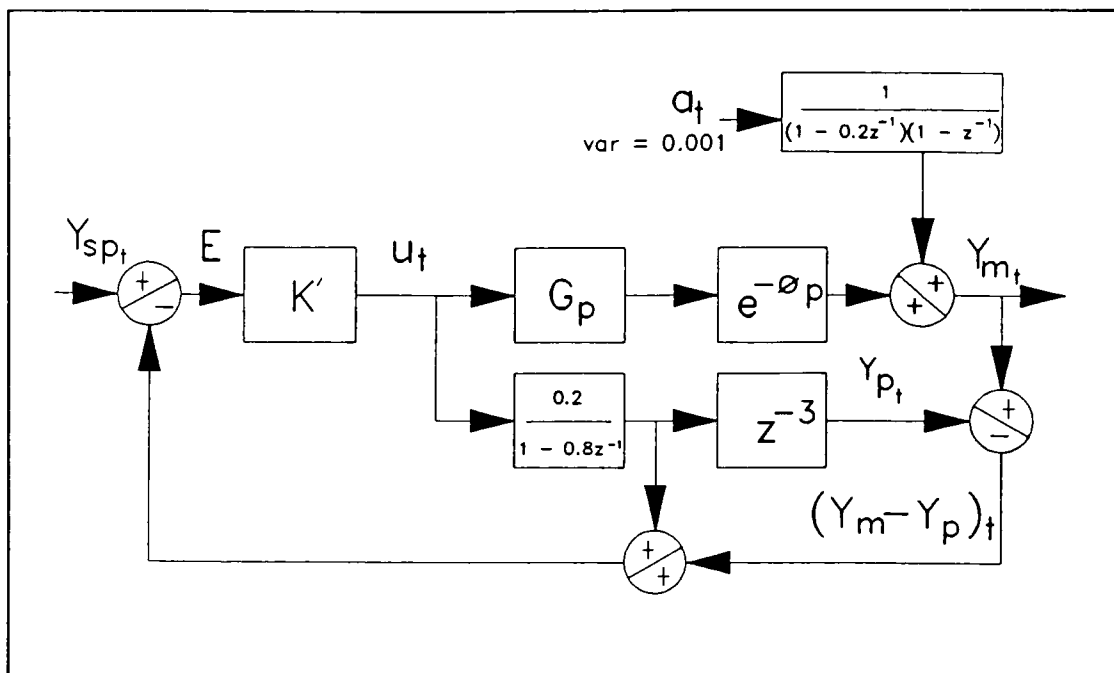


Figure 3.7 Smith Predictor Block Diagram

this quantity.

A base case was established for this system assuming a perfect process model and a minimum variance controller. The process response and correlation data are shown in Figure 3.8. The output autocorrelation is eliminated after the true process dead time of two periods, as is the crosscorrelation between the differenced input and the output, all of which is indicative of an MVC scheme. Moreover, the prediction for the theoretically minimum output variance of 0.00386, given the existing noise and disturbance conditions, agrees fairly well with the actual output variance of 0.00453. Much of the deviation can be attributed to the relatively small data

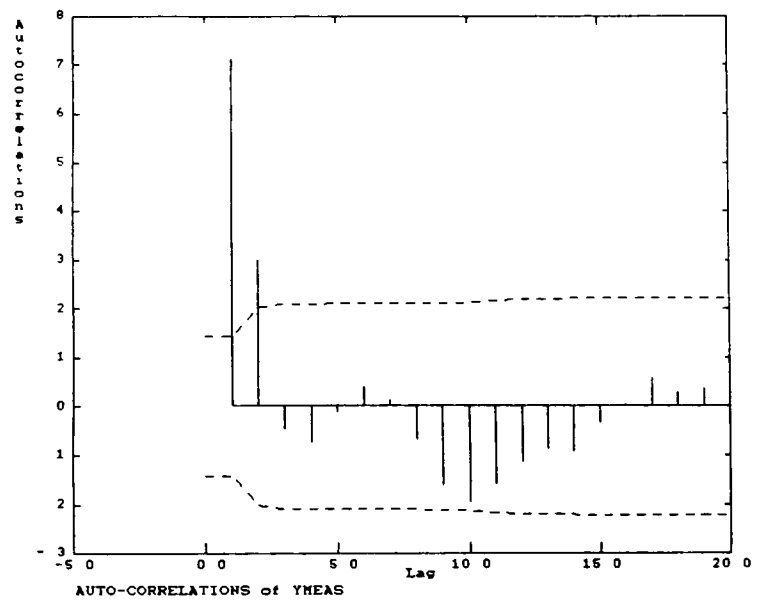
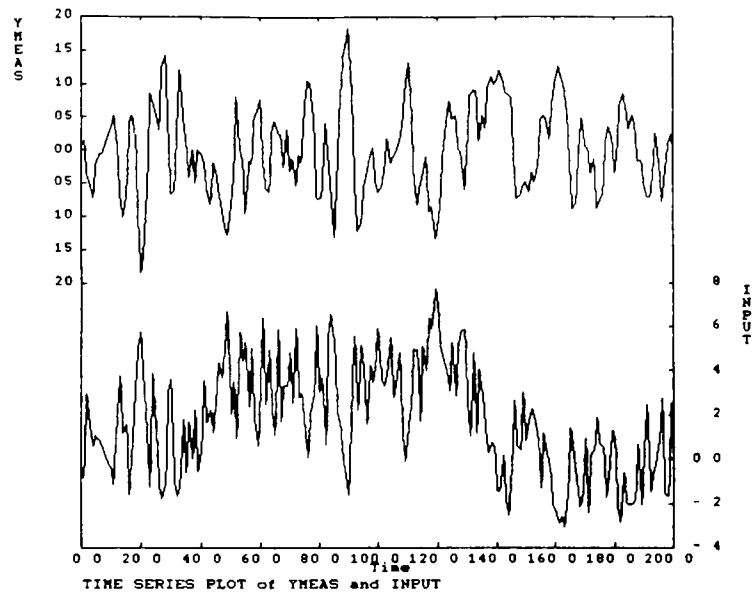


Figure 3.8(a,b) Smith Predictor (MVC), Base Case

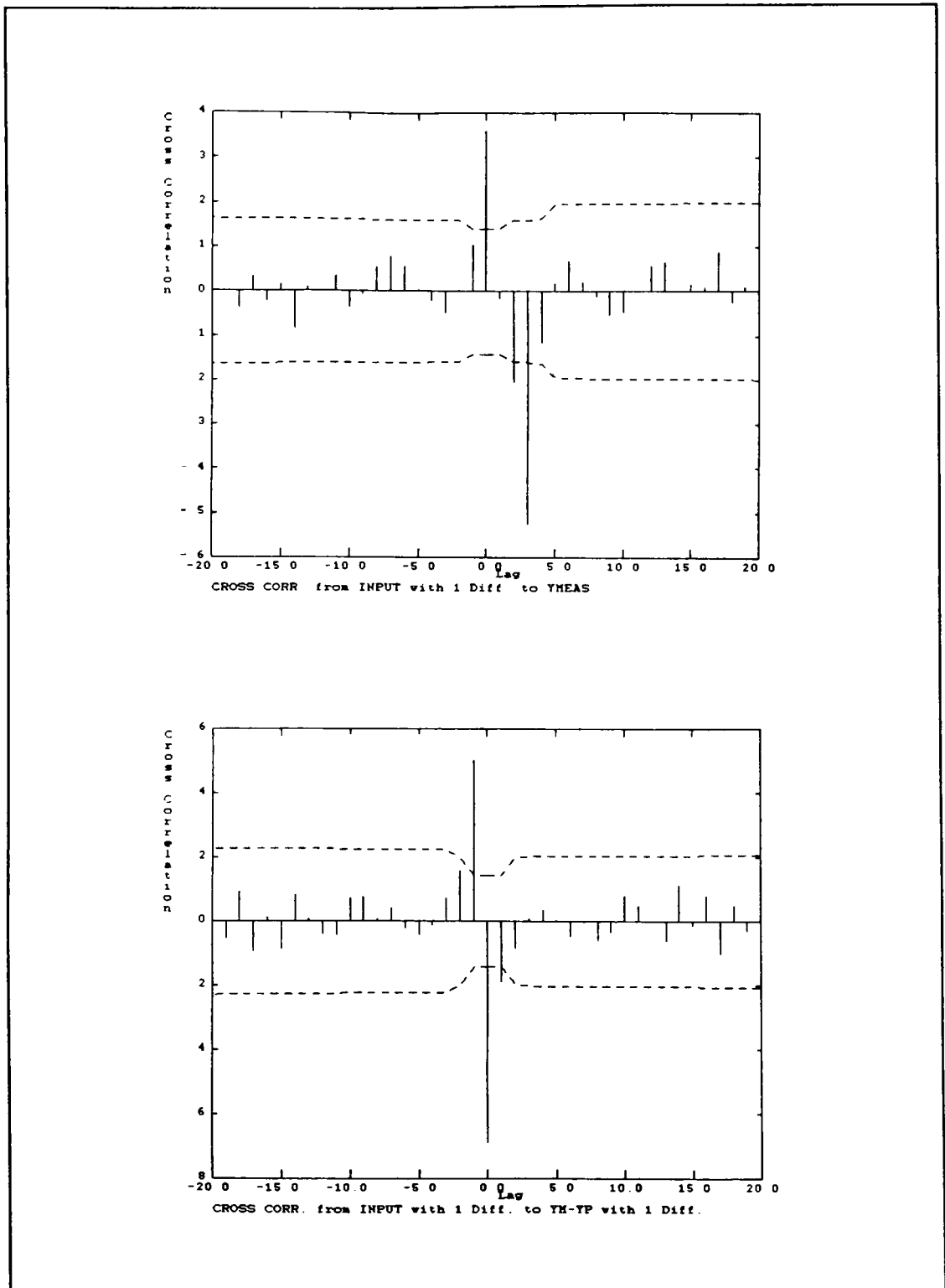


Figure 3.8(c,d) Smith Predictor (MVC), Base Case

sample consisting of 200 points. Averaging the results of several simulation cases resulted in an actual output variance of 0.00401 which differs by only 14% from the theoretical minimum value. All calculations are included in Appendix C. The crosscorrelation plot between the differenced input and the differenced prediction error shows an absence of significant correlation for positive lags. This implies that the present input has no effect on values of the future prediction error, hence the model is assumed to be correct. Therefore, upon examination of this correlation data it is possible to deduce that this controller is performing optimally.

Additional simulation cases were performed to further test the success of the diagnostic method. In order to verify the ability to distinguish between tuning and model error, cases of each were simulated and analyzed.

Figure 3.9 shows the results for a detuned controller based on a correct model. In this case a PI controller is used, given in Appendix C, designed using the Integral of Absolute Error (IAE) technique. The output autocorrelation and the crosscorrelation between the differenced input and the output show significant values beyond that of the true process dead time. The correlation plot of the differenced input to

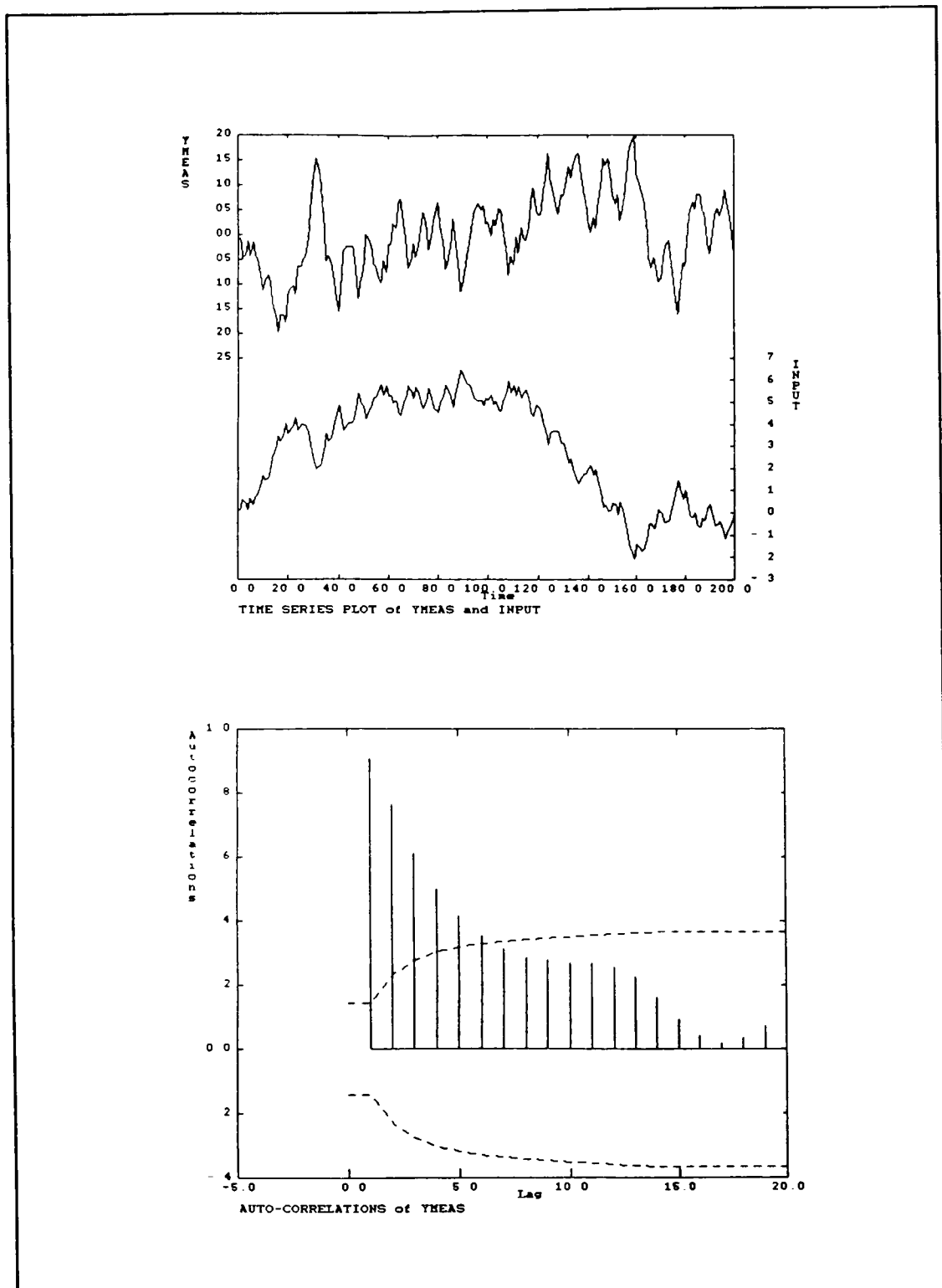


Figure 3.9(a,b) Smith Predictor (PI), Detuned Example

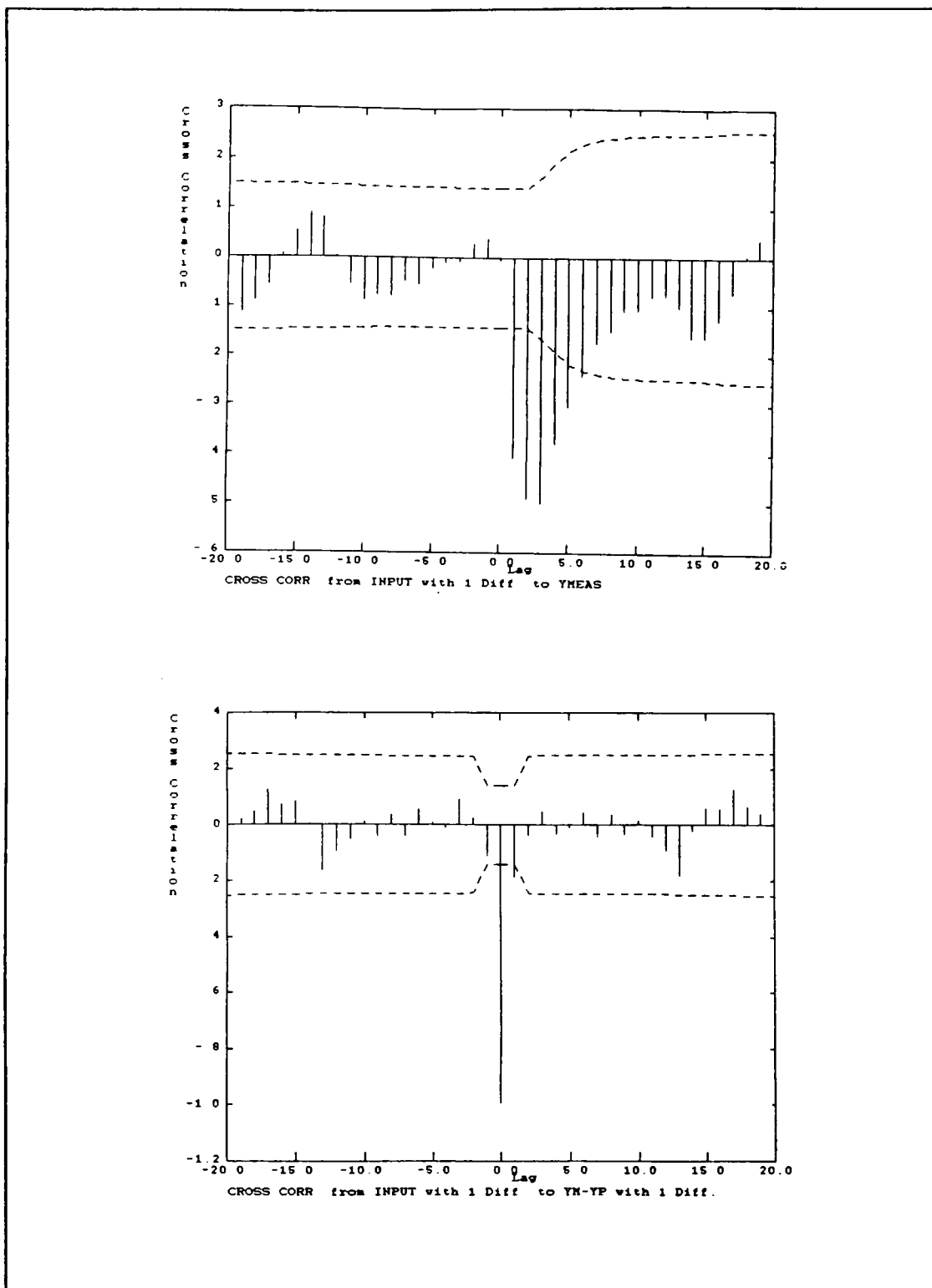


Figure 3.9(c,d) Smith Predictor (PI), Detuned Example

the differenced prediction term, $(Y_m - Y_p)_t$, however, does not show any correlation. This implies, therefore, that there is no model mismatch in the system and that non-optimal performance is the result of poor tuning.

Figure 3.10 shows the results of a minimum variance controller applied to an incorrect model. The mismatch occurs as a reduction of 50% in the actual process gain. Similar to Figure 3.9, the output autocorrelation and the cross correlation from the input to the output show significance beyond the dead time of the process. Unlike the detuned control case, however, this example shows significant correlation between the input and the prediction error. As described in Chapter 2, this significant correlation suggests model mismatch but is not necessarily conclusive. The significant correlation can be the result of model error or correlated noise. Model accuracy can only be unequivocally determined from data with controlled variable setpoint perturbations. Thus additional data, shown in Figure 3.11, was obtained. Similar to the results in Figure 3.10, the output autocorrelation and the crosscorrelation from the input to the prediction error show significant correlation. The presence of model error becomes conclusive in Figure 3.11d where significant correlation between $(Y_{sp})_t$ and $(Y_m - Y_p)_{t+k}$ is observed. Since model error exists, no evaluation of controller tuning can be made.

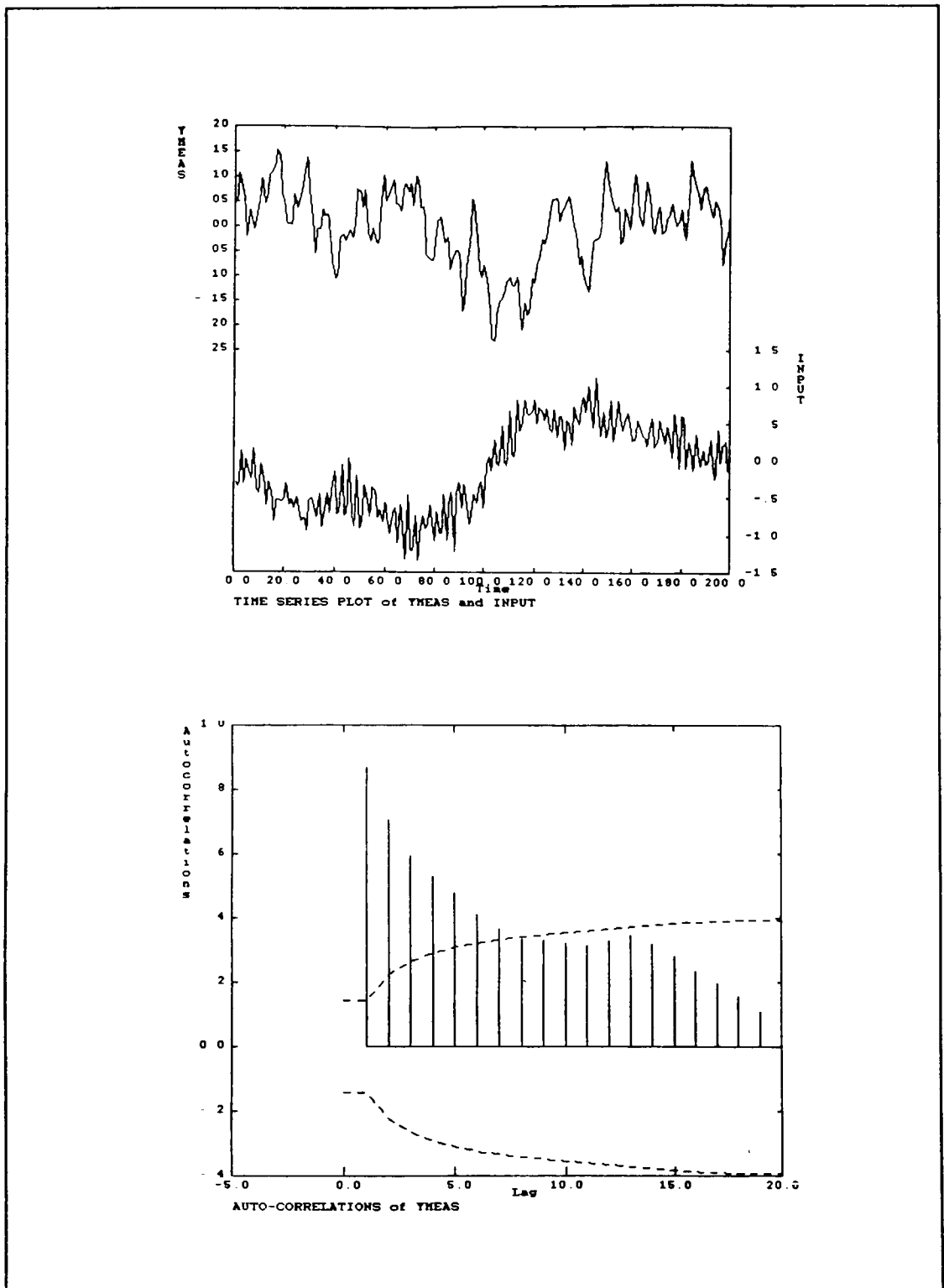


Figure 3.10(a,b) Smith Predictor (MVC), Model Mismatch Example

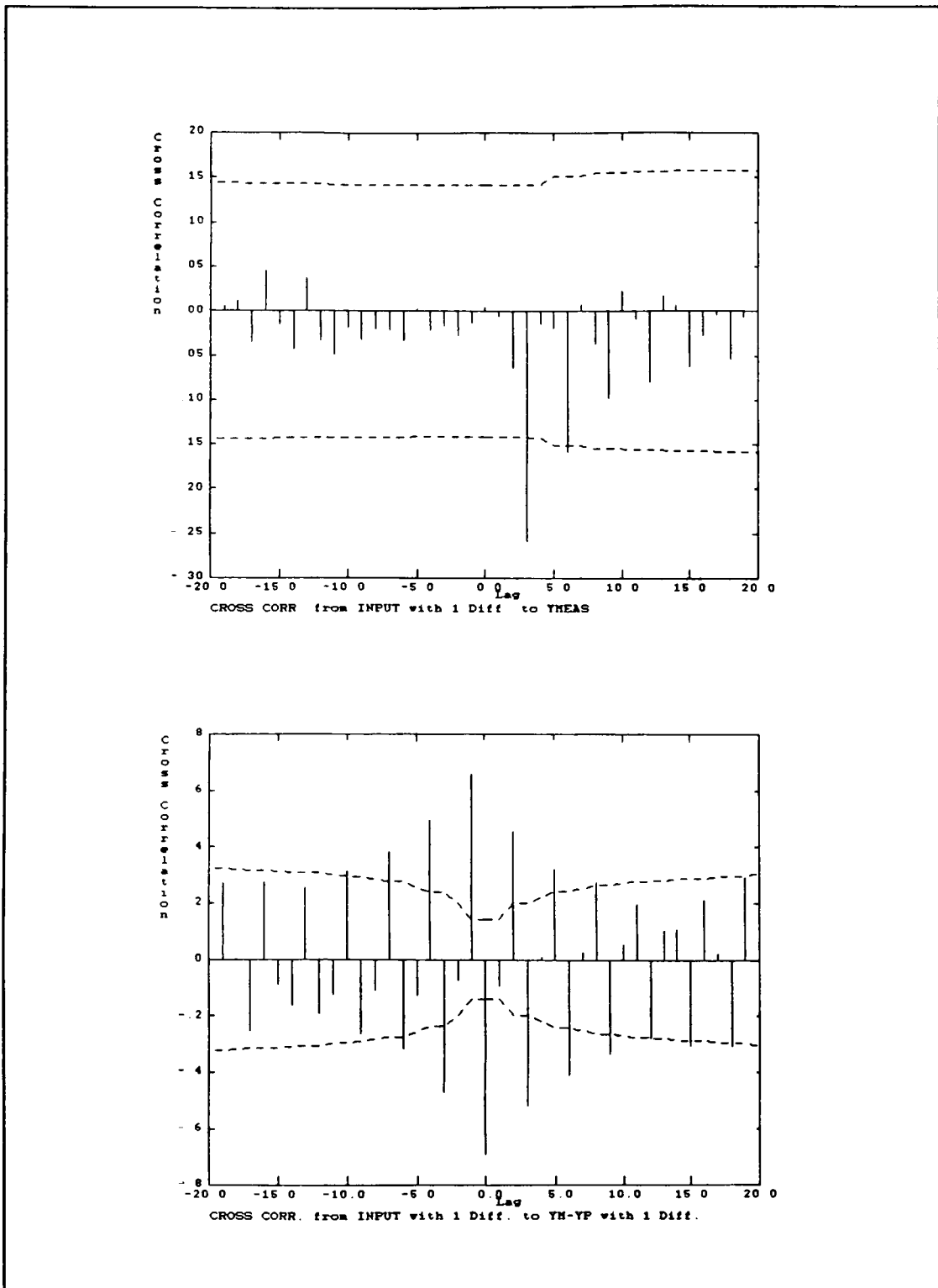


Figure 3.10(c,d) Smith Predictor (MVC), Model Mismatch Example

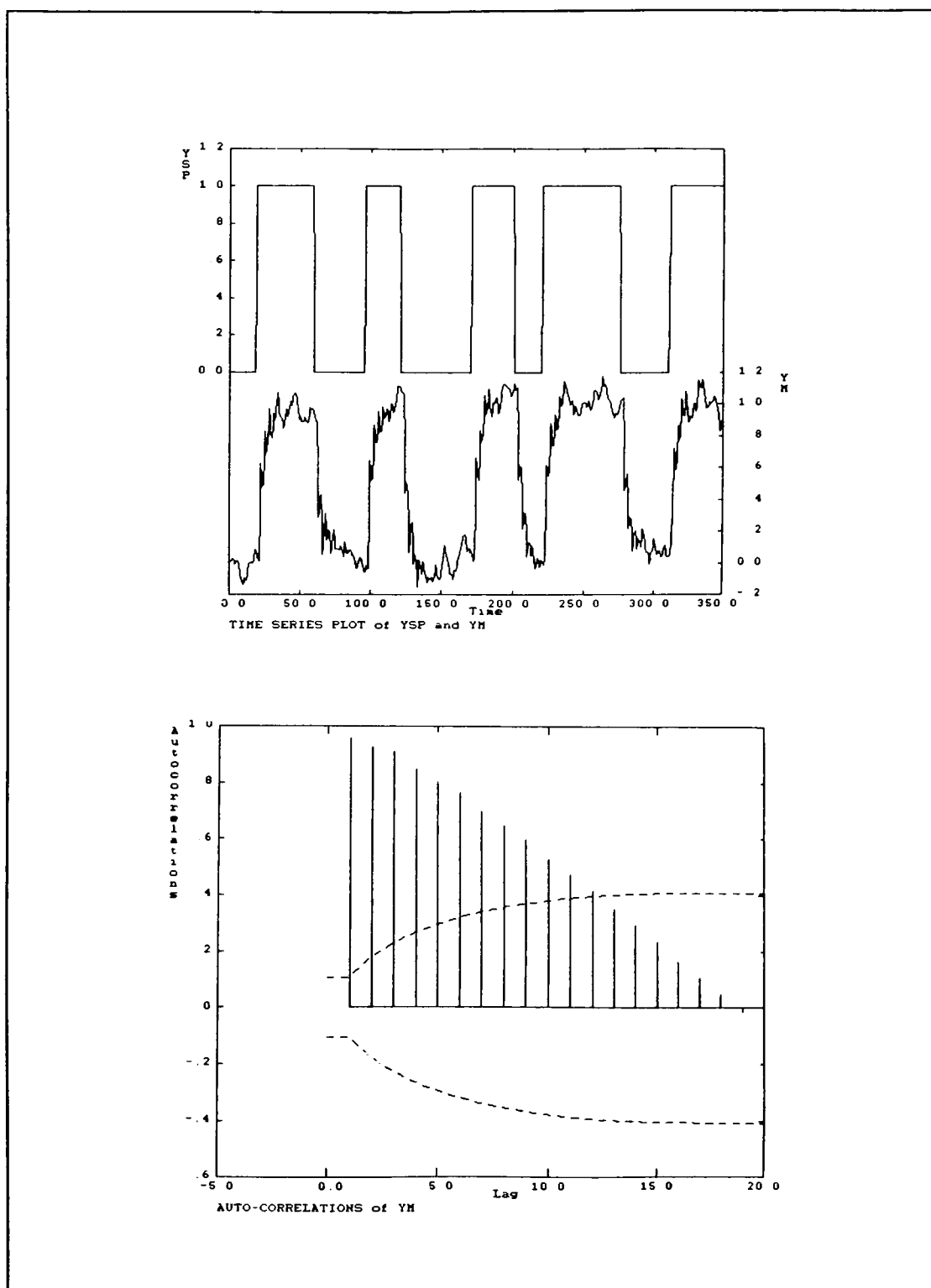


Figure 3.11(a,b) Smith Predictor (MVC), Model Mismatch Example (Setpoint Changes)

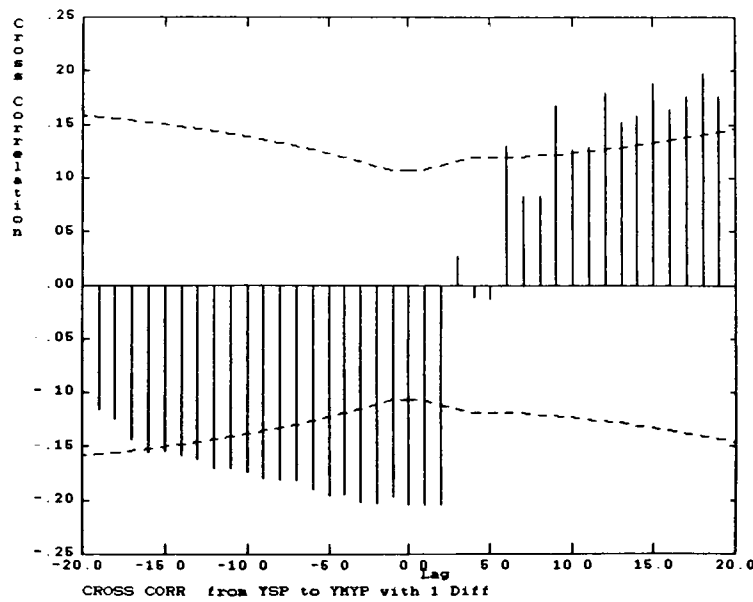
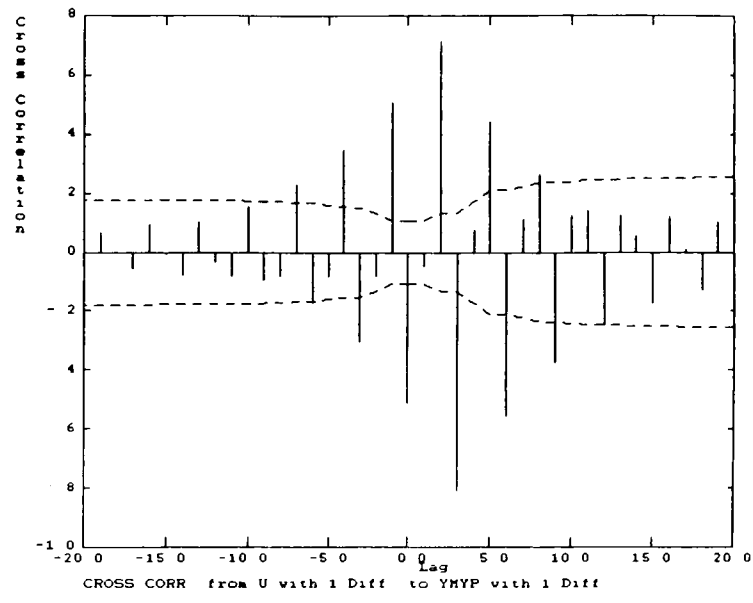


Figure 3.11(c,d) Smith Predictor (MVC), Model Mismatch Example (Setpoint Changes)

These examples demonstrate that non-optimal control performance can be diagnosed successfully to indicate errors in tuning or in modelling.

3.1.2 INDUSTRIAL CASE STUDY

Empirical Study of Pulp Base Weights at Domtar and Kruger Paper Mills

The initial industrial application for this research was in examining data from several Domtar and Kruger paper mills. In each case the pulp basis weight is being controlled with a commercial Dahlin controller.

Figure 3.12a and 3.12d show the output response for the Domtar uncontrolled and controlled cases. It is apparent from these responses that the controlled case is a great improvement over the uncontrolled case but this research questions whether further improvement is possible. The autocorrelations of the two cases are shown in Figure 3.12b and 3.12e. The uncontrolled plot is characteristic of a slowly drifting, nonstationary process while the autocorrelation of the controlled basis weight is eliminated after the second time interval. As the dead time of the process is approximately two units this latter case appears to

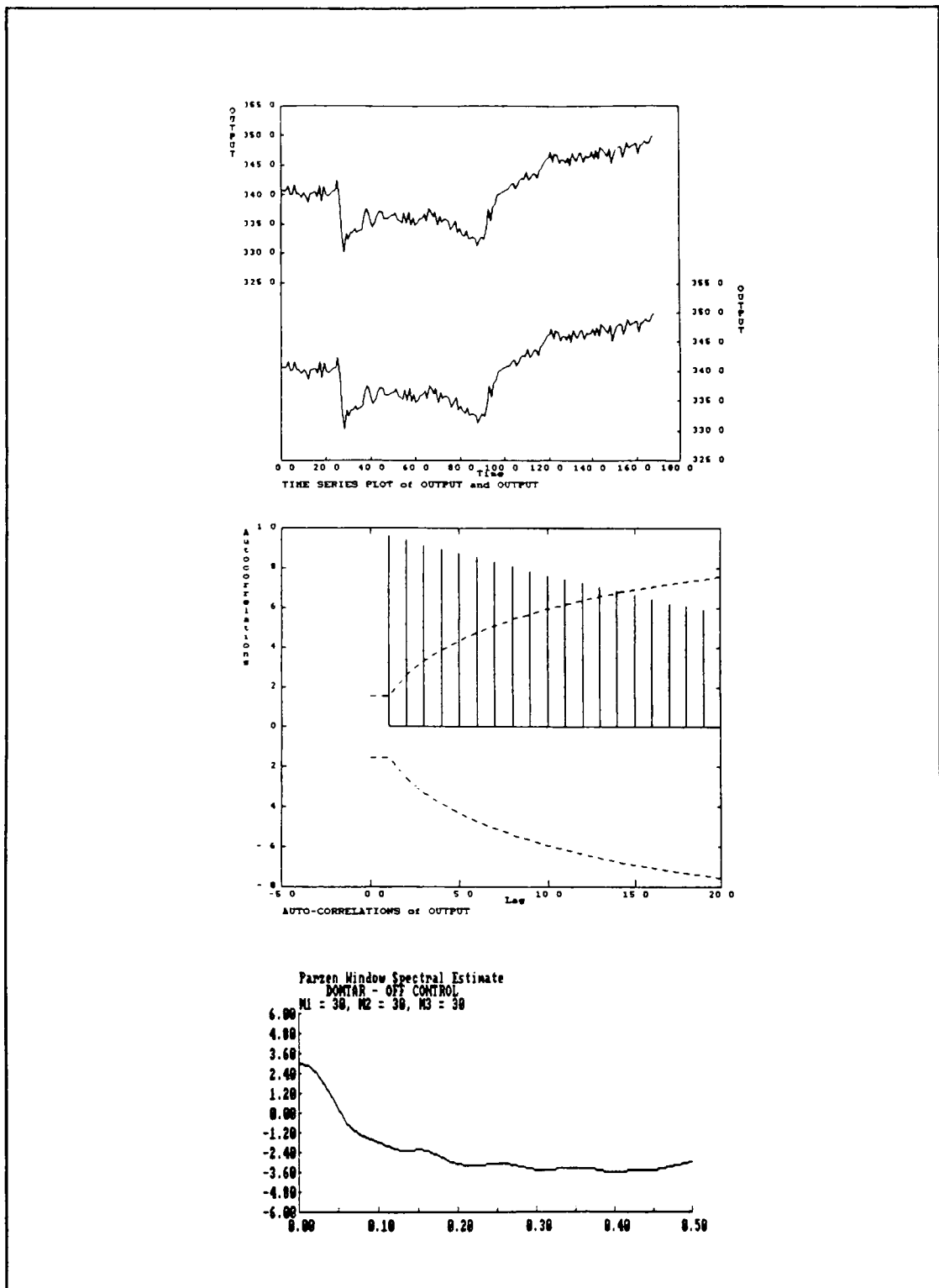


Figure 3.12(a,b,c) Domtar Paper Mill Data Case Study (Uncontrolled)

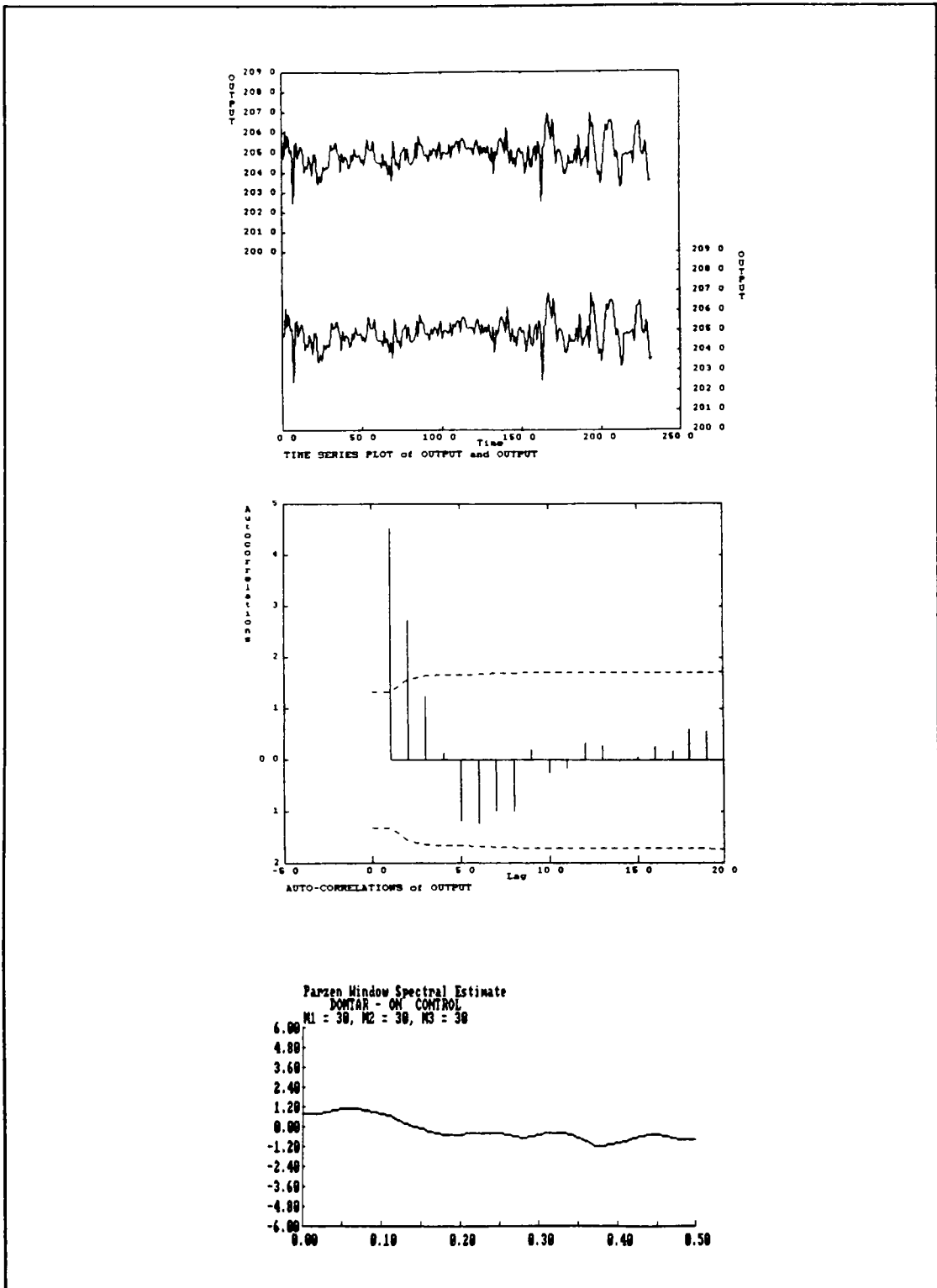


Figure 3.12(d,e,f) Domtar Paper Mill Data Case Study (Controlled)

be giving minimum variance performance. This is confirmed by the fact that the actual output variance of 0.452 is approximately equal to the predicted minimum of 0.485. Refer to Appendix D for calculations.

Figure 3.13a and 3.13d show the controlled and uncontrolled process response for basis weight data supplied by Kruger. Using simple observation it is difficult to differentiate between the two responses and to discern the superior performance. The autocorrelation plots for the two cases are shown in Figure 3.13b and 3.13e. Both plots show an alternating pattern in the autocorrelation function. This high frequency oscillation is also picked up as a large peak at high frequency in the power spectrum plots shown in Figures 3.13c and 3.13f. This information indicates a possible problem with the system sensor. When this problem was detected and remedied the performance improved significantly.

From these two simple industrial examples the utility of this diagnostic tool is apparent. The autocorrelation function and the power spectrum have been used successfully to confirm the presence of near optimal control in the first instance and to diagnose a sensor difficulty in the latter example.

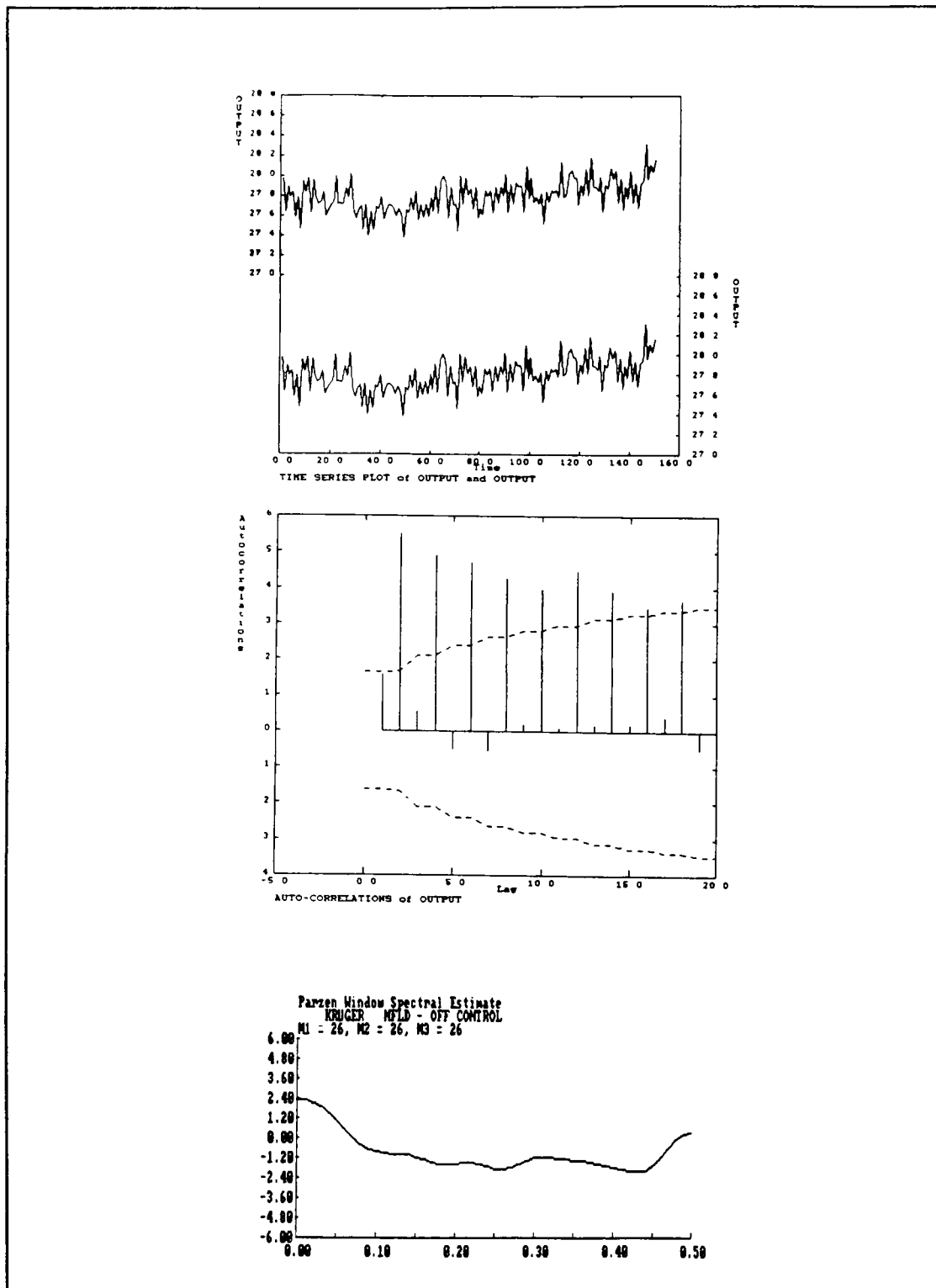


Figure 3.13(a,b,c) Kruger Paper Mill Data Case Study (Controlled)

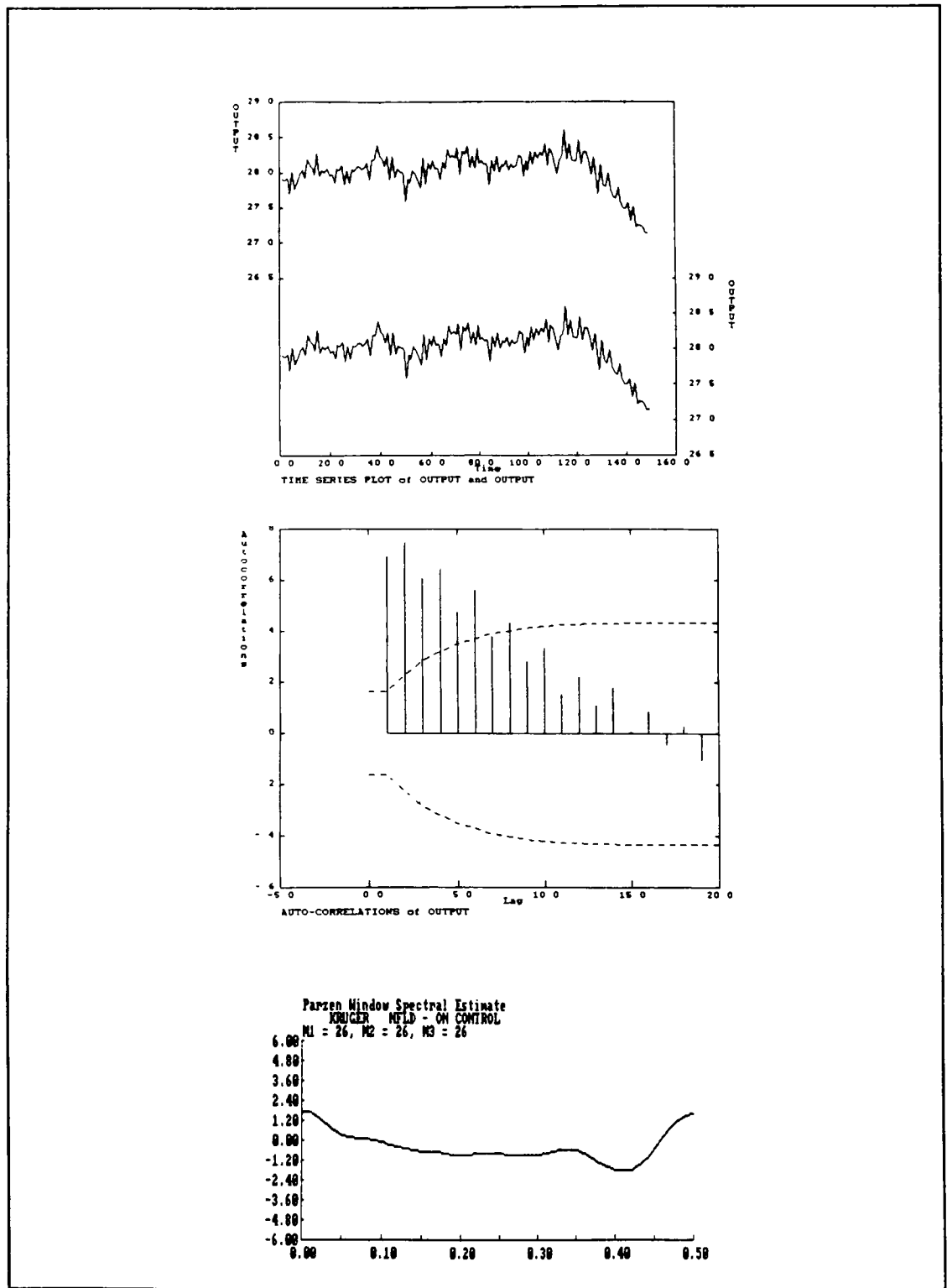


Figure 3.13(d,e,f) Kruger Paper Mill Data Case Study (Uncontrolled)

Empirical Study of a Heat Exchanger at Shell Scotford Refinery

A PI feedback control strategy was tested at the Shell Scotford Petroleum Refinery. A rich amine solution is being heated approximately 8 °C via exchange with low pressure steam before entering an amine flash drum. A process flow diagram is given in Figure 3.14. The heater is a double pipe heat exchanger, with steam in the outer tube, having an approximate duty of 1.10 MMBtu/hr. The rich amine outlet temperature is controlled by manipulating the steam flow through the exchanger.

A time series identification of the process yielded the following transfer function [Box & Jenkins, 1976],

$$T_m(z) = \frac{0.00852 z^{-2}}{1 - 0.568 z^{-1}} * F(z) + \frac{1}{1 - 0.8 z^{-1}} * a_t \quad (3.6)$$

with a variance of 0.05 (°C)² for a_t . A Pseudo-Random-Binary-Sequence (PRBS) signal was introduced into the steam flow with a magnitude of 100 kg/hr and a switching frequency of 4 minutes, while the sampling period was one minute. A continuous model which satisfies this discrete representation is given in equation 3.7.

$$T_m(s) = \frac{0.02 e^{-s}}{1.8s + 1} * F(s) \quad (3.7)$$

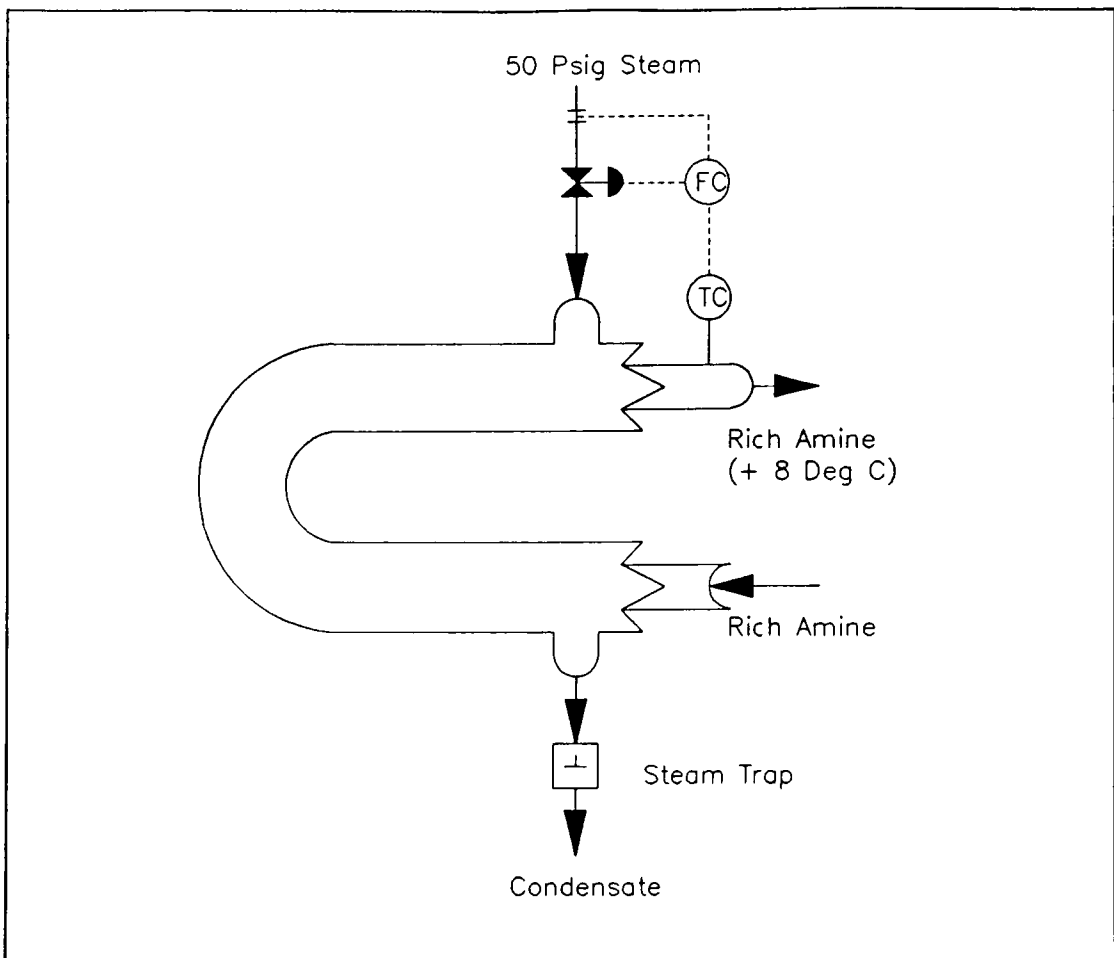


Figure 3.14 Process Schematic for Rich Amine Heat Exchanger

where F is the steam flow to the exchanger. A block diagram of the system is shown in Figure 3.15.

The identified transfer function relating the amine outlet temperature to the steam flow is used for the process model. The quantity $(T_p)_t$ represents the predicted temperature given the process model and the actual steam flow input. The difference between the actual temperature and the predicted

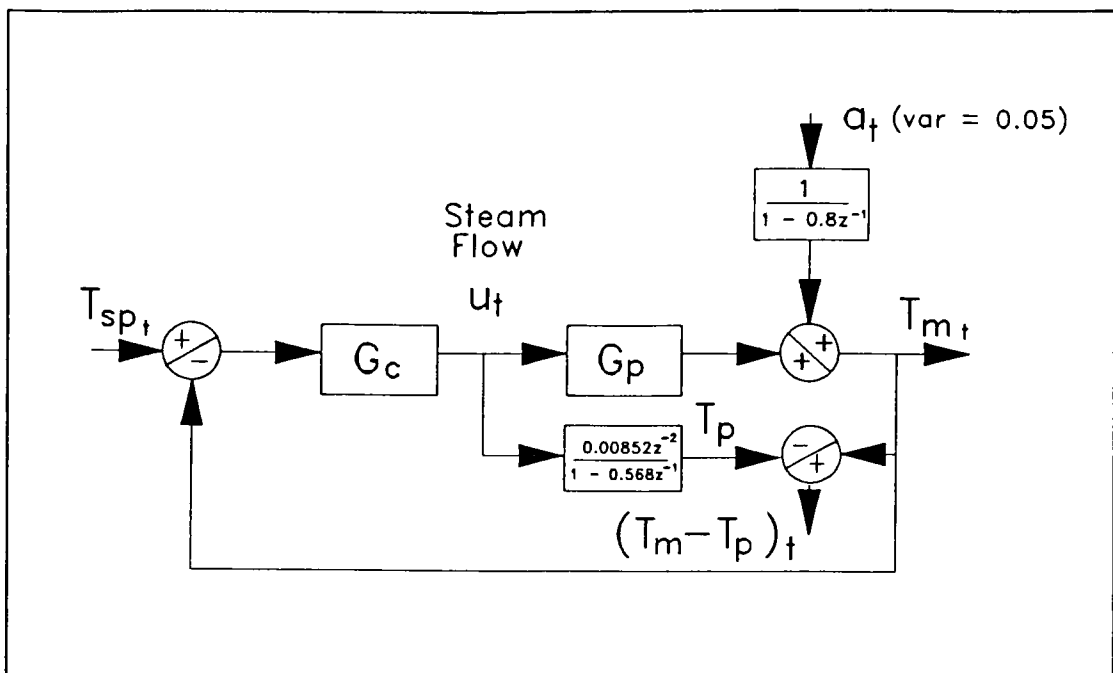


Figure 3.15 Rich Amine Heat Exchanger Control Block Diagram

temperature is given by the quantity $(T_m - T_p)_t$. Unlike the model based control case this quantity is not used by the control algorithm, but it will be used in the analysis to investigate possible modelling error.

Normal operating data was collected and analyzed for the original controller tuning constants. Figure 3.16 shows the process input and output response and the autocorrelation and crosscorrelation functions. The output and input are given by T13810 and F13023 respectively. The variance of the controlled variable is $1.943 \text{ (}^\circ\text{C)}^2$. The slowly decreasing autocorrelation plot is characteristic of a nonstationary process and indicates a detuned, poorly performing controller.

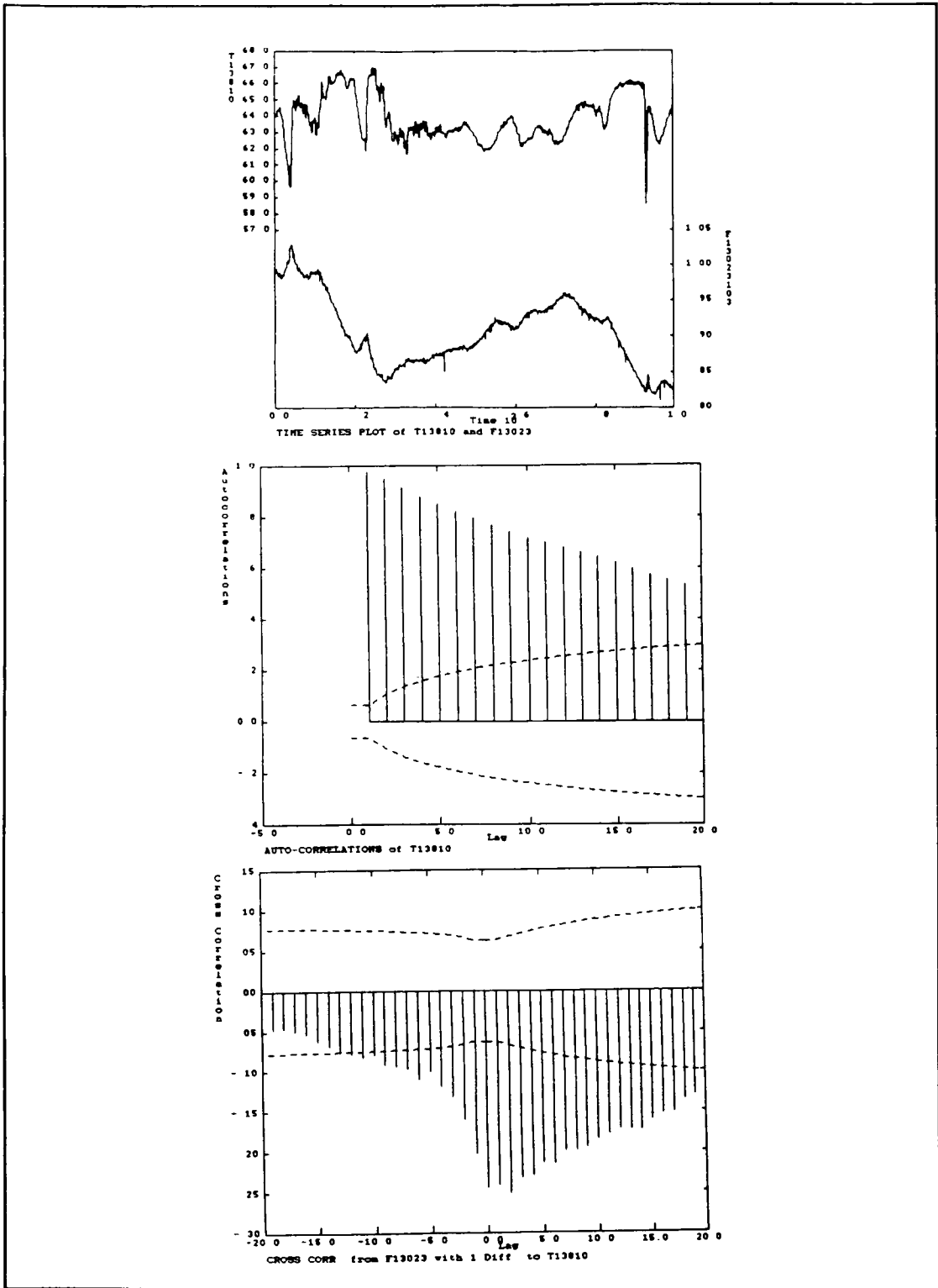


Figure 3.16(a,b,c) Rich Amine Heat Exchanger, Normal Operation

Given the ARMA model fit to the time response data and the true process dead time of one unit, the prediction of the minimum variance for the outlet temperature, using equation 2.12, yields $0.186 \text{ (}^\circ\text{C)}^2$. Appendix E shows the necessary calculations. This is a large reduction from the existing case indicating the need to modify the controller.

The controller parameters were changed gradually and an analysis was performed at each step. A summary of all the cases studied is given in Table 3.1. The controller gain required increasing while the reset time was decreased. Analysis results for trial number 3, shown in Table 3.1, are given in Figure 3.17. In this particular case the tuning parameters are approaching those of an MVC. A large improvement has been realized from the initial case as shown by the presence of only two significant autocorrelations beyond that of the process dead time. The best achievable performance was estimated to yield a variance of $0.042 \text{ (}^\circ\text{C)}^2$, as can be seen in Appendix E, which is virtually equivalent to the $0.048 \text{ (}^\circ\text{C)}^2$ variance of the sample. There seems to be a slight oscillation in autocorrelation function which may be an indication of control difficulty. If we examine Figure 3.17d it shows slight significance in the correlation between the differenced steam input and the differenced model prediction error. As stated before, this can be the result of either model inaccuracy or an autocorrelated disturbance. Although

TABLE 3.1 Summary of Rich Amine Heat Exchanger Study

	Tuning**	Temperature (C)		Predicted Minimum Variance	Percent Difference	Steam Flow (m ³ /hr)		K at last * significant autocorrelation	Number of significant u _t * (T _m - T _p) _{t+k} correlations
		mean	variance			mean	variance		
1	K _c =0.84 T _I =14.3	63.85	1.94	0.19	617	905.3	0.2E4	> 20	-
2	K _c =12 T _I =1.33	60.81	0.07	0.05	35	556.3	406.4	oscillatory	1
3	K _c =42 T _I =1.33	60.86	0.05	0.04	8	605.5	94.7	2	2
4	K _c =120 T _I =1.33	62.04	0.25	0.20	26	865.5	0.3E4	oscillatory	4
5	K _c =17 T _I =14.3	62.74	0.16	0.04	285	1110	0.2E4	30	-
6	K _c =24 T _I = 4	62.97	0.19	0.05	269	927.0	02.E4	30	0
7	K _c =60 T _I = 2	63.57	0.28	0.13	115	954.2	0.8E4	11	4

** K_c = (m³/hr) / deg C
T_I = min

* for MVC K=1

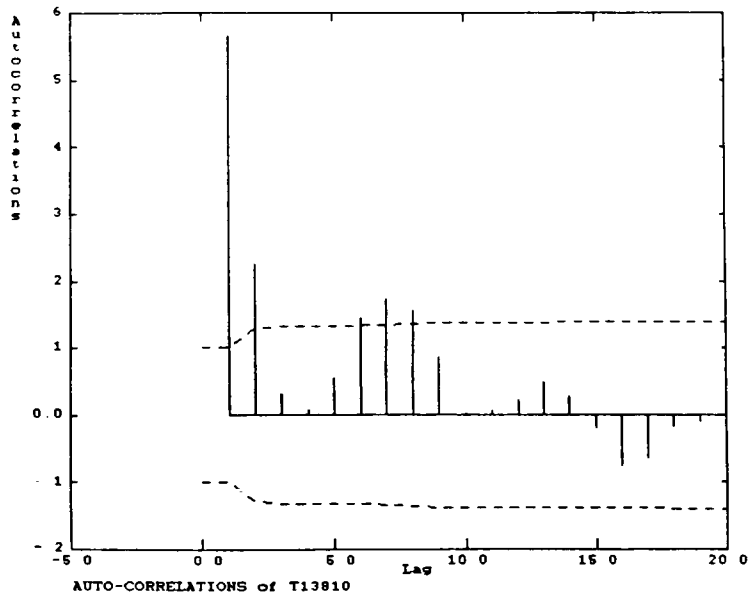
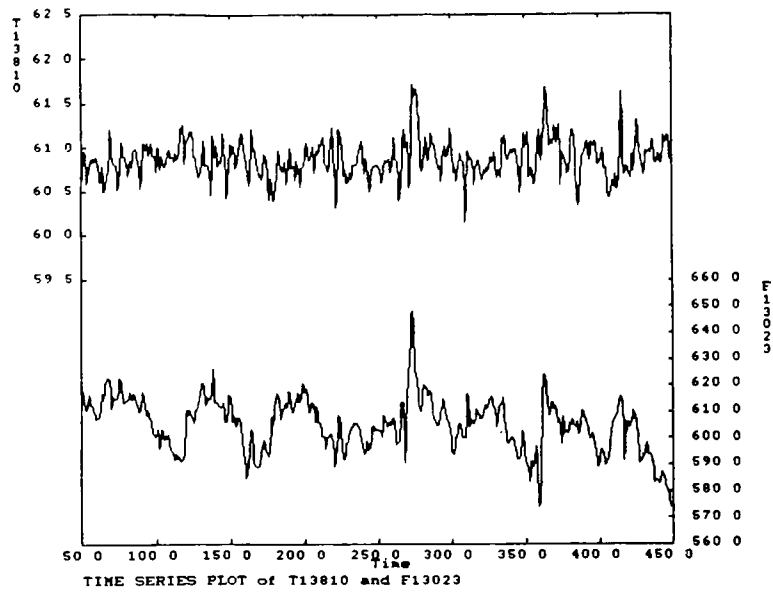


Figure 3.17(a,b) Rich Amine Heat Exchanger, MVC Case

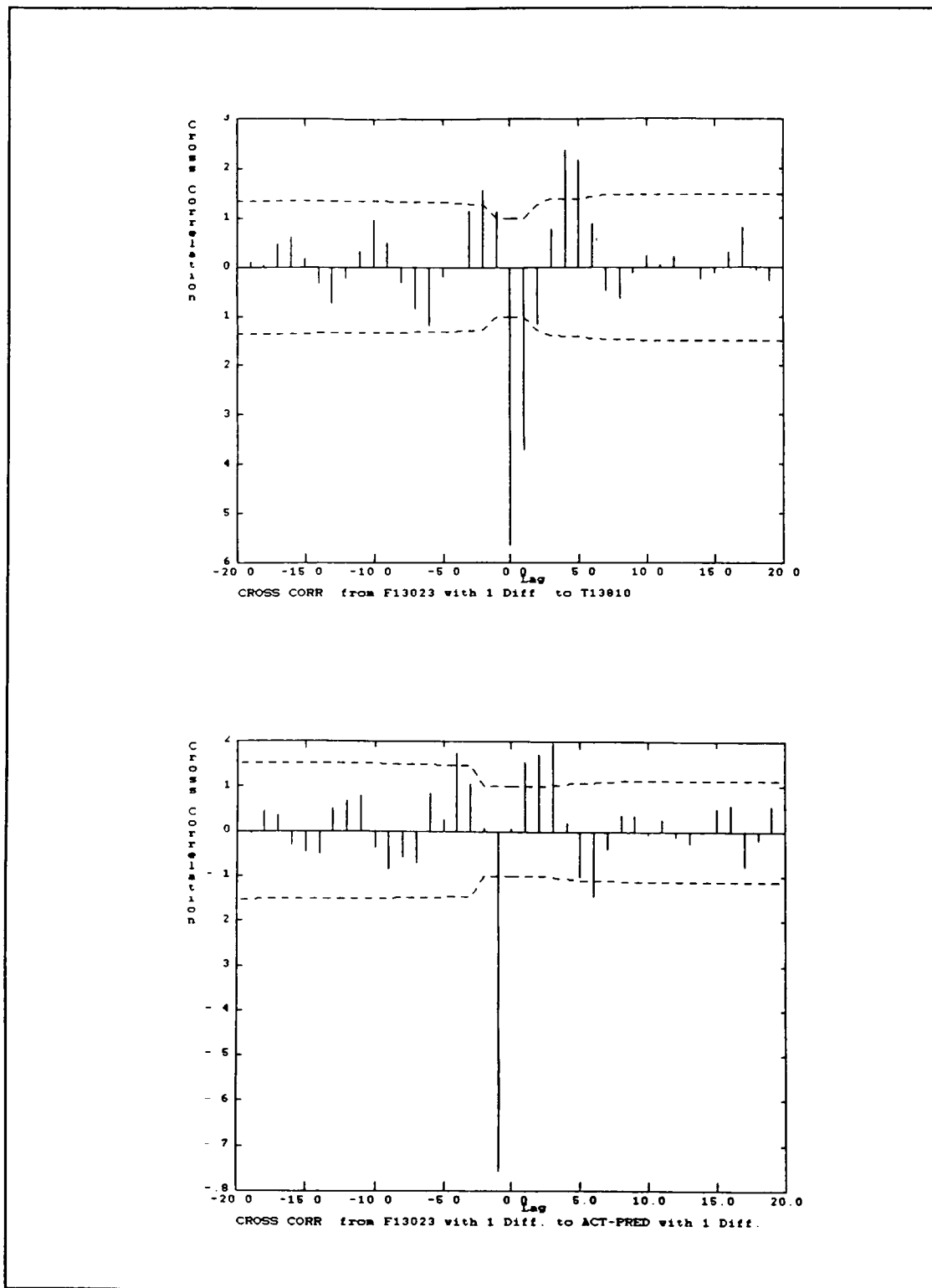


Figure 3.17(c,d) Rich Amine Heat Exchanger, MVC Case

there is no process model used directly in the control algorithm, an inherent model was assumed in deriving the control parameters. If the model accuracy is to be determined explicitly, data could be collected under the presence of controlled variable setpoint changes. This error, however, appears to have a minimal effect on the system and thus for the purposes of this application the performance may be acceptable.

Some further case studies were performed with Figure 3.18 showing a controller yielding an overly aggressive response, as can be seen in the highly oscillatory autocorrelation plot. These results correspond to case number 4 in Table 3.1. The temperature variance is moderately higher than in the MVC case while the steam flow variance has increased by two orders of magnitude. This overtuned controller is demanding overly aggressive manipulations of the input variable causing the controlled variable to be adversely affected. Although the temperature variance appears acceptable the large input manipulations accompanied by the oscillatory autocorrelation function indicate an overtuned controller, hence detuning would be advised.

These simple industrial examples have been used to demonstrate the use of the autocorrelation and crosscorrelation functions and the power spectrum. In the

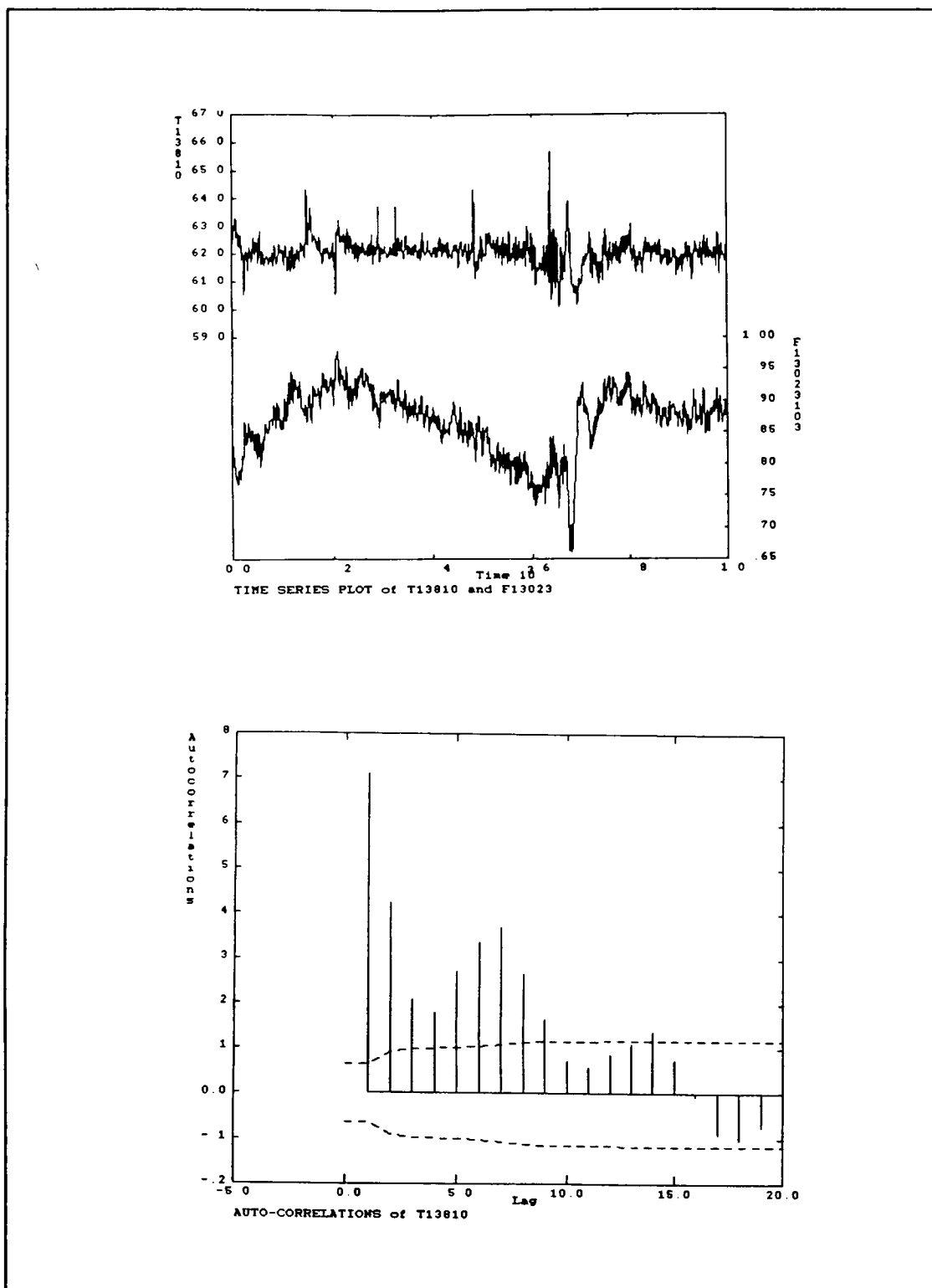


Figure 3.18(a,b) Rich Amine Heat Exchanger, Overtuned Case

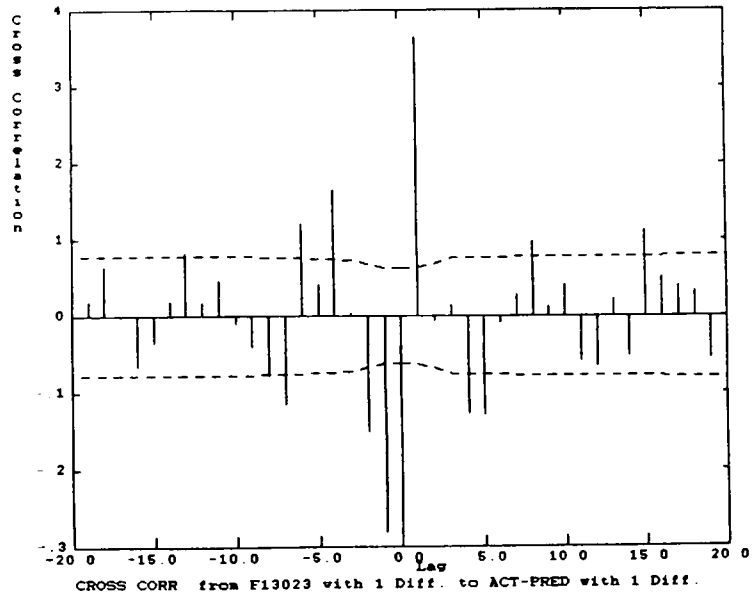
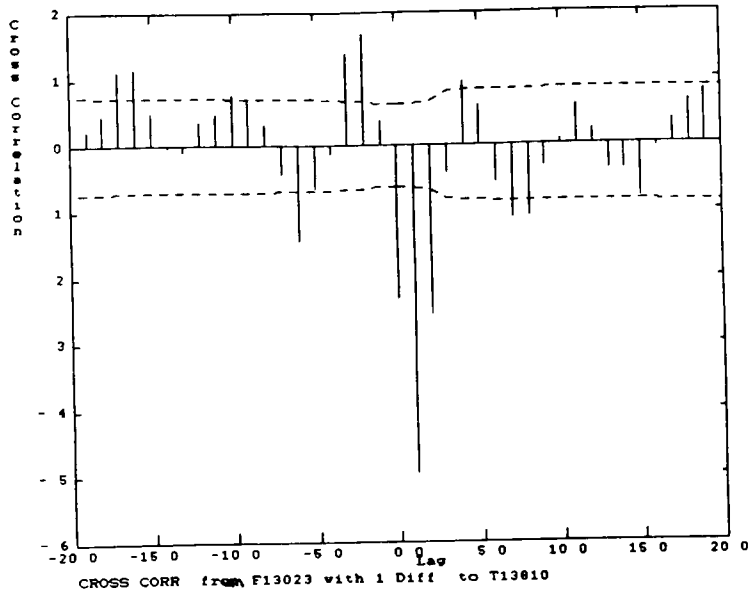


Figure 3.18(c,d) Rich Amine Heat Exchanger, Overtuned Case

'Shell Study' the correctness of the diagnosis was validated by further empirical cases which followed the recommendations based on the analysis of initial data. Therefore, this diagnostic procedure has proven effective in screening for the existence of a control performance inadequacy and in differentiating between mistuning and modelling errors in simple systems. In the latter case, however, the adequacy of tuning cannot be established until the modelling error has been eliminated.

3.2 SISO FEEDFORWARD - FEEDBACK CONTROL SYSTEM

It was the objective of this phase of the investigation to determine whether statistical techniques such as the autocorrelation and crosscorrelation functions could be used in evaluating control performance for a more complicated control scheme. To this end it was of interest to determine whether inadequacies in a feedforward-feedback control scheme could be successfully attributed to either the feedforward or the feedback controller in addition to distinguishing between mistuning and model mismatch, already discussed. Many of the results obtained in this phase of the study follow directly from the simple SISO pure feedback system discussed in the previous section. The concepts presented in this section will also introduce some of the methodology employed for the

multivariable applications in the following section.

3.2.1 SIMULATION RESULTS

A feedforward-feedback control scheme was designed for a first order with dead time process (FOPDT). The controller was designed for regulatory service with a FOPDT disturbance model. It is important to note that the process and disturbance models have an equivalent dead time. All process simulations were performed with a Pseudo-Random-Binary-Sequence, PRBS, disturbance input, d_t . A random walk, autoregressive noise model of order one, AR(1), was also added to the system. A block diagram for the process, showing the process and disturbance models, is given in Figure 3.19. The variance of a_t is 1.000. Using these models various feedforward and feedback controllers were designed and implemented. Refer to Appendix F for calculations.

This process was simulated in discrete time in a spreadsheet environment. [Stanfelj, 1990] The control details are provided in Appendix F. This technique was selected because of its simplicity, speed and ease of data modification and manipulation. Data generated from these simulations was then analyzed in the MIDSA™ software package.

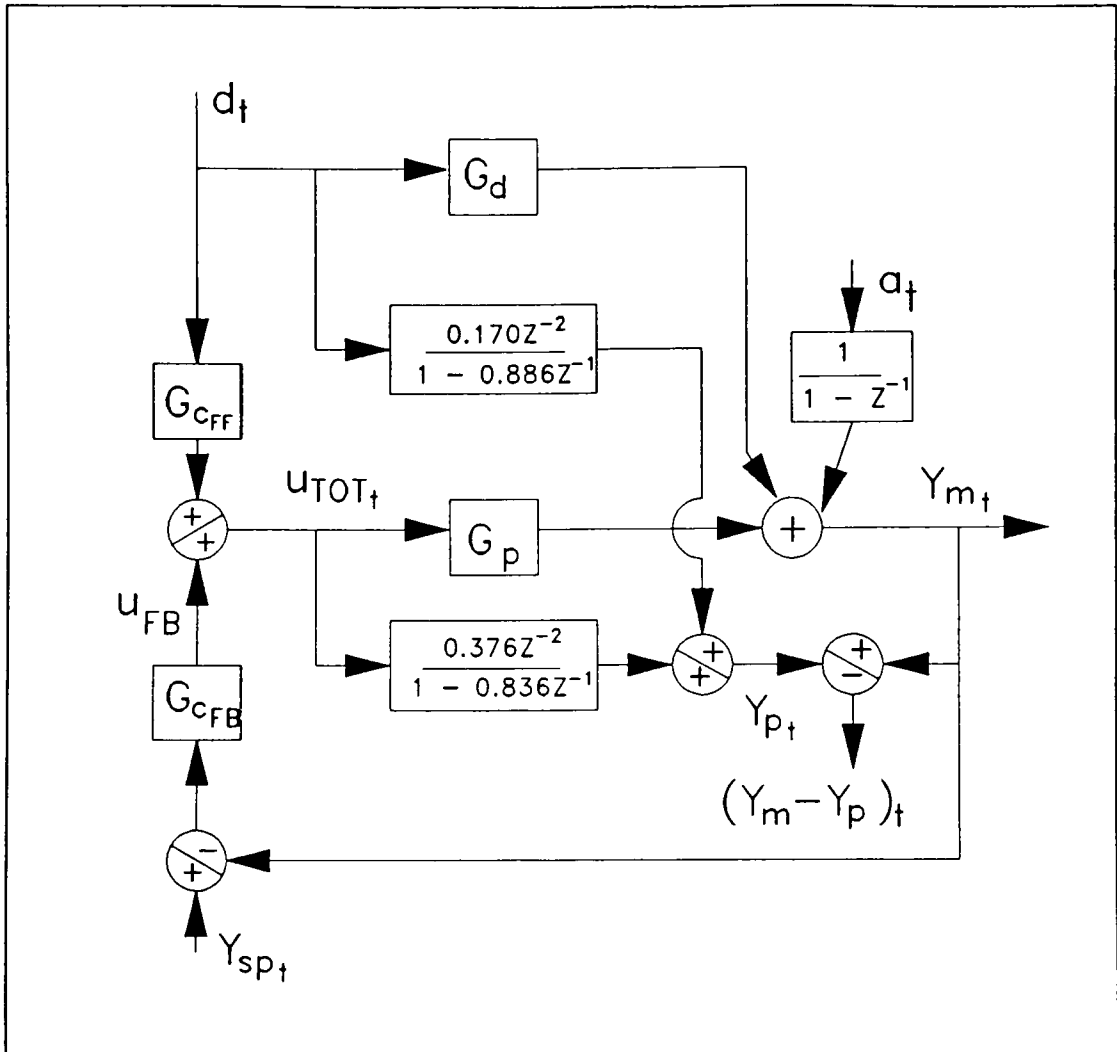


Figure 3.19 Feedforward-Feedback Control Block Diagram

The control performance evaluation and diagnosis methodology for combination feedforward-feedback controllers was presented in detail in Chapter 2. As we recall, the quantity $(Y_m - Y_p)_t$ represents the model prediction error and is composed of any error in both the process and disturbance models and the unmeasurable noise or disturbance entering the process. This quantity will again be used to check for

modelling errors. The procedure thus established will be demonstrated in the following examples.

Several cases having varying control equations were studied. A base case was selected having a perfect feedforward controller, defined as,

$$G_{c_{FF}}(s) = -\frac{G_d(s)}{G_p(s)} \quad (3.8)$$

and an MVC feedback algorithm, with both process and disturbance models being correct. In order to test the diagnostic procedure, the individual controllers were then detuned and the process and disturbance models mismatched. Recalling Figure 2.7, it is evident that the potential combinations causing poor performance are numerous, many of which will be discussed in the following section.

Case Studies

The first control scheme investigated was the base case having a perfect feedforward controller and a minimum variance feedback controller. The simulation results for this case are displayed in Figure 3.20. Figure 3.20b shows that no correlation exists between the measured disturbance and the

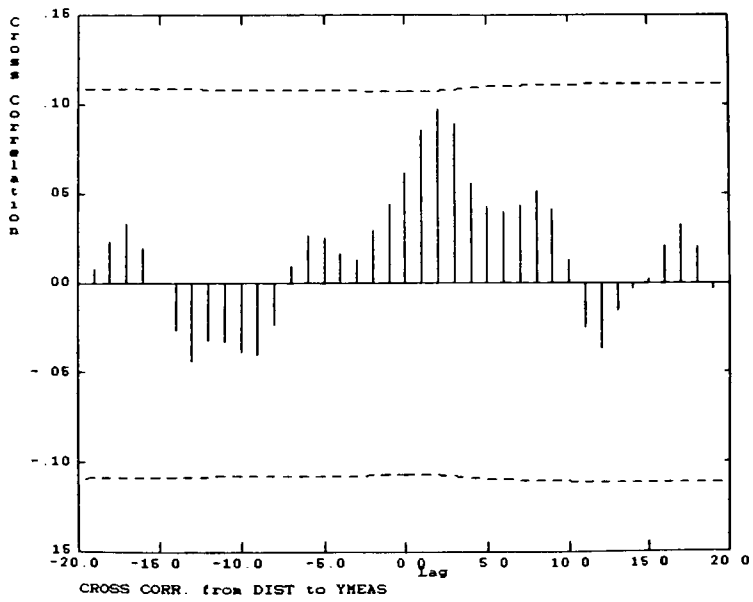
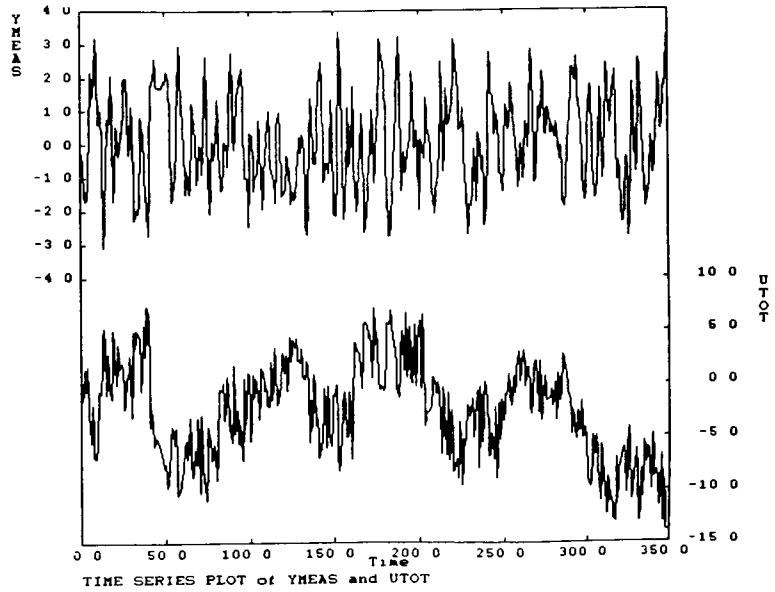


Figure 3.20(a,b) Feedforward-Feedback, Base Case

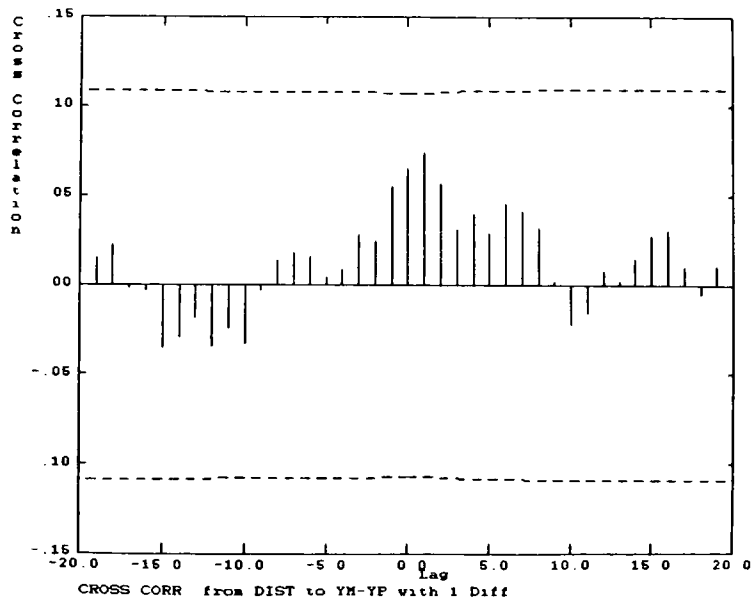
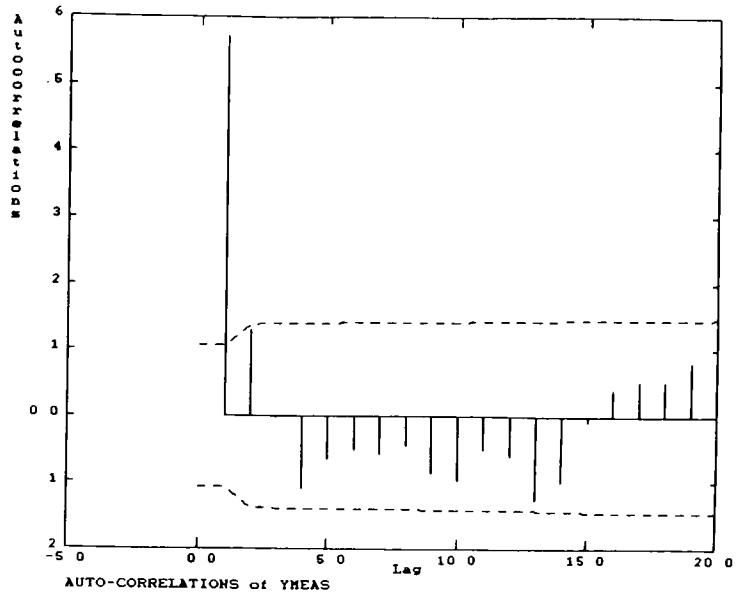


Figure 3.20(c,d) Feedforward-Feedback, Base Case

output which is expected for the perfect feedforward control case. The output autocorrelation establishes the presence of minimum variance feedback control, as all lags beyond the process dead time are within the confidence region. The output response is stationary with a variance of 1.957. This value agrees well with the predicted minimum of 1.921, as calculated in Appendix F. To confirm the absence of model mismatch Figure 3.20d shows that correlation does not exist between d_t and $(Y_m - Y_p)_{t+k}$. Therefore, the best possible control is being achieved given the structure of the process and control system. Control improvements can only be obtained through modifications of these structures.

The next control case analyzed retained the correct models but the feedback controller was detuned slightly by implementing a constrained minimum variance controller ($\lambda=1.0$). The results are shown in Figure 3.21. No correlation exists between the disturbance and the output, as visible in Figure 3.21b, which implies perfect feedforward compensation. The output autocorrelation has significant correlations appearing beyond the dead time, which indicates non-optimal feedback performance. The output response shown in Figure 3.21a is similar to that of the base case with the output variance being only marginally higher at 2.204. This variance is 24% greater than the lowest achievable value of 1.772. Although Figure 3.21d shows that no correlation exists

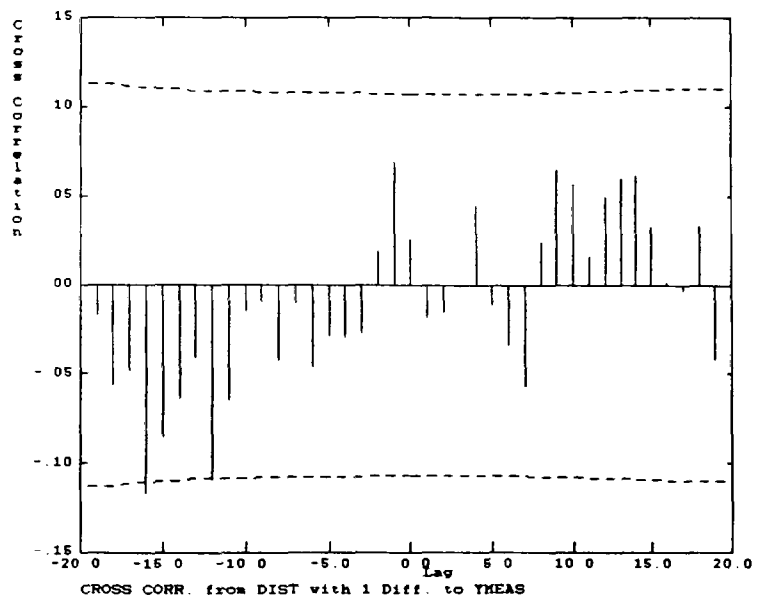
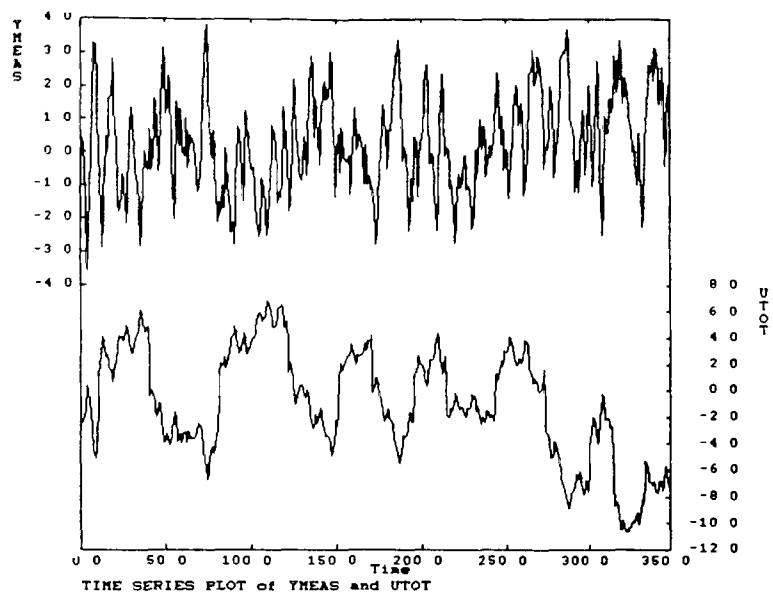


Figure 3.21(a,b) Feedforward-Feedback, Detuned Feedback Example

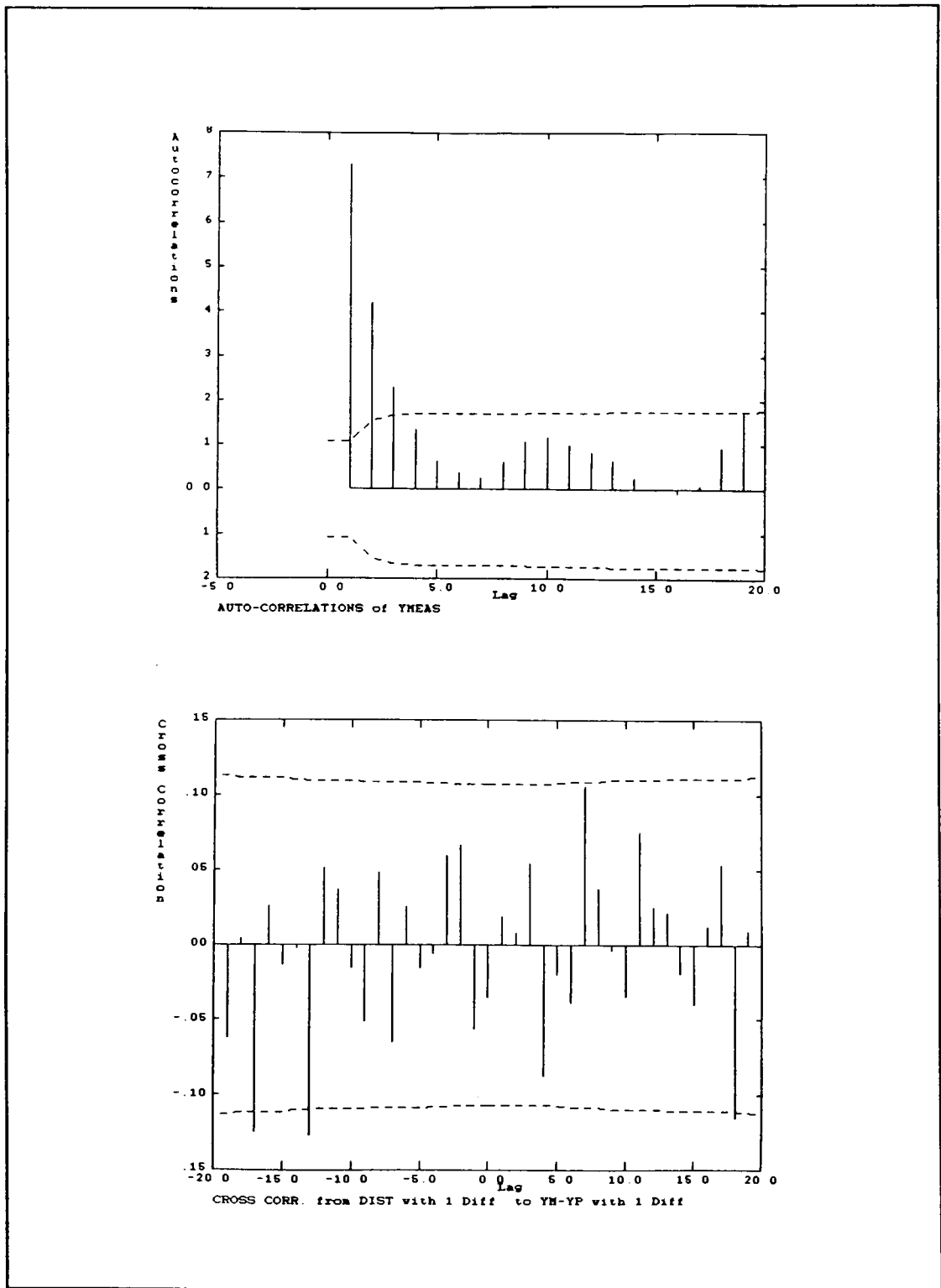


Figure 3.21(c,d) Feedforward-Feedback, Detuned Feedback Example

between the measured disturbance and the differenced model prediction error, the possibility of model error cannot be eliminated. As described in Chapter 2, the feedforward controller would have to be decommissioned and the data analyzed under those conditions. Therefore, given this analysis it is not certain whether the less than optimal performance is the result of a detuned feedback controller or compensating model errors.

Figure 3.22 shows the simulation results for the previous case with the feedforward control decommissioned. Unlike the previous example, Figure 3.22b shows significant correlation between the measured disturbance and the controlled variable, which is the result of the absence of feedforward control. The autocorrelation of $(Y_m)_t$ shows significant correlation beyond the process dead time of one unit, indicating non-optimal feedback performance. Similar to the last example, Figure 3.22d shows no correlation from the measured disturbance to the prediction error, therefore the models are deemed correct. Therefore, the non-optimal performance in the previous case is the result of a detuned feedback controller.

Figure 3.23 shows the results of the simulation in which perfect feedforward control was attained as a result of compensating errors in the process and disturbance models.

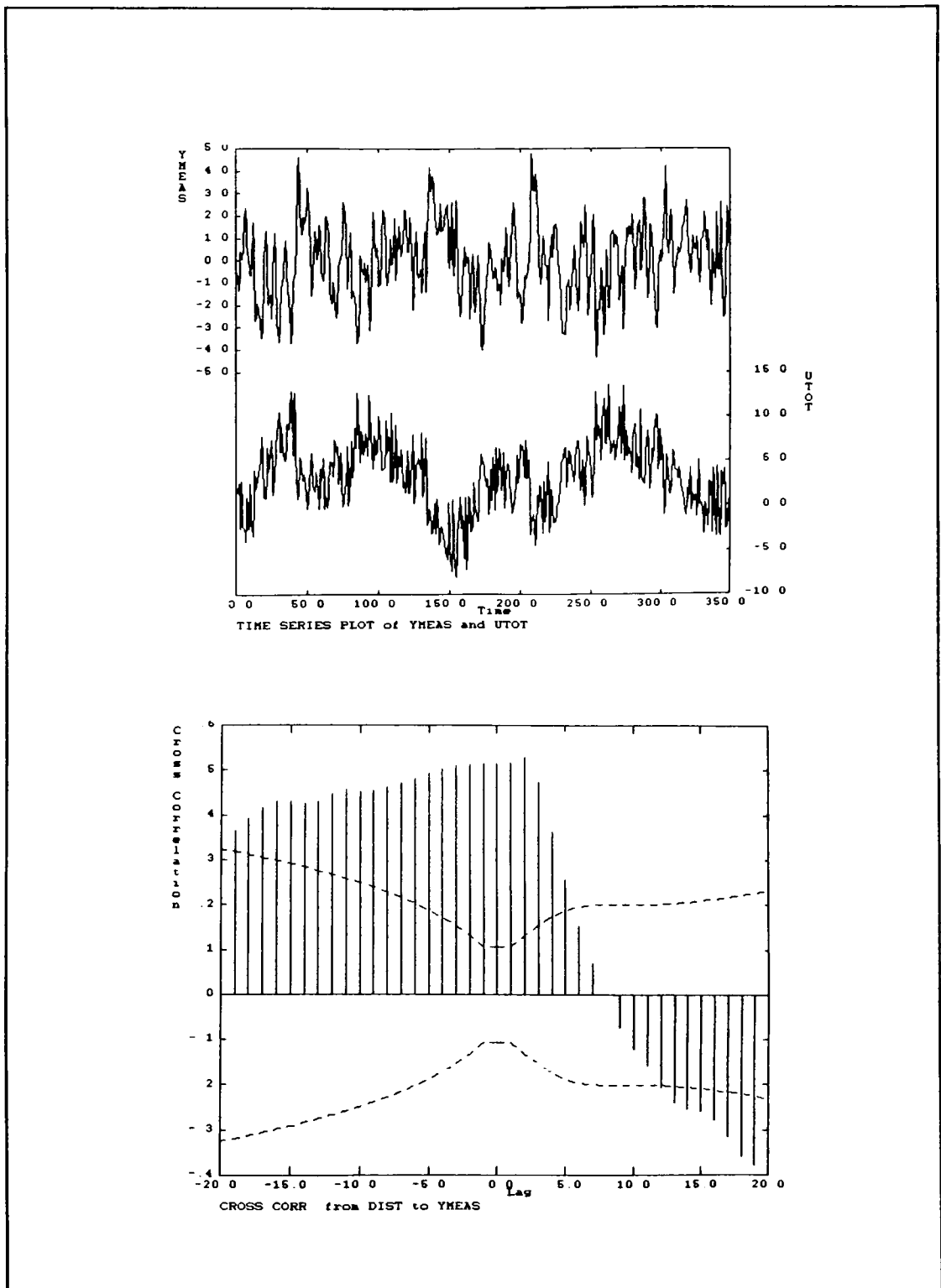


Figure 3.22(a,b) Feedforward Control Decommissioned, Perfect Models

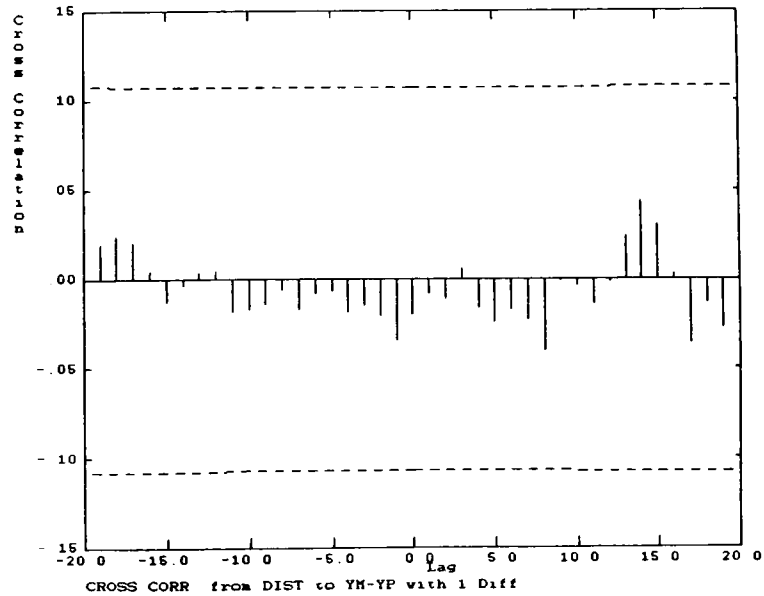
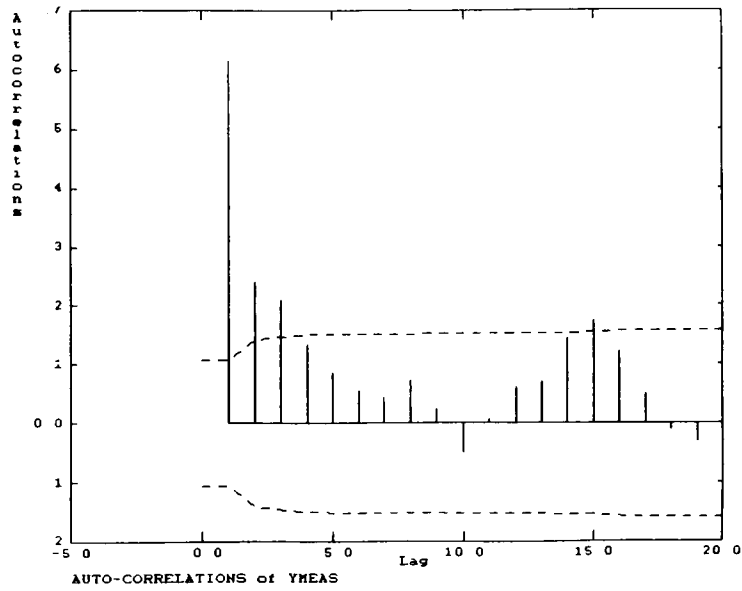


Figure 3.22(c,d) Feedforward Control Decommissioned, Perfect Models

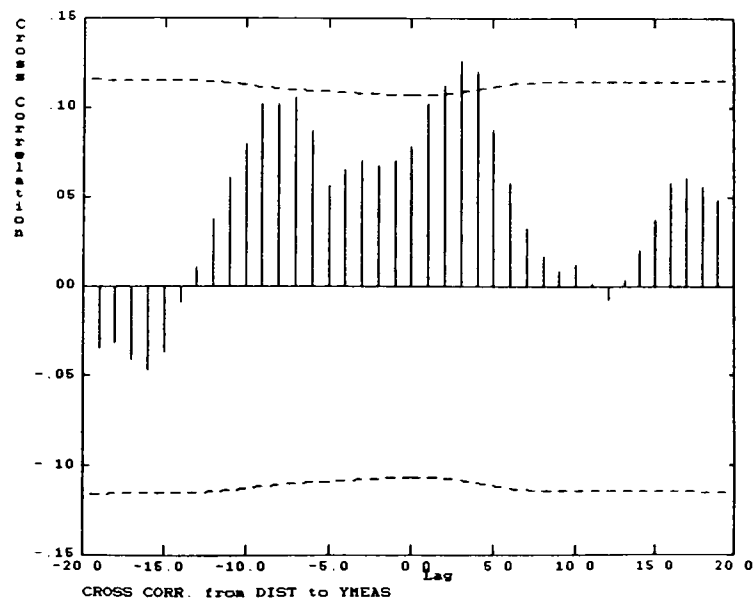
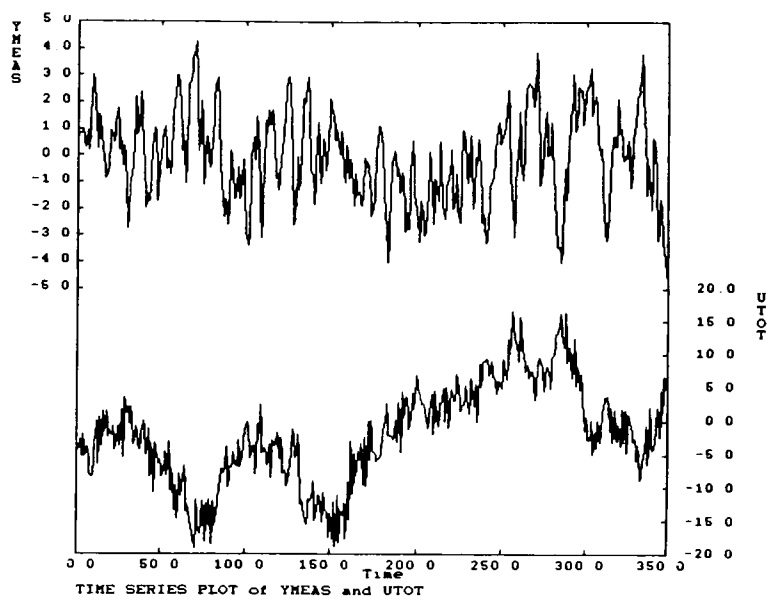


Figure 3.23(a,b) Feedforward-Feedback, Model Mismatch (Cancelling Errors)

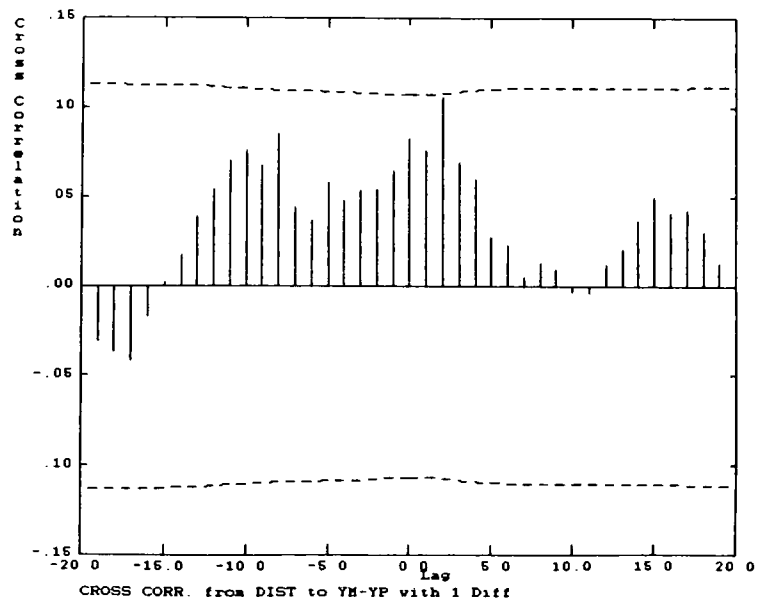
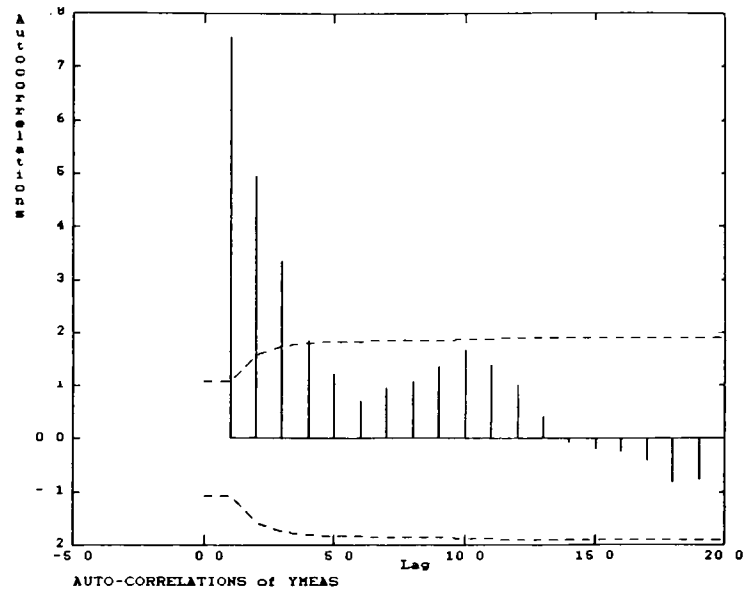


Figure 3.23(c,d) Feedforward-Feedback, Model Mismatch
(Cancelling Errors)

Figure 3.23b shows no significant correlation between d_t and $(Y_m)_{t+k}$ which implies perfect feedforward compensation. The autocorrelation of $(Y_m)_t$, however, shows significant correlation beyond the dead time of the process indicating non-optimal control performance. Figure 3.23d shows absence of correlation between the measured disturbance and the prediction error, which implies perfect models. As indicated in the last example, however, this result is not conclusive, thus further testing is necessary.

Using the same process and disturbance models, and the same feedback controller as the previous case, the system was simulated without the presence of feedforward control. The results of this simulation are shown in Figure 3.24. The only difference between these results and those of the previous case are in Figure 3.24d, the crosscorrelation between d_t and $(Y_m - Y_p)_{t+k}$. Unlike the previous example, significant correlation in this plot establishes the presence of model mismatch in the both models. Because the model errors are exactly compensating, they were not apparent in the crosscorrelation between the measured disturbance and the controlled variable.

The next example follows the right hand branch of the diagnosis presented in Figure 2.7. Figure 3.25, displays the analysis results for a perfect model of the measured

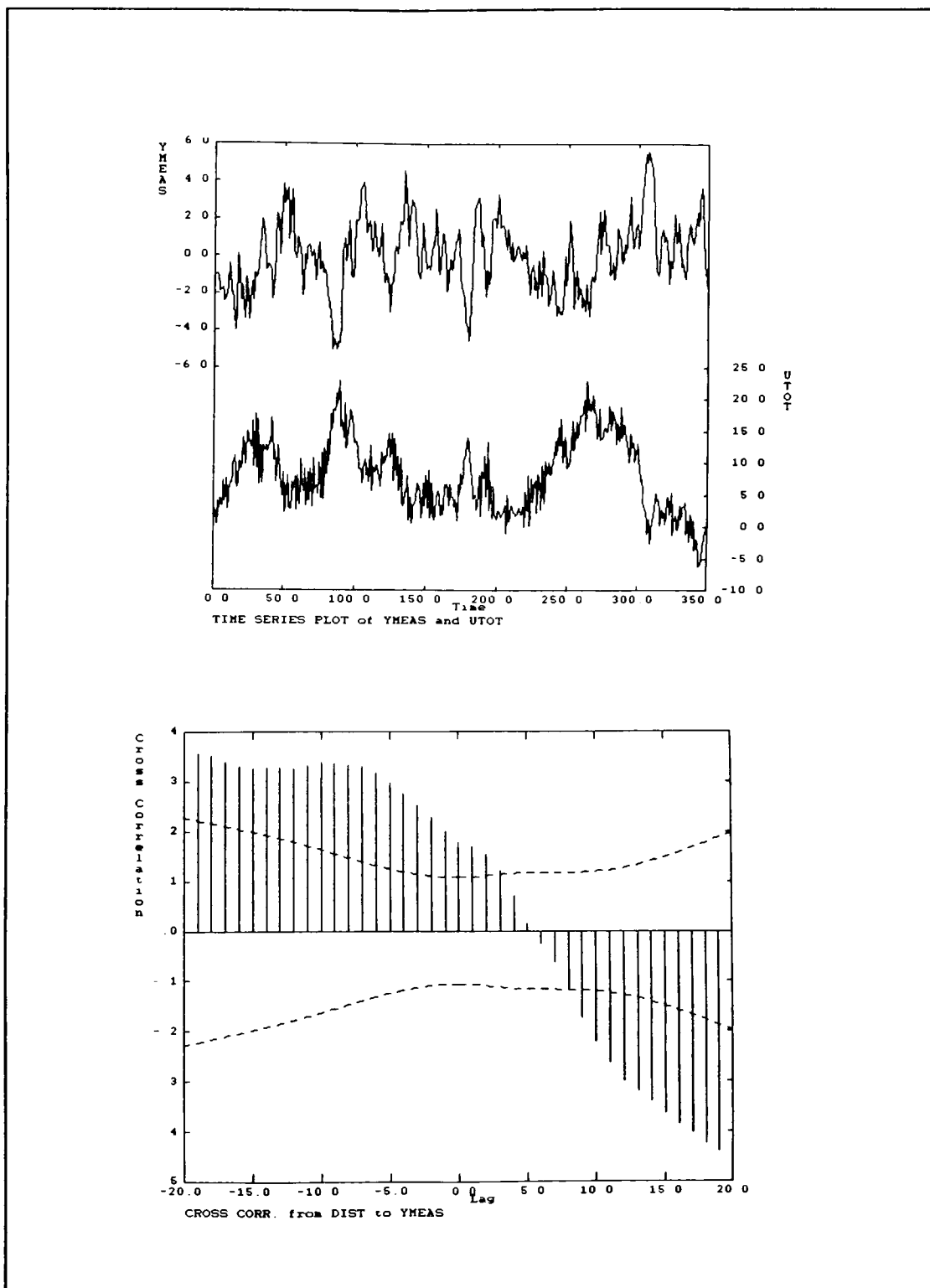


Figure 3.24(a,b) Feedforward Control Decommissioned
(Cancelling Model Errors)

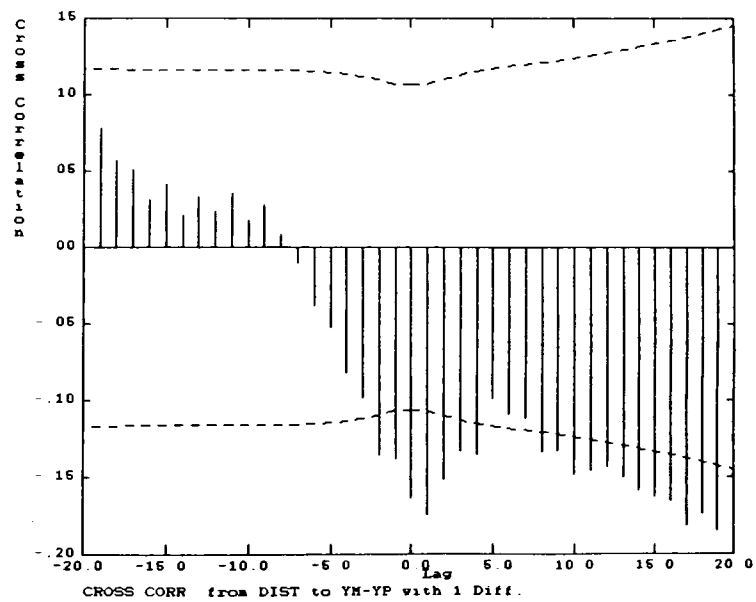
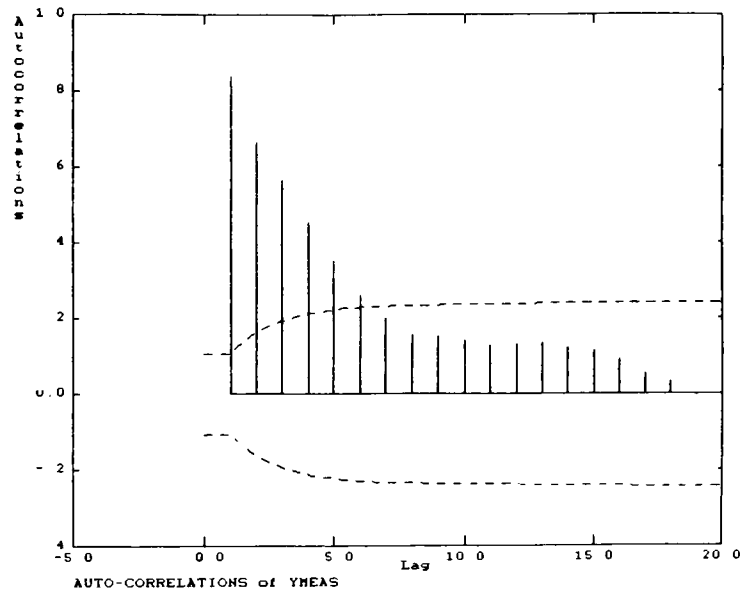


Figure 3.24(c,d) Feedforward Control Decommissioned
(Cancelling Model Errors)

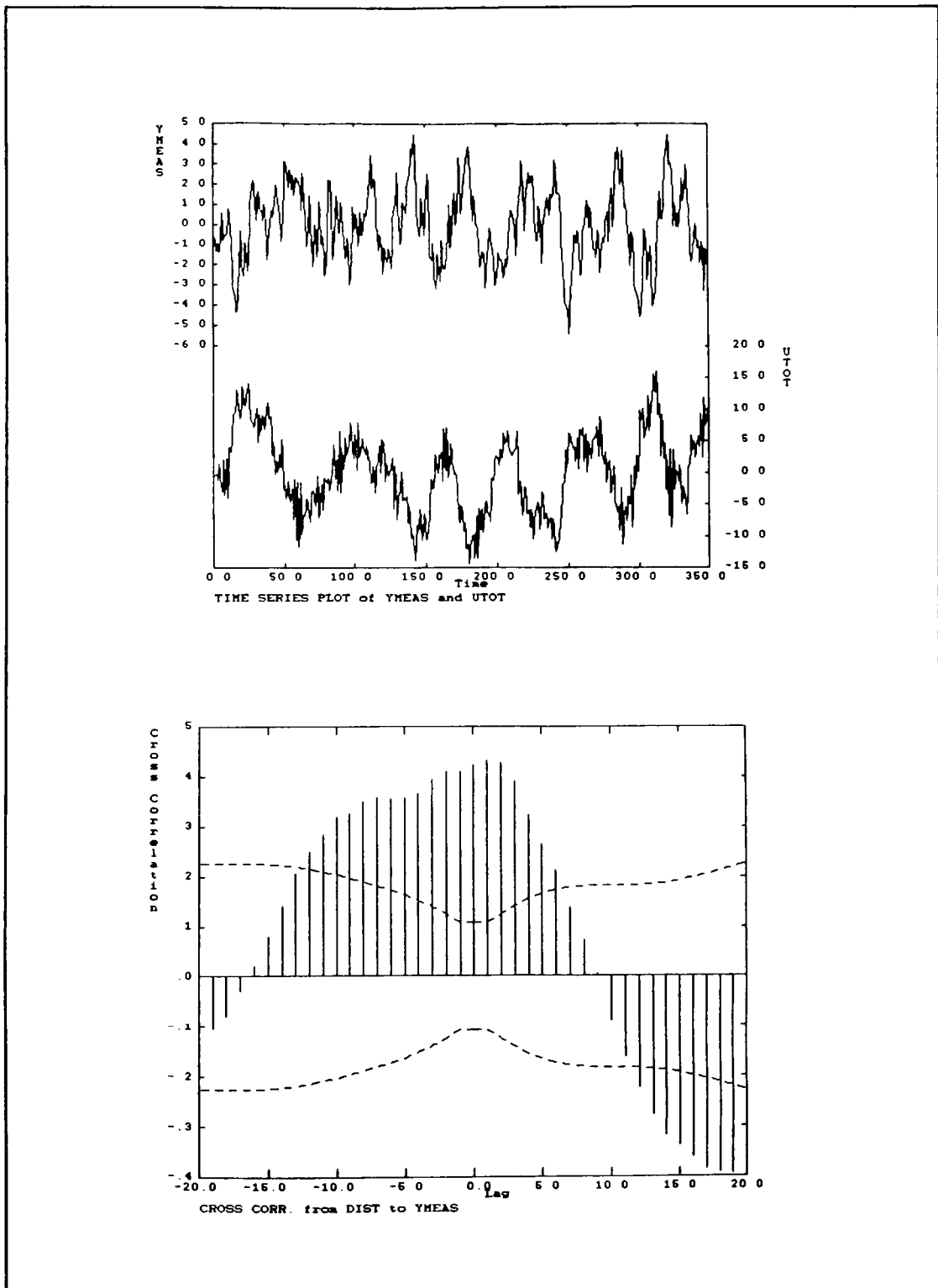


Figure 3.25(a,b) Feedforward-Feedback, Process Model Mismatch

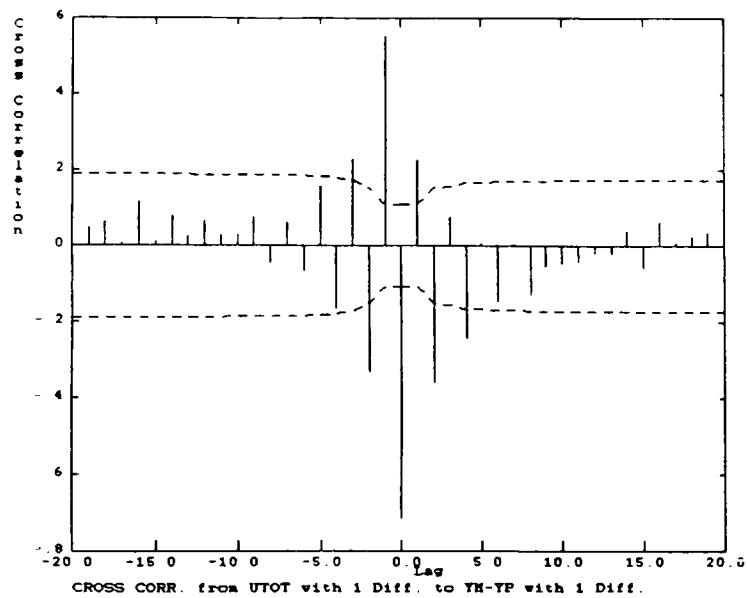
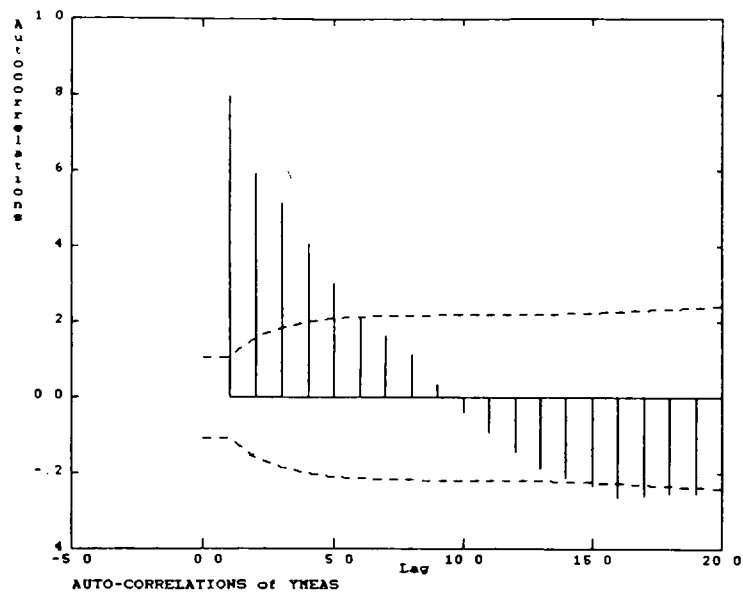


Figure 3.25(c,d) Feedforward-Feedback, Process Model Mismatch

disturbance and a model mismatched MVC feedback loop. The output response shows the controlled variable to be controlled less tightly which is quantified by the 59% higher variance of 3.483 as compared with the predicted minimum of 2.193. The disturbance-output crosscorrelation plot shows significant correlation which indicates a non-optimal feedforward controller. Moreover, the output autocorrelations remain significant beyond the dead time of the process, indicating that the best achievable control is not being attained. Figure 3.25d shows significant correlation between the differenced input and the differenced model prediction error which suggests model mismatch in the system. In order to clearly identify model error in G_d or in both G_d and G_p a controlled test with setpoint changes would have to be conducted and the data further analyzed.

The final combination examined is the case of non-compensating model errors in both the disturbance and the process models. In this instance both the feedforward and feedback controllers are not performing optimally. The output response shown in Figure 3.26a, accompanied with the large output variance of 16.472, confirms the poor control performance resulting from these modelling errors. The predicted minimum variance is calculated at 4.603 which represents a 72% reduction from the variance realized with this controller. This predicted minimum variance is

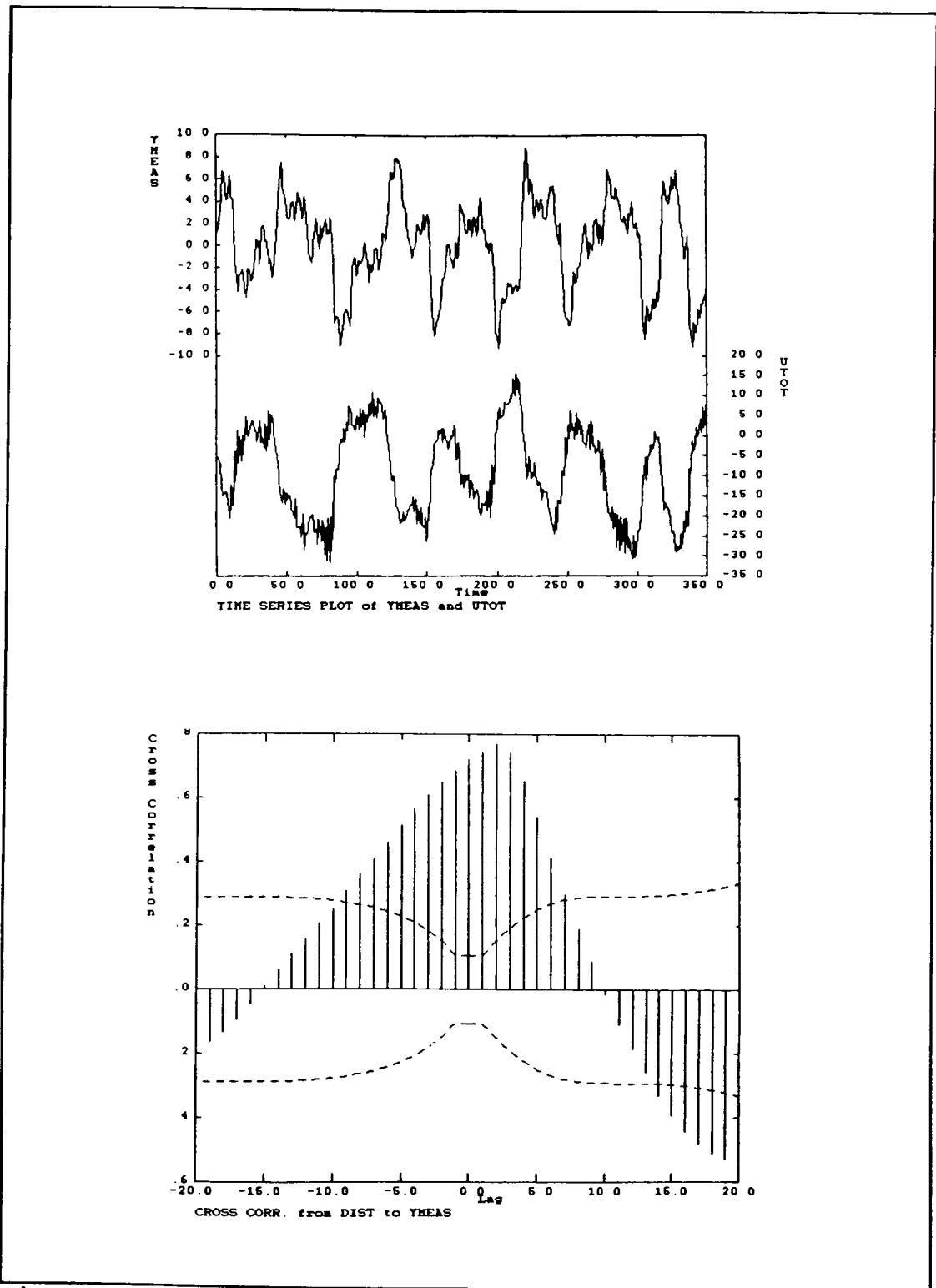


Figure 3.26(a,b) Feedforward-Feedback, Disturbance and Process Model Mismatch

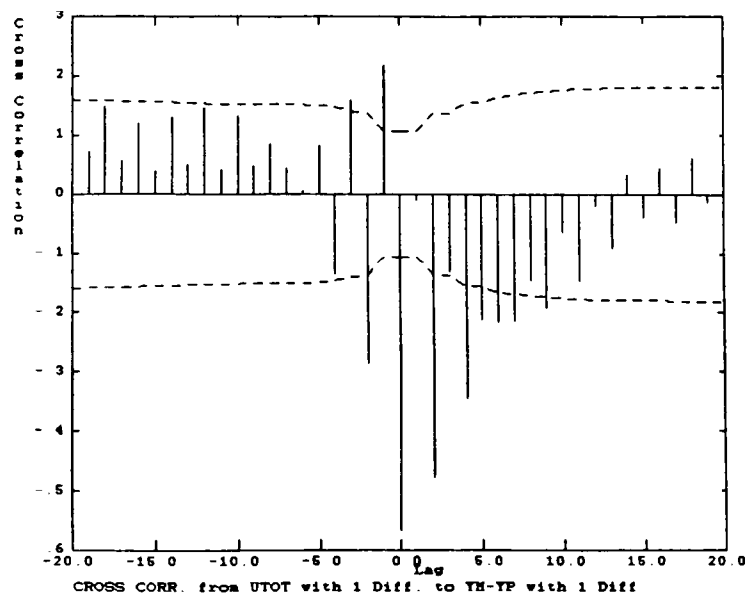
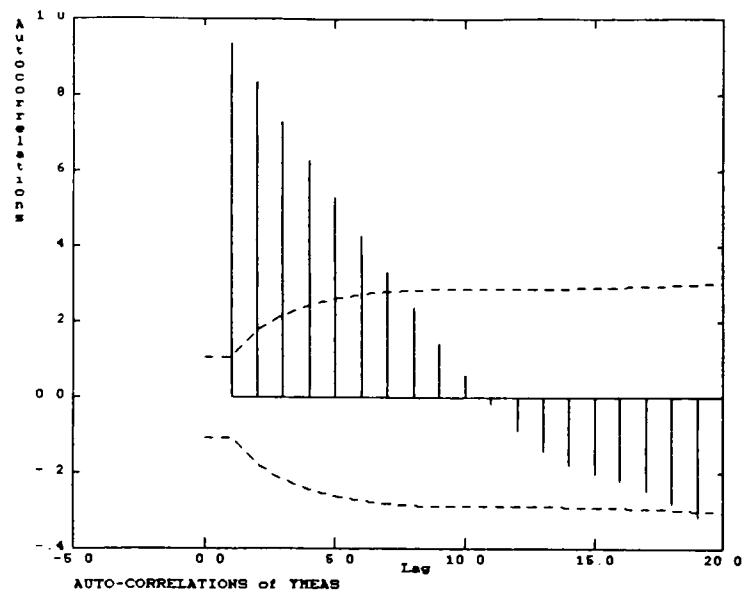


Figure 3.26(c,d) Feedforward-Feedback, Disturbance and Process Model Mismatch

considerably higher than that calculated for the previous cases. The reason for this discrepancy is that the poor feedforward control is acting like an additional disturbance which the feedback controller must attenuate. Therefore, the minimum variance predicted for this case reflects the larger inherent disturbance which results in a higher optimum value than that which would be obtained in the presence of good feedforward control, which would eliminate this disturbance. In cases such as these, which exhibit significantly degraded feedforward control, it is often possible to reduce the controlled variable variance to below that of the initially estimated minimum value, by improving the feedforward control. This is evident in Equation 2.12 by noting that σ_a^2 is reduced by the feedforward control.

The presence of significant correlation between the disturbance and the output indicates the inadequacy of the feedforward controller. As expected, the output autocorrelation demonstrates a deviation from the best achievable performance. Figure 3.26d suggests the presence of model mismatch in either or both of G_p and G_d , but is not conclusive. As in the previous example the accuracy of the individual models cannot be established with this normal operating data. This information can be obtained by conducting plant tests involving controlled variable setpoint changes if desired.

It is important to note that some of these examples required a large amount of mismatch in order to become apparent in the analysis. At this point it is important to note that the main issue is not to establish the amount of mismatch necessary for definitive observation of the error, but rather, upon observing poor performance to have the ability to deduce the source of that error. Obviously, if the mismatch or detuning in a process is not significant enough to emerge in the analysis, it is not likely that modifications are warranted nor would they necessarily improve the system performance. Let us consider a process under both detuned and tightly tuned control conditions. Given the same process-model mismatch it may not be diagnosed in the former control case because the controller is not as demanding while it may be clearly evident in the latter as the mismatch contributes more to the control moves. This difference will become apparent in the correlation analyses from the confidence intervals, as they allow true statistical properties to be distinguished from random error.

In order to facilitate the analysis a visual representation of all the information is beneficial. As discussed in Chapter 2 a correlation matrix is used to summarize the correlation information. Depending on which matrix elements show significant correlation, controller inadequacy may be deduced. Of course, the base or perfect

control case correlation matrix will exhibit no significant correlation in any of the correlation matrix elements other than the autocorrelation. In this latter case the correlation will be eliminated beyond the dead time lag of the process. Therefore, an "X" will only be placed in the $Y_t * Y_{t+k}$ element if correlation exists beyond the process dead time. Figures 3.27 and 3.28 show the correlation analysis results in correlation matrix format, taken from the examples shown in Figures 3.21 and 3.25. Figure 3.27 shows significant correlation occurring only in the output autocorrelation. Therefore, it is apparent that the feedback controller is only detuned as the feedforward controller is functioning well and no model mismatch exists in the system. Figure 3.28 shows significant correlation from the measured disturbance to the output variable, in addition to significant output autocorrelation beyond the dead time. As a result of the former, the feedforward control is determined to be non-optimal. Further data collection under controlled variable setpoint changes is then required. Analysis of the correlation between $(Y_{sp})_t$ and $(Y_m - Y_p)_{t+k}$, as shown in the feedback-only examples, is necessary to determine the exact cause of error. These are the same diagnoses made previously but the matrix format allows clearer access to all the information and therefore easier interpretation.

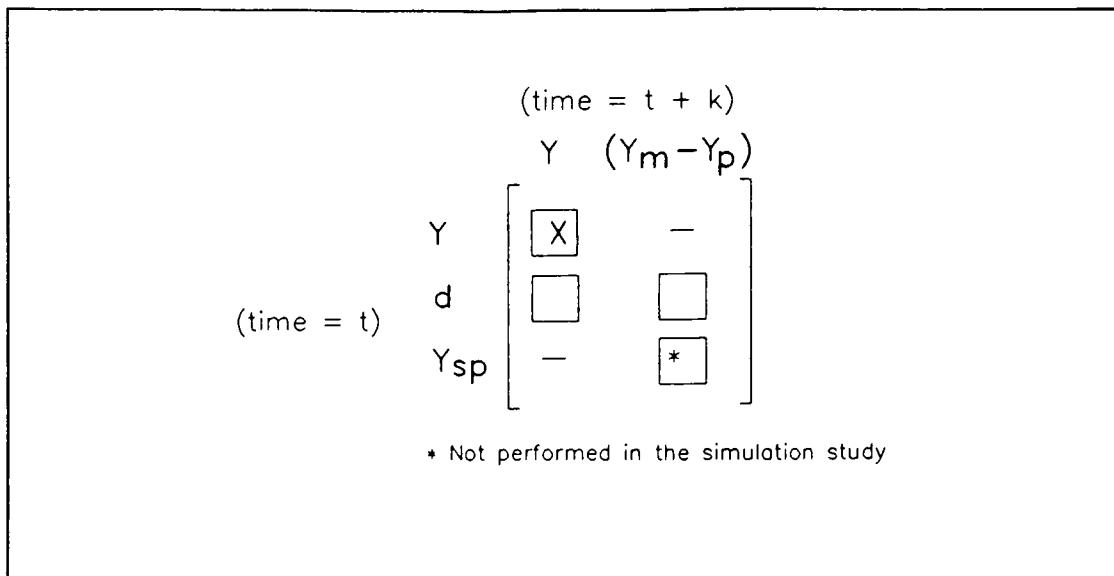


Figure 3.27 Feedforward-Feedback, Detuned Feedback Example

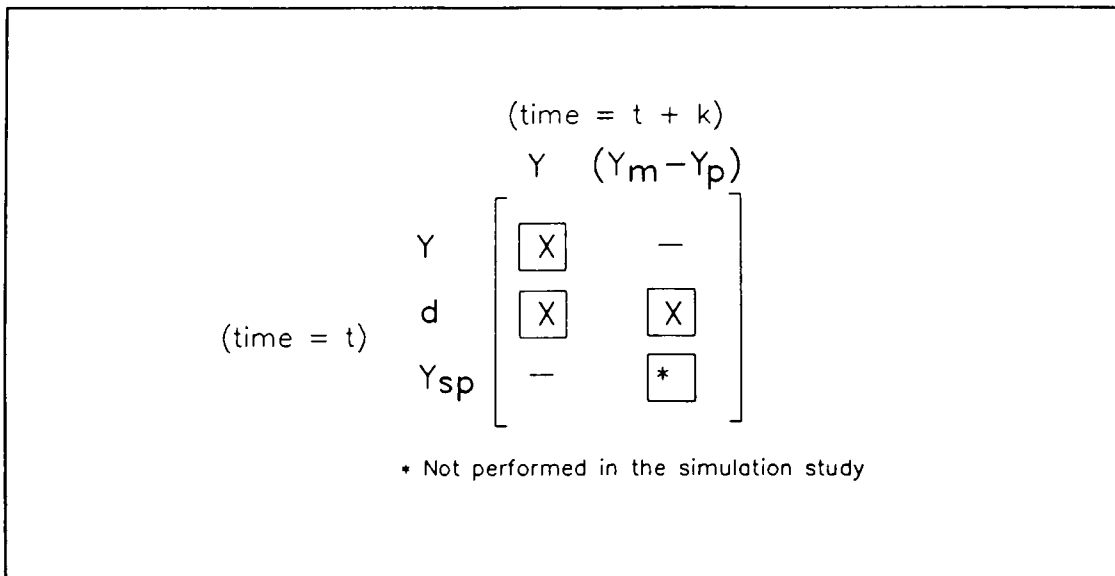


Figure 3.28 Feedforward-Feedback, Process Model Mismatch Example

This matrix representation may not be crucial in the analysis of this low dimension problem but it clearly simplifies diagnosis in the multidimensional problems to be encountered in the MIMO examples. Matrix representation will be further developed in the MIMO section of this report, but the concepts follow directly from the previous examples.

This investigation of a feedforward - feedback control system has shown that the use of the statistical autocorrelation and crosscorrelation functions is a successful performance diagnostic tool. The examples given have demonstrated the diagnostic procedure which allows control inadequacies to often be distinguished between tuning and model mismatch and in the case of the latter between the disturbance and process models.

3.2.2 EMPIRICAL STUDY OF A DISTILLATION TOWER AT SHELL SCOTFORD REFINERY

The approach used for the simulations in the previous section was then applied to an industrial example. A lead/lag feedforward - PI feedback controller was implemented on a Stabilizer bottom temperature at the Shell Canada Products Ltd., Scotford Refinery. The lead/lag feedforward controller

was reduced to a simple dead time block as the lead and lag elements cancelled. The bottom temperature is controlled via hot oil flow to the column reboiler while the tower liquid feed flow acts as the feedforward variable.

A simple schematic of the process is shown in Figure 3.29. The stabilizer is a 50 valve tray tower having two feed circuits, a liquid and a compressed vapour stream entering above trays 25 and 27 respectively. Both feeds come from the fractionator overhead drum where they are separated into the vapour and liquid streams. The overhead product consists primarily of C_3 , C_4 and C_5 components and feeds the gas recovery unit. The bottoms product is Light Hydrocrackate and consists mainly of C_6 components. The objective is to minimize iC_5 in the overhead product, which is measured by an on-line analyzer and is controlled by adjusting the Tray 45 temperature. This temperature controller is then cascaded to the top product flow while the accumulator level is maintained by adjusting the reflux flow. The vapour feed is only a small portion of the total feed to the column and the reflux to liquid feed ratio is approximately 0.85. The required heat input is supplied by a hot oil reboiler and an air cooler supplies overhead cooling.

An identification was performed on the process yielding the models shown in equations 3.9 and 3.10.

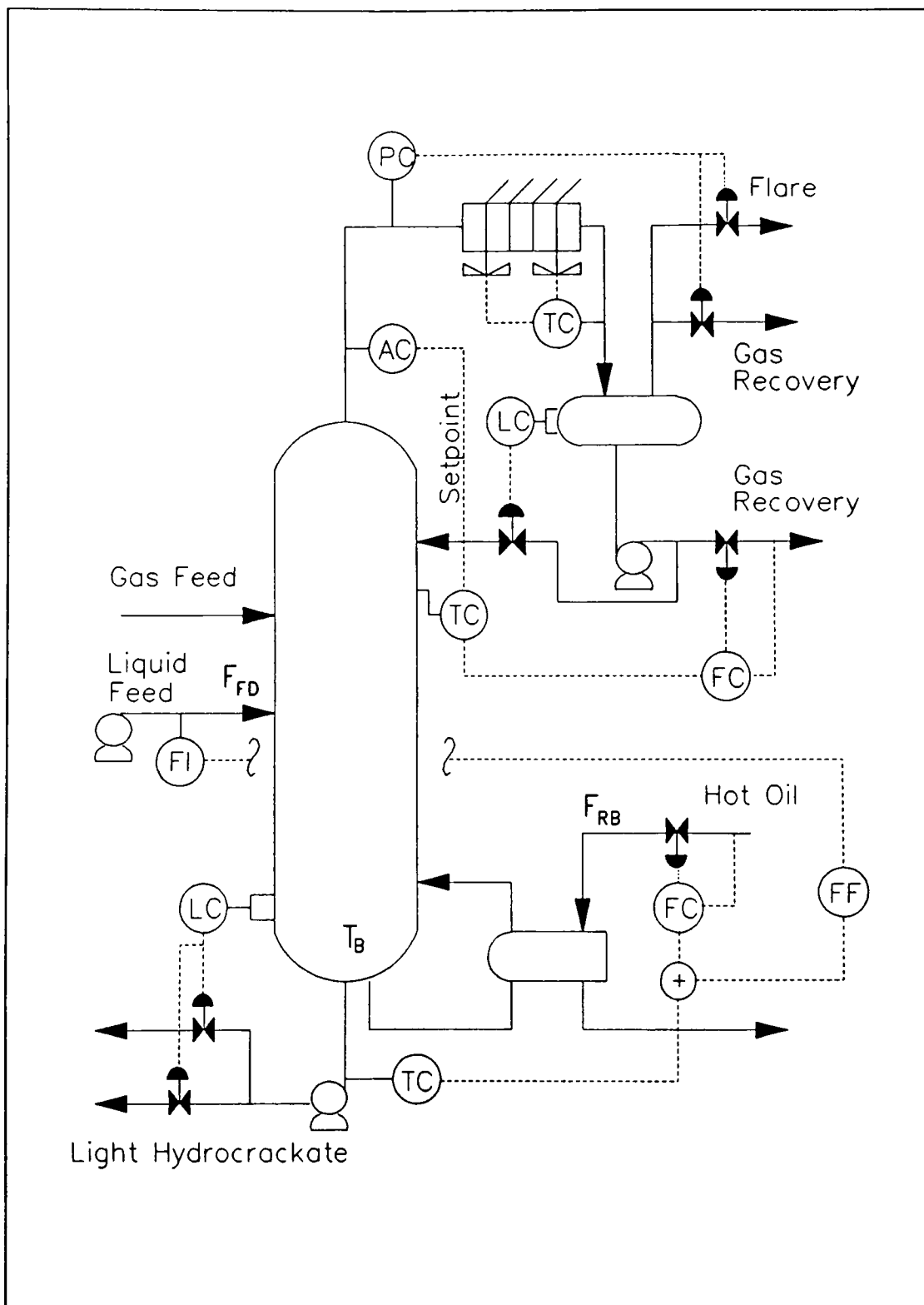


Figure 3.29 Process Schematic for the HCU Stabilizer

$$\frac{T_B(s)}{F_{RB}(s)} = G_p(s) = \frac{0.06 e^{-5s}}{7s + 1}$$

$$\frac{T_B(z)}{F_{RB}(z)} = G_p(z) = \frac{0.00761 z^{-6}}{1 - 0.875 z^{-1}}$$
(3.9)

$$\frac{T_B(s)}{F_{FD}(s)} = G_d(s) = \frac{0.07 e^{-9s}}{7s + 1}$$

$$\frac{T_F(z)}{F_{FD}(z)} = G_d(z) = \frac{-0.00932 z^{-10}}{1 - 0.873 z^{-1}}$$
(3.10)

The gain is in (°C)/(m³ flow) and the dead time and time constant are in minutes. The process and disturbance models were identified by imposing a pseudo-random-binary-sequence (PRBS) on the hot oil flow and the stabilizer feed flow, respectively, and using time series identification techniques to generate the appropriate relationships. [Box & Jenkins, 1976] The former had a magnitude of 10 m³/hr and a switching frequency of 5 minutes while the latter's magnitude and switching frequency were 7.5 m³/hr and 5 minutes, respectively. In both cases the sampling period used was one minute. The approximate conditions of the column are given in Table 3.2. During these identification experiments all overhead control loops were under automatic control and remained unchanged for the duration of the stabilizer study. An initial feedforward compensator and a PI feedback controller were then designed for the system. The

Table 3.2 HCU Stabilizer Conditions During Model Identification

HCU Stabilizer Conditions	
Feed Flow (F24039)	50 m ³ /hr
Bottom Temperature (T24835)	169 °C
Hot Oil Flow (UTOT)	107 m ³ /hr

following controller equations were used,

$$G_{cFF} = 0.73 z^{-4} \quad (3.11)$$

$$G_{cFB} : \quad K_c = 0.51 \quad (3.12)$$

$$T_I = 1$$

A block diagram is shown in Figure 3.30.

Data was collected and analyzed for the given process with various feedforward and feedback tuning parameters. In most of the test cases the stabilizer feed rate was perturbed using a PRBS signal in order to introduce forcing into the system. A PRBS of magnitude ranging from 3 to 5 m³/hr was used. It is important to note that initial model identification was performed under moderate rates to the unit, as given in Table 3.2, whereas the subsequent performance diagnosis was performed during both increases and decreases in the column throughput. This wide range in the operating point of the column introduced additional complexity in the

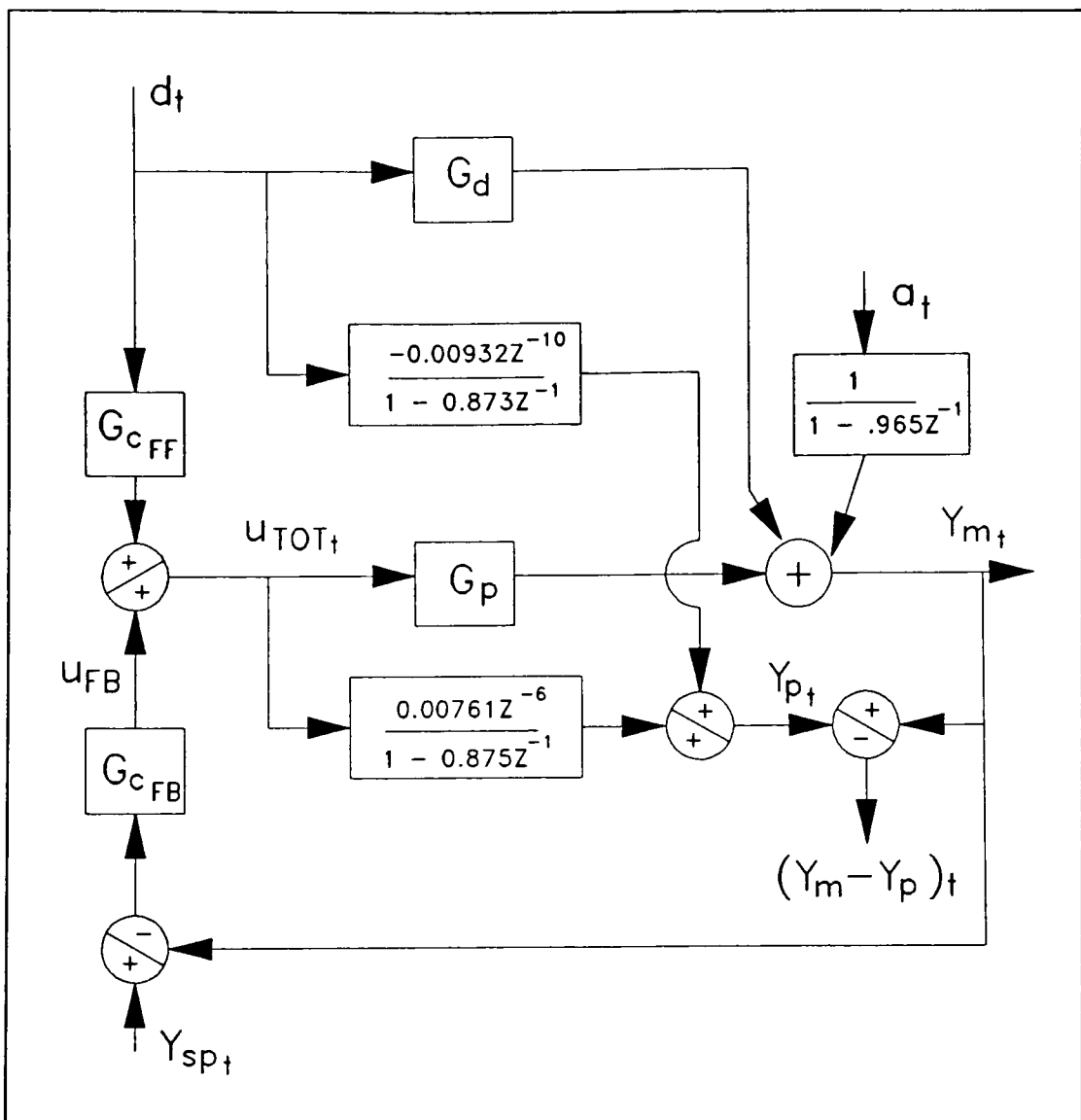


Figure 3.30 HCU Stabilizer Control Block Diagram

performance analysis. The relevant column conditions for each test case will be presented in the individual analyses and are included in the case summary presented in Table 3.3. The feedforward and feedback tuning parameters given in Table 3.3 have been scaled because of confidentiality concerns. The

TABLE 3.3 Summary of HCU Stabilizer Study

	** Tuning	Temperature (C)		Predicted Minimum Variance	Percent Difference	Feed (m ³ /hr)		UTOT Hot Oil (m ³ /hr)		UFB Hot Oil (m ³ /hr)	
		mean	variance			mean	variance	mean	variance	mean	variance
1	Kff = 0.73 Tid = Tig = 1 Kfb = 0.51 Ti = 1	165.871	0.077	0.0476	62	20.536	3.576	80.26	17.69	79.78	15.08
2	Kff = 0.40 Tid = Tig = 1 Kfb = 0.51 Ti = 1	165.905	0.133	0.0421	216	23.477	6.805	89.78	41.83	88.24	31.63
3	Kff = 0.73 Tid = Tig = 1 Kfb = 1.0 Ti = 1	165.008	0.0443	0.0328	35	21.706	2.954	78.22	20.49	76.72	17.33
4	Kff = 1.0 Tid = Tig = 1 Kfb = 1.0 Ti = 1	164.922	0.0935	0.0361	159	25.946	3.343	74.27	25.94	74.11	31.34
5	Kff = 0.0 Tid = Tig = 1 Kfb = 1.0 Ti = 1	163.048	0.0519	0.0219	137	59.847	9.593	111.50	20.16	111.54	21.14
6	Kff = 1.0 Tid = Tig = 1 Kfb = 1.0 Ti = 1	166.026	0.0243	0.0221	10	66.893	0.562	130.98	14.12	134.62	10.00
7	Kff = 2.0 Tid = Tig = 1 Kfb = 1.0 Ti = 1	163.453	0.127	0.0454	180	62.520	13.470	108.20	133.43	101.39	123.71

** Kff = Kfb = (m³/hr) / deg C
 Ti = Tid = Tig = min
 (scaled to a base of 1.0 for case no.4)

TABLE 3.3 Summary of HCU Stabilizer Study (continued)

	Tuning	K at last significant autocorrelation	significant [$d_t \cdot (Y_m - Y_p)_{t+k}$] correlations	number of significant [$u_{tot,t} \cdot (Y_m - Y_p)_{t+k}$] correlations
1	$K_{ff} = 0.73$ $T_{id} = T_{ig} = 1$ $K_{fb} = 0.51$ $T_i = 1$	9	9-12	1
2	$K_{ff} = 0.40$ $T_{id} = T_{ig} = 1$ $K_{fb} = 0.51$ $T_i = 1$	11	6-13	2
3	$K_{ff} = 0.73$ $T_{id} = T_{ig} = 1$ $K_{fb} = 1.0$ $T_i = 1$	9	9-12	1
4	$K_{ff} = 1.0$ $T_{id} = T_{ig} = 1$ $K_{fb} = 1.0$ $T_i = 1$	9	0	1
5	$K_{ff} = 0.0$ $T_{id} = T_{ig} = 1$ $K_{fb} = 1.0$ $T_i = 1$	12	1-7	1
6	$K_{ff} = 1.0$ $T_{id} = T_{ig} = 1$ $K_{fb} = 1.0$ $T_i = 1$	8	0	2
7	$K_{ff} = 2.0$ $T_{id} = T_{ig} = 1$ $K_{fb} = 1.0$ $T_i = 1$	12	15-23	2

* for MVC $K = 5$

tuning parameters corresponding to what was thought to be the best case, case 4 in Table 3.3, were given values of 1.0 and all other cases were scaled accordingly.

The process gain is the ratio of the change in the bottom temperature to the change in the reboiler flow. Similarly, the disturbance gain is the ratio of the change in the bottom temperature to the change in the feed flow. If we assume the top of the column to be under automatic control then both of these ratios and hence both gains are proportional to the feed flow rate. Since these gains are affected in the same manner the feedforward control gain, which is the ratio of these two values, should remain relatively constant in the event of feed flow rate changes. On the other hand the feedback controller gain is a function of the feed flow rate and as such should be in error as the feed flow fluctuates. As a result of the large feed flow changes experienced by the stabilizer during the testing phase it would be expected that the models originally identified would be incorrect and model mismatch would be observed at the more extreme flow rates.

Figure 3.31 shows the closed loop performance of the system under the feedforward and feedback control conditions given in Equations 3.11 and 3.12. This corresponds to trial number 1 in Table 3.3. The crosscorrelation between the feed

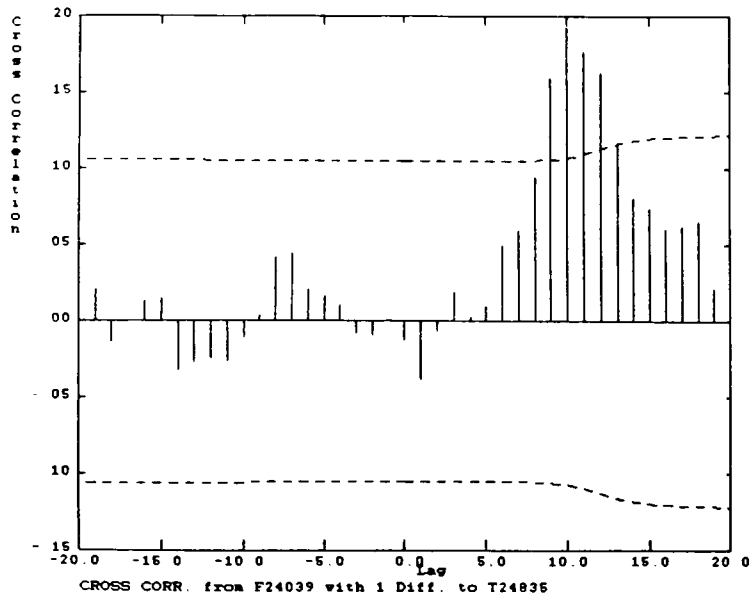
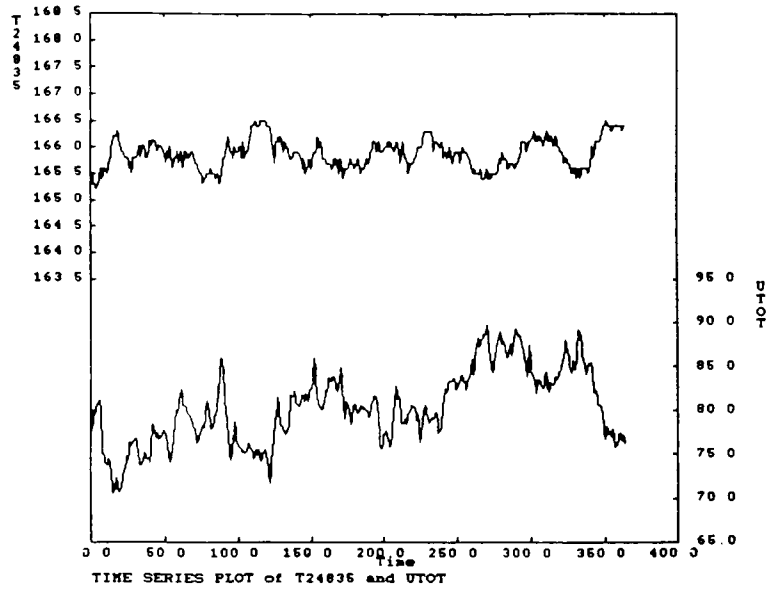


Figure 3.31(a,b) HCU Stabilizer, Initial Control Example

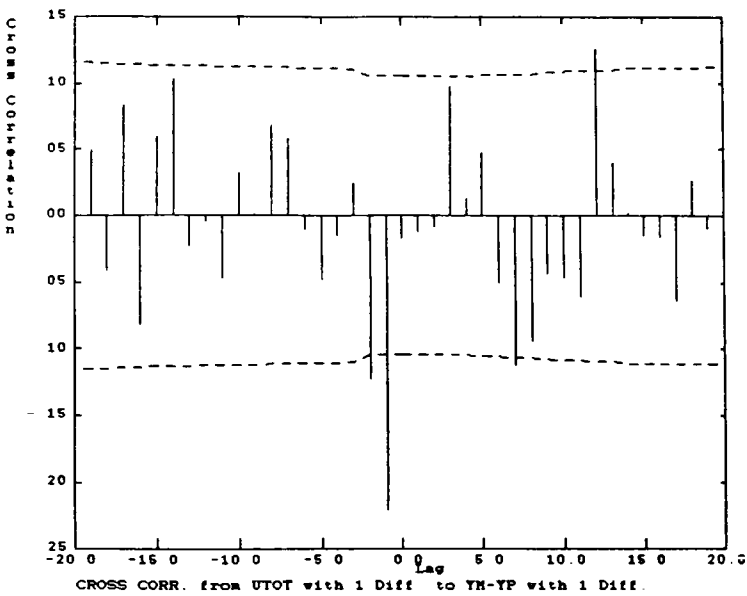
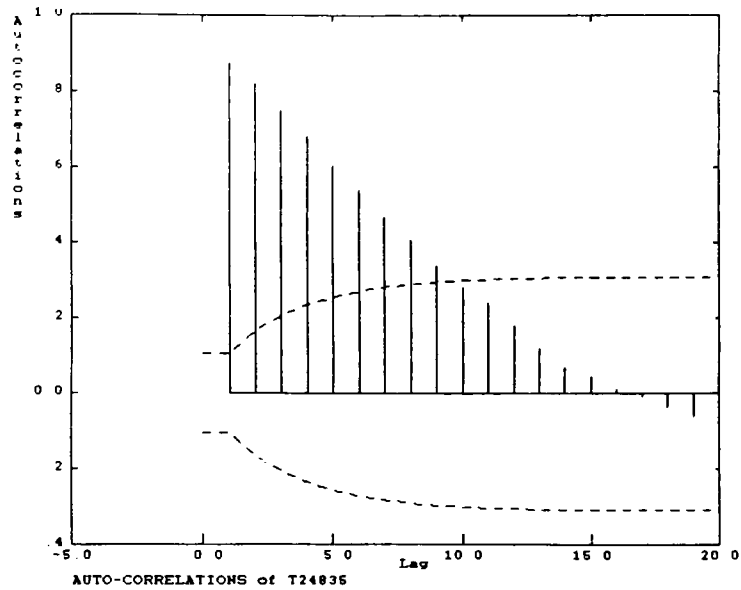


Figure 3.31(c,d) HCU Stabilizer, Initial Control Example

and the bottom temperature shows significant correlation at time intervals nine to twelve, which indicates inadequate feedforward compensation. The autocorrelation function is reduced to zero after nine time intervals which is greater than the five unit dead time, indicating less than minimum variance feedback performance. The bottom temperature appears stationary with a variance of $0.077 \text{ (}^\circ\text{C)}^2$. This is a 62% increase from the predicted minimum variance of $0.0476 \text{ (}^\circ\text{C)}^2$, as calculated in Appendix G. Although not conclusive, the crosscorrelation plot between the input and the model prediction error, showing only a couple small correlations, implies absence of model error. It is questionable whether this is statistically significant but may be interpreted as an indication of either correlated noise or model error.

In trial number 2 the feedforward gain was decreased by 45% yielding the results shown in Figure 3.32. It is important to note that when the feedforward gain is changed the corresponding change in the disturbance model gain is also made. In this manner the disturbance model is kept updated and thus model mismatch can be investigated. The feedback controller parameters remained unchanged. The control of the bottom temperature degraded with this lower feedforward gain as evident in both the temperature response and the higher temperature variance of $0.133 \text{ (}^\circ\text{C)}^2$. This variance represents a 216% increase from the calculated minimum variance of

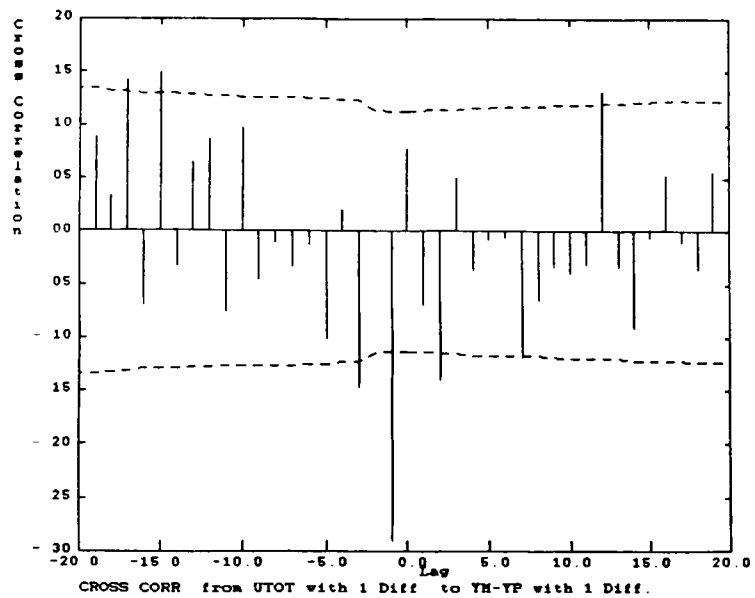
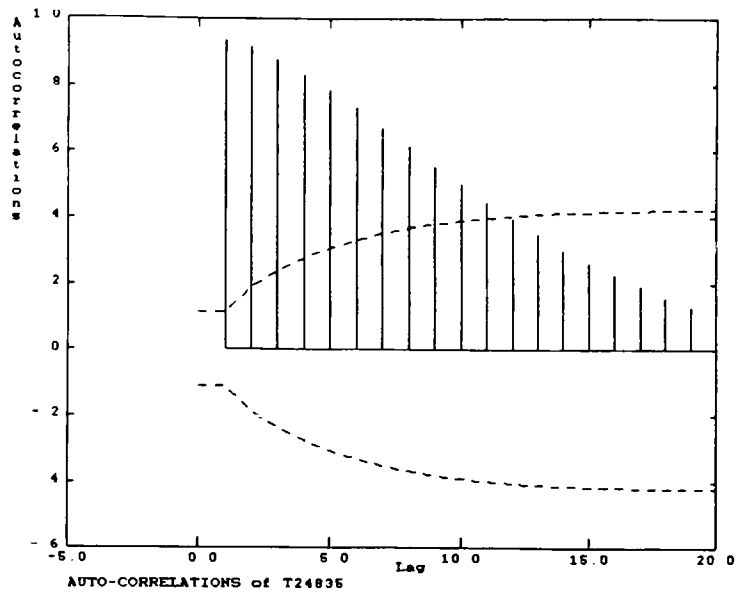


Figure 3.32(c,d) HCU Stabilizer, Decreased Feedforward Gain Example

0.0421 ($^{\circ}\text{C}$)². The crosscorrelation between the feed and the bottom temperature is shown in Figure 3.32b. This plot indicates poorer feedforward performance, as compared with the previous case, as the correlation values are larger and of a longer duration, existing between lags six and thirteen. The autocorrelation of the bottom temperature also shows degraded performance, requiring eleven time periods before damping out. The correlation plot between input and the model prediction error is not significantly different from the previous case. Once again, if model mismatch is present it does not appear to be a large contributing factor to the poor performance. It is evident, however, that the decrease in feedforward gain did not improve the performance of the control scheme. Therefore, other modifications must be made if improved performance is desired.

Figure 3.33 displays the control results obtained for the system with an increased feedback gain, corresponding to trial number 3. The feedback gain was doubled while the feedforward gain was returned to its initial value. The bottom temperature variance is at its lowest value thus far of 0.0443 ($^{\circ}\text{C}$)², which is only a 35% increase over the predicted minimum variance of 0.0328 ($^{\circ}\text{C}$)². The crosscorrelation plot between the feed and the bottom temperature is similar to the first case, as would be expected given the same feedforward tuning parameters. As in the former example significant

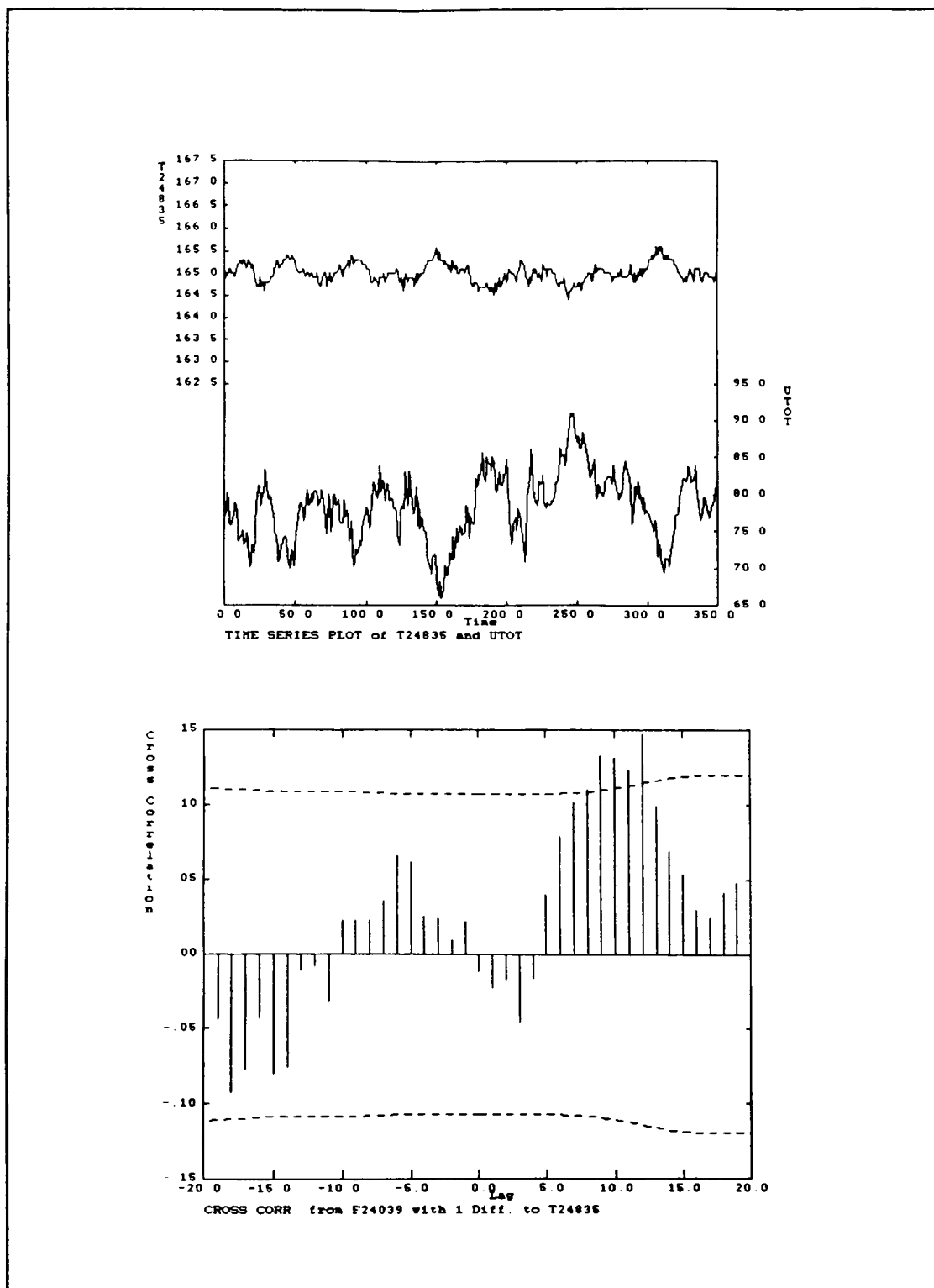


Figure 3.33(a,b) HCU Stabilizer, Increased Feedback Gain Example

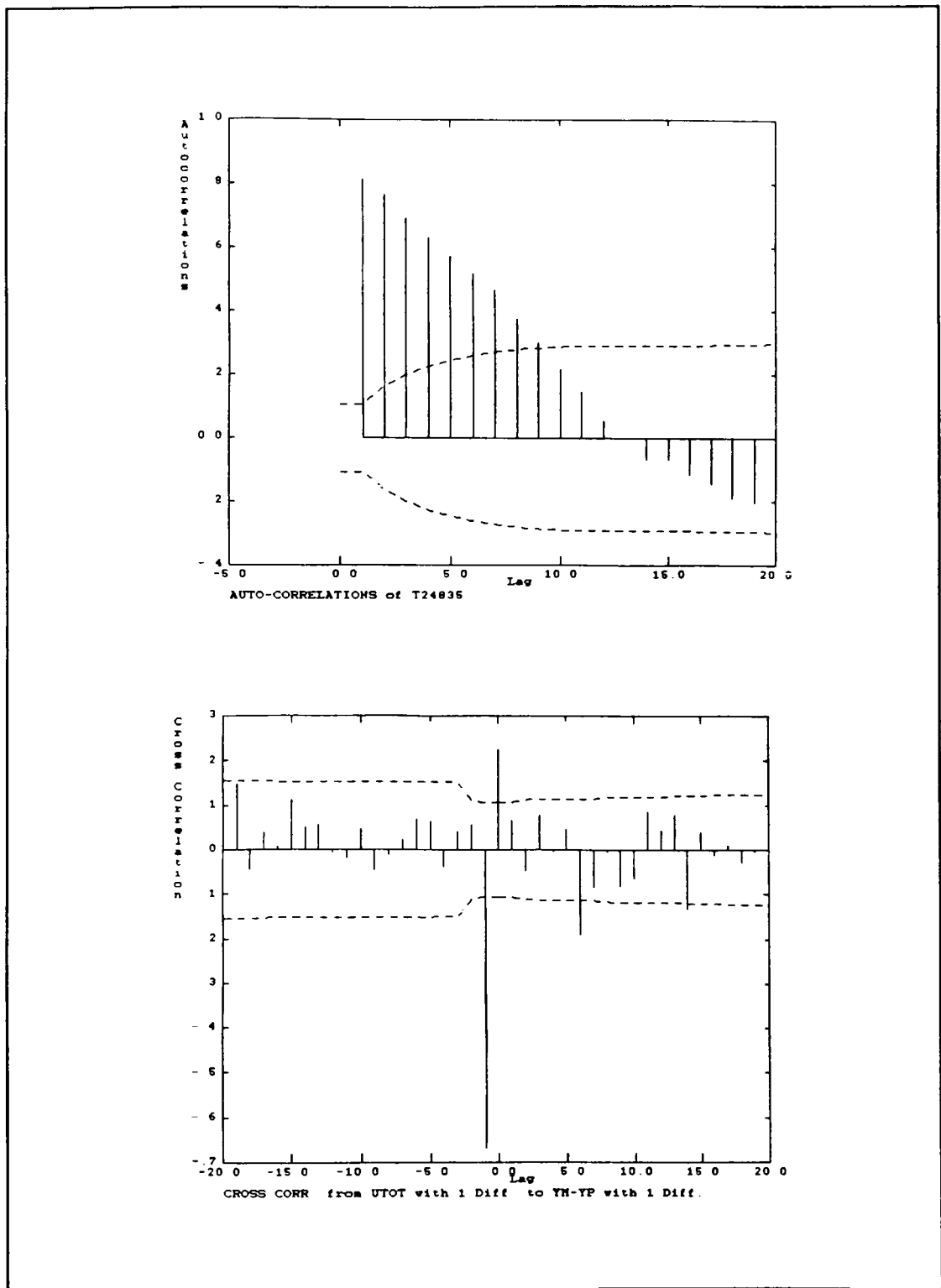


Figure 3.33(c,d) HCU Stabilizer, Increased Feedback Gain Example

correlation is observed between lags nine and twelve. This confirms the initial suspicion that feedforward modifications are required. Since decreasing the feedforward gain did not result in better control performance the next obvious step would be to increase the gain. The autocorrelation of the bottom temperature becomes negligible once again after nine time intervals. As with the previous cases, model mismatch does not appear to be a major concern as seen in the presence of only small, random correlation in Figures 3.33d. The higher feedback gain has resulted in improved performance over the first case and therefore should be maintained.

In the next trial the feedforward gain was increased by 40% while the feedback gain was maintained at its higher value. Refer to trial number 4 for actual control parameters. The correlation results for this case are shown in Figure 3.34. As was expected, the crosscorrelation between the feed and the bottom temperature has been completely eliminated, indicating perfect feedforward compensation. The autocorrelation of the bottom temperature, however, has not changed drastically, still being eliminated after nine time periods. Once again Figures 3.34d suggests acceptable models as only a few random lags show any significance. In order to confirm the presence of perfect models a case should be performed in which the feedforward controller is decommissioned and the data analyzed. This will be shown in

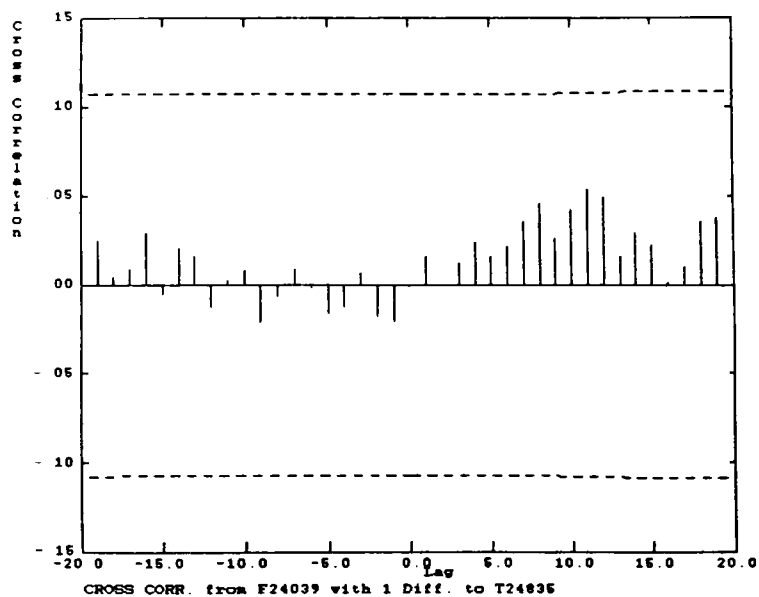
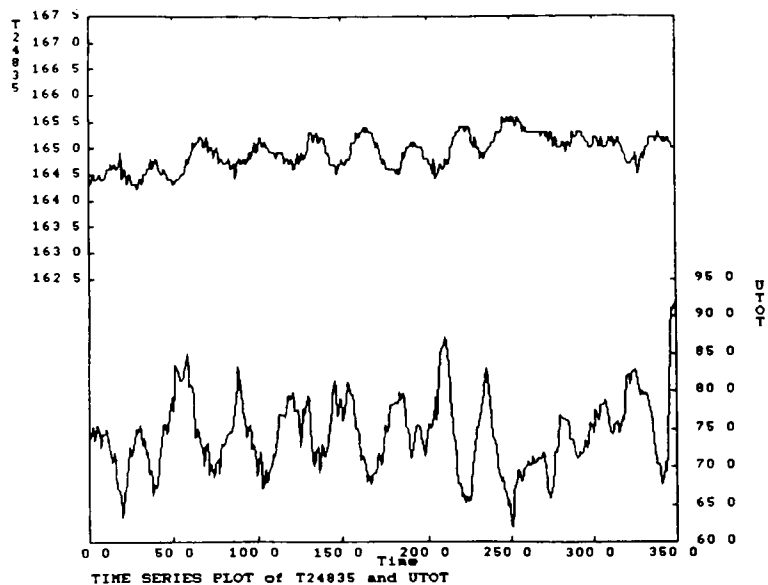


Figure 3.34(a,b) HCU Stabilizer, Increased Feedforward Gain Example

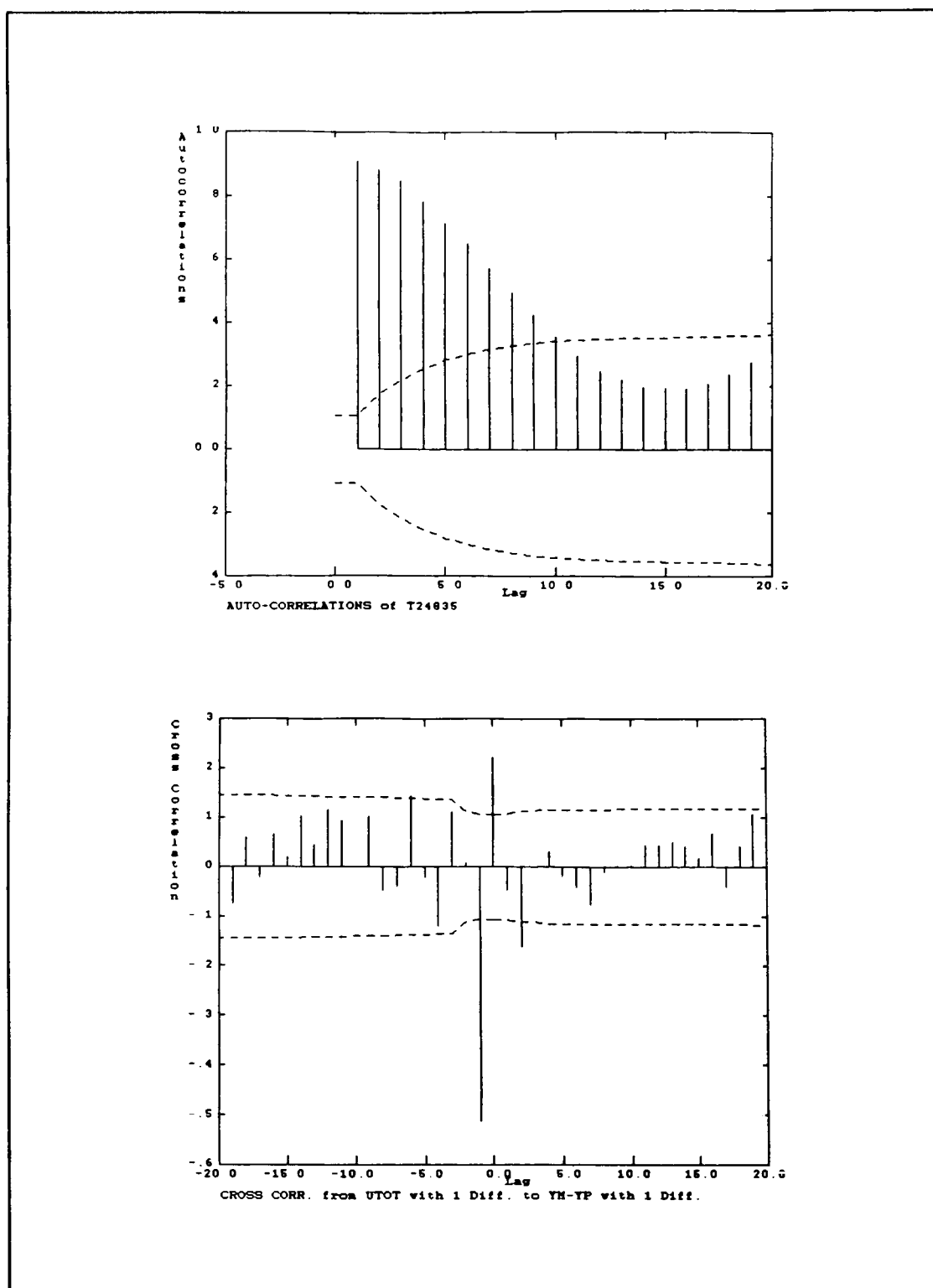


Figure 3.34(c,d) HCU Stabilizer, Increased Feedforward Gain Example

a following example. Nevertheless, this diagnosis suggests that the control scheme is adequate in all respects. Where this example deviates from what is expected is in the bottom temperature variance. A value of $0.0935\text{ }(^{\circ}\text{C})^2$ was calculated for the run which is a 159% increase from the predicted minimum variance of $0.0361\text{ }(^{\circ}\text{C})^2$. This large difference between the experienced variance and the lowest attainable variance is certainly not consistent with the correlation analysis results. It implies that the existing controller is not performing near the theoretical optimum while all the diagnostic criteria support a satisfactory control scheme. Additional investigation into this case study did not reveal any obvious causes for the discrepancy. Unmeasured disturbances may have adversely affected the analysis. A repetition of this test run may have produced other, more consistent results. The use of larger data sets over extended periods of time may have eliminated this difficulty.

The previous results were obtained for the system under the decreased feed flow rates. As discussed initially, it would be expected that the feedback controller would be affected by this deviation while the feedforward controller would not. The following examples were generated when the flow rate was increased by as much as 50%.

Trial number 6, the results of which are shown in Figure 3.35, was performed with the same tuning parameters as with the previous case but with no feed perturbation. As would be expected for the well controlled system the correlation analysis shows an output autocorrelation which damps out after eight time intervals and no correlation in any of the crosscorrelation plots. Furthermore, the attained temperature variance of $0.0243 \text{ (}^\circ\text{C)}^2$ is only 10% larger than the predicted minimum of $0.0221 \text{ (}^\circ\text{C)}^2$. Hence, it appears that these tuning parameters result in good control performance. This is consistent with the diagnosis obtained for the previous case, in which the feed was perturbed. The evaluation of the best achievable control performance for that example, however, was inconsistent as it implied significant improvement to be possible.

In order to verify the accuracy of the models, control of the bottom temperature was then attempted without feedforward control, although the feed flow rate was perturbed. Trial number 5 in Table 3.3 summarizes this case. The results of this example are given in Figure 3.36. The temperature variance of $0.0519 \text{ (}^\circ\text{C)}^2$ is 137% greater than the minimum variance calculated at $0.0219 \text{ (}^\circ\text{C)}^2$. The crosscorrelation between the feed flow and the bottom temperature shows significance between time interval one and seven which indicates poor feedforward compensation or in this

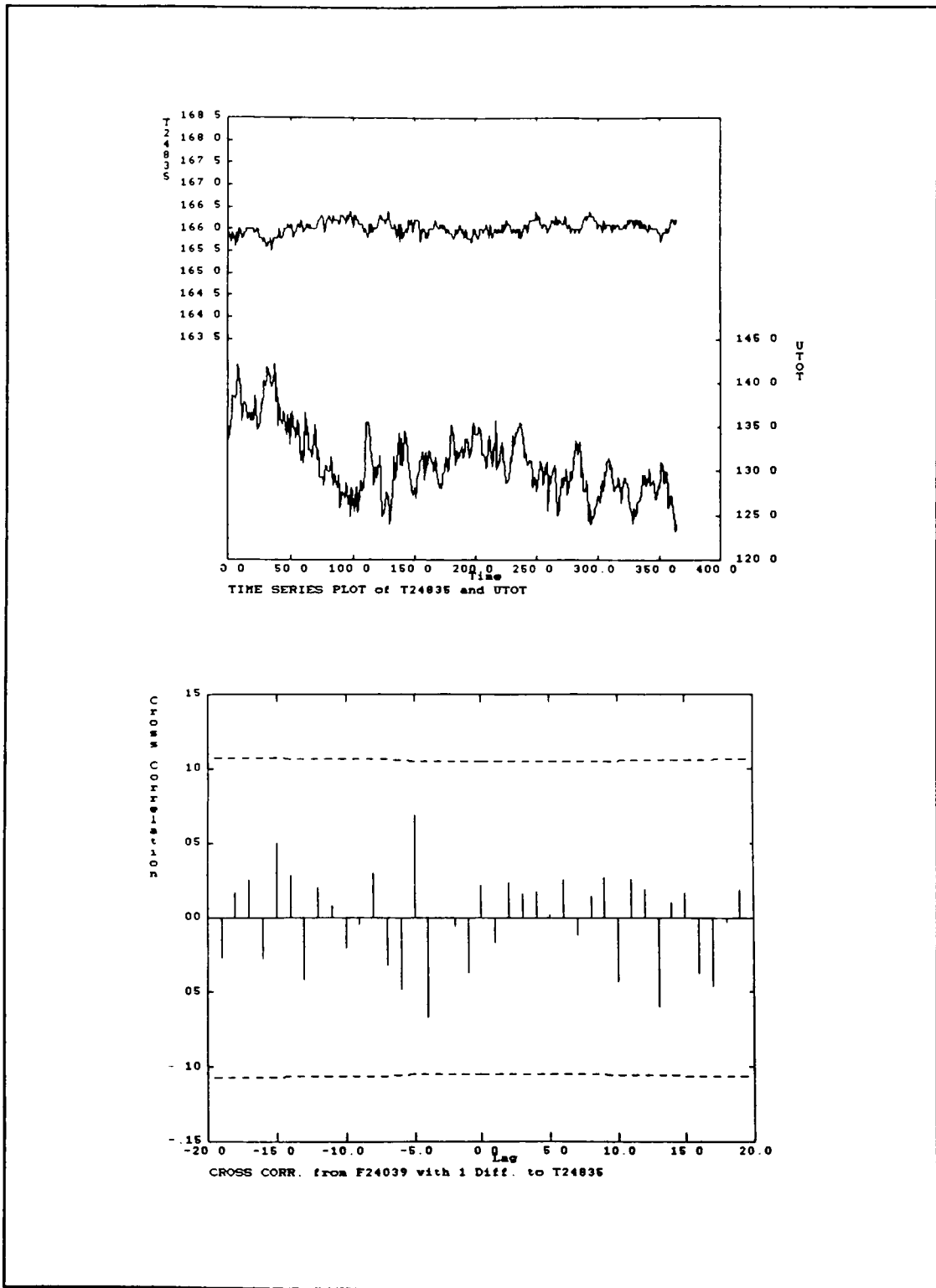


Figure 3.35(a,b) HCU Stabilizer, No Feed Perturbations Example

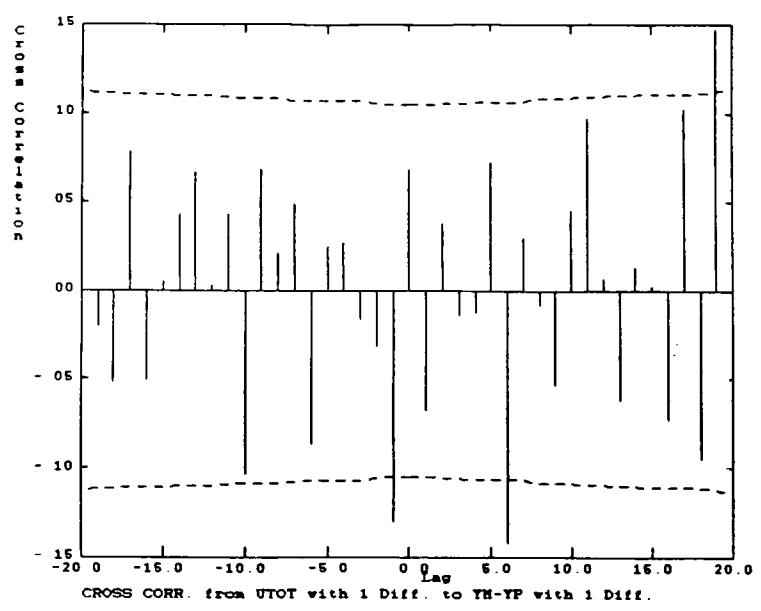
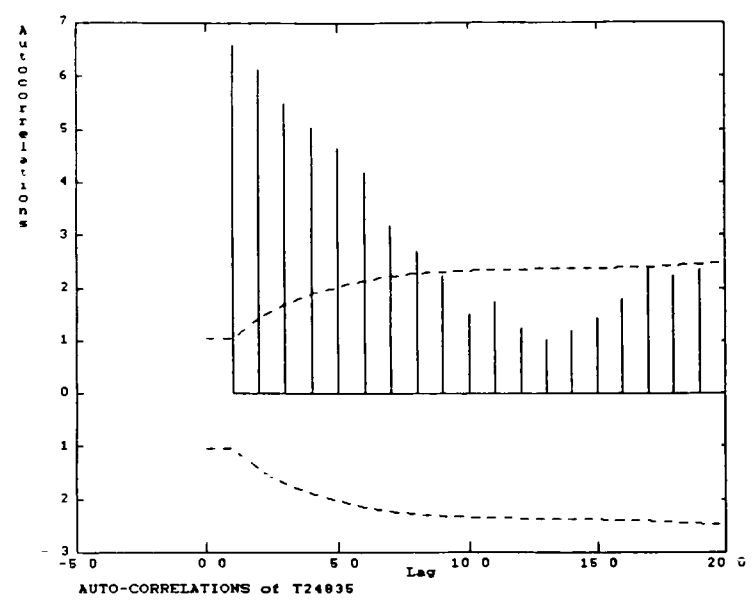


Figure 3.35(c,d) HCU Stabilizer, No Feed Perturbations Example

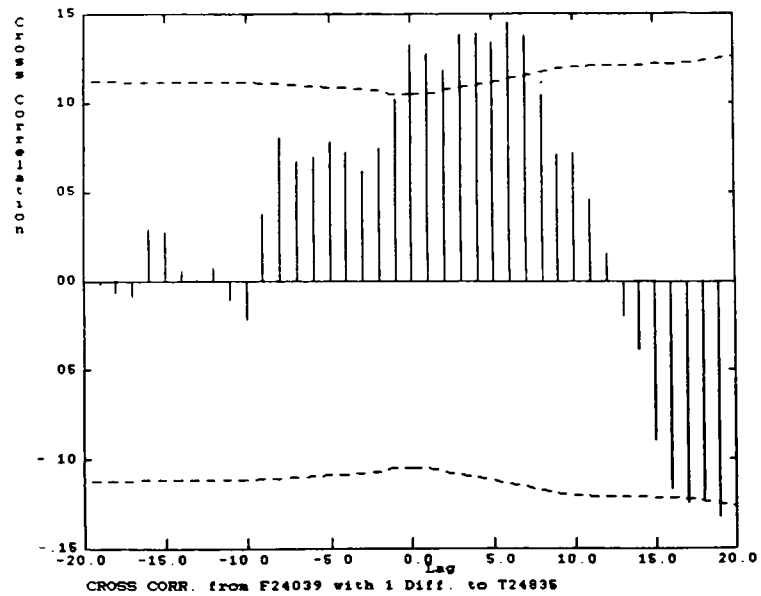
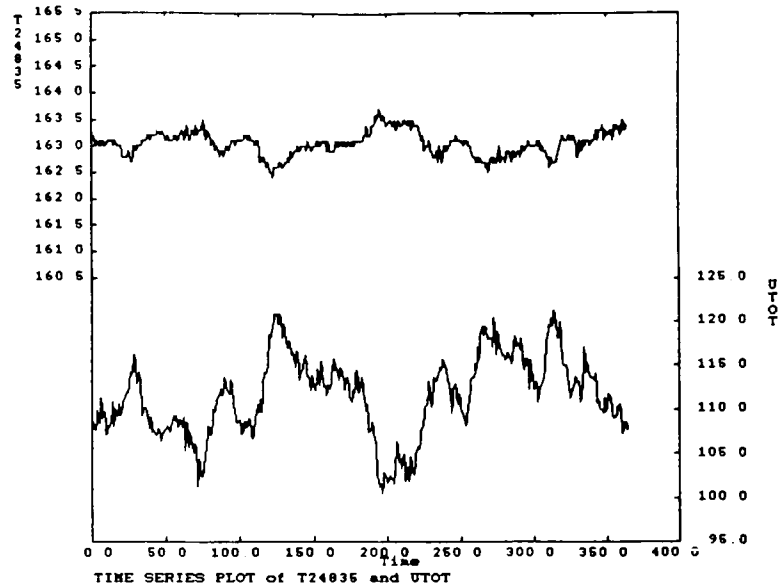


Figure 3.36(a,b) HCU Stabilizer, No Feedforward Control Example

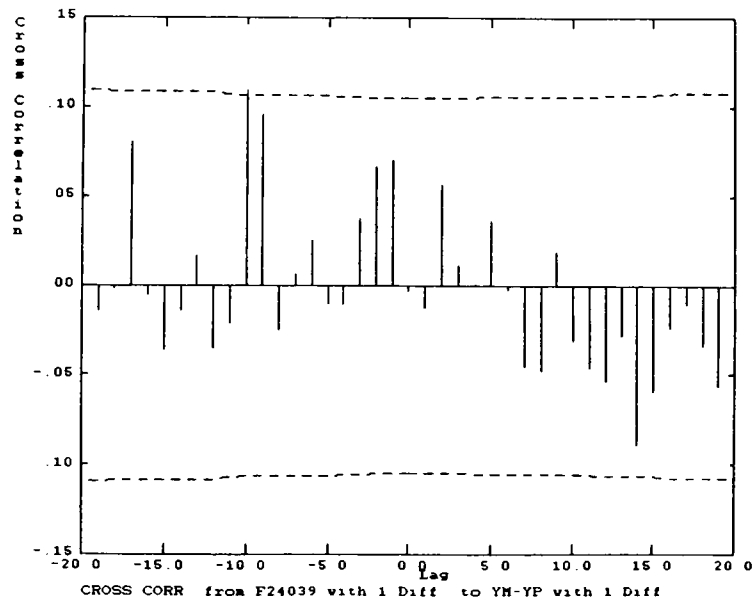
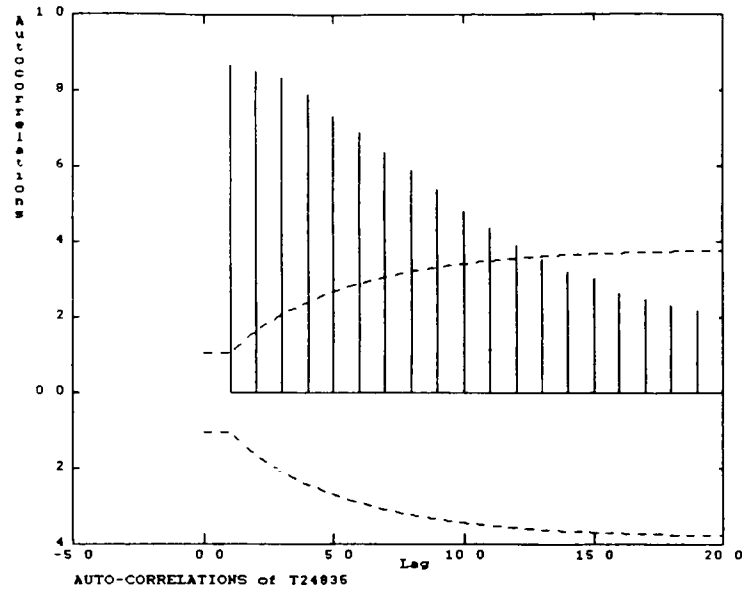


Figure 3.36(c,d) HCU Stabilizer, No Feedforward Control Example

case, the absence of it. The zero-crosscorrelation between the measured disturbance and the model prediction error indicates that the disturbance model is essentially perfect, hence the process model must also be perfect. Therefore, the performance in the last example could only be improved by tuning of the feedback controller or a different choice of feedback algorithm.

The final example studied, trial number 7, is displayed in Figure 3.37 which is the result of an excessive feedforward gain. The temperature variance is at its highest value thus far of $0.127 \text{ (}^\circ\text{C)}^2$ which is 180% greater than the predicted best achievable case. Inadequate feedforward control and possible model mismatch are apparent from the significant correlation obtained in the crosscorrelation plots between the feed flow and the bottom temperature and between the input and the model prediction error, respectively. Therefore, it is apparent that this modification to the feedforward controller has degraded the control system performance. The parameters of the feedforward controller should be returned to their previous values.

All of these results were summarized in Table 3.3 and all calculations are included in Appendix G. This industrial case study has illustrated some of the analysis methodology introduced in the simulation examples and has demonstrated the

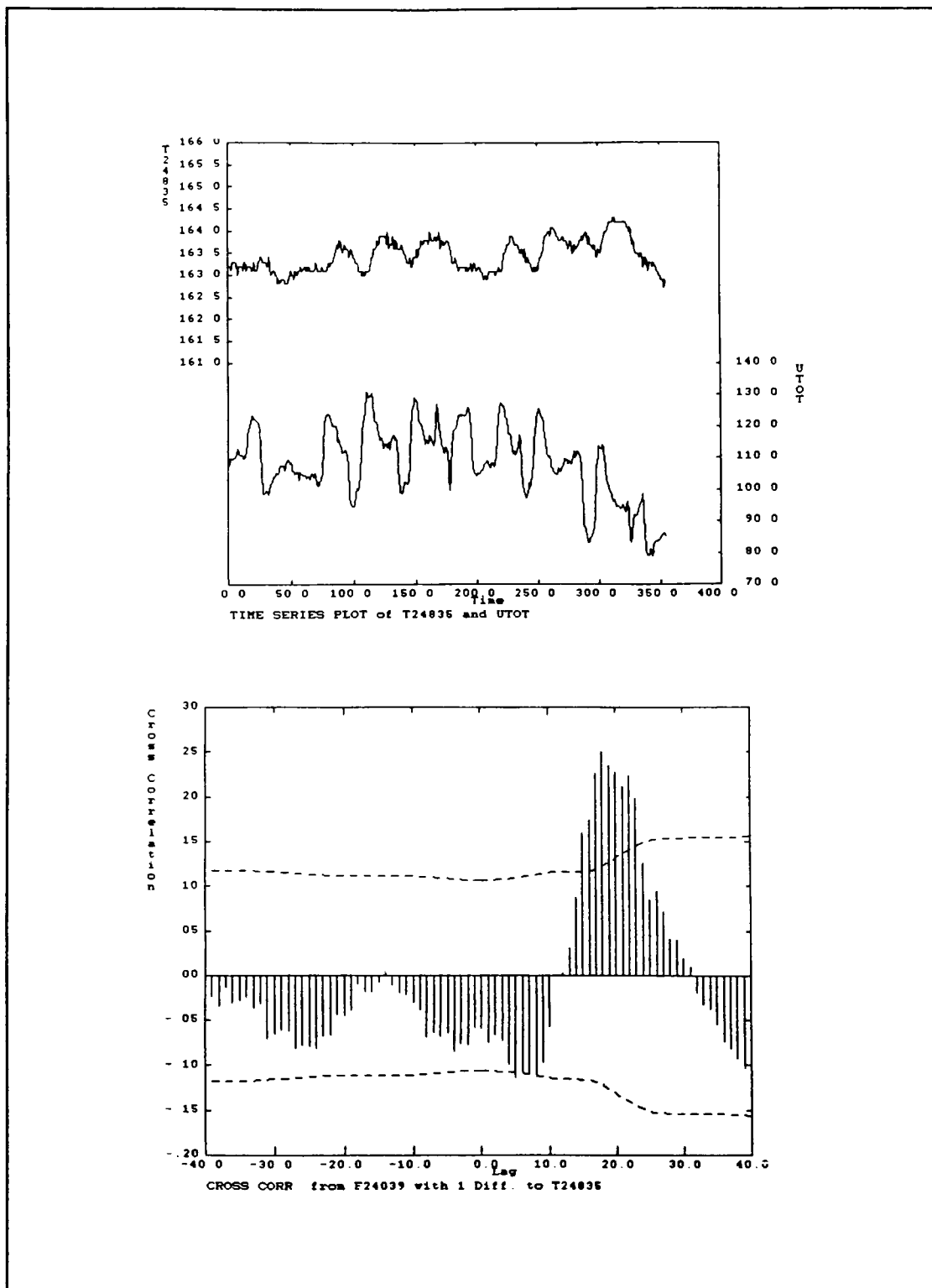


Figure 3.37 (a,b) HCU Stabilizer, Excessive Feedforward Gain Example

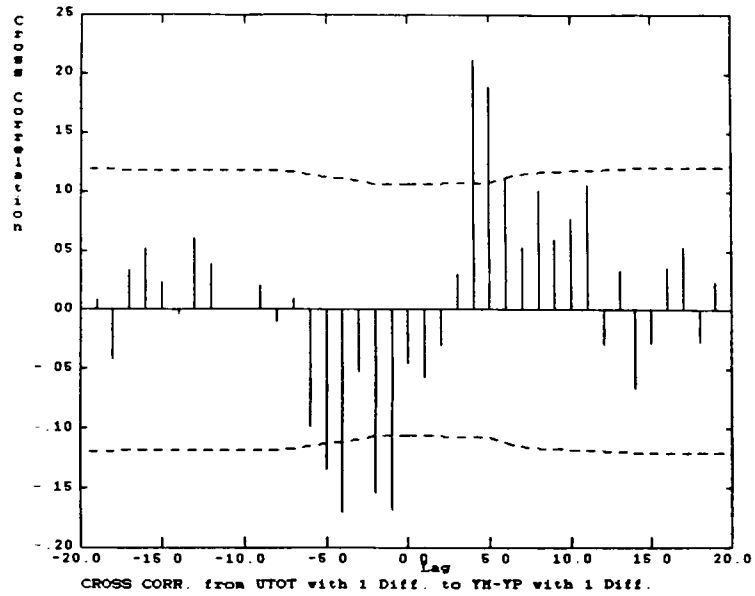
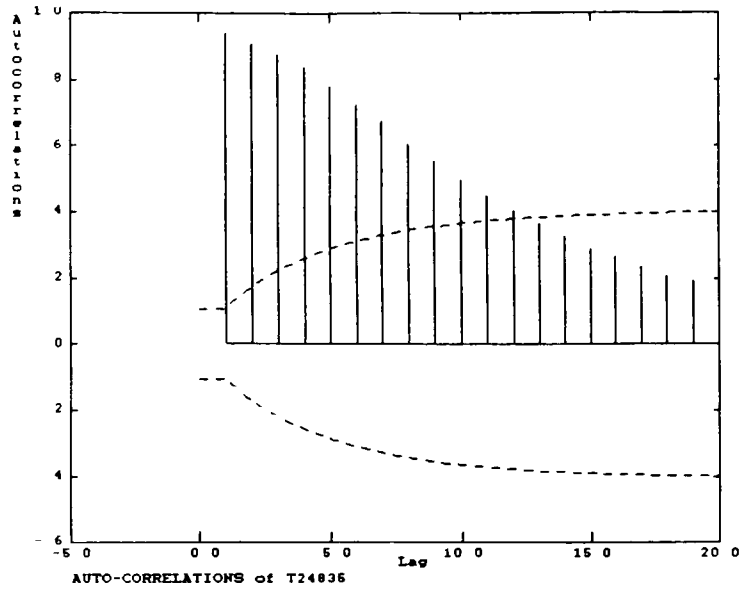


Figure 3.37(c,d) HCU Stabilizer, Excessive Feedforward Gain Example

usefulness of this control performance evaluation and diagnosis technique. Some inconsistencies have been observed as can be expected in dealing with relatively small sets of experimental data. Reproducing tests which lead to questionable results may be necessary for the successful use of this tool. The advantages of having this procedure on-line would be the recursive generation of the relevant statistical parameters. In this manner the results could be monitored over time and the results would be verified.

4.0 MIMO CONTROL SYSTEMS

The success of the diagnostic procedure was then examined for Multi-Input-Multi-Output (MIMO) systems. The basic interpretations developed in the SISO studies are still applicable here, as will be demonstrated. The analysis of the feedforward-feedback example with the introduction of the matrix representation serve as the foundation for the MIMO analysis.

Multivariable control schemes are becoming more common in industry and as such it is important to include them in this research. The sudden popularity of the (Quadratic) Dynamic Matrix Control, (Q)DMC, algorithm reflects an attitude that these schemes can solve a wide range of control problems. Because of their complexity and the interdependence of the inputs, outputs and disturbances, performance evaluation and diagnosis is challenging. The initial results in this chapter are from a simulation case on a 2x2 example which will illustrate the relevant concepts. Subsequently, the evaluation methodology developed is applied to an industrial QDMC case. These examples will present the capabilities and the limitations of the analysis methodology being used.

4.1 SIMULATION RESULTS

The control block diagram for the 2x2 system is shown in Figure 4.1. Several models with different degrees of interaction and the same process configuration were examined and analyzed. In all cases a Linear Quadratic Gaussian, LQG, controller [Astrom & Wittenmark, 1984] was designed for the processes with varying weights imposed on the inputs and outputs in order to realize a broad range of performance. The details for each case study, including the process model transfer functions and the control equations, are included in Appendix H.

Initially, a simple system was studied having uncorrelated disturbances and minimum dead times which appeared on the diagonal. Once these cases were studied and a methodology was developed and proven, variations were added to the analysis. Complexities such as correlated disturbances, which are more common in industrial settings, and dead time imbalances were introduced in order to determine the capabilities and limitations of the diagnostic procedure. Finally, sparsity was introduced in the system matrix and the analysis simplifications were observed. The specific concerns associated with each of these configurations were discussed in Chapter 2. The procedure outlined in the section pertaining to MIMO systems is followed in the succeeding examples.

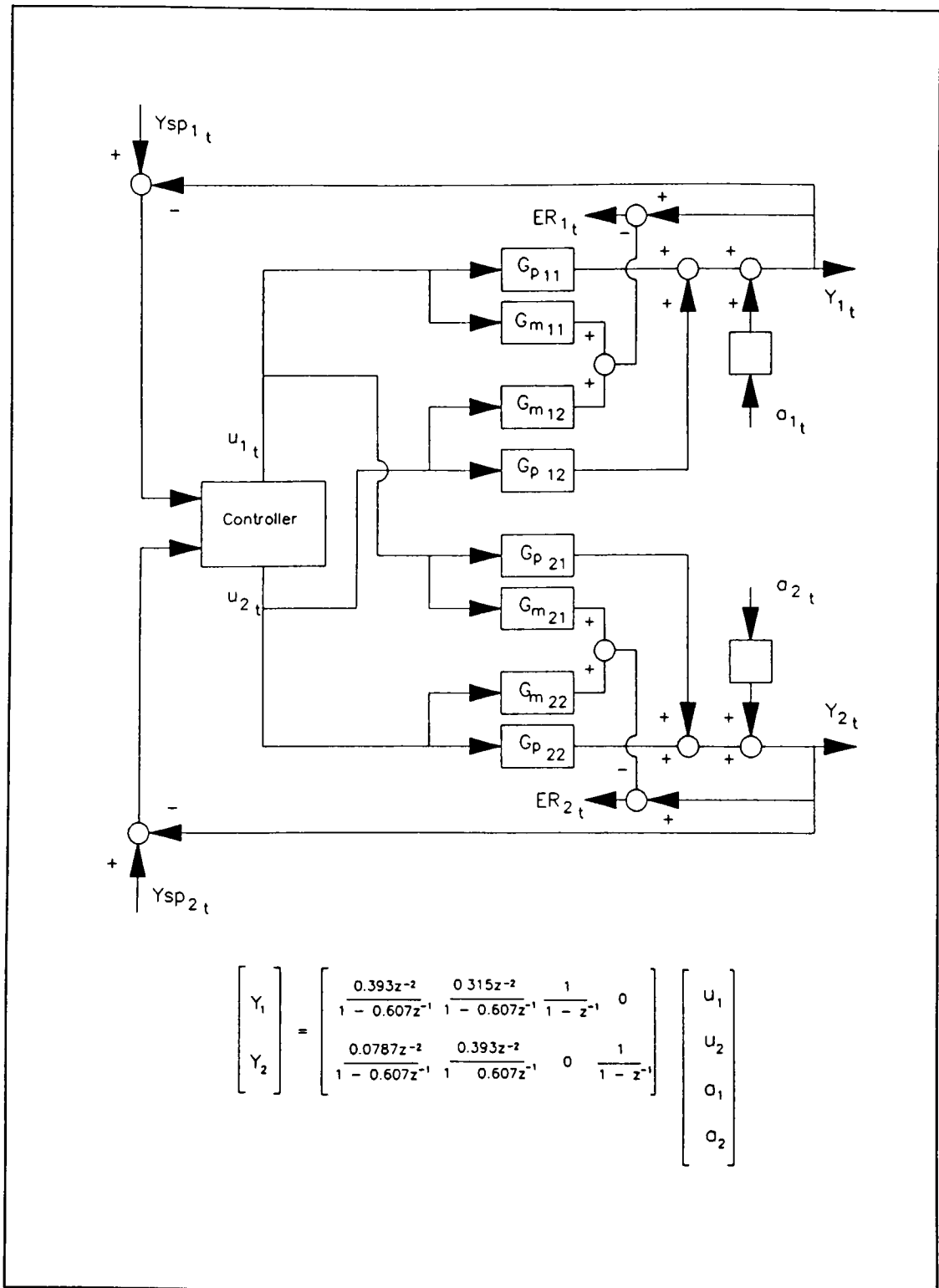


Figure 4.1 Control Block Diagram for 2x2 MIMO System

As introduced in Chapter 2, the correlation matrix will be used to summarize the information required for performance diagnosis. Individual correlation plots for the cases examined can be examined in the Control Performance Evaluation and Diagnosis Laboratory Manual. [Stanfelj, 1990]

The following results pertain to the simple process configuration having uncorrelated noise and minimum dead times appearing on the diagonal. The latter information is critical in establishing the minimum number of lags for each output, prior to which control can have no effect and beyond which all correlation can be eliminated given perfect control. In the instance that the minimum dead times do appear on the diagonal, the minimum number of significant lags for each output corresponds to this minimum dead time. This analysis is not as straightforward in the case when all of the minimum dead times do not appear on the diagonal and will be discussed in more detail presently.

Figure 4.2 shows the analysis matrix results for the base case. The base case consists of a perfect LQG controller, based on a correct process model, having equal weighting on both outputs and unlimited input moves. The autocorrelation of both outputs is reduced to zero after their respective minimum dead times of one unit. This is confirmed in the crosscorrelation between the inputs and the outputs

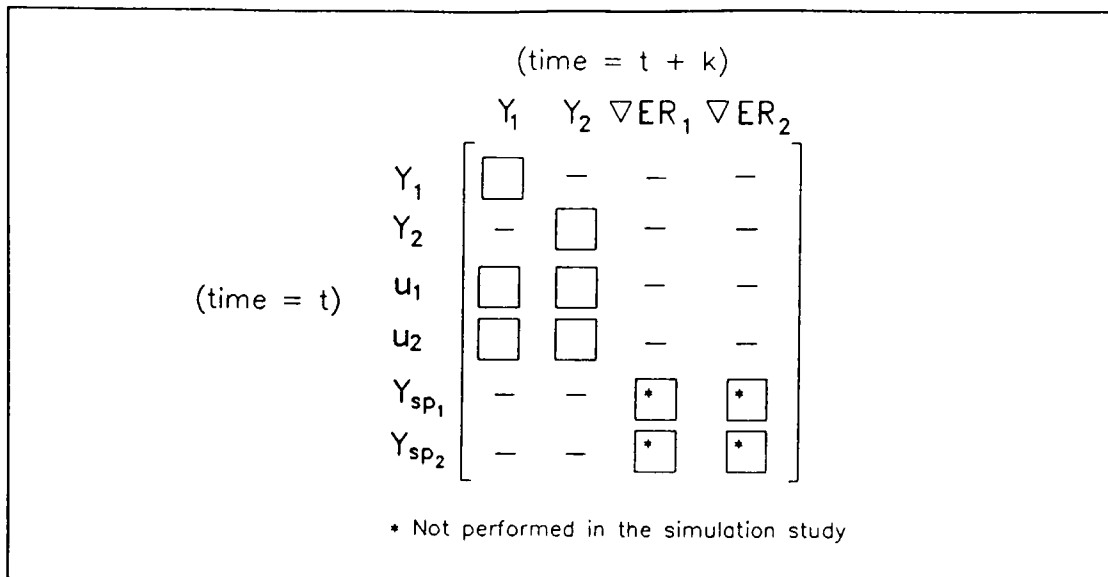


Figure 4.2 MIMO Base Case

which are also eliminated after the dead time. The variances of Y_1 and Y_2 are 2.127 and 1.908 while u_1 and u_2 experienced variances of 273.599 and 228.232, respectively. Although not shown in the correlation matrix, there was no correlation between the inputs and the model prediction errors. As described in Chapter 2, however, this diagnostic does not conclusively indicate the presence or absence of model error, under correlated noise conditions. Therefore, as described in the feedback-only case, setpoint changes would have to be introduced into the system and the data analyzed accordingly. Nevertheless, in the case of perfect models there should not be an "X" in any of the elements representing the crosscorrelation from $(Y_{sp})_i$ to ER_i .

This controller can be detuned by imposing penalties on the variances of the input manipulations. The results of the case in which equal penalties of 2.0 units are placed on both inputs are displayed in Figure 4.3. The output autocorrelations and the crosscorrelations between the inputs and the outputs show significant correlation beyond their respective minimum dead times, which suggests non-optimal control. Both outputs experienced greater variances than in the optimal control case, measuring 4.376 and 6.716 respectively. Once again, there was absence of correlation in the elements representing the crosscorrelation between the inputs and the model prediction errors, suggesting perfect models but not definitively. As in the last case, analysis should be done on plant tests having controlled variable

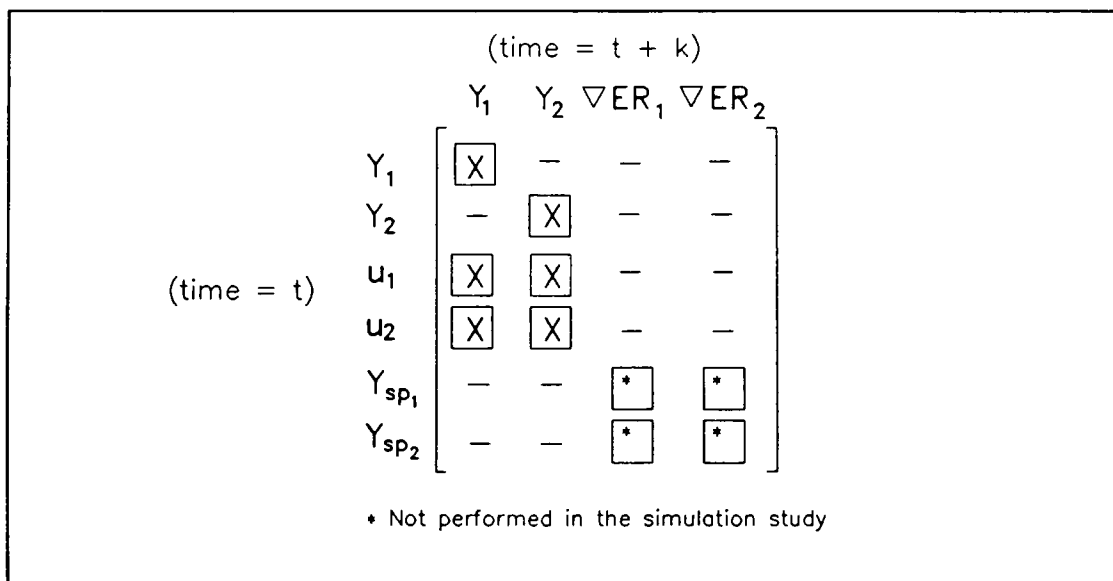


Figure 4.3 MIMO, Penalty Weights On u_1 and u_2

setpoint changes. The significant correlations in elements 1 through 6, however, do indicate improvement in the control performance of both Y_1 and Y_2 is possible.

The correlation matrix for the case in which only one of the inputs, u_1 , is penalized is shown in Figure 4.4. In this particular case the weight placed on u_1 was also 2.0 units. As with the previous example both output autocorrelations are marked with an 'X', indicating non-perfect control. Contrary to the previous example, however, this correlation matrix only shows significance between the first input and both outputs. This fact establishes that the degraded performance observed is the result of the first input only. Furthermore, model mismatch would be discounted as there would be no significant crosscorrelation between any

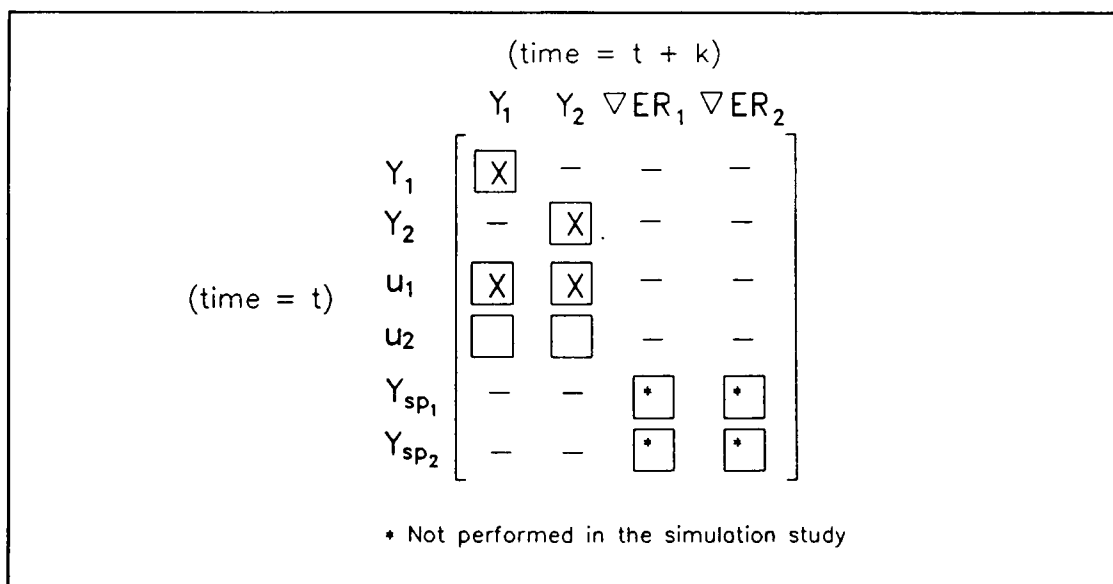


Figure 4.4 MIMO, Penalty Weight On u_1

setpoint changes and the prediction error. These last two examples demonstrate the success of differentiating between poor performance resulting from one or both of the inputs.

Figure 4.5 shows the correlation matrix representing several cases of model mismatch in which either or both of $G_m(1,1)$ and $G_m(1,2)$ are incorrect. In the particular case presented here, the gain of $G_m(1,1)$ was decreased while the gain of $G_m(1,2)$ was increased. Output weights remained constant at 1.0 units each and no penalty weights were put on the input moves. As is expected for non-optimal control, the

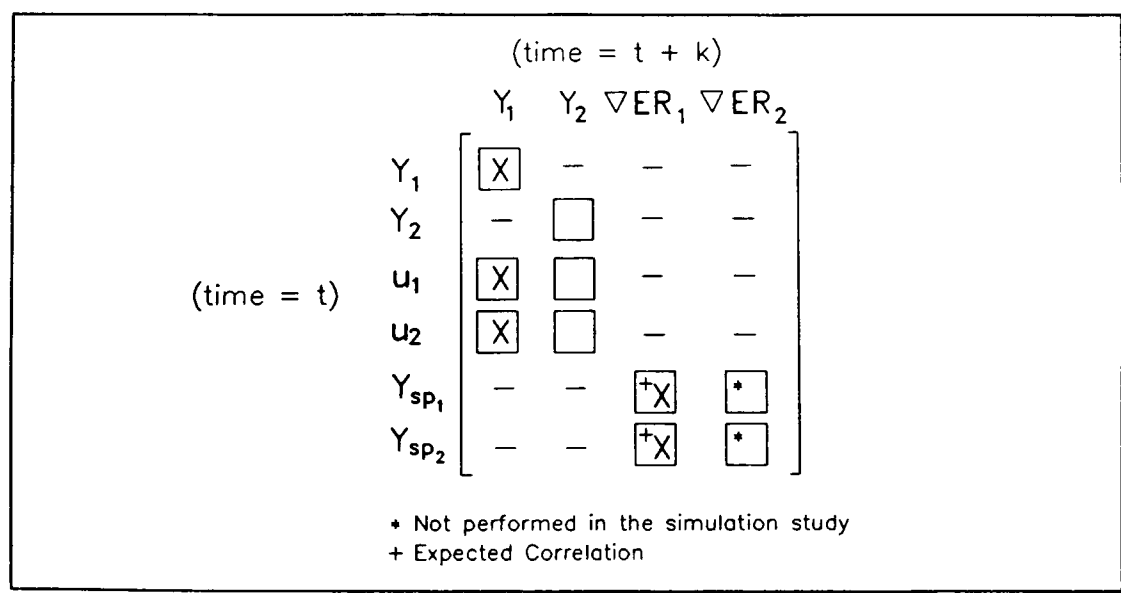


Figure 4.5 MIMO, Model Mismatch in $G_m(1,1)$ and/or $G_m(1,2)$

autocorrelation for Y_1 shows significant correlation beyond the dead time. Moreover, the variance of this output has increased 200%, measuring 6.639. The control of Y_2 is not affected, as apparent in the autocorrelation function and confirmed by a variance of 1.927, which compares well with the minimum value. The former is expected as the inaccurate models pertain only to Y_1 . Because of non-optimal control resulting from the modelling errors in Y_1 , however, it would be expected that the disturbance to Y_2 is different than that expected, hence the variance of Y_2 could be higher than the estimated minimum value. The variance obtained in this case, however, does not reflect this probability. As with many of the unexpected results obtained using this method it can be argued that the errors introduced to the system are not statistically significant and as such are not apparent in the analysis. Moreover, if the errors cannot be observed in this analysis they are not likely to be degrading the performance of the particular control scheme in question. Both of the input variances have increased dramatically from the base case, having values of 5.44×10^3 and 709.383 respectively for u_1 and u_2 . The crosscorrelation between both inputs and the first output show significance beyond the dead time regardless of which or both of the models is mismatched. Similarly, the crosscorrelation between both inputs and the model prediction error for the first output also showed significant correlation, which suggests model mismatch. Any deviation in

Y_1 from its setpoint is recognized by the LQG controller which then adjusts both inputs accordingly. Therefore, both inputs become correlated with Y_1 and ER_1 . This model error, however, would have to be confirmed once setpoint changes were added to the system. The modelling error would be apparent from significant crosscorrelations between $(Y_{sp})_1$ and ER_1 and $(Y_{sp})_2$ and ER_1 .

Figure 4.6 shows the correlation matrix for the case in which at least one of the models for each of the outputs is mismatched. In this example the gain of $G_m(1,1)$ is decreased and the gain of $G_m(2,1)$ is increased, while the input and output weights remain unchanged. For this example all of the elements in the matrix would show significant correlation. The two controlled variable variances have increased to 5.901 and 2.958. A similar increase was experienced by the input variables whose variances increased to 1.60×10^4 and 5.75×10^3 . The analysis shows that both outputs are affected by incorrect relationships but it cannot further deduce which of the models is responsible. In a case such as this, however, the likely solution would involve complete process reidentification if the performance is unacceptable.

In order to more closely represent plant conditions a simulation study was performed on the same system but with correlated noise sequences. This was accomplished in the

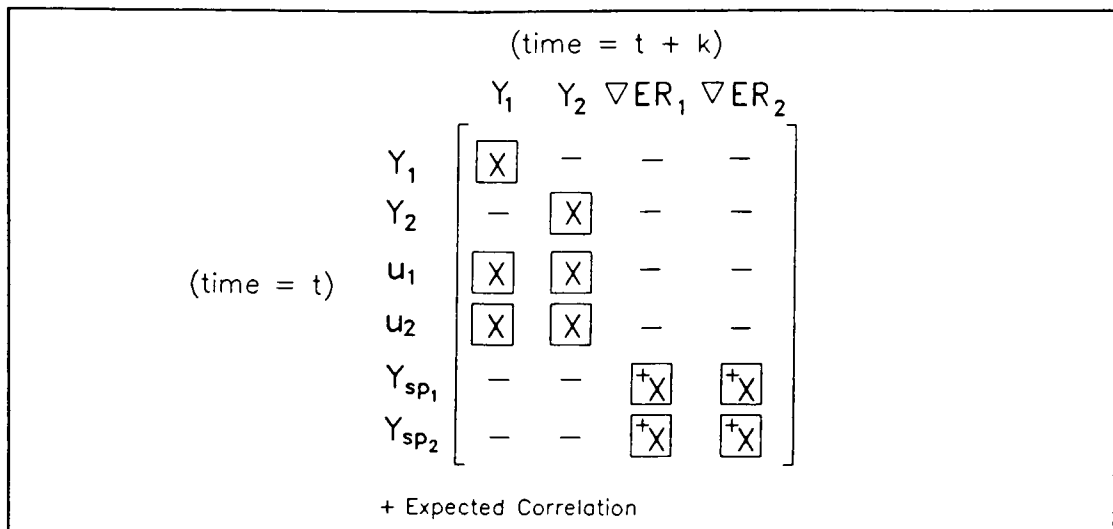


Figure 4.6 MIMO, Model Mismatch In Y_1 and Y_2

simulation by specifying a nonzero covariance between the two noise sequences. Various covariance values can be used, ranging from slightly correlated series, $\gamma=0.1$, to perfectly correlated series, $\gamma=1.0$. In physical terms this may correspond to a flow rate and a flow composition disturbance. Although not always true, the two are often experienced simultaneously. As an example we can consider the product of one column feeding another whose cutpoint is changed. The change in stream composition is often reflected in the volume which is produced, hence the two inputs are correlated. Several examples were studied with varying noise crosscovariance values. The results reported here are for the extreme case of perfectly correlated noise sequences. The base case is equivalent to that of the uncorrelated noise example in that the autocorrelations greater than lag f are

eliminated and the crosscorrelations are all zero.

Figure 4.7 shows the analysis results for the process having perfectly correlated disturbance sequences and model mismatch, consisting of a decreased gain, occurring solely in element $G_m(2,2)$. We can compare this correlation matrix with that shown in Figure 4.8 which corresponds to the same control problem only with independent disturbances. The variance of the controlled variables is comparable for the two cases with values of 2.131 and 2.128 for Y_1 , and 5.754 and 5.656 for Y_2 . The manipulated variable variance is lower for the correlated noise case registering 680.44 and 1.47×10^3 for inputs one and two, respectively, while the independent noise example showed variances of 1.08×10^4 and 1.56×10^4 . In the latter case the disturbances are moving independently, hence the inputs must compensate for both effects, causing the greater variance. Elements 1 through 6 show the same significant correlations in both cases of independent and correlated noise. If both of these systems were tested in the presence of independent controlled variable setpoint changes, both cases would exhibit model mismatch only in the crosscorrelation from $(Y_{sp})_1$ and $(Y_{sp})_2$ to ER_2 . If the setpoint perturbations were not independent, however, then both setpoint changes would be correlated with both model prediction errors. It is apparent, therefore, that in the presence of independent controlled variable setpoint changes, correlated noise disturbances do

		(time = t + k)			
		Y_1	Y_2	∇ER_1	∇ER_2
(time = t)	Y_1		-	-	-
	Y_2	-	X	-	-
	u_1		X	-	-
	u_2		X	-	-
	Y_{sp1}	-	-	*	+X
	Y_{sp2}	-	-	*	+X

* Not performed in the simulation study
 + Expected Correlation

Figure 4.7 MIMO, Correlated Noise With Model Mismatch in $G_m(2,2)$

		(time = t + k)			
		Y_1	Y_2	∇ER_1	∇ER_2
(time = t)	Y_1		-	-	-
	Y_2	-	X	-	-
	u_1		X	-	-
	u_2		X	-	-
	Y_{sp1}	-	-	*	+X
	Y_{sp2}	-	-	*	+X

* Not performed in the simulation study
 + Expected Correlation

Figure 4.8 MIMO, Independent Noise with Model Mismatch in $G_m(2,2)$

not have an effect on the multivariable control system diagnosis.

The complication of imbalanced dead times was also studied. The system matrix is given below.

$$Y(z) = \begin{bmatrix} \frac{0.393 z^{-3}}{1 - 0.6 z^{-1}} & \frac{0.315 z^{-5}}{1 - 0.6 z^{-1}} \\ \frac{0.0787 z^{-4}}{1 - 0.6 z^{-1}} & \frac{0.393 z^{-8}}{1 - 0.6 z^{-1}} \end{bmatrix} * u(z) \quad (4.1)$$

In this particular example we have the minimum dead times appearing in column 1 of the matrix. Because the one input cannot perfectly control both outputs the minimum process dead times achieved under perfect control cannot correspond to these minimum values. The results for this case under best achievable control are shown in Figure 4.9. The output autocorrelations are only eliminated after two and four lags, respectively, for Y_1 and Y_2 . This follows the Holt & Morari [1985] results discussed in Chapter 2, stating that the minimum possible settling time must lie between the upper and lower dead time limits given by the transfer function relationships. In this particular case the lower and upper limits for Y_1 are 2 and 3, respectively, and are 3 and 5 for Y_2 . Refer to Appendix H for calculation details. If the minimum dead times appeared on the diagonal, as shown in Equation 4.2,

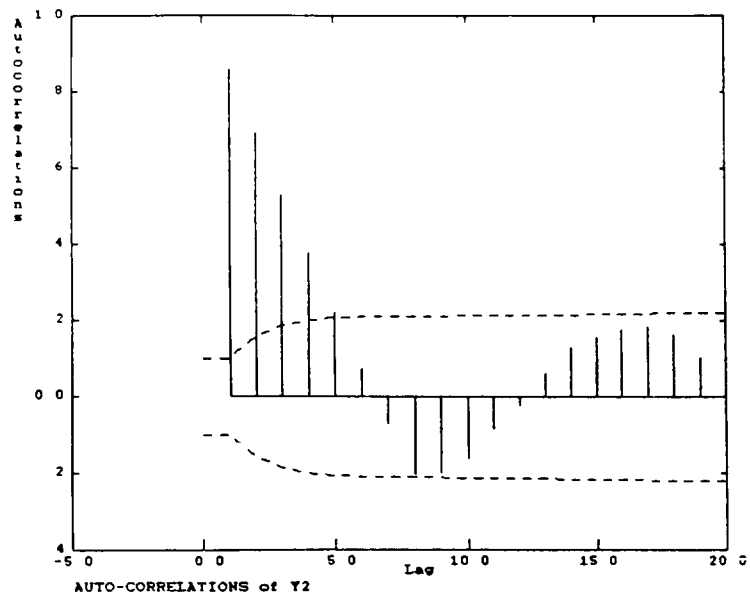
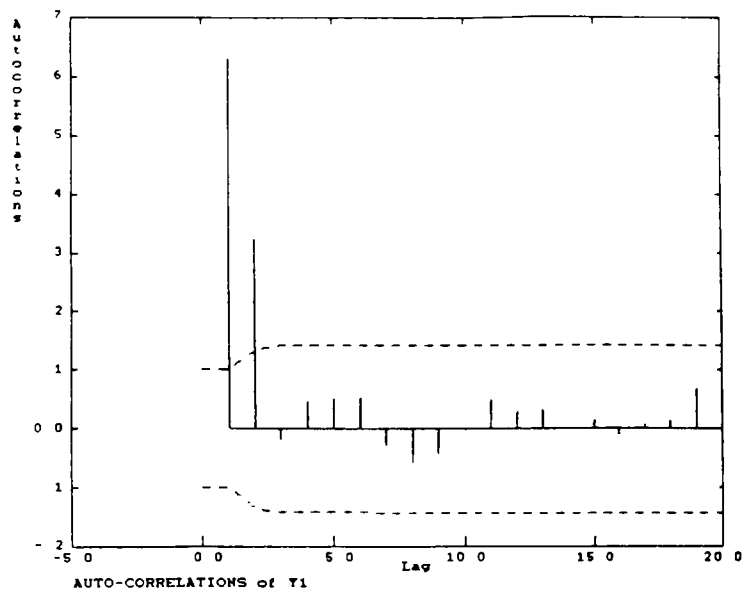


Figure 4.9 MIMO, Imbalanced Dead Time Example

$$Y(z) = \begin{bmatrix} \frac{0.393 z^{-3}}{1 - 0.6 z^{-1}} & \frac{0.315 z^{-5}}{1 - 0.6 z^{-1}} \\ \frac{0.0787 z^{-8}}{1 - 0.6 z^{-1}} & \frac{0.393 z^{-4}}{1 - 0.6 z^{-1}} \end{bmatrix} * U(z) \quad (4.2)$$

the output autocorrelations would have been eliminated after two and three time intervals for Y_1 and Y_2 respectively, as shown in Figure 4.10. Furthermore, while the variance of both inputs and of Y_1 are comparable between the two configurations, the variance of Y_2 is 88% greater in the former case, measuring 6.437 as compared to 3.426 for the latter. As expected, both outputs cannot be controlled optimally given the imbalanced dead time configuration. The balanced dead time system produces minimum output variance estimates of 3.009 and 3.143, which compare well with the actual values of 3.180 and 3.426 for Y_1 and Y_2 respectively. Refer to Appendix H for calculations. As discussed in Chapter 2, minimum variance predictions for the imbalanced dead time system cannot be determined using this simplified procedure. The exact estimates can only be obtained by solving the LQG design problem.

A process having a sparse dynamic matrix was then studied. In most cases sparsity simplifies the diagnosis as the effects of specific variables are eliminated due to the physical aspects of the process. If we assume a lower

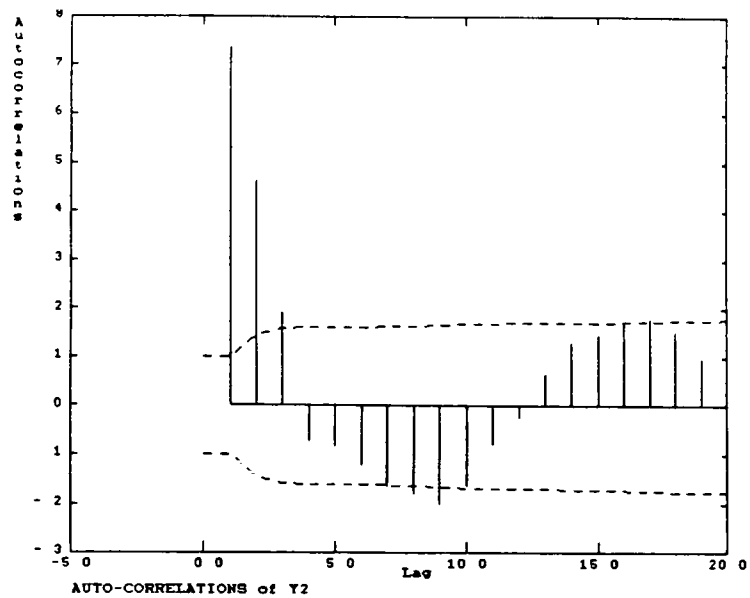
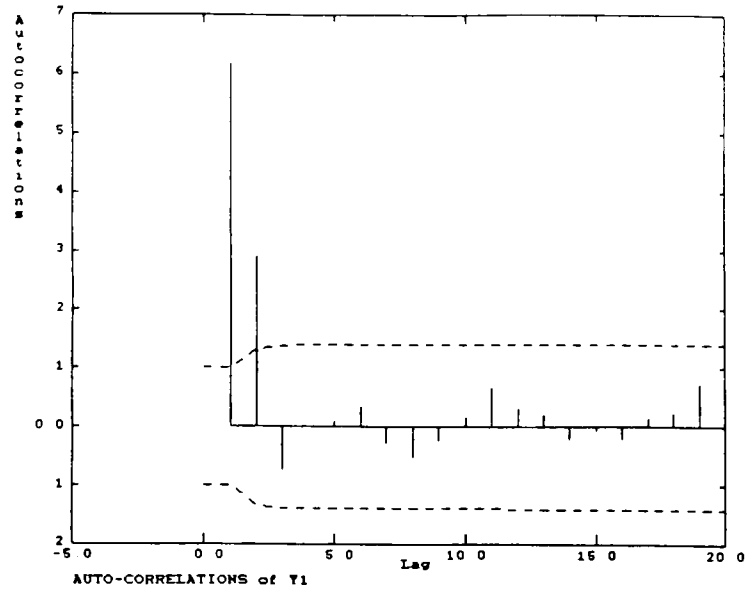


Figure 4.10 MIMO, Balanced Dead Time Example

triangular matrix thereby reducing $G_m(1,2)$ to zero only one input variable and one model remain which have an effect on Y_1 . The correlation matrix for this sparse system is shown in Figure 4.11. Therefore, any inadequacy observed in the control of Y_1 is due to excessive penalization of u_1 or an incorrect model relating the two. Of course, this rationalization is only correct if due to the physical system $G_m(1,2)$ is indeed negligible. The multivariable example discussed in the next section will show this triangular nature as the reactor examined experiences downward interaction only. It is important to note, however, that inadequate control of Y_1 could be the direct result of violation of this assumption. If a significant relationship exists between Y_1 and u_2 which is not incorporated into the controller, poor control performance may result and the correlation between u_2 and Y_1 must be examined. In this case the sparse system is returned to its full state and the simplifications no longer apply. Therefore, in the analysis of sparse systems certain assumptions can be made which simplify the analysis by eliminating certain variables, but care must be taken to ensure that these assumptions are valid.

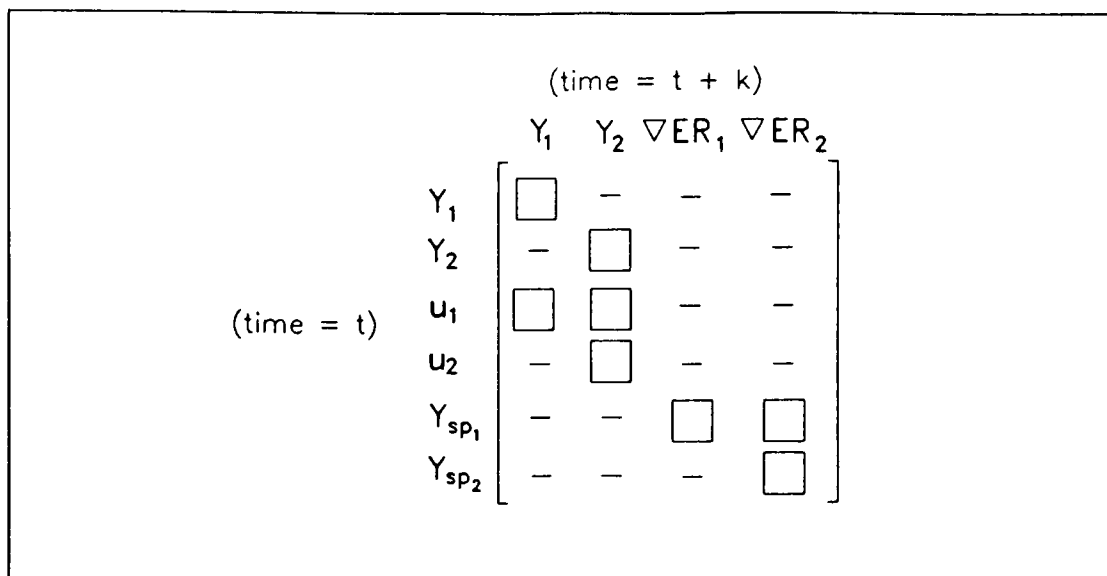


Figure 4.11 MIMO, Sparse System Correlation Matrix

4.2 MULTIVARIABLE INDUSTRIAL CASE STUDY USING QDMC

The control performance evaluation methodology was tested on an industrial control system using the QDMC algorithm. This control scheme regulates key variables on a multibed hydrocracking reactor at Shell Canada's Scotford refinery. The relevant information and design for this control scheme has been presented in Kelly, Rogers & Hoffman.[1988] The primary objective is to control the overall reaction severity which is represented by the Weighted Average Bed Temperature (WABT). This is accomplished through the control of the individual Average Bed Temperatures (ABT). Many combinations of the ABT's will give the same WABT;

therefore, a secondary objective is needed to uniquely specify the control objective. The secondary objective is to control the ABT's either to a specified profile or to minimize energy utilization.

The analysis was performed on the temperature profile operating mode which yields a 6x5 control matrix. In this operating mode the four individual ABT's are controlled to a predetermined profile that optimizes selectivity. The WABT, which is a linear combination of the four ABT's, is regulated to maintain a desired level of denitrification of the feed.[Kelly, Rogers & Hoffman, 1988] The final control variable is the valve position adjusting hydrogen quench to the first reactor bed. The five manipulated variables are the four bed inlet and reactor inlet temperature setpoints. The problem is not overspecified as the WABT is a linear combination of the four ABT's and is therefore not independent. Hence, the apparent 6x5 problem is actually a square 5x5 system. The four bed outlet temperatures are included in the QDMC design as associated variables in order to safeguard against temperature excursions. Constraints were also placed on the quench valve positions in order to ensure reserve quench capacity in the case of temperature runaways. These constraints were never active during the plant tests described in this chapter nor are they active in typical plant operation. Thus, the control system was always "square".

A schematic of the process is given in Figure 4.12. High purity hydrogen is heated in a furnace and is added to the hydrocarbon feed at high pressure. This combined stream is reacted over a hydrotreating catalyst on the four reactor beds. Unheated hydrogen is added at the inlet of each bed as an intermediate quench for the exothermic reaction. The quench stream to the first bed also provides fine adjustment of the reactor inlet temperature. The reactor inlet temperature is controlled by adjustment of the fuel gas flow to the preheat furnace. The hydrogen quench valves to each bed are adjusted to control the bed inlet temperatures. The first stage reactor effluent is then fed to the second stage hydrocracking reactor.

The controlled variable dynamic matrix is shown in Figure 4.13. [Kelly, Rogers & Hoffman, 1988] The lower triangular nature of the dynamic matrix illustrates the downward interaction of the reactor beds. This is to be expected as a result of the downward flow through the reactor beds. Assuming there is negligible backflow through the reactor, occurrences in lower beds will have no effect on the upper beds. Therefore, changes in a given bed inlet temperature introduce disturbances to the lower beds only. The sparsity of the dynamic matrix reflects this one-way interaction and thus simplifies the control performance diagnosis, as the effects of certain variables can be

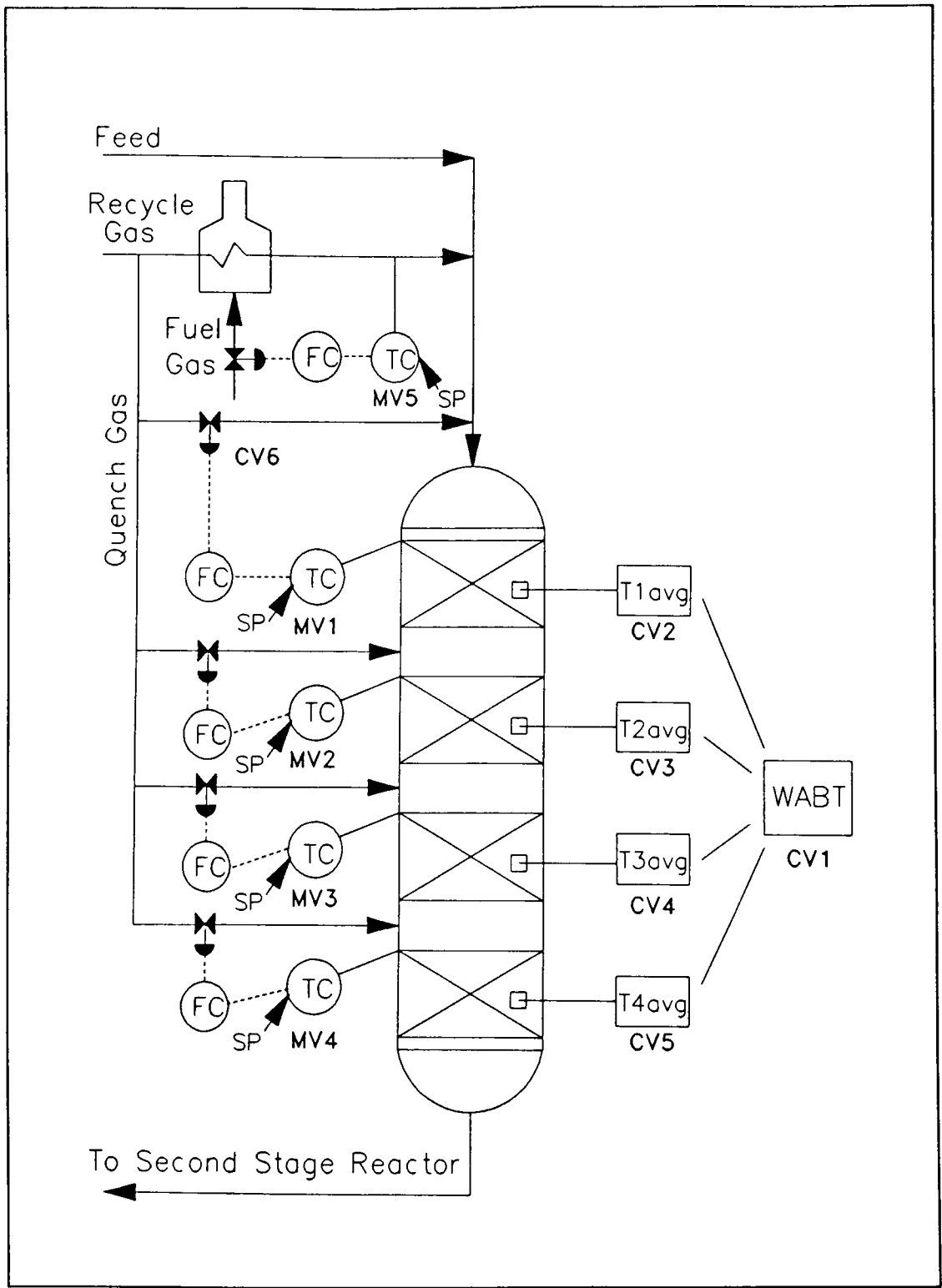


Figure 4.12 Schematic for First Stage Hydrotreater

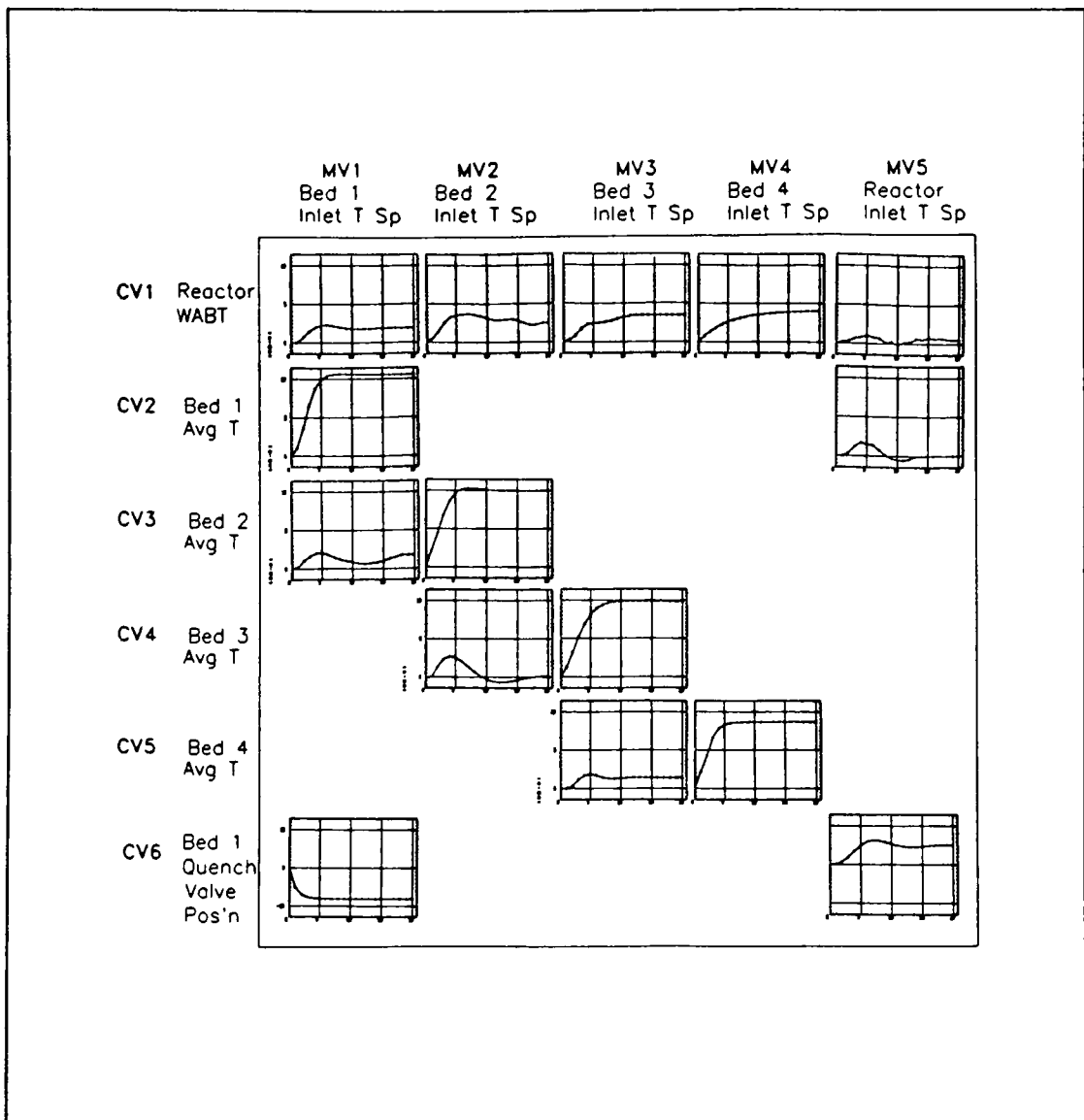


Figure 4.13 HCU QDMC Dynamic Matrix

eliminated.

Initially, an analysis was performed on the existing control system under normal operation. This first step compared actual control performance to theoretically best

achievable performance. The output weighting factors are such that the WABT has the greatest importance, the four individual ABT's have equal weightings substantially less than that of the WABT and the reactor inlet quench valve position has the lowest weighting. There is a move suppression for each of the manipulated variables as well as a maximum move size. The latter constraint was never active during any of the testing nor is it active during normal operation. It is important to note that the terms in the objective function are the deviations from setpoint of the controlled variables.

The correlation analysis showed good control of the WABT and poor control of the individual ABT's, which reflects the priorities as defined in the QDMC objective function. The WABT autocorrelation exhibited slight oscillatory behaviour, however, which may be indicative of overly aggressive control action or model mismatch. The crosscorrelations from each of the five manipulated variables to the WABT also showed this oscillation. The autocorrelation function for each of the four ABT's dampened very slowly and also showed slight oscillation. Finally, the autocorrelation of inlet quench valve position was eliminated soon after the dead time. As with the other controlled variables the autocorrelation did show slight oscillation. It is important to note that these oscillations did appear outside the confidence limits and are

therefore taken as being significant. Oscillations can be induced in the autocorrelation, however, as a result of large initial correlation. Coinciding with the controlled variable priorities given previously were the variances experienced by each of these variables. The WABT experienced the least variation at 0.0119 ($^{\circ}\text{C}$)², followed by the four ABT's having variances of 0.154 , 0.0557 , 0.0471 and 0.0253 ($^{\circ}\text{C}$)², and finally the valve position with a variance of 11.754 (%)².

The crosscorrelation function from the input variables to the model prediction errors showed significant values in all elements. This is either the result of model error and/or autocorrelated disturbances. Furthermore, definite patterns were distinguishable for the crosscorrelations corresponding to each controlled variable, and these patterns were similar for all input-output combinations. This result indicates that the input variables themselves are highly correlated and any disturbances affecting the process are also correlated. The specific data set examined represents normal unit operation affected by routine disturbances and was not subject to external forcing. Because of the relatively steady operation during the time in which data was collected the system dimensionality was most probably low. Although there may be several degrees of freedom in the system some of these could be so highly correlated that they are statistically dependent.

If this is the case then the effective degrees of freedom are reduced. The QDMC system itself is of high dimension but enough information was not available in the data to completely represent these dimensions. Crosscorrelating the manipulated variables with one another demonstrated significant correlation, following the downward trend of process interaction. This confirms that the input variables are highly correlated as a result of the low system dimensionality. Hence, the full benefits of this performance analysis procedure could not be attained as individual correlation relationships could not be observed. Therefore, inadequacy in the control scheme could not be distinguished as the errors present were propagated throughout the scheme and this statistically based analysis method could not differentiate the cause.

Process disturbances were then introduced to the system in order to increase the system dimensionality. Initially a PRBS disturbance, of magnitude 5% and switching frequency 30 minutes was introduced into the recycle gas feed. The collection frequency was 6 minutes and a total of 300 data points were collected. The results obtained in this case study are not significantly different from the previous example. Once again the WABT control is near optimal as shown in the autocorrelation function displayed in Figure 4.14. The

autocorrelation is eliminated after two lags. Contrary to the previous example, however, the WABT autocorrelation and the crosscorrelation from the inputs to the WABT are not oscillatory. The ABT's are still not controlled optimally as apparent from slowly decaying autocorrelation functions. Figure 4.14 also illustrates the Bed 1 Avg T autocorrelation.

Given the dynamic matrix in Figure 4.13 it is difficult to establish the transfer functions having the minimum dead times. Intuitively, it can be assumed that among the transfer functions relating each ABT to the input variables the one having the minimum dead time would be the corresponding bed inlet temperature. Therefore, the criteria of having minimum dead times appearing on the diagonal is satisfied and the performance evaluation and minimum variance prediction can be generated as discussed in Chapter 2. In the case of the WABT, however, all of the input variables would have the same time delay. The control interval used in this system is six minutes. This is also the data collection frequency which was used. Given this time interval the minimum dead time for each controlled variable appears to be less than the sampling period, thus "f" equals zero. Given this information the minimum variance calculated for all of the outputs is given in Table 4.1. All calculations are included in Appendix I. The actual WABT variance differs

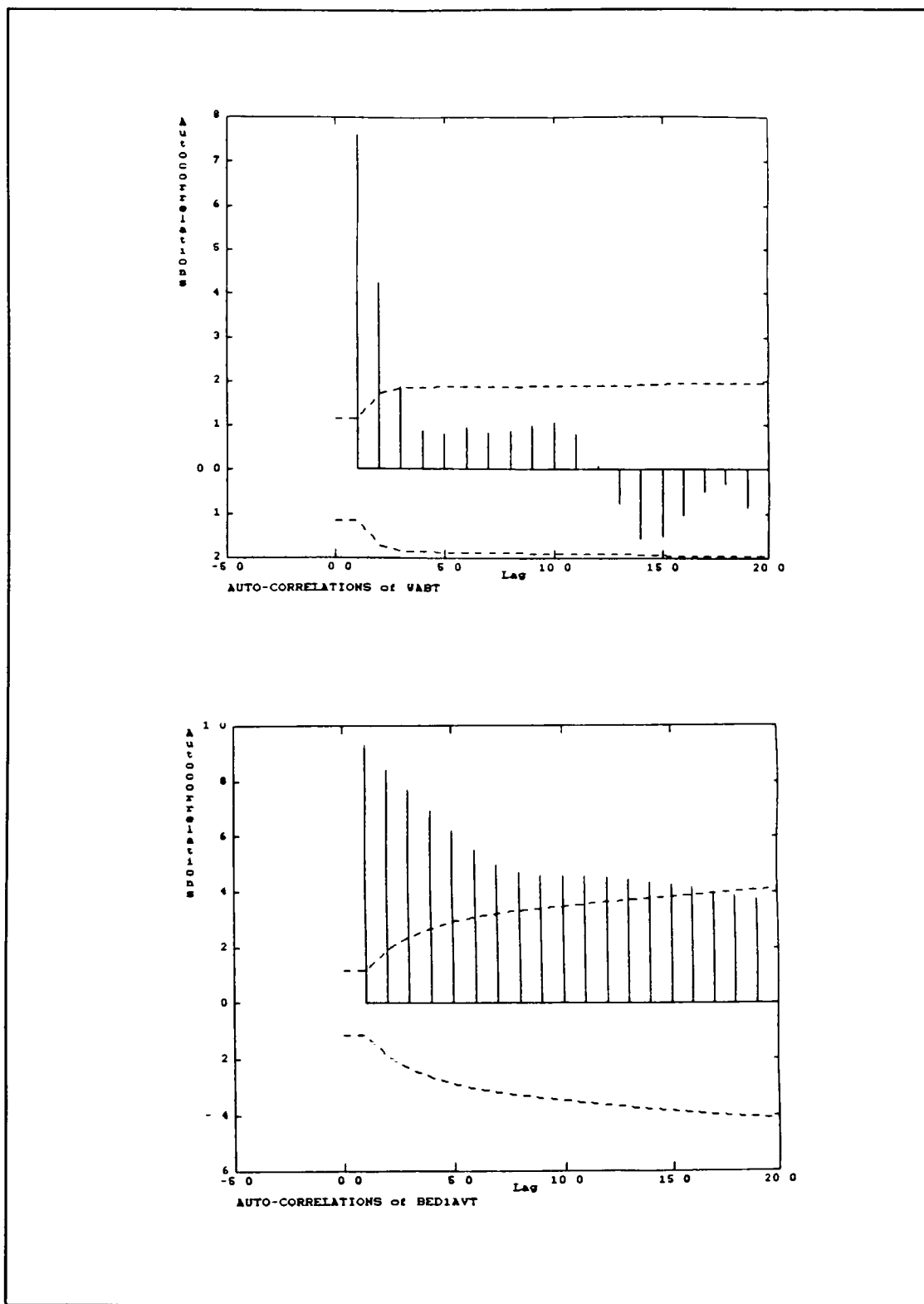


Figure 4.14 HCU QDMC, Autocorrelation

the least from its optimal value as is expected given the objective function weighting. The remaining control variables show room for improvement if this improvement is desired.

Table 4.1 Minimum Variance Predictions

Variable	Minimum Variance (°C) ²	Actual Variance (°C) ²	% Difference
WABT	0.00434	0.012	176
Bed 1 Avg T	0.0274	0.226	725
Bed 2 Avg T	0.0105	0.0486	363
Bed 3 Avg T	0.00712	0.0345	385
Bed 4 Avg T	0.00706	0.0661	836
Bed 1 Quench Valve Pos'n	13.811 *	41.201 *	198

* (%)²

Crosscorrelating the disturbance to the controlled variables shows significant correlation which confirms the presence of forcing. Figure 4.15 shows the crosscorrelation between the recycle gas feed and both the WABT and the Inlet quench valve position. As with the base case, the crosscorrelation from the inputs to the model prediction errors also show significant correlation. Similarly, the

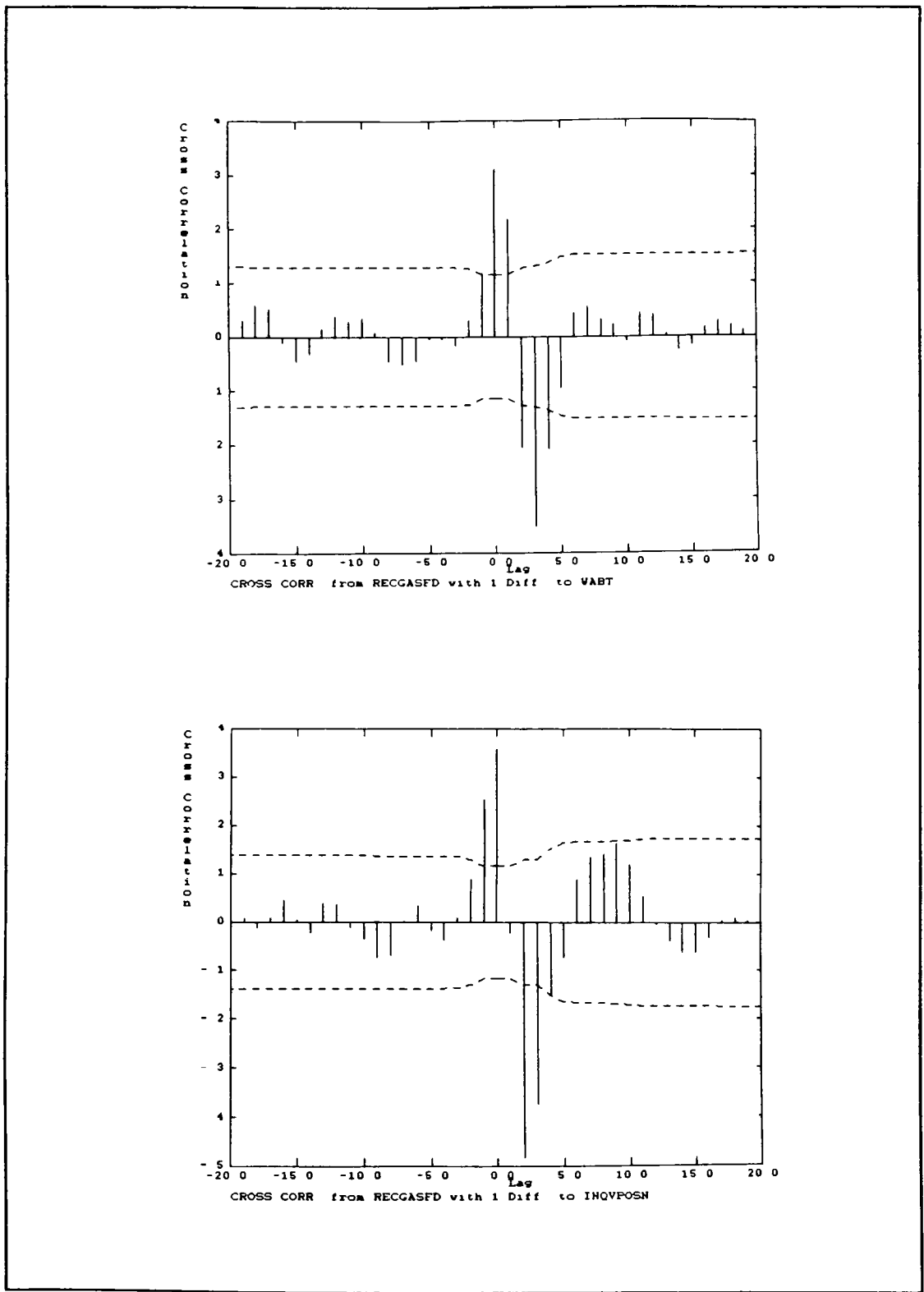


Figure 4.15 HCU QDMC, Crosscorrelation ($d_t \times C.V._{t+k}$)

correlation patterns produced are consistent, as shown in Figure 4.16, which again implies a lack of independent information. Figure 4.16 shows the crosscorrelation from the Bed 2 and Bed 3 inlet temperature setpoints (BED2INTSP, BED3INTSP) to the model prediction error for the WABT (PREDE1). A definite similarity is apparent upon observation of these two correlation plots. This pattern is also visible in Figure 4.17 which shows the crosscorrelation from the Reactor and Bed 2 inlet temperature setpoints (REACINTSP, BED2INTSP) to the model prediction error for the Bed 2 average temperature (PREDE3). The crosscorrelations between the input variables themselves also shows significance and pattern reproduction which confirms this lack of independent information. Figure 4.18 shows the crosscorrelation from the Reactor inlet temperature setpoint to the Bed 1 and Bed 2 inlet temperature setpoints. These plots indicate a definite correlation exists between the manipulated variables and moreover a similar pattern is apparent in this correlation. At this point it can only be stated whether the controller is meeting its objectives and how close the performance is to the best achievable. The causes of inadequate performance cannot be identified due to insufficient dimensionality in the problem.

A similar experiment was done with three perturbations affecting the process in order to increase independent system

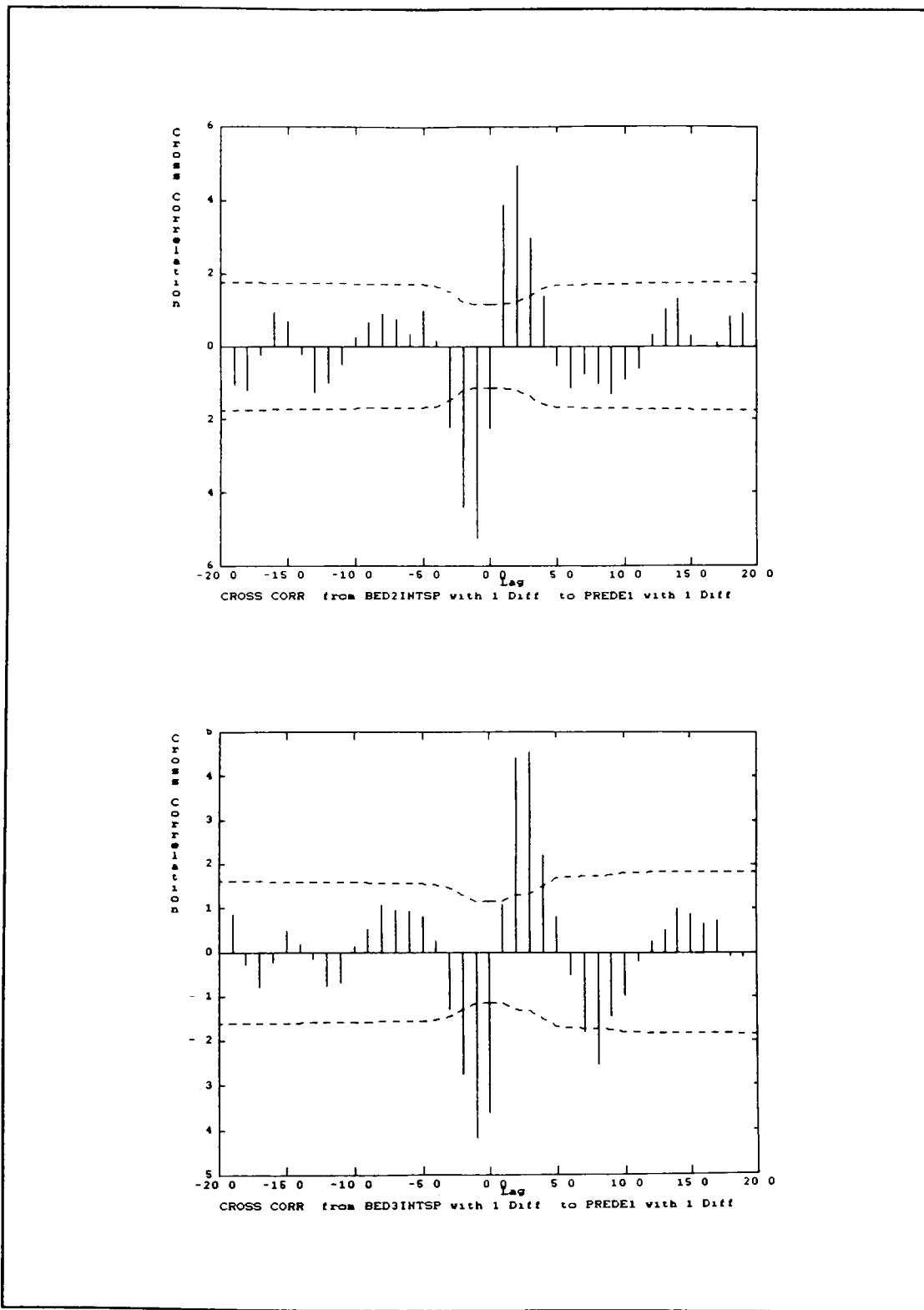


Figure 4.16 HCU QDMC, Crosscorrelation ($u_t \times ER_{t+k}$)

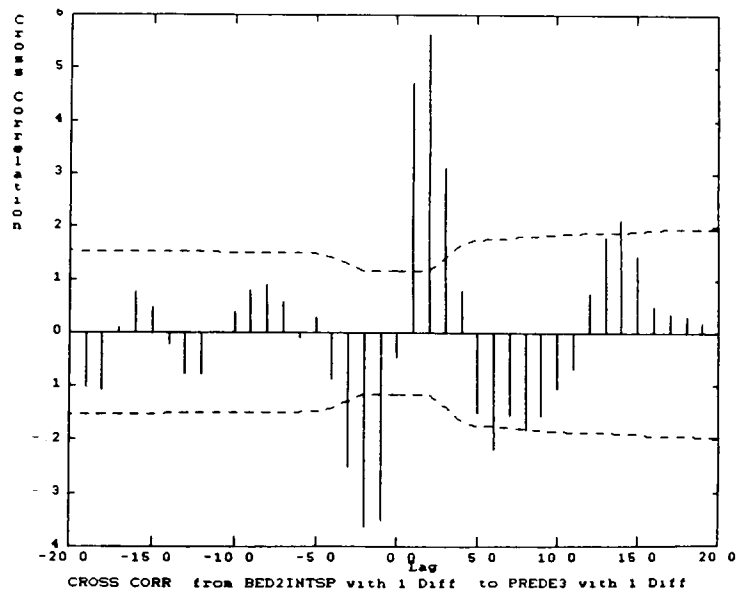
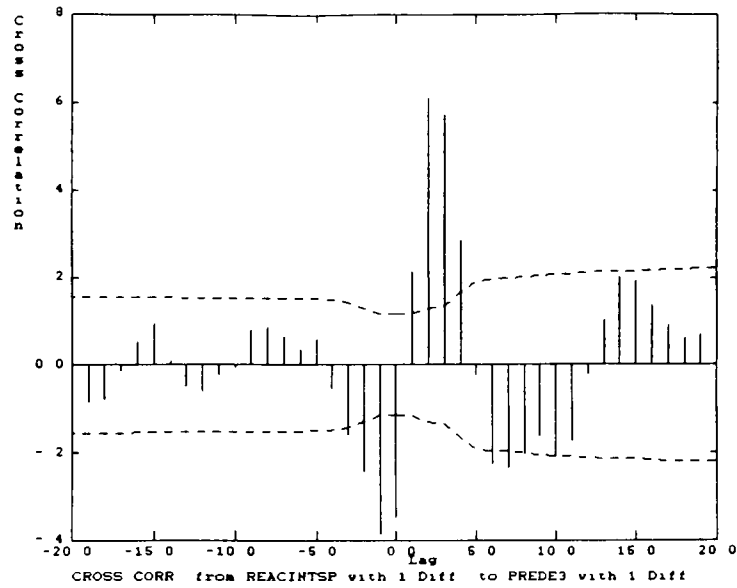


Figure 4.17 HCU QDMC, Crosscorrelation ($u_t \times ER_{t+k}$)

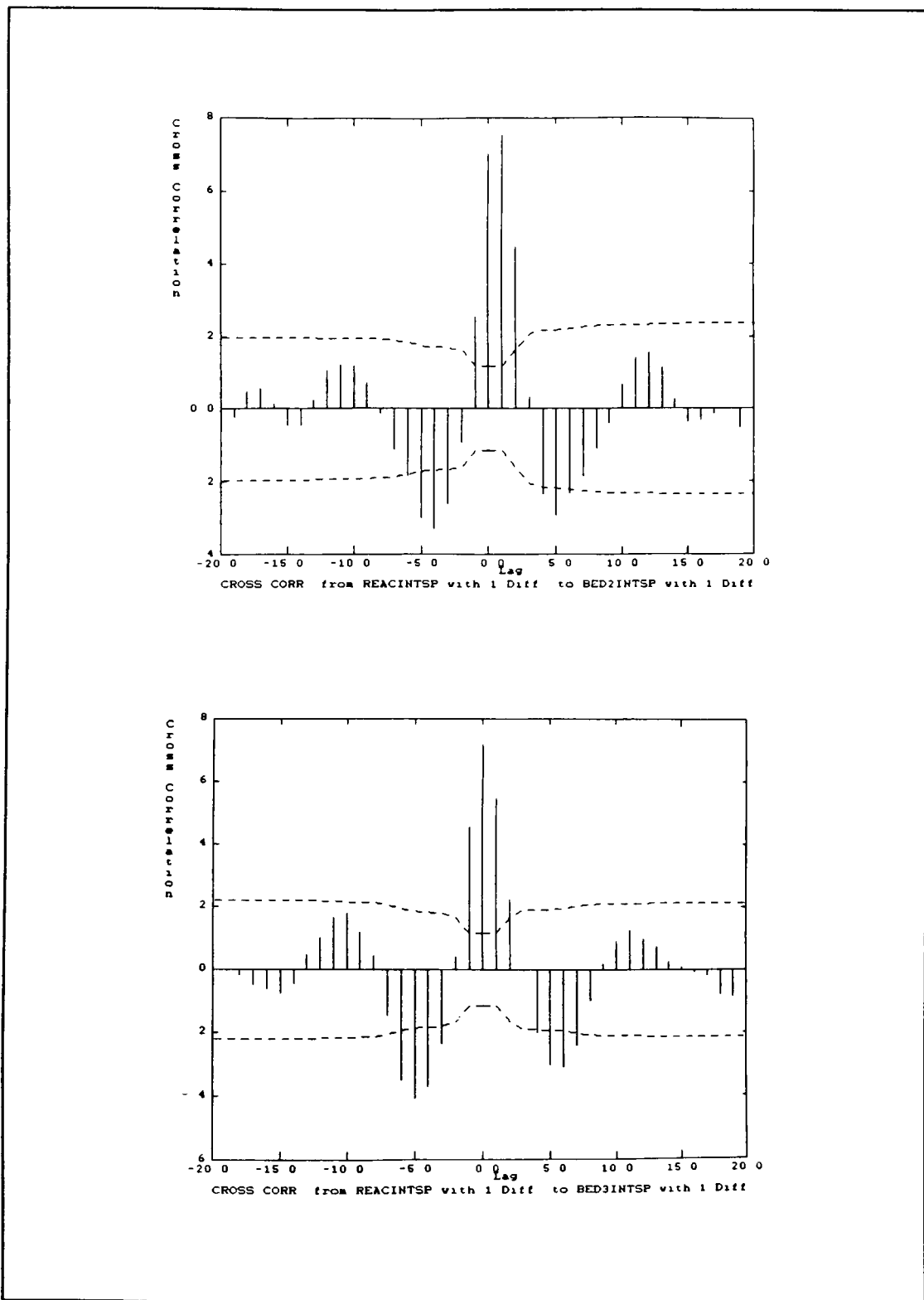


Figure 4.18 HCU QDMC, Crosscorrelation ($u_t \times u_{t+k}$)

forcing and hence, dimensionality. The recycle gas feed was once again perturbed in a PRBS fashion with a magnitude of 5% of normal operation and a switching frequency of 30 minutes, as was the WABT setpoint with a magnitude of 0.3% and a switching frequency of 60 minutes, while the inlet quench valve position setpoint was manually changed 10% every several hours. Additional forcing was not possible as the existing facilities only allow for two PRBS signals and the need for steady plant operation did not allow for larger disturbances. Data was collected every 6 minutes for a total of 500 data points. The results obtained for this example are consistent with the previous case and hence will not be discussed in detail. Although the forcing was increased in this test case, the perturbations may not have been sufficiently large or spaced adequately to provide three distinct dimensions. The results show that once again essentially only one dimension can be recognized in the data sample. This question of dimensionality should be addressed in a further study.

A simulation study was also performed on the closed loop system in order to investigate various aspects of control performance. The program used for these simulations was developed by Shell and uses the same step weight models used in the on-line QDMC program. Therefore, these models are considered proprietary information and cannot be reported in this document. The first case represents the actual unit

operation reflecting the objective function weighting and the imposed system constraints. The correlation results obtained resemble those of the actual plant. The WABT and inlet quench valve position control are near-optimal while the ABT's are poorly controlled. In the next case equal weighting was placed on all of the outputs leading to sluggish control of all the controlled variables, as concluded from the slowly damping autocorrelation functions. In order to get good control of the ABT's the WABT weighting was decreased to 1 unit while the ABT's weighting was increased to 100 units. This resulted in sluggish control of the WABT, as seen in a slowly decaying autocorrelation, and minimum variance control of the ABT's. Of course, the output weighting and input penalties are selected to suit the system objectives, which is not the concern of this research. This exercise shows, however, that the control performance evaluation procedure can be used to confirm whether the objectives are being met.

The MIMO simulation and industrial examples presented here have demonstrated the analysis techniques used in the evaluation and diagnosis of these complex schemes. The analysis of the simplest MIMO system has been shown to be a direct extension of the SISO analysis presented in Chapter 3. This extension in the analysis procedure, however, cannot be made with the addition of imbalanced dead times, as was demonstrated. In these cases, the evaluation and diagnosis

procedure being used is limited in its results. Correlated noise and inadequate forcing, which reduce the dimensionality of the MIMO system, have also been shown to limit the ability of this statistical analysis procedure. Nevertheless, the present analysis method does enable the user to verify that control objectives are being met and identify whether further improvement is possible. To address these complex examples, however, further study should be focused on the dimensionality of the MIMO problem. Additional analysis tools should be investigated for their potential use in this application.

5.0 CONCLUSIONS AND RECOMMENDATIONS

A hierarchial method for monitoring and diagnosing control performance has been developed and successfully tested in an industrial environment.

The Minimum Variance and Linear Quadratic Gaussian Controllers are useful bases against which to evaluate actual control performance and establish potential for improvement. The output autocorrelations of a SISO process under MVC are reduced to zero after lag f , where f is the process dead time. Similarly, the output autocorrelations of a MIMO process, whose minimum dead times appear on the diagonal, are eliminated after this minimum dead time value. If the dead time values on the diagonal are less than the other values appearing in their respective rows, the best achievable control performance can be estimated using an extension of the SISO procedure. The output autocorrelations of a MIMO process, whose minimum dead times do not appear on the diagonal, are eliminated sometime between upper and lower limits, as established by the transfer function settling times. In this case it is not possible to establish the best achievable performance with the method used in this research.

Statistical analyses such as autocorrelation and crosscorrelation functions and power spectra can be used to evaluate control performance, indicating the possibility of improvement if it exists and if it is warranted. Model-plant mismatch in a feedback-only control scheme can be detected in the crosscorrelation between the controlled variable setpoint and the model prediction error. If this is the case the model error must be eliminated before the controller tuning can be examined. In feedforward-feedback control schemes these statistical tools can often distinguish between an imperfect feedforward or feedback controller and between mistuning and model mismatch. It is sometimes necessary, however, to decommission the feedforward controller in order to evaluate the model accuracy. Once again if model error is present, tuning cannot be investigated until this mismatch is eliminated.

In MIMO control schemes this diagnostic tool has proven successful in deducing tuning or modelling difficulties and in locating a specific input or output responsible for non-optimal performance. In the presence of correlated noise, affecting a MIMO control scheme, the analysis procedure cannot always distinguish the cause of inadequate performance. In evaluating MIMO control schemes it is necessary that enough independent forcing is present in order to ensure adequate problem dimension. This should be addressed in greater detail

in a further study.

Finally, the matrix representation of correlation data is a useful visual tool for successful interpretation of control performance.

6.0 REFERENCES

- [1] K.J. Astrom, B. Wittenmark, Computer Controlled Systems: Theory and Design, Prentice-Hall Inc., Englewood Cliffs N.J., 1984.

- [2] G.E.P. Box, G.M. Jenkins, Time Series Analysis - Forecasting and Control, Holden-Day, California, 1976.

- [3] G.E.P. Box, J.F. MacGregor, "The Analysis of Closed Loop Dynamic Stochastic Systems", *Technometrics*, Vol. 16, No. 3, August, 1974.

- [4] G.E.P. Box, J.F. MacGregor, "Parameter Estimation with Closed-Loop Operating Data", *Technometrics*, Vol. 18, No. 4, November, 1976.

- [5] T.J. Harris, "Assessment of Control Loop Performance", *The Canadian Journal of Chemical Engineering*, Volume 67, October, 1989.

- [6] B.R. Holt, M. Morari, "Design of Resilient Processing Plants - V The Effect of Deadtime on Dynamic Resilience", Chemical Engineering Science, Volume 40, No. 7, 1985.
- [7] S.J. Kelly, M.D. Rogers, D.W. Hoffman, "Quadratic Dynamic Matrix Control of Hydrocracking Reactors", American Control Conference, Session WA9, Atlanta Georgia, 1988.
- [8] D.K. Kozub, R. Swanson, J. Wong, LQDESIGN, 1988.
- [9] Dr. J.F. MacGregor, "Optimal Stochastic Control : Theory and Applications - An Intensive Short Course on Digital Computer Techniques for Process Identification and Control", Department of Chemical Engineering - McMaster University, 1988.
- [10] Dr. J.F. MacGregor, Dr. P.A. Taylor, Dr. J.D. Wright, "Advanced Process Control - An Intensive Short Course on Digital Computer Techniques for Process Identification and Control", Department of Chemical Engineering - McMaster University, 1988.

- [11] Dr. J.F. MacGregor, Dr. P.A. Taylor, Dr. J.D. Wright, "Advanced Process Control - An Intensive Short Course Laboratory Manual", Department of Chemical Engineering McMaster University, 1988.
- [12] T.E. Marlin, J.D. Perkins, G.W. Barton, M.L. Brisk, "Advanced Process Control Applications", Warren Centre for Advanced Engineering, The University of Sydney, October 1987.
- [13] C. Pryor, "Autocovariance and Power Spectrum Analysis Derive New Information from Process Data", Control Engineer, October 1982.
- [14] H.J. Newton, TIMESLAB: A Time Series Analysis Laboratory, Wadsworth & Brooks/Cole Publishing Company Advanced Books & Software Pacific Grove, California, 1988.
- [15] C.A. Smith, A.B. Corripio, Principles and Practice of Automatic Process Control, John Wiley & Sons, USA, 1985.
- [16] O.J.M. Smith, "Close Control of Loops with Dead Time", Chemical Engineering Progress, 53(5), pg 217, 1957.

- [17] N. Stanfelj, "Control Performance Evaluation and Diagnosis Laboratory Report", Department of Chemical Engineering, McMaster University, 1990.

- [18] B.D. Stanton, "Characteristics and Control of Process Disturbances", Hydrocarbon Processing, June 1984.

- [19] T.M. Stout, R.P. Cline, "Control System Justification", Instrumentation Technology, September 1976.

- [20] P.A. Taylor, MIDSA - A Program for Computer Aided Identification of Multivariable Processes using Time Series Methods, 1990 - An Integrated Computer Aided Tutorial for Advanced Digital Controller Designs, Transfer Function Simulation and Analysis of Discrete Control Systems, 1989.

7.0 GLOSSARY OF TERMS

a	random noise sequence
ABT	average bed temperature
AR(p)	Autoregressive model of order p
ARIMA(p,d,q)	Autoregressive Integrated Moving Average model of order p,d,q
ARMA(p,q)	Autoregressive Moving Average model of order p,q
c(k)	estimated covariance function
CMVC	Constrained Minimum Variance Control
d	disturbance sequence
DMC	Dynamic Matrix Control
E	Expectation operator
Er	variable deviation from setpoint
ER	model prediction error
f	process delay
FOPDT	First Order plus Dead Time
G_c	controller transfer function
G_d	disturbance transfer function
$G_{c_{FB}}$	feedback controller transfer function
$G_{c_{FF}}$	feedforward controller transfer function
G_{m_d}	disturbance transfer function model
G_{m_p}	process transfer function model

G_p	process transfer function
IAE	Integral of Absolute Error
k	lag
K	controller transfer function (IMC form)
K'	controller transfer function (Smith Predictor form)
LQG	Linear Quadratic Gaussian
MA(q)	Moving Average model of order q
MIMO	Multi-Input-Multi-Output
MMSE	Minimum Mean Square Error
MVC	Minimum Variance Control
N	sample size
N_t	time series of noise function
$N(z)$	noise transfer function
PRBS	Pseudo-Random-Binary-Sequence
Q	Chi-Squared distribution
QDMC	Quadratic Dynamic Matrix Control
$r(k)$	estimated correlation function
S, σ	standard deviation
$S(f)$	power content at frequency, f
SISO	Single-Input-Single-Output
u	process input
u_{FB}	input signal from feedback controller
u_{FF}	input signal from feedforward controller
u_{TOT}	total process input, feedforward plus feedback
V	polynomial in z^{-1}

V, σ^2	variance
WABT	Weighted Average Bed Temperature
Y	output
\bar{Y}, μ	mean output
Y_m, Y_{meas}	measured output
Y_p, Y_{pred}	predicted output
$Y_m - Y_p$	model prediction error
z^{-1}	backward shift operator
∇	$(1 - z^{-1})$
λ	Dahlin closed loop time constant constraining constant for CMVC
$\gamma(k)$	covariance function
$\rho(k)$	correlation function
$\theta(z^{-1})$	transfer function numerator
$\phi(z^{-1})$	transfer function denominator
$\psi(z^{-1})$	transfer function expansion weights

Appendix A

Time Series Review

Some of the time series techniques and properties used in this research are discussed briefly in the following section. If more detail is desired please refer to Box and Jenkins.[1976]

ARMA Models (Autoregressive Moving Average)

In most cases adequate process models can be obtained directly from the dynamic data collected from the process. If this information is summarized in the form of an empirical model with parameters estimated from the data it is referred to as a parametric model.[MacGregor, Taylor & Wright, 1988] These models can then be used directly in a control algorithm. The parametric model identification methods used in this research were developed for sampled data systems. This discrete time representation is the most relevant to digital computer control applications.

Given the general univariate system shown in Figure A.1, the output Y_t is the result of changes made in the process input u_t and the process noise or disturbance N_t .

$$Y_t = V(z^{-1}) u_t + N_t \quad (\text{A.1})$$

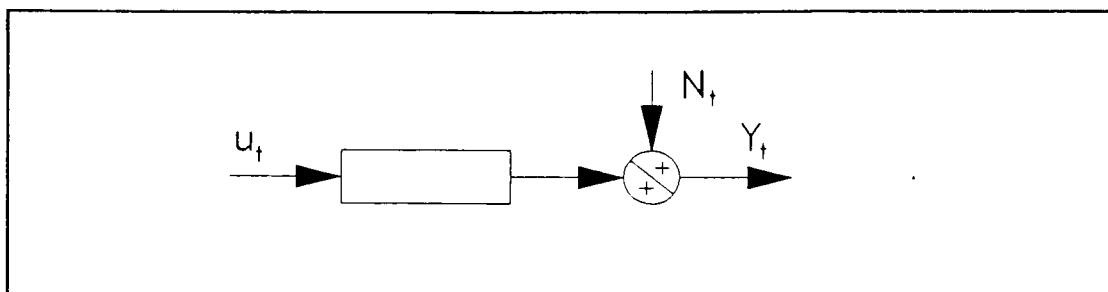


Figure A.1 Univariate System Block Diagram

V is a polynomial in z^{-1} , the backward shift operator where,

$$(z^{-k}) u_t = u_{t-k} \quad (\text{A.2})$$

and therefore can be expressed as a difference equation. The stochastic disturbance N_t can also be represented by difference equations or by an autoregressive moving average model.

A stochastic process is one which evolves in time according to probabilistic laws. "White Noise" is the simplest of all stochastic processes and consists of a sequence of independent, identically distributed random

variables, a_t . The underlying assumption, common to most stochastic control, is that a stochastic process can be described by a transfer function driven by random shocks. [Box & Jenkins, 1976]

$$Y_t = \frac{\theta(z^{-1})}{\phi(z^{-1}) \nabla} a_t \quad (\text{A.3})$$

$$\text{where, } \nabla = 1 - z^{-1}$$

A highly correlated series such as N_t can therefore be generated by passing a white noise sequence through a linear dynamic filter. [MacGregor, Taylor & Wright, 1988] This transfer function representation is referred to as an autoregressive integrated moving average (ARIMA) model of order (p,d,q) . If the process is stationary d become zero and the model is reduced to an autoregressive moving average (ARMA) model of order (p,q) . If the numerator reduces to unity then a pure autoregressive model, $AR(p)$, results. Conversely, a pure moving average model, $MA(q)$, is obtained if the denominator is simply unity. The values of θ ($i=1, \dots, p$) and ϕ ($i=1, \dots, q$) are the parameters of the model and must be estimated from the process data. Almost any time series or disturbance process encountered in practice can be modelled adequately with some choice of model order (p,q) and parameters (θ, ϕ) . [MacGregor, Taylor & Wright, 1988]

The ARMA models apply to stationary processes. A stochastic process is described as being stationary if its statistical properties or moments are unaffected by time. Therefore, a stochastic process will have a constant mean, variance and covariance. The latter will be discussed in the next section.

$$\begin{aligned}\mu_y &= E(Y_t) \\ \sigma_y^2 &= E(Y_t - \mu_y)^2\end{aligned}\tag{A.4}$$

These formulas are written in expectation notation. In practical circumstances an estimate of these theoretical properties must be calculated for the sample being examined.

$$\begin{aligned}\mu_y &= \bar{y} = \sum_{i=1}^N \frac{y_i}{N} = \frac{1}{N} \sum_{i=1}^N y_i \\ \sigma_y^2 &= \frac{1}{N} \sum_{i=1}^N (y_i - \bar{y})^2\end{aligned}\tag{A.5}$$

If the process being examined is nonstationary then stationarity conditions must be imposed before the model parameters are estimated from the data. Stationarity can be achieved by differencing the raw process data the required number of times, d .

$$\nabla^d Y_t\tag{A.6}$$

where,

$$\nabla Y_t = Y_t - Y_{t-1} \quad (\text{A.7})$$

The drifting nature of the series is corrected as only the difference between successive values is used and not the absolute value itself. The first difference will eliminate a drifting mean while the second difference will remove a changing slope. Once the data exhibits a constant mean and slope stationarity has been attained. The order of the numerator and denominator and the model parameters can then be estimated. The number of times the data is differenced becomes the value of d in the estimated process transfer function.

For more information on model identification refer to Box & Jenkins.[1976]

Autocorrelation and Crosscorrelation

The covariance between values of a stationary stochastic process separated by k periods of time will be constant and only a function of the separation time, k . The autocovariance is defined by,

$$\gamma_{yy}(k) = E[(Y_t - \mu_y)(Y_{t+k} - \mu_y)] \quad k=0,1,2,\dots \quad (\text{A.8})$$

and can be calculated with the Minimum Mean Square Error (MMSE) estimate given by,

$$c_{yy}(k) = \frac{1}{N} \sum_{t=1}^{N-k} (Y_t - \bar{Y})(Y_{t+k} - \bar{Y}) \quad k=0,1,2,\dots \quad (\text{A.9})$$

The autocovariance at lag zero is equivalent to the process variance. The autocovariance function represents the dependency between successive values in a series separated by k time intervals. The autocorrelation function is a normalized or dimensionless autocovariance which is convenient due to its independence from units.

$$\rho_{yy}(k) = \frac{\gamma_{yy}(k)}{\gamma_{yy}(0)} \quad k=0,1,2,\dots \quad (\text{A.10})$$

Similarly, this value can be estimated for a data sample with

$$r_{yy}(k) = \frac{c_{yy}(k)}{c_{yy}(0)} \quad k=0,1,2,\dots \quad (\text{A.11})$$

The absolute value of ρ_{yy} and r_{yy} are always less than or equal to one, with values near ± 1 indicating a high dependency while those near zero imply independence for normally distributed Gaussian processes.

The graphical representation of the autocovariance will produce various patterns. In the case of an oscillatory function the position of the peaks and valleys is dependent on the frequency of the variations in the error. Thus, visual inspection of the autocovariance plot, noting the period of oscillation, can determine the major frequencies of the process disturbances. [Box & Jenkins, 1976]

In the case of two Gaussian processes Y_t and u_t , the crosscovariance between u and Y at lag $+k$ is similarly defined as,

$$\gamma_{uy}(k) = E[(u_t - \mu_u)(Y_{t+k} - \mu_y)] \quad k=0,1,2,\dots \quad (\text{A.12})$$

and the crosscovariance between Y and u at lag $+k$ as,

$$\gamma_{yu}(k) = E[(Y_t - \mu_y)(u_{t+k} - \mu_u)] \quad k=0,1,2,\dots \quad (\text{A.13})$$

These parameters can be calculated using the estimates given in Equation A.14.

$$\begin{aligned} c_{uy}(k) &= \frac{1}{N} \sum_{t=1}^{N-k} (u_t - \bar{u}) (Y_{t+k} - \bar{Y}) \\ c_{yu}(k) &= \frac{1}{N} \sum_{t=1}^{N-k} (Y_t - \bar{Y}) (u_{t+k} - \bar{u}) \end{aligned} \quad (\text{A.14})$$

where, $k = 0, 1, 2, \dots$

Whereas in the autocovariance case, $\gamma_{yy}(+k) = \gamma_{yy}(-k)$, for the crosscovariance function, $\gamma_{uy}(+k) = \gamma_{yu}(-k)$. The dimensionless crosscorrelation is defined by Equation A.15 and can be estimated from Equation A.16.

$$\rho_{uy}(k) = \frac{\gamma_{uy}(k)}{\sigma_u \sigma_y} \quad k = 0, \pm 1, \pm 2, \dots \quad (\text{A.15})$$

$$r_{uy}(k) = \frac{c_{uy}(k)}{\sqrt{c_{uu}(0) c_{yy}(0)}} \quad (\text{A.16})$$

Differencing

The autocorrelation and crosscorrelation functions are only defined for stationary processes. Most processes, however, do exhibit some nonstationarity in the mean or slope.

A slowly drifting flow rate of a stream exiting a vessel under level flow smoothing or the changing ambient temperature throughout the day are examples of variables exhibiting nonstationarity. This violates the initial assumption of constant mean and variance. These nonstationary processes are highly autocorrelated and as such crosscorrelating these series will result in the correlation estimates, for the sample set, at successive lags being highly dependent. Therefore, the raw crosscorrelation analysis of autocorrelated series can be misleading. In order to calculate valid correlation functions for a sample of nonstationary data, stationarity conditions are induced by differencing the series themselves as discussed in the previous section. By differencing the series the appropriate number of times, d , the nonstationarity in mean and slope can be eliminated.

In the analyses used in this research the differencing of nonstationary series is demonstrated. In most cases the controlled variable is maintained at its desired setpoint and is stationary, therefore it is not differenced in the analyses. On the contrary, the manipulated and disturbance variables are generally nonstationary and are differenced for the correlation analysis.

Confidence Intervals

The autocorrelation and crosscorrelation described previously are theoretical functions of a stochastic process. In practice, only estimates of these correlation functions can be obtained from the available finite time series of N observations (Y_1-Y_N, u_1-u_N) . In order to check whether these correlation estimates are effectively zero beyond a certain lag, the corresponding estimates, $r_{uy}(k)$ and $r_{yy}(k)$, are compared with their approximate standard errors. In the case of 'larger lags' the standard errors of the estimated autocorrelations can be computed from the simplified form of Bartlett's formula, where the sample estimates replace the theoretical autocorrelations [Box & Jenkins, 1976]. Thus, the 'large-lag standard error' is given by,

$$\hat{\sigma} [r_{yy}(k)] = \frac{1}{N^{1/2}} \{1 + 2(r_{yy}(1))^2 + r_{yy}(2)^2 + \dots + r_{yy}(q)^2\}^{1/2} \quad (\text{A.17})$$

where $k > q$. Approximate expressions are given by Bartlett for the covariance between estimated correlations, r_k and r_{k+s} . Similarly, the 'large-lag' approximation is represented by Equation A.18.

$$\text{cov}[r_{yy}(k) r_{yy}(k+s)] = \frac{1}{N} \sum_{v=-\infty}^{\infty} \rho_{yy}(v) \rho_{yy}(v+s) \quad (\text{A.18})$$

The importance of these confidence intervals is in establishing the statistical significance of the parameters being estimated for each dataset. Therefore, it is not the absolute size of variations which is the key issue but whether this variation has statistical significance and can thus be distinguished from random error. The confidence intervals used throughout this reasearch, which are displayed in all the correlation plots, are 95% limits which translates to $\pm 2\sigma$.

Power Spectrum

The power spectrum of a stationary stochastic process shows how the variance of the process is distributed with frequency, and it can be obtained by taking the Fourier transform of the autocovariance function.

$$S_{yy}(f) = \frac{1}{N} \left| \sum_{t=-n}^{n-1} Y_t e^{-i2\pi ft} \right|^2 \quad -\frac{1}{2} \leq f \leq \frac{1}{2} \quad (\text{A.19})$$

This definition, however, is not satisfactory for stochastic signals undergoing random changes in frequency, amplitude and phase. The sample spectrum for a stochastic series fluctuates about the true spectrum and improvements are not obtained by increasing the sample size. Therefore, in most case some form of smoothing is necessary. For more information on smoothed spectral estimators please refer to Box & Jenkins [1976] and Timeslab [Newton, 1988].

The area under the spectral curve is equal to the process variance. Hence, the percentage of the total area which lies between two frequencies is the percentage of the variance occurring in that frequency band. Cyclical disturbances can be ascertained from peaks on the curve. Therefore, an important application of the power spectrum is the determination of these disturbances from their observed frequency.

Appendix B

SISO Feedback-Only Control Simulation Results

The minimum variance controller designed for the FOPDT process,

$$Y_m(z) = \frac{0.2 z^{-3}}{1 - 0.8 z^{-1}} * u(z) + \frac{1}{(1 - 0.8 z^{-1}) \nabla} * a_t \quad (\text{B.1})$$

is given by,

$$G_c(z) = \frac{14.760 - 21.568 z^{-1} + 7.808 z^{-2}}{1.0 - 2.952 z^{-3} + 1.952 z^{-4}} \quad (\text{B.2})$$

The constrained minimum variance controller, with a constraint factor ($\lambda=0.4$), designed for the same process is given by,

$$G_c(z) = \frac{4.009 - 6.079 z^{-1} + 2.297 z^{-2}}{1.0 - 1.187 z^{-1} + 0.414 z^{-2} - 0.802 z^{-3} + 0.574 z^{-4}} \quad (\text{B.3})$$

The model mismatch cases performed on the system consisted of the same CMVC given above but the process transfer function was modified to create the mismatch. The two mismatch cases examined are given by the following process

transfer functions. A 50% increase in process gain yields,

$$Y_m(z) = \frac{0.3z^{-1}}{1 - 0.8z^{-1}} * u(z) + \frac{1}{(1 - 0.8z^{-1})\nabla} * a_t \quad (\text{B.4})$$

and a 50% decrease in process gain gives,

$$Y_m(z) = \frac{0.1z^{-1}}{1 - 0.8z^{-1}} * u(z) + \frac{1}{(1 - 0.8z^{-1})\nabla} * a_t \quad (\text{B.5})$$

Appendix C

SISO Model-Based (Smith Predictor Algorithm) Feedback Control Simulation Results

The minimum variance controller designed for the FOPDT process shown in Figure 3.7,

$$Y_m(z) = \frac{0.2 z^{-1}}{1 - 0.8 z^{-1}} * u(z) + \frac{1}{(1 - 0.2 z^{-1}) \nabla} * a_t \quad (\text{C.1})$$

is given by,

$$G_c(z) = \frac{6.0 - 5.8 z^{-1} + 0.8 z^{-2}}{1.0 - 1.2 z^{-1} + 0.2 z^{-2}} \quad (\text{C.2})$$

It is important to note that the plant and model dead times were equivalent.

In order to estimate the best achievable performance an ARMA model is fit to the time series data, yielding the following relationship,

$$\begin{aligned} Y_m(z) &= \frac{1.0 + 0.520 z^{-1} + 0.302 z^{-2}}{1.0 - 0.694 z^{-1}} * a_t \\ &= (1 + 1.214 z^{-1} + 1.145 z^{-2} + \dots) * a_t \end{aligned} \quad (\text{C.3})$$

where the variance of a_t is 0.00102. Given the true process dead time of two units the minimum variance achievable is given by,

$$\begin{aligned} \text{Var}\{Y_m\}_{MVC} &= (1^2 + 1.214^2 + 1.145^2) * 0.00102 \\ &= 0.00386 \end{aligned} \quad (\text{C.4})$$

A PI controller was designed for the process in order to generate more realistic control conditions. The controller was designed using the Integral of Absolute Error (IAE) technique [Smith & Corripio, 1985] yielding the following,

$$G_c(z) = \frac{1.212 - 1.0z^{-1}}{1.0 - 1.0z^{-1}} \quad (\text{C.5})$$

The model mismatch case performed on the system consisted of the same MVC given above but the process transfer function was modified to create the mismatch. The mismatch case examined is given by the following process transfer function. A 50% decrease in process gain yields,

$$Y_m(z) = \frac{0.1z^{-1}}{1 - 0.8z^{-1}} * u(z) + \frac{1}{(1 - 0.2z^{-1})V} * a_t \quad (\text{C.6})$$

Appendix D

Paper Mill Data Industrial Case Study

DOMTAR - Controlled case

In order to estimate the best achievable performance an ARMA model is fit to the time series data, yielding the following relationship,

$$\begin{aligned} Y_m(z) &= \frac{1.0 - 0.145z^{-1}}{1.0 - 0.576z^{-1}} * a_t \\ &= (1 + 0.431z^{-1} + 0.248z^{-2} + \dots) * a_t \end{aligned} \quad (\text{D.1})$$

where the variance of a_t is 0.389. Given the true process dead time of two units the minimum variance achievable is given by,

$$\begin{aligned} \text{Var}\{Y_m\}_{MVC} &= (1^2 + 0.431^2 + 0.248^2) * 0.389 \\ &= 0.485 \end{aligned} \quad (\text{D.2})$$

Appendix E

Shell Heat Exchanger Industrial Case Study

In order to estimate the best achievable performance an ARMA model was fit to the time series data obtained under original control conditions (shown as Case 1 in Table 3.1), yielding the following relationship,

$$Y_m(z) = \frac{1.0}{1.0 - 0.975z^{-1}} * a_t \quad (\text{E.1})$$
$$= (1 + 0.975z^{-1} + 0.951z^{-2} + \dots) * a_t$$

where the variance of a_t is 0.0952. Given the true process dead time of one unit the minimum variance achievable is given by,

$$\text{Var}\{Y_m\}_{MVC} = (1^2 + 0.975^2) * 0.0952 \quad (\text{E.2})$$
$$= 0.186$$

Given the case in which the control parameters were approaching those of a minimum variance controller, Case 3, the ARMA model fit to the process data resulted in,

$$Y_m(z) = (1.0 + 0.625z^{-1} + 0.264z^{-2}) * a_t \quad (\text{E.3})$$

with a variance of 0.0304 for a_t . The estimate of the lowest achievable variance is then obtained,

$$\begin{aligned} \text{Var}\{Y_m\}_{MVC} &= (1^2 + 0.625^2) * 0.0304 \\ &= 0.042 \end{aligned} \quad (\text{E.4})$$

Case 4 demonstrated overly aggressive control. The ARMA model fit to the process data resulted in,

$$Y_m(z) = (1.0 + 0.825z^{-1} + 0.582z^{-2}) * a_t \quad (\text{E.5})$$

with a variance of 0.118 for a_t . The estimate of the lowest achievable variance is then obtained,

$$\begin{aligned} \text{Var}\{Y_m\}_{MVC} &= (1^2 + 0.825^2) * 0.118 \\ &= 0.198 \end{aligned} \quad (\text{E.6})$$

Appendix F

SISO Feedforward-Feedback Control Simulation Results

The minimum variance controller designed for the FOPDT process,

$$\begin{aligned} G_p(z) &= \frac{0.376 z^{-2}}{1 - 0.836 z^{-1}} * u(z) + \frac{1}{1 - z^{-1}} * a_t \\ G_d(z) &= \frac{0.17 z^{-2}}{1 - 0.886 z^{-1}} \end{aligned} \quad (\text{F.1})$$

is given by,

$$G_{c_{FB}}(z) = \frac{2.660 - 2.223 z^{-1}}{1.0 - 1.0 z^{-1}} \quad (\text{F.2})$$

and the feedforward controller resulting in complete disturbance rejection is given by,

$$G_{c_{FF}}(z) = \frac{-0.440 + 0.366 z^{-1}}{1.0 - 0.886 z^{-1}} \quad (\text{F.3})$$

It is important to note that the best achievable performance refers specifically to optimal feedback control given the specific system configuration and disturbances. If the feedforward controller is not attenuating disturbances adequately the minimum variance calculated under these conditions will not be the lowest possible variance given a perfect feedforward controller. Hence, in order to establish the absolute best achievable performance, the feedforward controller must be performing satisfactorily. Otherwise the minimum variance calculated is that which is attainable under the given adverse disturbance conditions. In the cases which follow, the calculation of the minimum variance corresponds to the disturbance conditions present and does not take into consideration the adequacy of the feedforward controller and whether this estimated minimum variance can in fact be further reduced.

In order to estimate the best achievable performance an ARMA model is fit to the time series data, yielding the following relationship,

$$Y_m(z) = \frac{1.0}{1.0 - 0.726z^{-1} + 0.455z^{-2} - 0.335z^{-3} + 0.178z^{-4}} * a_t \quad (\text{F.4})$$

$$- (1 + 0.726z^{-1} + \dots) * a_t$$

where the variance of a_t is 1.258. Given the true process dead time of one unit the minimum variance achievable is given by,

$$\begin{aligned} \text{Var}\{Y_m\}_{MVC} &= (1^2 + 0.726^2) * 1.258 \\ &= 1.921 \end{aligned} \quad (\text{F.5})$$

A CMV controller, $\lambda=1.0$, was designed for the process in order to generate more sluggish control conditions, yielding the following control equation,

$$G_{c_{FB}}(z) = \frac{0.672 - 0.595 z^{-1}}{1.0 - 1.147 z^{-1} + 0.147 z^{-2}} \quad (\text{F.6})$$

In order to estimate the best achievable performance an ARMA model is fit to the time series data, yielding the following relationship,

$$\begin{aligned} Y_m(z) &= \frac{1.0}{1.0 - 0.908 z^{-1} + 0.242 z^{-2}} * a_t \\ &= (1 + 0.908 z^{-1} + \dots) * a_t \end{aligned} \quad (\text{F.7})$$

where the variance of a_t is 0.971. The minimum variance achievable is then given by Equation F.8.

$$\begin{aligned} \text{Var}\{Y_m\}_{MVC} &= (1^2 + 0.908^2) * 0.971 \\ &= 1.772 \end{aligned} \quad (\text{F.8})$$

The model mismatch cases performed on the system consisted of using the same controllers given previously but the process and disturbance transfer functions were modified to create the mismatch.

The first mismatch case consisted of compensating model errors where both the model gains were decreased by 50%, and is given by the following process transfer functions,

$$\begin{aligned} G_p(z) &= \frac{0.188 z^{-2}}{1 - 0.836 z^{-1}} * u(z) + \frac{1}{1 - z^{-1}} * a_t \\ G_d(z) &= \frac{0.085 z^{-2}}{1 - 0.886 z^{-1}} \end{aligned} \quad (\text{F.9})$$

The next mismatch case examined is given by the following process transfer functions in which the process transfer function is decreased by 50% but the disturbance model remains correct,

$$\begin{aligned} G_p(z) &= \frac{0.188 z^{-2}}{1 - 0.836 z^{-1}} * u(z) + \frac{1}{1 - z^{-1}} * a_t \\ G_d(z) &= \frac{0.17 z^{-2}}{1 - 0.886 z^{-1}} \end{aligned} \quad (\text{F.10})$$

The ARMA model fit to the time series data generated the relationship given in equation F.11, where the variance of a_t is 1.201. The minimum variance achievable is then calculated as shown in equation F.12.

$$Y_m(z) = \frac{1.0}{1.0 - 0.904z^{-1} + 0.292z^{-2} - 0.211z^{-3}} * a_t \quad (\text{F.11})$$

$$= (1 + 0.904z^{-1} + \dots) * a_t$$

$$\text{Var}\{Y_m\}_{MVC} = (1^2 + 0.904^2) * 1.207 \quad (\text{F.12})$$

$$= 2.193$$

The final case studied is given by the following, in which case both the disturbance and process transfer functions are mismatched but the errors do not compensate,

$$G_p(z) = \frac{0.188z^{-2}}{1 - 0.836z^{-1}} * u(z) + \frac{1}{1 - z^{-1}} * a_t \quad (\text{F.13})$$

$$G_d(z) = \frac{0.34z^{-2}}{1 - 0.886z^{-1}}$$

The ARMA model fit to the time series data resulted in the following relationship,

$$Y_m(z) = \frac{1.0}{1.0 - 1.260z^{-1} + 0.344z^{-2}} * a_t \quad (\text{F.14})$$

$$= (1 + 1.260z^{-1} + \dots) * a_t$$

where the variance of a_t is 1.779. The minimum variance achievable is calculated as,

$$\begin{aligned}\text{Var}\{Y_m\}_{MVC} &= (1^2 + 1.260^2) * 1.779 && \text{(F.15)} \\ &= 4.603\end{aligned}$$

Appendix G

Shell Stabilizer Industrial Case Study

The original control test yielded the following ARMA model fit to the time series data,

$$Y_m(z) = \frac{1.0}{1.0 - 0.633z^{-1} - 0.281z^{-2}} * a_t \quad (\text{G.1})$$
$$= (1 + 0.633z^{-1} + 0.682z^{-2} + 0.610z^{-3} + 0.578z^{-4} + 0.537z^{-5} + \dots) * a_t$$

where the variance of a_t is 0.0159. This corresponds to Case 1 in Table 3.3. Given the true process dead time of five units the minimum variance achievable is given by,

$$\text{Var}\{Y_m\}_{MVC} = (1^2 + 0.633^2 + 0.682^2 + 0.610^2 + 0.578^2 + 0.537^2) * 0.0159 \quad (\text{G.2})$$
$$= 0.0476$$

The feedforward gain was then decreased, as shown in Case 2, and a time series model fit to the data resulted in Equation G.3, where the variance of a_t is 0.0130. The minimum variance achievable is then given by Equation G.4.

$$Y_m(z) = \frac{1.0}{1.0 - 0.618z^{-1} - 0.351z^{-2}} * a_t$$

$$= (1 + 0.618z^{-1} + 0.733z^{-2} + 0.670z^{-3} + 0.671z^{-4} + 0.650z^{-5} + \dots) * a_t \quad (\text{G.3})$$

$$\text{Var}\{Y_m\}_{MVC} = (1^2 + 0.618^2 + 0.733^2 + 0.670^2 + 0.671^2 + 0.650^2) * 0.0130$$

$$= 0.0421 \quad (\text{G.4})$$

The feedback gain was increased according to Case 3 and a time series model fit to the data resulted in the following,

$$Y_m(z) = \frac{1.0}{1.0 - 0.563z^{-1} - 0.308z^{-2}} * a_t$$

$$= (1 + 0.563z^{-1} + 0.625z^{-2} + 0.525z^{-3} + 0.489z^{-4} + 0.437z^{-5} + \dots) * a_t \quad (\text{G.5})$$

where the variance of a_t is 0.0136. The minimum variance achievable is then given by,

$$\text{Var}\{Y_m\}_{MVC} = (1^2 + 0.563^2 + 0.625^2 + 0.525^2 + 0.489^2 + 0.437^2) * 0.0136$$

$$= 0.0328 \quad (\text{G.6})$$

In Case 4 the feedforward gain was increased and a time series model fit to the data resulted in the relationship given in equation G.7, where the variance of a_t is 0.0135.

$$Y_m(z) = \frac{1.0}{1.0 - 0.590z^{-1} - 0.245z^{-2} - 0.107z^{-3}} * a_t \quad (\text{G.7})$$

$$= (1 + 0.590z^{-1} + 0.593z^{-2} + 0.602z^{-3} + 0.563z^{-4} + 0.542z^{-5} + \dots) * a_t$$

The minimum variance achievable is then given by equation G.8.

$$\text{Var}\{Y_m\}_{MVC} = (1^2 + 0.590^2 + 0.593^2 + 0.602^2 + 0.563^2 + 0.542^2) * 0.0135 \quad (\text{G.8})$$

$$= 0.0361$$

The tuning parameters were then kept constant and a run, Case 6, was performed having no feed perturbations. The time series model fit to that data resulted in the following,

$$Y_m(z) = \frac{1.0}{1.0 - 0.449z^{-1} - 0.319z^{-2}} * a_t \quad (\text{G.9})$$

$$= (1 + 0.449z^{-1} + 0.521z^{-2} + 0.377z^{-3} + 0.335z^{-4} + 0.270z^{-5} + \dots) * a_t$$

where the variance of a_t is 0.0123. The minimum variance achievable is then given by,

$$\text{Var}\{Y_m\}_{MVC} = (1^2 + 0.449^2 + 0.521^2 + 0.377^2 + 0.335^2 + 0.270^2) * 0.0123 \quad (\text{G.10})$$

$$= 0.0221$$

The feedforward controller was then turned off but the feed perturbations were reintroduced. Refer to Case 5 in Table 3.3. The time series model fit to that data resulted in the following,

$$Y_m(z) = \frac{1.0}{1.0 - 0.445z^{-1} - 0.280z^{-2} - 0.219z^{-3}} * a_t$$

$$- (1 + 0.445z^{-1} + 0.478z^{-2} + 0.557z^{-3} + 0.480z^{-4} + 0.475z^{-5} + \dots) * a_t \quad (\text{G.11})$$

where the variance of a_t is 0.00999. The minimum variance achievable is then given by,

$$\text{Var}\{Y_m\}_{MVC} = (1^2 + 0.445^2 + 0.478^2 + 0.557^2 + 0.480^2 + 0.475^2) * 0.00999$$

$$= 0.0219 \quad (\text{G.12})$$

The final example, given as Case 7, resulted from an excessive feedforward gain. The time series model fit to the data produced the following,

$$Y_m(z) = \frac{1.0}{1.0 - 0.562z^{-1} - 0.318z^{-2}} * a_t$$

$$- (1 + 0.562z^{-1} + 0.634z^{-2} + 0.535z^{-3} + 0.503z^{-4} + 0.453z^{-5} + \dots) * a_t \quad (\text{G.13})$$

where the variance of a_t is 0.0113. The minimum variance achievable is then given by,

$$\begin{aligned} \text{Var}\{Y_m\}_{MVC} &= (1^2 + 0.562^2 + 0.634^2 + 0.535^2 \\ &\quad + 0.503^2 + 0.453^2) * 0.0113 \quad \text{(G.14)} \\ &= 0.0278 \end{aligned}$$

Appendix H

MIMO Control System Simulation Results

The LQG controller designed for the base case process,

$$\begin{aligned}
 G_m(z) = G_p(z) = & \begin{vmatrix} \frac{0.393 z^{-2}}{1 - 0.607 z^{-1}} & \frac{0.315 z^{-2}}{1 - 0.607 z^{-1}} \\ \frac{0.0787 z^{-2}}{1 - 0.607 z^{-1}} & \frac{0.393 z^{-2}}{1 - 0.607 z^{-1}} \end{vmatrix} * \underline{u(z)} \\
 & + \begin{vmatrix} \frac{1}{1 - z^{-1}} & 0 \\ 0 & \frac{1}{1 - z^{-1}} \end{vmatrix} * \underline{a_t}
 \end{aligned} \tag{H.1}$$

is given by,

$$G_{cij}(z) = \frac{\alpha_{ij}(z^{-1})}{1 - \beta_{ij}(z^{-1})} \tag{H.2}$$

where i and j refer to the row and column, respectively, of the controller matrix and α and β are polynomials in the backward shift operator, z^{-1} . The coefficients of $\alpha(z^{-1})$ and $\beta(z^{-1})$ for this example are given in Tables H.1 and H.2. It is important to note that in all cases studied the output weights were equal, at 1.0 units.

Table H.1 Coefficients of $\alpha(z^{-1})$

z^0	3.031	-2.429
	-.6070	3.031
z^{-1}	-5.520	4.424
	1.105	-5.520
z^{-2}	3.350	-2.685
	-.6709	3.350
z^{-3}	-.6779	.5433
	.1357	-.6779
z^{-4}	.3044E-6	-.2389E-6
	-.3790E-7	.2050E-6
z^{-5}	-.1322E-6	.9533E-7
	.1729E-7	-.6499E-7

Table H.2 Coefficients of $\beta(z^{-1})$

z^{-1}	-1.214
z^{-2}	.3684
z^{-3}	-.1039E-6
z^{-4}	.1064E-6

The control equations for the case in which equal penalty weights of 2.0 units were placed on both inputs is obtained by using the coefficients given in Tables H.3 and H.4 in Equation H.2.

Table H.3 Coefficients of $\alpha(z^{-1})$

z^0	.5327	-.2125
	.1077	.5327
z^{-1}	-1.580	.5431
	-.4072	-1.580
z^{-2}	1.899	-.5592
	.5825	1.899
z^{-3}	-1.155	.2931
	-.4014	-1.155
z^{-4}	.3557	-.7924E-1
	.1347	.3557
z^{-5}	-.4435E-1	.8970E-2
	-.1770E-1	-.4435E-1

Table H.4 Coefficients of $\beta(z^{-1})$

z^{-1}	-3.536
z^{-2}	5.268
z^{-3}	-4.329
z^{-4}	1.946
z^{-5}	-.4842
z^{-6}	.5106E-1

Mismatch was then introduced into the system by modifying the process transfer function to yield,

$$G_p(z) = \begin{vmatrix} \frac{0.200 z^{-2}}{1 - 0.607 z^{-1}} & \frac{0.500 z^{-2}}{1 - 0.607 z^{-1}} \\ \frac{0.0787 z^{-2}}{1 - 0.607 z^{-1}} & \frac{0.393 z^{-2}}{1 - 0.607 z^{-1}} \end{vmatrix} * \underline{u(z)} \quad (\text{H.3})$$

$$+ \begin{vmatrix} \frac{1}{1 - z^{-1}} & 0 \\ 0 & \frac{1}{1 - z^{-1}} \end{vmatrix} * \underline{a_t}$$

while the controller remained the same as designed for the base case given in Equation H.2, and Tables H.1 and H.2.

The next mismatch case had the following transfer function matrix,

$$G_p(z) = \begin{vmatrix} \frac{0.200 z^{-2}}{1 - 0.607 z^{-1}} & \frac{0.315 z^{-2}}{1 - 0.607 z^{-1}} \\ \frac{0.200 z^{-2}}{1 - 0.607 z^{-1}} & \frac{0.393 z^{-2}}{1 - 0.607 z^{-1}} \end{vmatrix} * \underline{u(z)} \quad (\text{H.4})$$

$$+ \begin{vmatrix} \frac{1}{1 - z^{-1}} & 0 \\ 0 & \frac{1}{1 - z^{-1}} \end{vmatrix} * \underline{a_t}$$

while the base controller remained unchanged.

Model mismatch was then introduced to the process model itself to give Equation H.5.

$$G_p(z) = \begin{bmatrix} \frac{0.393 z^{-2}}{1 - 0.607 z^{-1}} & \frac{0.315 z^{-2}}{1 - 0.607 z^{-1}} \\ \frac{0.0787 z^{-2}}{1 - 0.607 z^{-1}} & \frac{0.100 z^{-2}}{1 - 0.607 z^{-1}} \end{bmatrix} * \underline{u(z)} \quad (\text{H.5})$$

$$+ \begin{bmatrix} \frac{1}{1 - z^{-1}} & 0 \\ 0 & \frac{1}{1 - z^{-1}} \end{bmatrix} * \underline{a_f}$$

The problem of imbalanced dead times was also studied. The system matrix is given in Equation H.6.

$$G_m(z) - G_p(z) = \begin{bmatrix} \frac{0.393 z^{-3}}{1 - 0.607 z^{-1}} & \frac{0.315 z^{-5}}{1 - 0.607 z^{-1}} \\ \frac{0.0787 z^{-4}}{1 - 0.607 z^{-1}} & \frac{0.393 z^{-8}}{1 - 0.607 z^{-1}} \end{bmatrix} * \underline{u(z)} \quad (\text{H.6})$$

$$+ \begin{bmatrix} \frac{1}{1 - z^{-1}} & 0 \\ 0 & \frac{1}{1 - z^{-1}} \end{bmatrix} * \underline{a_f}$$

The control equation is the same as that given in Equation H.2 with coefficients for polynomials $\alpha(z^{-1})$ and $\beta(z^{-1})$ as given in Tables H.5 and H.6. The minimum possible settling time for each controlled variable must lie between the upper and lower

dead time limits given by the transfer function relationships. The procedure outlined here follows the Holt & Morari results [1985]. A lower bound for the settling time of output "i" is given by $\tau_i = \min_j(p_{ij})$ where p_{ij} is the minimum delay in the numerator of element "ij" of the transfer function matrix G. In the case of the transfer function shown in Equation H.6, the lower bounds for Y_1 and Y_2 are 2 and 3, respectively. Note that the true process dead times are used, from the continuous domain. An upper bound on settling time is given by,

$$r_{jj} = \exp\{-s_i (\text{Max}_i (\text{Max}(0, (\hat{Q}_{ij} - \hat{P}_{ij}))))\}$$

where,

(H.7)

\hat{P}_{ij} - minimum delay in numerator of element ij of G^{-1}
 \hat{Q}_{ij} - minimum delay in denominator of element ij of G^{-1}

Considering only dead times in Equation H.6, G and G^{-1} are given by Equation H.8.

$$G = \begin{vmatrix} e^{-2s} & e^{-4s} \\ e^{-3s} & e^{-7s} \end{vmatrix}$$

$$G^{-1} = \frac{1}{e^{-9s} - e^{-7s}} \begin{vmatrix} e^{-7s} & -e^{-4s} \\ -e^{-3s} & e^{-2s} \end{vmatrix}$$
(H.8)

Applying Equation H.7 to the above, the upper bounds on the settling time for Y_1 and Y_2 are 3 and 5, respectively.

Balancing the dead times, by placing the minimum dead times on the diagonal yields the transfer function matrix shown in Equation H.9.

$$G_m(z) - G_p(z) = \begin{vmatrix} \frac{0.393 z^{-3}}{1 - 0.607 z^{-1}} & \frac{0.315 z^{-5}}{1 - 0.607 z^{-1}} \\ \frac{0.0787 z^{-8}}{1 - 0.607 z^{-1}} & \frac{0.393 z^{-4}}{1 - 0.607 z^{-1}} \end{vmatrix} * \underline{u(z)} \quad (\text{H.9})$$

$$+ \begin{vmatrix} \frac{1}{1 - z^{-1}} & 0 \\ 0 & \frac{1}{1 - z^{-1}} \end{vmatrix} * \underline{a_t}$$

The coefficients for the control equation are given in Tables H.7 and H.8. The minimum achievable variance for the two controlled variables can be calculated for this final example. ARMA models were fit to the two output series yielding the relationships displayed in Equations H.10 and H.11. The variances of a_{1t} and a_{2t} are 1.972 and 1.573 respectively.

$$Y_1(z) = \frac{1.0}{1 - 0.617 z^{-1}} * a_t \quad (\text{H.10})$$

$$= (1.0 + 0.617 z^{-1} + 0.381 z^{-2} + \dots) * a_t$$

$$Y_2(z) = \frac{1.0}{1 - 0.737 z^{-1}} * a_t \quad (\text{H.11})$$

$$= (1.0 + 0.737 z^{-1} + 0.543 z^{-2} + 0.400 z^{-3} + \dots) * a_t$$

The minimum achievable variance is then derived from,

$$\begin{aligned} \text{VAR}\{Y_1\}_{MVC} &= (1^2 + 0.617^2 + 0.381^2) * 1.972 \\ &= 3.009 \end{aligned} \quad (\text{H.12})$$

$$\begin{aligned} \text{VAR}\{Y_2\}_{MVC} &= (1^2 + 0.737^2 + 0.543^2 + 0.400^2) * 1.573 \\ &= 3.143 \end{aligned} \quad (\text{H.13})$$

given minimum dead times of 2 and 3 units for outputs Y_1 and Y_2 , respectively.

Table H.5 Coefficients of $\alpha(z^{-1})$

z^0	2.446	.4899
	-.5096	2.545
z^{-1}	-4.455	-.8921
	.9279	-4.634
z^{-2}	2.704	-1.498
	-.5632	2.813
z^{-3}	-.5471	3.604
	.1140	-.5691
z^{-4}	-.9811E-1	-2.744
	-.1334E-6	.3059E-6
z^{-5}	-.1787	1.348
	.9982E-7	-.1128E-6
z^{-6}	.1084	-.5415
	-.1330E-6	.1597E-6
z^{-7}	-.2194E-1	.1096
	.1910E-6	-.3787E-6
z^{-8}	.8214E-6	-.5509E-6
	-.2586E-6	.6725E-6
z^{-9}	-.6723E-6	.4366E-6
	.1852E-6	-.5401E-6
z^{-10}	.1829E-6	-.1288E-6
	-.4650E-7	.1435E-6

Table H.6 Coefficients of $\beta(z^{-1})$

z^{-1}	-1.214
z^{-2}	.2079
z^{-3}	.1949E-6
z^{-4}	-.5914E-1
z^{-5}	-.6633E-7
z^{-6}	.1538E-6
z^{-7}	-.2093E-6
z^{-8}	.3787E-6
z^{-9}	-.1520E-6

Table H.7 Coefficients of $\alpha(z^{-1})$

z^0	2.545	.8924E-5
	-.9585E-6	2.545
z^{-1}	-4.634	-.1666E-6
	.1677E-5	-4.634
z^{-2}	2.813	-2.039
	-.1031E-5	2.813
z^{-3}	-.5691	3.714
	-.1446E-6	-.5691
z^{-4}	.1110E-5	-2.254
	-.5096	-.1573E-5
z^{-5}	-.3538E-6	.4561
	.9279	-.3031E-5
z^{-6}	.3318E-6	-.4563E-6
	-.5632	-.1600E-5
z^{-7}	-1864E-6	.2196E-6
	.1140	.8997E-7
z^{-8}	.7741E-7	.2549E-7
	-.5269E-7	.2169E-6
z^{-9}	-.1160E-6	.7015E-7
	.4622E-7	-.1919E-6

Table H.8 Coefficients of $\beta(z^{-1})$

z^{-1}	-1.214
z^{-2}	.3684
z^{-3}	-.1129E-6
z^{-4}	.1273E-6
z^{-5}	-.2276E-6
z^{-6}	-.1605
z^{-7}	.1949
z^{-8}	-.5914E-1

Appendix I

Shell HCU QDMC Industrial Case Study Results

The minimum variance estimates for the six controlled variables were calculated for the test run in which the recycle gas feed to the reactor was perturbed in a PRBS fashion. ARMA models were fit to the time response data collected for the six variables and the minimum variance predictions were estimated as described in Chapter 2. As discussed in Chapter 4, the minimum dead time of all the transfer functions related to each of the controlled variables was estimated to be less than the sampling time of 6 minutes. Therefore, the minimum dead time lag, f , was chosen as zero. This means that the best achievable performance for each controlled variable corresponds to the residual variance obtained after the ARMA model is fit to the process response. Equations I.1 to I.6 display the models fit to each of the controlled variables and the corresponding residual variance obtained. These results were summarized in Table 4.1.

$$WABT_t = (1 + 1.044 z^{-1} + \dots) a_t \quad (\text{I.1})$$

where, $\sigma_{a_t}^2 = 0.00434$

$$BED1AVT_t = (1 + 1.161 z^{-1} + \dots) a_t \quad (\text{I.2})$$

where, $\sigma_{a_t}^2 = 0.0274$

$$BED2AVT_t = (1 + 1.044 z^{-1} + \dots) a_t \quad (\text{I.3})$$

where, $\sigma_{a_t}^2 = 0.0105$

$$BED3AVT_t = (1 + 0.892 z^{-1} + \dots) a_t \quad (\text{I.4})$$

where, $\sigma_{a_t}^2 = 0.00712$

$$BED4AVT_t = (1 + 0.946 z^{-1} + \dots) a_t \quad (\text{I.5})$$

where, $\sigma_{a_t}^2 = 0.00706$

$$INQVPOSN_t = (1 + 1.120 z^{-1} + \dots) a_t \quad (\text{I.6})$$

where, $\sigma_{a_t}^2 = 13.811$

